Departamento de Edafología y Química Agrícola

Behaviour of fuel organic compounds in contaminated soils and development of a phytoremediation procedure

Memoria para optar al Grado de Doctora en Medio Ambiente y Recursos Naturales

Mención Internacional

María Balseiro Romero

Santiago de Compostela, Diciembre 2014

USC
UNIVERSIDADE
DE SANTIAGO
DE COMPOSTELA

Dra. Mª del Carmen Monterroso Martínez, Profesora titular del Departamento de Edafología y Química Agrícola de la Universidad de Santiago de Compostela

INFORMA:

Que la presente memoria titulada *Behaviour of fuel organic compounds in contaminated soils and development of a phytoremediation procedure* presentada por **Dña. María Balseiro Romero** para optar al Grado de Doctora en Medio Ambiente y Recursos Naturales, fue realizada bajo mi dirección.

Y considerando que representa trabajo de Tesis Doctoral, autorizo su presentación ante el Tribunal correspondiente.

Y para que así conste, firmo el presente en Santiago de Compostela a 16 de Diciembre de 2014.

Fdo.: Dra. Mª del Carmen Monterroso Martínez

USC
UNIVERSIDADE
DE SANTIAGO
DE COMPOSTELA

A mi familia

USC
UNIVERSIDADE
DE SANTIAGO
DE COMPOSTELA

CONTENT

LIST OF ABBREVIATIONS

ACV	Absorbance of crystal violet
APL	Absorbance of planktonic cells
ASE	Accelerated solvent extraction
BS	Biosurfactants
BTEX	Benzene, toluene, ethylbenzene, xylene
CFU	Colony forming units
CPI	Carbon preference index
DCPIP	2,6-dichlorophenol indophenol
DOC	Dissolved organic carbon
DRO	Diesel range organics
ETBE	Ethyl *tert*-butyl ether
FO	Fuel oxygenates
GC	Gas chromatography
HS	Headspace
K_{oc}	Organic carbon partition coefficient
K_{ow}	Octanol-water partition coefficient
L/HMW	low to high molecular weight alkanes concentration ratio
LOD	Limit of detection
LOQ	Limit of quantification
MS	Mass spectrometry
MTBE	Methyl *tert*-butyl ether
OD	Optical density
OST	Organic solvent tolerance
PCA	Principal components analysis
PEL	Pellet
PGP	Plant growth promotion
PP	Polypropylene
PS	Polystyrene
REC	Root exudate components
RFT	Range finding test
RT	Room temperature

SN	Supranatant
SOM	Soil organic matter
SPME	Solid-phase microextraction
SRL	Specific root length
SSL	Specific shoot length
SVE	Soil vapour extraction
US	Ultrasonic
USEPA	U. S. Environmental Protection Agency
VOA	Volatile organic analysis
VOC	Volatile organic compounds

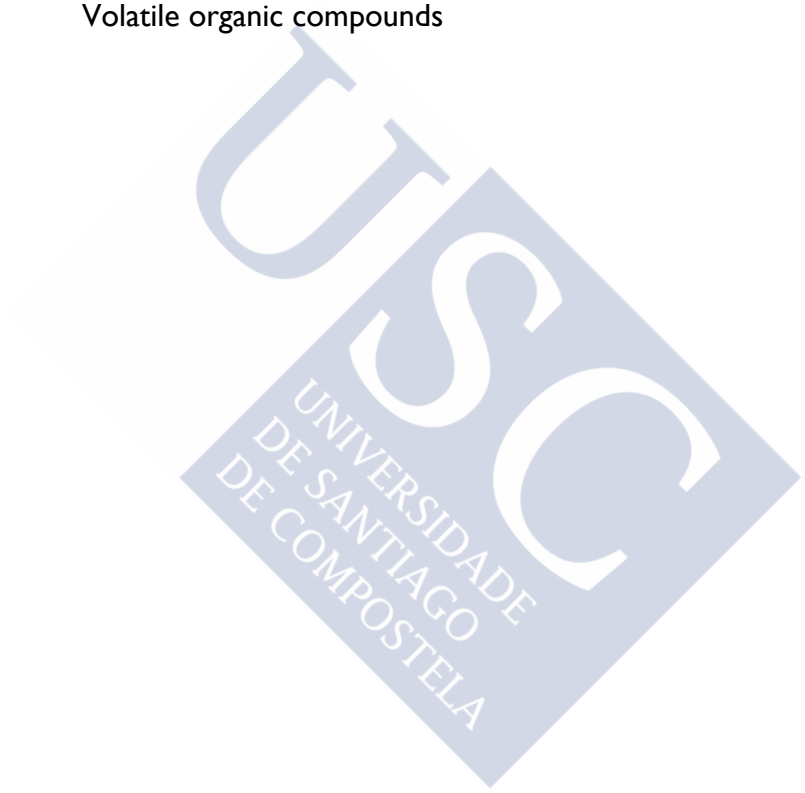

USC
UNIVERSIDADE
DE SANTIAGO
DE COMPOSTELA

USC
UNIVERSIDADE
DE SANTIAGO
DE COMPOSTELA

RESUMEN

INTRODUCCIÓN Y OBJETIVOS

La contaminación del suelo es un problema de gran preocupación medioambiental, debido a que conlleva grandes riesgos para la salud humana y los ecosistemas. El suelo es un recurso valioso y considerado como no renovable a escala de tiempo humana (Hasset y Banwart, 1992), por lo que es importante evitar al máximo episodios de contaminación y desarrollar técnicas de limpieza efectivas y poco invasivas.

Los principales contaminantes del suelo incluyen fertilizantes, pesticidas, metales pesados, hidrocarburos aromáticos policíclicos (PAH), bifenilos policlorados (PCB), pero son los metales pesados y los hidrocarburos derivados del petróleo los que suponen un 60% de la contaminación total del suelo en Europa (Panagos *et al.*, 2013). En concreto, la contaminación del suelo con compuestos derivados del petróleo es un problema causado, principalmente, por emisiones y residuos de la industria petroquímica, accidentes de tráfico, vertidos accidentales en tuberías o fugas de los tanques de almacenamiento subterráneo de combustibles (Hentati *et al.*, 2013). Como ejemplo, el CONCAWE (Conservation of Clean Air and Water in Europe), registró cerca de 457 vertidos en tuberías de fuel entre 1971 y 2012, que liberaron más de 80,000 m^3 de petróleo y contaminaron más de 100,000 m^2 de suelo por año.

Los combustibles derivados del petróleo, gasolina y diesel, son mezclas complejas de compuestos orgánicos, muchos de los cuales son tóxicos y están incluidos en la lista de contaminantes prioritarios de la USEPA. Entre ellos, benceno, tolueno, etilbenceno y xileno (BTEX), son, junto con los alcanos hasta C_{10}, cicloalcanos y oxigenados (éteres, como MTBE y ETBE, y alcoholes) los componentes principales de la gasolina (Xiao *et al.*, 2014). Los compuestos orgánicos de rango diesel (DRO), alcanos de C_{10} a C_{25}, son los componentes mayoritarios del diesel, además de cicloalcanos y compuestos poliaromáticos (Pitz y Mueller, 2011). Dada la gran variedad de propiedades fisicoquímicas de los compuestos orgánicos derivados del fuel (diferentes presiones de vapor, solubilidad en agua y pesos moleculares (Fine *et al.*, 1997)), los suelos contaminados con gasolina y/o diesel generan un gran riesgo medioambiental, dado que pueden contaminar otros compartimentos medioambientales, con los riesgos que ello conlleva (Al-Mutairi *et al.*, 2008). La adsorción a las partículas de suelo, volatilización, lixiviación, degradación (oxidación química, fotoquímica, biológica), absorción por plantas, etc., son los principales procesos que van a influir en el destino final de los contaminantes del suelo en el medio ambiente (Asquith *et al.*, 2012). Por ello, resulta esencial estudiar la dinámica de cada contaminante particular en el suelo, en función de las propias características físico-químicas del compuesto y el suelo donde tenga lugar el episodio contaminante. La adsorción de contaminantes al suelo, es el proceso más ampliamente estudiado, ya que influye en el resto de procesos anteriormente citados (Serrano y Gallego, 2006): en función del grado de adsorción, el contaminante se evaporará o lixiviará con mayor o menor facilidad, o estará más o menos biodisponible para su degradación por los organismos del suelo o absorción por la plantas.

La descontaminación de suelos se realiza tradicionalmente mediante técnicas, *ex situ* o *in situ*, que incluyen tratamientos físicos y químicos (extracción

de vapor, inyección de disolventes, desorción térmica, etc.), que provocan grandes impactos en el suelo y requieren elevadas inversiones económicas (Kuiper *et al.*, 2004). Las tendencias más recientes buscan tratamientos de limpieza menos agresivos, basados en procesos naturales, que permitan la conservación del recurso edáfico y que sean económicamente viables. La biorremediación es el uso de organismos vivos (plantas, bacterias y/o hongos), para la recuperación de suelos contaminados (Wenzel, 2009). Particularmente, la rizodegradación (fitorremediación en la rizosfera asistida con microorganismos), es una de las técnicas más utilizadas para degradar hidrocarburos derivados del petróleo (MacKinnon y Duncan, 2013). En esta técnica, se aprovecha la relación entre plantas y microorganismos, para mejorar de forma significativa la degradación microbiana.

El objetivo de la presente tesis doctoral fue estudiar el comportamiento de los contaminantes orgánicos derivados del petróleo (MTBE, ETBE, BTEX y DRO) en el suelo y desarrollar un procedimiento de limpieza de suelos contaminados, efectivo y de bajo impacto, por rizodegradación utilizando las asociaciones planta-bacteria. Para ello fue esencial desarrollar métodos analíticos sensibles y precisos y entender los procesos que sufren los contaminantes en el suelo y su toxicología (Drozdova y Rosenberg, 2013), a través de estudios a diferente escala (laboratorio, invernadero, campo).

De acuerdo con este objetivo general, diferentes estudios se llevaron a cabo con los siguientes objetivos específicos:

- Desarrollar y optimizar los métodos de análisis de compuestos volátiles (MTBE, ETBE y BTEX) y compuestos orgánicos de rango diesel (DRO) en muestras ambientales (suelos y aguas).
- Aplicación de estos métodos a la caracterización de la contaminación de un entorno contaminado por hidrocarburos alrededor de una gasolinera.

- Estudiar el comportamiento de los compuestos volátiles del fuel en el suelo (*in vitro*), a través de estudios de adsorción y evaluar el efecto que inducen las plantas en la movilidad de los contaminantes en el suelo a través de la producción de exudados en la raíz.
- Evaluar la toxicidad de combustibles derivados del petróleo, diesel y gasolina, mediante bioensayos con plantas.
- Seleccionar cepas bacterianas con capacidad de degradación de diesel y de promoción del crecimiento vegetal para su aplicación como inoculantes en técnicas de fitorremediación.
- Evaluar el efecto de la inoculación de *Lupinus luteus* con cepas bacterianas con capacidad de degradación de diesel y promoción del crecimiento vegetal, sobre el crecimiento de la planta y la disipación de hidrocarburos de diesel en suelos con distinto contenido en materia orgánica.

ESTUDIOS REALIZADOS Y PRINCIPALES RESULTADOS

Para la consecución de los objetivos planteados, durante el desarrollo de la tesis doctoral se llevaron a cabo los estudios que se describen a continuación, junto con los principales resultados.

Desarrollo y optimización del análisis de compuestos volátiles del petróleo (MTBE, ETBE y BTEX) e hidrocarburos de rango diesel (DRO) en matrices medioambientales (Capítulos 3 y 4)

En este trabajo se optimizaron los métodos de extracción y análisis cromatográfico de compuestos orgánicos volátiles (MTBE, ETBE y BTEX) e hidrocarburos de rango diesel (DRO) (capítulo 3 y 4, respectivamente). Para ello se utilizaron muestras de suelos con distinto contenido en materia orgánica y aguas, contaminadas de forma artificial con aquellos contaminantes. Para el

análisis de compuestos volátiles, se optimizaron métodos de "head-space" (HS) y "head-space solid phase microextraction" (HS-SPME), variando los principales parámetros de extracción: temperatura, tiempos de incubación, tamaño de muestra y velocidad de agitación. Para el análisis de DRO se optimizaron las condiciones de extracción por fluidos presurizados (ASE) y HS-SPME para muestras de suelos, y de ultrasonidos (US) y HS-SPME para muestras de agua. Para ASE se testaron diferentes temperaturas y ciclos de extracción; y para US, se probaron diferentes tiempos, disolventes y ratios muestra/disolvente. En el caso de HS-SPME, la optimización fue similar a la extracción de volátiles. Además, se optimizaron los parámetros de los métodos de análisis por cromatografía de gases acoplada a espectrometría de masas (GC/MS): rampas de temperatura de columna, flujo de split, temperatura del inyector, etc.

Las condiciones óptimas de extracción para el análisis de contaminantes derivados del petróleo en muestras ambientales dependían del tipo de compuestos, la matriz y la concentración. La extracción de compuestos volátiles de muestras de suelo y agua con HS (80°C, 15 min, 500 rpm) es la adecuada cuando la concentración sea relativamente alta (del orden de mg Kg^{-1} ó mg L^{-1}). En el mismo rango de concentraciones, los métodos óptimos de extracción de DRO en muestras de suelo y aguas eran, respectivamente, ASE (100 °C, hexano y 2 ciclos de extracción), y US (1 h, hexano, 1:2 muestra/disolvente). HS-SPME (80°C, 30 min, 500 rpm para volátiles; 90°C, 30 min, 500 rpm, para DRO) resultó ser un método más sensible (límites de detección más bajos), y por ello adecuado para muestras con baja concentración de ambos grupos de compuestos (del orden de µg Kg^{-1} ó µg L^{-1}). Para el análisis de suelos resultaba esencial la adición de patrones internos a la muestra ("surrogate") para la corrección del efecto matriz, especialmente en suelos con materia orgánica que adsorbían fuertemente los contaminantes.

Caracterización e identificación de las fuentes de contaminación del suelo y el agua en el entorno de una gasolinera en Galicia (Capítulo 5)

Se caracterizó la contaminación originada en el entorno de una gasolinera de Tomiño (Pontevedra, España). Para ello se tomaron muestras de suelo, a diferentes profundidades, y de agua subterránea, en las que se analizaron compuestos volátiles (MTBE, ETBE y BTEX) y DRO mediante los métodos anteriormente optimizados.

Los resultados obtenidos permitieron identificar dónde tenía lugar la contaminación (suelos superficiales, subsuperficiales, o agua subterránea), así como el tipo de contaminante y la edad de los vertidos (Alimi *et al.*, 2003). Los datos analíticos y los índices de "fingerprinting" indicaban que el foco de contaminación era una fuga de combustibles de los tanques de almacenamiento subterráneo. Esto contaminó los suelos cercanos, y de ahí los contaminantes migraron a los suelos circundantes y al agua subterránea por lixiviación. Los datos revelaron altas concentraciones de MTBE en agua, no detectado en los combustibles actuales, indicando una antigüedad del vertido de más de 10 años y constatando la elevada persistencia de este contaminante en el medio acuoso. La alta presencia de volátiles en el agua, que sólo aparecen en vertidos relativamente recientes, indicaba, además, la continuidad del vertido.

Estudio de la adsorción de compuestos volátiles derivados del petróleo en diferentes suelos y componentes del suelo mediante una aproximación HS (Capítulo 6)

Se utilizó la mayor limitación del análisis HS, el efecto matriz (Rosell *et al.*, 2006), para caracterizar comparativamente la adsorción ejercida por diferentes suelos (horizontes A un Andosol y un Podzol y horizontes B de un Ferralsol y un Cambisol), y componentes del suelo (ácido húmico, montmorillonita, caolinita y

goetita). Además, se ensayaron varias temperaturas de extracción para estudiar el efecto de la misma sobre la desorción de los compuestos, y como base para la remediación mediante extracción por vapor (SVE).

Los ensayos de desorción en HS constataron que la presencia de materia orgánica resulta clave en la adsorción de MTBE, ETBE y BTEX en el suelo, siendo además más rápida que la adsorción sobre los componentes minerales del suelo. Altas temperaturas fueron necesarias para la obtención de recuperaciones significativas, especialmente de los compuestos BTEX. Los componentes minerales del suelo ejercieron una fuerza de adsorción más débil, obteniéndose incluso altas recuperaciones a bajas temperaturas de extracción. Los resultados indicaron que la remediación de suelos contaminados con MTBE, ETBE y BTEX, mediante extracción de vapor (SVE), a baja temperatura, podría ser exitosa en suelos con baja concentración de materia orgánica. En presencia de materia orgánica, la combinación de SVE a baja temperatura con bioremediación sería la alternativa más adecuada.

Influencia de los exudados radiculares en la movilidad de compuestos volátiles derivados del fuel en suelos contaminados (Capítulo 7)

Se utilizó el análisis HS, sin corrección de matriz, para estudiar de forma comparativa, el efecto de los exudados radiculares sobre los procesos de adsorción-desorción de compuestos volátiles en el suelo (Zhu *et al.*, 2009), y por lo tanto, sobre la movilidad de los mismos. Para ello, se utilizaron muestras de suelo (horizonte A de un Cambisol úmbrico) y componentes coloidales del suelo (ácido húmico y montmorillonita) contaminadas artificialmente con MTBE, ETBE y BTEX. A estas muestras se añadieron disoluciones de: a) exudados naturales extraídos de *Holcus lanatus* y *Cytisus striatus,* b) exudados artificiales elaborados a partir de la disolución de 10 de los componentes más frecuentes de los exudados

de las raíces vegetales (ácidos carboxílicos y compuestos fenólicos) y c) cada unos de estos compuestos separadamente con distintas concentraciones.

En general, los exudados radiculares de *Holcus lanatus* y *Cytusis striatus* disminuyeron la movilidad de MTBE, ETBE y BTEX, excepto en presencia de una alta cantidad de materia orgánica (ácido húmico), donde aumentaron la solubilidad de la misma y, por ello, la de los compuestos adsorbidos a ella. Los componentes individuales tuvieron diferentes efectos en función de sus propiedades: los compuestos fenólicos se comportaron como los exudados naturales, mientras que los compuestos carboxílicos, tanto en presencia como ausencia de materia orgánica, aumentaron la movilidad de los contaminantes.

Fitotoxicidad de suelos contaminados con gasolina y diesel: Influencia del suelo, tipo de combustible y tolerancia de la planta (Capítulo 8)

En base al bioensayo con plantas definido por la OECD (Organization for Economic Cooperation and Development) (OECD, 2006), se evaluó la toxicidad de muestras suelo con diferentes propiedades (obtenidas de horizontes A y B de un Cambisol úmbrico) contaminados con diesel y gasolina en diferentes concentraciones (0, 1.25, 2.5, 5 y 10 %, *p/p*). Se utilizaron una gran variedad de plantas (*Zea mays* L., *Avena sativa* L., *Trifolium repens* L., *Pisum sativum* L., *Brassica oleracea* L., *Lactuca sativa* L.) y se evaluó el efecto de los contaminantes sobre su germinación, supervivencia y desarrollo temprano.

Los bioensayos con planta indicaban una elevada fitotoxicidad del diesel, especialmente acusada en ausencia de materia orgánica del suelo y una baja fitotoxicidad de la gasolina, lo que se relacionaba con su menor tiempo de vida medio en el suelo. Las plantas con las semillas más pequeñas (*Brassica oleracea*, *Trifolium repens* y *Lactuca sativa*) fueron aquellas con el menor índice de germinación (EC_{50} entre 1.25 y 2.5%), reflejando que la dureza del recubrimiento y reservas nutritivas de la semilla eran factores clave en la supervivencia y

desarrollo de las plantas en suelos contaminados con fuel. Los combustibles afectaron al desarrollo de la raíz en mayor medida que al del tallo, y a la biomasa más que a la elongación, reflejando el efecto negativo de los contaminantes sobre la ramificación de la raíz. *Brassica oleracea* y *Trifolium repens* fueron las especies más sensibles, pudiendo ser utilizadas como bioindicadores de contaminación.

Caracterización y potencial degradador de cepas bacterianas degradadoras de diesel para su aplicación en la descontaminación de suelos (Capítulo 9)

Una colección de cepas bacterianas aisladas de un suelo con contaminación real por diesel (aisladas y cedidas por el Centre for Environmental Sciences, University of Hasselt) fueron sometidas a diferentes protocolos de detección de las principales propiedades de interés en procesos de bio- y fitorremediación: producción de biosurfactantes (Bordoloi and Konwar, 2009), formación de biofilm (Singh *et al.*, 2006), y tolerancia a disolventes orgánicos. Un número reducido de cepas con resultado positivo en el protocolo de degradación de diesel (Protocolo TCPIP) (Kubota *et al.*, 2008), se utilizaron para cuantificar su potencial degradador. Para ello se cultivaron en un medio mínimo con diesel como única fuente de carbono, y se analizó periódicamente la concentración de los hidrocarburos de rango diesel (DRO) durante la incubación.

Tres bacterias degradadoras aisladas de suelos contaminados con diesel fueron las que obtuvieron los mejores resultados en producción de biosurfactantes, formación de biofilm y tolerancia a disolventes orgánicos, propiedades importantes para su aplicación a la remediación de suelos contaminados. Las bacterias 5 y 12 degradaron entre el 15 y el 25% de los DRO presentes en el medio líquido tras 10 días de incubación. La cepa 26, llegó a tasas mucho más altas, del orden del 90% del total de DRO, resultando en una clara

candidata para su aplicación en suelos contaminados con diesel, en procesos de rizodegradación.

Mejora de la degradación de diesel en la rizosfera de *Lupinus luteus* tras la inoculación con cepas bacterianas degradadoras de diesel y PGP (Capítulo 10)

Se realizó un ensayo en maceta utilizando como sustrato suelo de los horizontes A o B de un Cambisol úmbrico, sin contaminar y contaminados con 1.25-1.5% de diesel (*p*/*p*). Los suelos fueron plantados con *Lupinus luteus* L. e inoculados con una cepa bacteriana con capacidad de degradación (seleccionada a partir del trabajo descrito anteriormente) y/o un consorcio de cepas con capacidad de promoción del crecimiento vegetal (PGP) (seleccionado a partir de ensayos previos en perlita). Como control se utilizaron plantas sin inocular. Se realizaron dos inoculaciones, a tiempo 0 y 14 días, y se tomaron muestras de suelo a tiempo 0, 14 y 30 días. Se analizó la cantidad total de DRO en suelo mediante extracción con ASE, así como la cantidad fácilmente disponible y lixiviable, con una extracción en agua (agitación 24h y extracción con US). Tras la cosecha, se determinó la elongación de raíz y tallo de las plantas, así como su biomasa, además de la actividad microbiológica del suelo.

La inoculación de *Lupinus luteus* con un consorcio bacteriano formado por la cepa degradadora y dos cepas PGP inducía una disipación de hidrocarburos de rango diesel (DRO) superior al 50% tras 30 días (un 15-20% mayor que la disipación en suelos no inoculados), en suelos con una contaminación moderada (1.25-1.5%, *p*/*p*), y con un contenido en carbono orgánico de 42.6 g C Kg^{-1} (horizonte A úmbrico). En ausencia de materia orgánica del suelo (horizonte B), los mejores resultados se obtuvieron con la inoculación de la cepa degradadora sola: un 10% más de DRO fue eliminado, con respecto a suelos no inoculados.

CONCLUSIONES

De forma general se puede concluir que:

- Los métodos de extracción y análisis de contaminantes del petróleo desarrollados en este estudio son fiables, sensibles y robustos. Sirvieron de base para el resto estudios realizados en esta tesis y son adecuados para su aplicación en episodios de contaminación real.
- Los datos analíticos y de "fingerprinting" permitieron identificar, caracterizar y datar la contaminación por hidrocarburos alrededor de una gasolinera en Tomiño (Pontevedra, España).
- El uso de HS sin corrección de matriz es un método simple, rápido y limpio que permite evaluar la adsorción/desorción de compuestos volátiles (MTBE, ETBE y BTEX) en el suelo en una gran variedad de escenarios. La materia orgánica es el componente más importante del suelo en la absorción de BTEX y determina la temperatura de desorción. Los resultados aportan información de gran utilidad para la planificación de medidas de descontaminación.
- Los exudados radiculares modifican de forma significativa la movilidad de compuestos volátiles del fuel (MTBE, ETBE y BTEX) en el suelo. Este efecto depende del contenido en materia orgánica del suelo, y de la composición de los exudados, por lo que será específico de cada sistema suelo-planta particular y puede variar a lo largo del crecimiento vegetal.
- Los carburantes más comunes, gasolina y diesel, son fitotóxicos y afectan especialmente al desarrollo de la raíz. El alcance de este efecto depende de la especie vegetal, las características del suelo y el combustible. Ya que en un proceso de fitorremediación la descontaminación se produce en el entorno radicular, es necesario seleccionar plantas tolerantes en cada

situación particular y sería útil mejorar su crecimiento a través de su inoculación con bacterias PGP.

- La combinación de *Lupinus luteus* con cepas bacterianas degradadoras del diesel y/o PGP es una asociación prometedora en la rizodegradación inducida de hidrocarburos del diesel. Exudados radiculares y biosurfactantes bacterianos juegan un papel clave en el proceso.

En conclusión, la presente tesis ayuda a entender en comportamiento de las fracciones más móviles del fuel (compuestos oxigenados y monoaromáticos) en el suelo y avanza en el desarrollo de un procedimiento efectivo de rizodegradación de diesel (una fracción menos lábil) en suelos contaminados.

REFERENCIAS

Al-Mutairi N, Bufarsan A, Al-Rukaibi F. 2008. Ecorisk evaluation and treatability potential of soils contaminated with petroleum hydrocarbon-based fuels. Chemosphere 74:142-148.

Alimi H, Ertel T, Schug B. 2003. Fingerprinting of Hydrocarbon Fuel Contaminants: Literature Review. Environ Forensics 4:25-38.

Asquith EA, Geary PM, Nolan AL, Evans CA. 2012. Comparative bioremediation of petroleum hydrocarbon-contaminated soil by biostimulation, bioaugmentation and surfactant addition. J Environ Sci Eng A 1:637-650.

Bordoloi NK, Konwar BK. 2009. Bacterial biosurfactant in enhancing solubility and metabolism of petroleum hydrocarbons. J Hazard Mater 170:495-505.

Drozdova S, Rosenberg E. 2013. Petroleum: Hydrocarbon Contamination, In: Jorgensen SE (ed.). Encyclopedia of Environmental Management. CRC Press, Taylor & Francis group, Abingdon.

Fine P, Graber ER, Yaron B. 1997. Soil interactions with petroleum hydrocarbons: Abiotic processes. Soil Technol 10:133-153.

Hasset JJ, Banwart WL.1992. Soils and their environment. Prentice Hall Inc., Englewood Cliffs.

Hentati O, Lachhab R, Ayadi M, Ksibi M. 2013. Toxicity assessment for petroleum-contaminated soil using terrestrial invertebrates and plant bioassays. Environ Monit Assess 185:2989-2998.

Kubota K, Koma D, Matsumiya Y, Chung S, Kubo M. 2008. Phylogenetic analysis of long-chain hydrocarbon-degrading bacteria and evaluation of their

hydrocarbon-degradation by the 2,6-DCPIP assay. Biodegradation 19:749-757.

Kuiper I, Lagendijk EL, Bloemberg GV, Lugtenberg BJJ. 2004. Rhizoremediation: A beneficial plant-microbe interaction. Mol Plant-Microbe Interact 17:6-15.

MacKinnon G, Duncan HJ. 2013. Phytotoxicity of branched cyclohexanes found in the volatile fraction of diesel fuel on germination of selected grass species. Chemosphere 90:952-957.

Organization for Economic Cooperation and Development (OECD). 2006. Guidelines for the Testing of Chemicals. Test 208: Terrestrial plant test. Seedling emergence and seedling growth test.

Panagos P, Van Liedekerke M, Yigini Y, Montanarella L. 2013. Contaminated sites in Europe: Review of the current situation based on data collected through a European Network. J Environ Public Health 2013:1-11.

Pitz WJ, Mueller CJ. 2011. Recent progress in the development of diesel surrogate fuels. Prog Energ Combust Sci 37:330-350.

Rosell M, Lacorte S, Barceló D. 2006. Simultaneous determination of methyl tert-butyl ether, its degradation products and other gasoline additives in soil samples by closed-system-purge-and-trap gas chromatography-mass spectrometry. J Chromatogr A 1132:28-38.

Serrano A, Gallego M. 2006. Sorption study of 25 volatile organic compounds in several Mediterranean soils using headspace–gas chromatography–mass spectrometry. J Chromatogr A 1118:261-270.

Singh R, Paul D, Jain RK. 2006. Biofilms: implications in bioremediation. Trends Microbiol 14:389-397.

Xiao J, Wu L, Wu Y, Liu B, Dai L, Li Z, Xia Q, Xi H. 2014. Effect of gasoline composition on oxidative desulfurization using a phosphotungstic acid/activated carbon catalyst with hydrogen peroxide. Appl Energy 113:78-85.

Wenzel W. 2009. Rhizosphere processes and management in plant-assisted bioremediation (phytoremediation) of soils. Plant Soil 321:385-408.

Zhu Y, Zhang S, Huang H, Wen B. 2009. Effects of maize root exudates and organic acids on the desorption of phenanthrene from soils. J Environ Sci 21:920-926.

USC
UNIVERSIDADE
DE SANTIAGO
DE COMPOSTELA

USC
UNIVERSIDADE
DE SANTIAGO
DE COMPOSTELA

USC
UNIVERSIDADE
DE SANTIAGO
DE COMPOSTELA

1

Introduction

SOIL ENVIRONMENT AND ITS CONTAMINATION

Soil is a dynamic, living system that constitute a vital part of the environment. It is an interphase among atmosphere, lithosphere, and hydrosphere, and provides a base for life, conforming a part of the biosphere (White, 2013). Soil is also a support for all human activities: food production, forestry, agriculture or mineral extraction are some of the life-supported activities that depend on soils (Yong *et al.*, 2012). Soil is considered a non-renewable resource at human scale, due to its slow regeneration rate. Therefore, it is very important to understand the soil environment composition and its processes to prevent it from degradation.

Soil is three-dimensional system comprised of solids (minerals and organic matter, 45 and 5%, respectively), liquid (soil water, about 25%) and gases (soil air,

about 25%) (Mirsal, 2008). The organization of soil solid phase forms a complex pore matrix which allows the residence and circulation of water and air and creates a favourable habitat for soil organisms. The soil solid phase is mainly composed aluminosilicates, oxides and organic matter. One of the most important components are minerals of colloidal size (<2μm), including clays (kaolinite, montmorillonite, vermiculite, chlorite); oxides (of iron hematite, maghemite, ferrihydrite); hydroxides (of aluminium, gibbsite); and oxihydroxides (of iron, goethite) (Evangelou, 1998). These minerals have high surface areas, depending both on internal and external surfaces and on their crystallinity. The surface charges (either positive or negative), due to surface functional edge groups and isomorphic substitutions, make them good sorbents for ions (Sparks, 2003). Soil organic matter (SOM) consists of plant and animal residues at various stages of decomposition, and substances synthesized by soil organisms. Humus is the major component of soil organic matter (Gerrard, 2000). SOM contributes to plant growth through its effects on chemical, biological and physical properties of soil: it supplies nutrients (N, P and S), serves as energy source for soil microorganisms, and promotes soil structure, aeration and moisture retention. On the other hand, the high porosity and cation exchange capacity of SOM make it a good sorbent for contaminants, either inorganic and organic (Bohn *et al.*, 2001).

Chemical pollution of soils is one of the most important environmental problems concerning soil ecosystems, and the most spread pollutants are phosphorous and nitrogen fertilizers, heavy metals (lead, cadmium, chromium, cobalt, copper, mercury, nickel, zinc, etc.), pesticides, polycyclic aromatic hydrocarbons (PAH), polychlorinated biphenyls (PCB), or petroleum hydrocarbons (Mirsal, 2008). Panagos *et al.* (2013), from European Commission Joint Research Centre, reviewed the European contaminated sites, based on data collected through an European network, under the European Union (EU)

Thematic Strategy for Soil Protection. According to 2011-2012 data from 33 EU countries, there are more than 1 million of potentially contaminated sites, but only 58,000 were remediated. The sectors which contributed most to soil contamination were (i) waste disposal (municipal and industrial) (37.2%); (ii) industrial and commercial activities (mining, oil extraction and production, and power plants) (33.3%); (iii) storages (oil storage, obsolete chemicals storage, and other storages) (10.5%); (iv) transport spills on land (oil spill sites and other hazardous substance spills sites) (7.9%); (v) military (military sites and war affected zones) (3.4%); (vi) nuclear (0.1%); and (vii) other sources (7.9%). The distribution of the contaminants affecting soil is similar to that of groundwater (Panagos *et al.*, 2013). The main contaminant categories are heavy metals and mineral oil contributing jointly to around 60% of soil contamination and 53% of groundwater contamination (Figure 1.1).

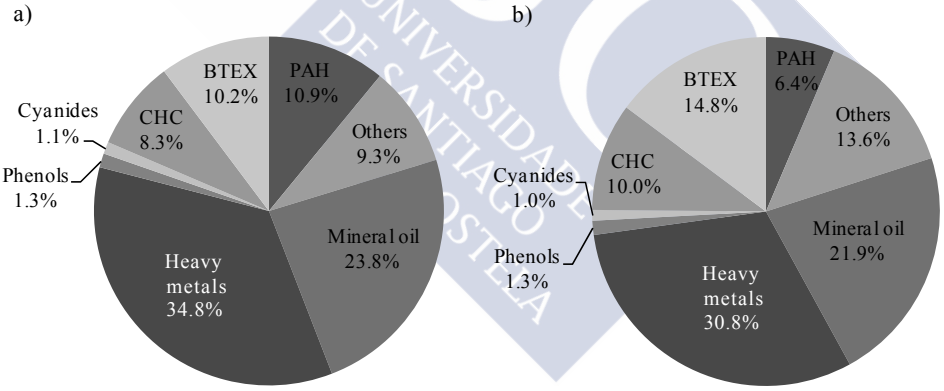

Figure 1.1. Distribution of contaminants affecting soil (a) and groundwater (b) in Europe (2011-2012 data) (*CHC: chlorinated hydrocarbons*) (from Panagos *et al.*, 2013).

Spanish law on contaminated soils (Real Decreto 9/2005), established a list of potentially soil-contaminating activities and limit concentrations above which a soil is considered contaminated and should be cleaned. The contaminants included are principally organics, as pesticides, BTEX, PAH, phenols and several

organic solvents. Levels for heavy metals are established by regional governments. In Galicia (NW Spain), Decreto 60/2009, established the maximum contamination concentrations of trace elements, based on background levels due to Galician geological substrate (Macías y Calvo de Anta, 2009).

When soil is contaminated by a chemical, the extent to which it will be distributed among the soil phases (solids, water and gas) depends on the characteristics of the contaminant and the soil, in addition to environmental factors as topography, humidity, solar radiation, climate conditions and other biosphere characteristics. Knowing the association of the contaminant with the different phases will determine its fate in the soil environment. Sorption or retention is a major process influencing the transport of contaminants in soils (Tarradellas *et al.*, 1997). Soil can retain substances by several mechanisms. Cation exchange at negatively charged sites is the major retention mechanism for some inorganic cations. The retention of some polar or induced-polar organics can also be governed by the same mechanisms. In case of low-polarity organic chemicals, in general, the predominant sorbent is the organic matter associated with soils. "Like dissolves like" rule can be used to explain sorption of chemicals by soil particles (Goss and Schwarzenbach, 2003).

PETROLEUM PRODUCTS AND THEIR IMPACTS

Petroleum or crude oil is a thick, dark brown inflammable liquid formed by the anaerobic decay of organic matter in conditions of increased temperature and pressure in enclosing sedimentary rocks. Petroleum is extracted from reservoirs, and refined by distillation. The refined products include kerosene, benzene, gasoline, diesel fuel, paraffin wax, asphalt, etc. The lightest hydrocarbons are all gases, and are used as fuel (methane, ethane, propane and butane). The carbon range from C_6 to C_{10} is normally used in gasoline, C_{10}-C_{15} in kerosene and C_{10}-C_{25} in diesel fuel. Higher carbon numbers form paraffin wax,

tar, or asphaltic bitumen (van der Perk, 2006) (Figure 1.2). Compounds of crude oil can be divided into three general classes consisting of saturated hydrocarbons (chain alkanes and cycloalkanes), aromatic hydrocarbons, and polar organic compounds (Riser-Roberts, 1998). These fuel hydrocarbons are usually characterized using three fractions: gasoline range organics (GRO, including aromatics and aliphatics of C_6 to C_{10} range); diesel range organics (DRO, including aromatics and aliphatics of C_{10} to C_{25} range); and residual range organics (RRO, including aromatics and aliphatics of C_{25} to C_{35} range). Chain alkanes represent more than 65% of the total volume of gasoline and diesel (Riser-Roberts, 1998).

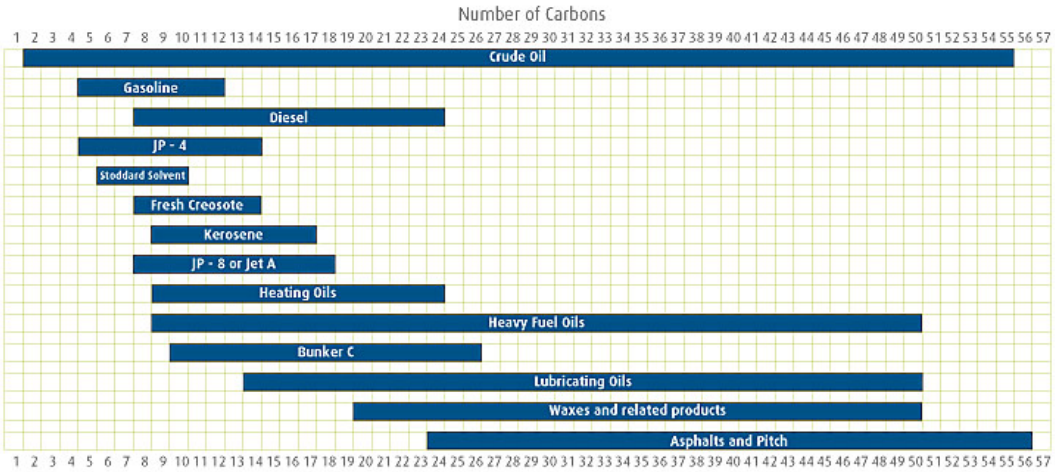

Figure 1.2. Petroleum hydrocarbon ranges in refined products (from: http://www.caslab.com/Petroleum-Hydrocarbon-Ranges/)

Monocyclic aromatic hydrocarbons are compounds consisting of carbon and hydrogen and containing one benzene ring. The most common monocyclic aromatic hydrocarbons are benzene, toluene, ethylbenzene and xylene isomers (*ortho*-, *meta*- and *para*-xylene), which are commonly known as BTEX. BTEX can make up a significant percentage of petroleum products, i.e. about 18% (*w*/*w*) of standard gasoline are BTEX compounds. They are normally used as solvents for

paints, rubber, or leather industries, and for the production of plastics, ink or nylon (van der Perk, 2006). Some of their physicochemical properties are detailed in Appendix A.

BTEX are among the most hazardous constituents of fuel. Indeed, benzene, toluene and ethylbenzene are included in the List of Priority Pollutants of the United States Environmental Protection Agency (USEPA). Acute exposures to high levels of BTEX may cause irritation of the skin, eyes, and respiratory tract, and depression of the central nervous system. Chronic inhalation or contaminated water consumption can cause adverse effects to the liver, kidneys, heart, lungs, and central nervous system. Benzene is the most dangerous of BTEX and is carcinogenic to humans (van der Perk, 2006).

Other volatile components of fuel, principally of gasoline, are oxygenate ethers, commonly known as fuel oxygenates (FO), including principally, methyl *tert*-butyl ether (MTBE) and ethyl *tert*-butyl ether (ETBE) (Appendix A). The use of FO as octane enhancers in gasoline started in the early 2000s, when the Fuel Quality European Directive 98/70/EC required all EU countries to use completely lead free gasoline. The use of MTBE was questioned in many countries since it is a carcinogen. Furthermore, it caused several contamination episodes of aquifers and wells, due to its high mobility (Appendix A) but poor degradation rates (high persistency), especially under anaerobic conditions (Atienza *et al.*, 2005). In EU, European Renewable Energy Directive (2009/28/EC) and Fuel Quality Directive (2009/30/EC) encouraged the use of bio-components (synthesised from agricultural feedstocks), such as ETBE and ethanol in gasoline, and limited the use of MTBE as a fuel oxygenate.

Diesel range organics (DRO) is a widely spread term to only refer to the range of saturated *n*-alkanes present in diesel (C_{10}-C_{25}), which is the major fraction and the most commonly analyzed, together with PAH. They are not of such environmental or human hazard concern as aromatic contaminants, but

they are usually analyzed as a marker for the presence of a spilled oil, for the identification of the product type, or for monitoring chemical composition changes due to weathering and/or biodegradation (Wang and Fingas, 1997). Some of their physicochemical properties are detailed in Appendix B.

ENVIRONMENTAL FATE OF PETROLEUM CONTAMINANTS

Environmental pollution by petroleum products may occur during extraction, refinement, transport, storage and use. Spills and leaks are the principal causes of oil pollution of soil, groundwater, and surface water, and involve a threat to soil and water quality, plant and animal life, and human health (van der Perk, 2006). Most spills take place on marine environment, by tanker spills, and on land, including oil spills from pipelines, underground storage tanks, and aboveground storage containers (Wang *et al.*, 2006).

ITOPF (International Tankers Owners Pollution Federation Limited) reported in its Oil tanker spill statistics of 2013, more than 800 spills from 1970, with more than 5.74 million tonnes of oil released in the marine environment. However, the volume spilt improved through the decades; i.e. 386,000 tonnes were spilt in 1970, while only 7,000 were spilt in 2013. CONCAWE (Conservation of Clean Air and Water in Europe) reported 457 spills in oil pipelines from 1971 to 2012, which released more than 80,000 m^3 of oil, and contaminated more than 100,000 m^2 of land per year.

The environmental fate and behaviour of soil spilled oil, depends on a wide variety of natural processes known as weathering, including volatilization, biodegradation, photodecomposition, chemical oxidation, bioaccumulation, plant detoxication, dispersion, diffusion, binding to soil (sorption) and leaching to groundwater (Asquith *et al.*, 2012) (Figure 1.3). These processes can be divided in two groups: transfer processes (that relocate the contaminant without altering

their structure) and degradation processes (that alter the chemical structure) (Pierzynsky *et al.*, 2005).

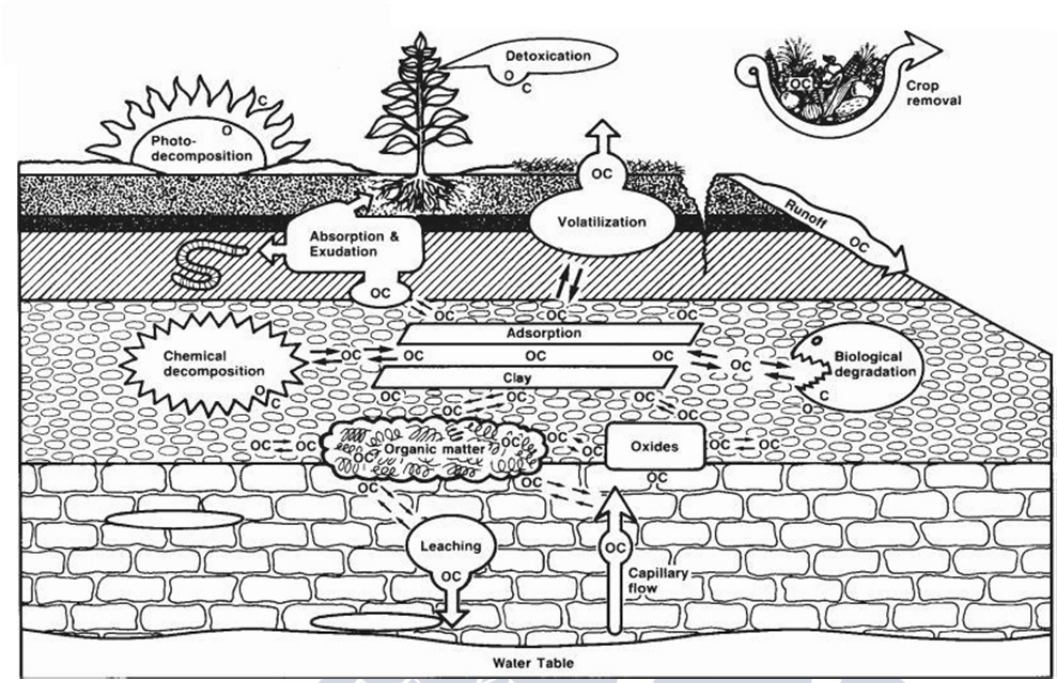

Figure 1.3. Processes and fate of organic contaminants (OC) in the soil environment (from Webber and Miller, 1989).

i. **Leaching:** is the lateral or downward migration of soil contaminants to groundwater reservoirs. Water solubility of hydrocarbons and its octanol-water partition coefficient (K_{ow}), can be used to predict the leachability of contaminants from soil to groundwater. Furthermore, the porosity, SOM content, or texture of soil, apart from rainfall or irrigation intensity will highly influence on the leaching potential of petroleum hydrocarbons.

ii. **Volatilization:** is the migration of contaminants from soil and water to the atmosphere. The solubility and vapour pressure of the contaminants as well as sorption-desorption processes, and soil characteristics (porosity, texture, SOM content, etc.) are factors influencing the

volatilization of petroleum hydrocarbons from soils. For example, fuel volatile compounds such as BTEX and fuel oxygenates (FO), due to their high vapour pressure and water solubility (Appendix A), tend to rapidly migrate into the atmosphere or leach into groundwater. BTEX can be sorbed on soil particles, but not so strongly as other fuel components, such as aliphatic hydrocarbons.

iii. **Degradation**: is the breakdown of the molecules due to sunlight (photochemical degradation), hydrolysis or redox reactions (chemical degradation), and/or microorganisms metabolism (microbial degradation).

iv. **Sorption**: is the most important factor affecting the fate of organic contaminants, and involves the interaction between the contaminant and the soil mineral and organic matter through one or more of the following interactions: H-bonding, dipole-dipole interactions, ion-exchange, covalent bonding, protonation, ligand exchange, cation bridging, water bridging, and/or hydrophobic partitioning (Pierzynsky *et al.*, 2005). The organic carbon partition coefficient (K_{oc}), which describes the distribution of the contaminant between aqueous and organic matter phases, is usually used to predict the sorption of petroleum hydrocarbons in soils. Sorption of petroleum hydrocarbons, can substantially reduce its mobility, and therefore its biodegradability, bioavailability, leachability, and volatility.

All the described weathering processes can alter the composition of spilled oil, modifying its toxicity, and can also provoke the contamination of other environmental compartments. Thus, soil contamination with petroleum products involves important environmental and health risks, giving huge importance to the development of tools for assessing those risks and to the application of effective clean-up technologies (Wang *et al.*, 2006).

REMEDIATION OF PETROLEUM CONTAMINATED SOILS

Soil is a very slowly renewable natural resource and it is important that our use of soil does not lessen its value to future generations or irreversibly alter its value for other purposes (Hasset and Banwart, 1992).

The soil system itself is sometimes capable of recovering its functions and diversity through natural processes (chemical, physical and biological) in a reasonable amount of time. This is called natural attenuation. Although natural attenuation may be used at numerous sites, it is rarely used as a sole treatment, since it is a very slow process. When contamination levels are very high, contaminants can inhibit the biological activity and therefore persist in the soil environment, with the intrinsic risks for other environmental compartments, such as aquatic systems (Mulligan and Yong, 2004). In these cases, soil remediation techniques are essential.

Soil remediation technologies are processes or methods for treating contaminants in soil by containing, removing, degrading, or transforming pollutants in less harmful forms. The most common technologies for the remediation of soils contaminated with organic compounds are summarized in Table 1.1.

Conventional remediation methods are based on removal or containment, an often present high costs and environmental risks, due to soil excavation and removal, application of chemicals, such as solvents or surfactants, application of hot water or air at high pressure, etc. These disadvantages encouraged researchers for developing "environmental-friendly" remediation technologies, cheaper and with less impact on the soil environment.

Table 1.1. Remediation techniques for soils contaminated with organic pollutants.

Remediation technique		Description	Target contaminants	References
Ex situ/ In situ	**Physicochemical stabilization**	Reducing the mobility of contaminants in the environment through both physical and chemical means: vitrification, asphalt batching.	Limited to low concentrations of organic contaminants.	Suthersan, 1997
	Thermal desorption	Heating soils to 100–600 °C to vaporize and separate from the soil those contaminants with boiling points in that range.	VOC, petroleum hydrocarbons, PAH, PCB, pesticides.	Roland *et al.*, 2010
	Bioremediation	Use of (micro)organisms to detoxify or remove soil pollutants owing to diverse metabolic capabilities.	Petroleum hydrocarbons, VOC, SVOC, PCB, PAH, chlorinated hydrocarbons, pesticides.	Megharaj *et al.*, 2011
Ex situ	**Landfarming**	Enhancing contaminant bioremediation by the addition of nutrients and water, aerating and mixing the soil.	Light petroleum hydrocarbons.	McCarthy *et al.*, 2004
	Biopiles	Piling contaminated soils and stimulating aerobic microbial activity by aeration and the addition of minerals, nutrients, and moisture.	Petroleum products, VOC, SVOC, pesticides.	Khan *et al.*, 2004
In situ	**Natural attenuation**	Use of natural processes to reduce the concentration and contain the spread of contamination from chemical spills.	VOC, chlorinated hydrocarbons, pesticides.	Mulligan and Yong, 2004
	Soil washing	Use of liquids (usually water, occasionally combined with solvents) and mechanical processes, to scrub soils.	SVOC, petroleum and fuel residuals, PCB, PAH, pesticides	Khan *et al.*, 2004
	Soil vapour extraction (SVE)	Application of vacuum to soil, producing an airflow that transports the contaminants in extraction wells.	VOC, SVOC.	Soares *et al.*, 2010
	Soil flushing	Flushing contaminated soils with an extracting solution that moves the contaminants to an area where they can be removed from soil by pumps.	VOC, SVOC, fuels, pesticides	Khan *et al.*, 2004
	Phytoremediation	Use of plants and associated microorganisms to clean up contaminated soils, by extracting, accumulating, and/or degrading the contaminants.	Chlorinated solvents, petroleum hydrocarbons, PCB, PAH, insecticides, explosives, biosurfactnts.	Vangronsveld *et al.*, 2009

VOC: volatile organic compounds; SVOC: semivolatile organic compounds.

In situ bioremediation of fuel contaminated soil is often chosen as remediation option because of the reduced soil disturbance, low maintenance, and overall low costs. Phytoremediation is defined as the use of green plants and its associated microorganisms to remove, contain or render harmless environmental substances (Chaney *et al.*, 1997; Kidd *et al.*, 2009; Pilon-Smits, 2004; Salt *et al.*, 1998; Schnoor *et al.*, 1995). This definition applies to all plant-influenced biological, chemical, and physical processes that aid in remediation of contaminated substrates (Schwab and Banks, 1999).

There are several processes which plants can use to remediate contaminated soils, divided in two groups: *containment processes*, such as phytostabilization; and *removal process*, such as phytoextraction, phytovolatilization, and phytodegradation (Wenzel *et al.*, 1999) (Figure 1.4):

i. **Phytostabilization:** is the use of plant-tolerant species to reduce mobilization of either organic and inorganic contaminants and limit their diffusion in soil, by incorporating them into the lignin of the cell wall of roots cells or into soil humus (Dary *et al.*, 2010).

ii. **Phytoextraction** (also phytoaccumulation, phytoabsorption or phytosequestration)**:** is mainly used for metal contaminants (Cd, Ni, Cu, Zn or Pb) and other elements (Se or As), and involves the absorption of soil contaminants by plant roots and their translocation and accumulation in the aerial biomass (Kidd and Monterroso, 2005).

iii. **Phytovolatilization:** relies on the ability of some plants to absorb, transform and volatilize certain contaminants, such as metals and metalloids (Favas *et al.*, 2014). Plants can also uptake volatile organic pollutants, such as BTEX (Boonsaner *et al.*, 2011), from soils and soil water, and translocate them to the atmosphere, via the transpiration stream. As found by Briggs *et al.* (1982), plant uptake and transpiration is

more efficient for organic contaminants with intermediate polarity (log K_{ow} between -1 and 5, and a maximum in 1.8).

iv. **Phytodegradation:** is the degradation of organic contaminants *in planta*, sometimes using endophytic degrading bacteria colonizing plant tissues, either in shoots and roots (Afzal *et al.*, 2014; Weyens *et al.*, 2009).

v. **Phytostimulation or rhizodegradation:** is based on the rhizosphere effect (Kaksonen *et al.*, 2006) of plant roots on promoting the proliferation of degrading rhizosphere microorganisms which utilize exudates, plant metabolites and the contaminants as a source of carbon and energy (Wojtera-Kwiczor *et al.*, 2014).

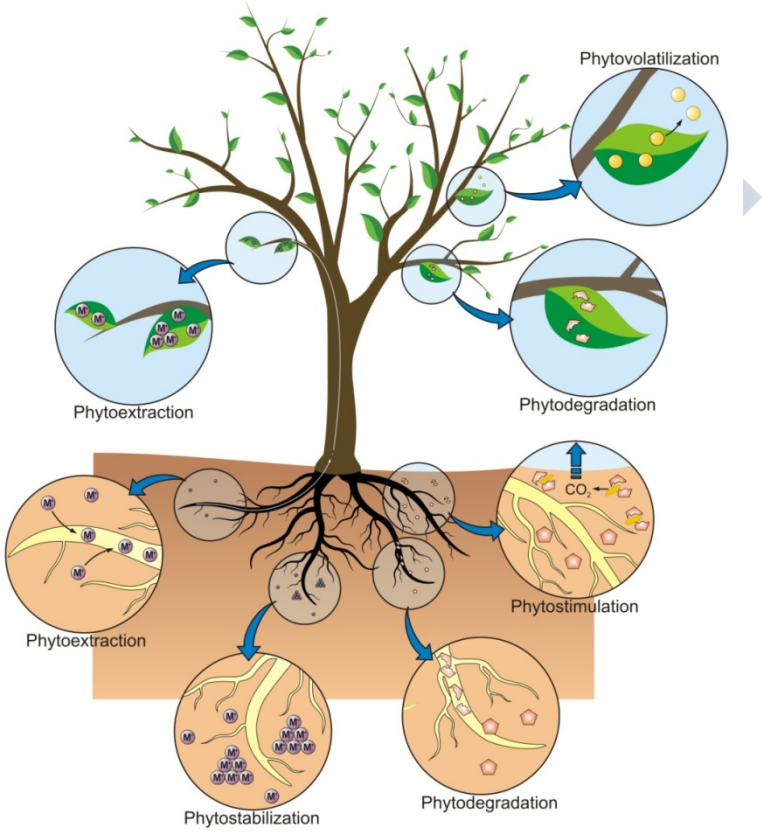

Figure 1.4. Schematic representation of the main phytoremediation processes (from Favas *al.*, 2014).

Phytoremediation (alone or in combination with other processes) is one of the most promising techniques for the remediation of petroleum products. It is usually carried out by rhizodegradation or rhizoremediation (degradation in the rhizosphere), taking advantage of synergic effects of the plant-bacteria association. Plants can enhance microbial biomass production by providing readily carbon sources, nutrients, oxygen and favourable redox conditions (Wang *et al.*, 2011). Furthermore, they can stimulate hydrocarbon degradation by secreting organic substances with similar chemical structures (Wojtera-Kwiczor *et al.*, 2014), and/or by increasing contaminant bioavailability (LeFevre *et al.*, 2013). In addition, plants further get benefits from their associated-bacteria possessing hydrocarbon-degradation potential, leading to enhanced hydrocarbon mineralization and lowering both the phytotoxicity and the evapotranspiration of volatile hydrocarbons. Bacteria with plant-growth promotion properties, can mitigate plant responses to stress, and enhance plant growth and development on contaminated substrates (Khan *et al.*, 2013).

The understanding of plant-bacteria and soil-plant-bacteria partnerships are very important to enhance soil rhizoremediation: the selection of appropriate plants and bacterial strains, which can symbiotically work, and the study of the characteristics of each contaminated site are essential to carry out a successful remediation of petroleum-contaminated soils.

REFERENCES

Afzal M, Khan QM, Sessitsch A. 2014. Endophytic bacteria: Prospects and applications for the phytoremediation of organic pollutants. Chemosphere 117:232-242.

Asquith EA, Geary PM, Nolan AL, Evans CA. 2012. Comparative bioremediation of petroleum hydrocarbon-contaminated soil by biostimulation, bioaugmentation and surfactant addition. J Environ Sci Eng A 1:637-650

Atienza J, Aragón P, Herrero MA, Puchades R, Maquieira Á. 2005. State of the art in the determination of MTBE in natural waters and soils. Crit Rev Anal Chem 35:317-337.

Bohn HL, McNeal BL, O'Connor GA. 2001. Soil Chemistry. John Wiley and Sons Inc., New York.

Boonsaner M, Borrirukwisitsak S, Boonsaner A. 2011. Phytoremediation of BTEX contaminated soil by *Canna×generalis*. Ecotoxicol Environ Saf 74:1700-1707.

Briggs GG, Bromilow RH, Evans AA. 1982. Relationships between lipophilicity and root uptake and translocation of non-ionised chemicals by barley. Pestic Sci 13:495-504.

Chaney RL, Malik M, Li YM, Brown SL, Brewer EP, Angle JS, Baker AJ. 1997. Phytoremediation of soil metals. Curr Opin Biotechnol 8:279-284.

Dary M, Chamber-Pérez MA, Palomares AJ, Pajuelo E. 2010. "In situ" phytostabilisation of heavy metal polluted soils using *Lupinus luteus* inoculated with metal resistant plant-growth promoting rhizobacteria. J Hazard Mater 177:323-330.

Evangelou VP. 1998. Environmental soil and water chemistry: Principles and applications. John Wiley & Sons Inc., New York.

Favas PJC, Pratas J, Varun M, D'Souza R, Paul MS. 2014. Phytoremediation of soils contaminated with metals and metalloids at mining areas: Potential of native flora. In: Hernandez Soriano MC (ed.). Environmental risk assessment of soil contamination. InTech Open access. http://www.intechopen.com/

Gerrard J. 2000. Fundamentals of soils. Routledge, London.

Goss KU, Schwarzenbach RP. 2003. Rules of thumb for assessing equilibrium partitioning of organic compounds: success and pitfalls. J Chem Educ 80:450-455.

Hasset JJ, Banwart WL. 1992. Soils and their environment. Prentice Hall Inc., Englewood Cliffs.

Kaksonen AH, Jussila MM, Lindström K, Suominen L. 2006. Rhizosphere effect of *Galega orientalis* in oil-contaminated soil. Soil Biol Biochem 38:817-827.

Khan FI, Husain T, Hejazi R. 2004. An overview and analysis of site remediation technologies. J Environ Manage 71:95-122.

Khan S, Afzal M, Iqbal S, Khan QM. 2013. Plant–bacteria partnerships for the remediation of hydrocarbon contaminated soils. Chemosphere 90:1317-1332.

Kidd P, Monterroso C. 2005. Metal extraction by *Alyssum serpyllifolium* sp. *lusitanicum* on mine-spoil soils from Spain. Sci Total Environ 336:1-11.

Kidd P, Barceló J, Bernal MP, Navari-Izzo F, Poschenrieder C, Shilev S, Clemente R, Monterroso C. 2009. Trace element behaviour at the root–soil interface: Implications in phytoremediation. Environ Exp Bot 67:243-259.

LeFevre GH, Hozalski RM, Novak PJ. 2013. Root exudate enhanced contaminant desorption: An abiotic contribution to the rhizosphere effect. Environ Sci Technol 47:11545-11553.

Macías F, Calvo de Anta R. 2009. Niveles genéricos de referencia de metales pesados y otros elementos traza en suelos de Galicia. Xunta de Galicia, Santiago de Compostela.

McCarthy K, Walker L, Vigoren L, Bartel J. 2004. Remediation of spilled petroleum hydrocarbons by in situ landfarming at an arctic site. Cold Reg Sci Technol 40:31-39.

Megharaj M, Ramakrishnan B, Venkateswarlu K, Sethunathan N, Naidu R. 2011. Bioremediation approaches for organic pollutants: A critical perspective. Environ Int 37:1362-1375.

Mirsal IA. 2008. Soil pollution: Origin, monitoring and remediation. Springer, Berlin.

Mulligan CN, Yong RN. 2004. Natural attenuation of contaminated soils. Environ Int 30:587-601.

Panagos P, Van Liedekerke M, Yigini Y, Montanarella L. 2013. Contaminated sites in Europe: Review of the current situation based on data collected through a European Network. J Environ Public Health 2013:1-11.

Pierzynski GM, Sims JT, Vance GF. 2005. Soils and environmental quality. CRC Press, Boca Raton.

Pilon-Smits E. 2004. Phytoremediation. Annu Rev Plant Biol 56:15-39.

Riser-Roberts E. 1998. Remediation of petroleum contaminated soils. Lewis Publishers, Boca Raton.

Roland U, Bergmann S, Holzer F, Kopinke F. 2010. Influence of *in situ* steam formation by radio frequency heating on thermodesorption of hydrocarbons from contaminated soil. Environ Sci Technol 44:9502-9508.

Salt DE, Smith RD, Raskin I. 1998. Phytoremediation. Annu Rev Plant Physiol Plant Mol Biol 49:643-668.

Schnoor J, Licht L, McCutcheon SC, Wolfe NL, Carreira LH. 1995. Phytoremediation of organic and nutrient contaminants. Environ Sci Technol 29:318-323.

Schwab P, Banks K. 1999. Phytoremediation of petroleum-contaminated soils. In: Adriano DC, Bollag JM, Frankenberger WT, Sims RC (eds.). Bioremediation of contaminated soils. American Society of Agronomy Inc., Madison.

Soares AA, Albergaria JT, Domingues VF, Alvim-Ferraz MdCM, Delerue-Matos C. 2010. Remediation of soils combining soil vapor extraction and bioremediation: Benzene. Chemosphere 80:823-828.

Sparks, DL. 2003. Environmental soil chemistry. Academic Press, San Diego.

Suthersan SS. 1997. Remediation engineering: Design concepts. Lewis Publishers, Boca Raton.

Tarradellas J, Bitton G, Rossel D (eds.). 1997. Soil ecotoxicology. CRC Press, Boca Raton.

van der Perck M. 2006. Soil and water contamination. Taylor & Francis Group, London.

Vangronsveld J, Herzig R, Weyens N, Boulet J, Adriaensen K, Ruttens A, Thewys T, Vassilev A, Meers E, Nehnevajova E, van der Lelie D, Mench M. 2009. Phytoremediation of contaminated soils and groundwater: lessons from the field. Environ Sci Pollut Res. 16:765-794.

Wang Z, Fingas M. 1997. Developments in the analysis of petroleum hydrocarbons in oils, petroleum products and oil-spill-related environmental samples by gas chromatography. J Chromatogr A 774:51-78.

Wang Z, Stout SA, Fingas M. 2006. Forensic fingerprinting of biomarkers for oil spill characterization and source identification. Environ Forensics 7:105-146.

Wang Z, Xu Y, Zhao J, Li F, Gao D, Xing B. 2011. Remediation of petroleum contaminated soils through composting and rhizosphere degradation. J Hazard Mater 190:677-685.

Webber JB, Miller CT. 1989. Reactions and movement of organic chemicals in soils. Soil Science Society of America, Madison.

Wenzel WW, Adriano DC, Salt D, Smith R. 1999. Phytoremediation: a plant-microbe-based remediation system. In: Adriano DC, Bollag JM, Frankenberger WT, Sims RC (eds.). Bioremediation of contaminated soils. American Society of Agronomy Inc., Madison.

Weyens N, van der Lelie D, Taghavi S, Vangronsveld J. 2009. Phytoremediation: plant–endophyte partnerships take the challenge. Curr Opin Biotechnol 20:248-254.

White RE. 2013. Principles and practice of soil science. The soil as a natural resource. Wiley Blackwell Publishing, Hoboken.

Wojtera-Kwiczor J, Żukowska W, Graj W, Małecka A, Piechalak A, Ciszewska L, Chrzanowski Ł, Lisiecki P, Komorowicz I, Barałkiewicz D, Voss I, Scheibe R, Tomaszewska B. 2014. Rhizoremediation of diesel-contaminated soil with two rapeseed varieties and petroleum degraders reveals different responses of the plant defense mechanisms. Int J Phytoremediation 16:770-789.

Yong RN, Nakano M, Pusch R. 2012. Environmental soil properties and behaviour. CRC Press, Taylor & Francis Group, Boca Raton.

USC
UNIVERSIDADE
DE SANTIAGO
DE COMPOSTELA

2

Objectives and scope

The contamination of soil with petroleum derived products is an environmental problem with a considerable concern, since it involves important risks for human health and for the ecosystems. Soil is a slowly renewable resource, and therefore, it is very important to understand its processes, study the behaviour and dynamics of the fuel contaminants in the soil system and develop effective remediation procedures to protect it from degradation.

A great number of literature and investigation studies have been yet developed in this field. However, processes governing the behaviour of fuel organic compounds in contaminated soils and the success of remediation procedures will depend on the particular properties of each soil system. Therefore, it is essential to perform specific research on every contaminated site under study.

Within this context, the aim of this thesis was to evaluate the behaviour of fuel organic compounds (volatiles, such as MTBE, ETBE and BTEX; and diesel range organics) released in the soil environment and to develop an appropriate remediation procedure by rhizodegradation, using the profits of plant-bacteria partnerships. Thus, it is very important to develop precise and sensitive analytical methods and to understand the environmental fate and behaviour of those contaminants and its toxicology, through studies at different scale (laboratory, greenhouse and field).

Accordingly, specific studies were carried out in order to achieve those objectives:

- Development and optimization of analytical methods for volatile compounds (MTBE, ETBE and BTEX) and diesel range organics (DRO) in environmental samples (soil and water).
- Application of those analytical methods to the characterization and fingerprinting of the hydrocarbon contamination sources around a fuel distribution station.
- Study of the behaviour of fuel volatile contaminants in soil (*in vitro*) through sorption studies and evaluation of the effect of plants on contaminant mobility in soils due to root exudation.
- Characterization of the phytotoxicity of petroleum derived fuels (gasoline and diesel) with crop plants bioassays.
- Selection of bacterial strains with diesel degrading potential and plant growth promoting characteristics for its application as inoculants in phytoremediation procedures.
- Evaluation of the effect of *Lupinus luteus* inoculation with diesel degrading and plant growth promoting bacterial strains on plant growth and on the enhancement of diesel dissipation from soils with different organic matter content.

3

Development and optimization of VOC analysis in environmental samples

The application of an effective and sensitive analytical method to determine soil contaminants is a crucial step in monitorization and remediation processes. In the present work, we optimized the analysis of volatile organic compounds (VOC) commonly present in fuel: oxygenates (FO -MTBE and ETBE-) and monoaromatic hydrocarbons such as benzene, toluene, ethylbenzene and xylene (BTEX). Headspace (HS) and headspace-solid phase microextraction (HS-SPME) were optimized in water samples, and validated for contaminated soils, using artificially spiked soils. Contaminants were identified and quantified by gas chromatography coupled to mass spectrometry (GC/MS). Matrix effect correction with surrogate standards resulted essential when analyzing soil samples, especially when the sample exerted a strong sorption on the contaminants.

This work was included in the publication:

Balseiro-Romero M, Monterroso C. 2014. Development and optimization of headspace (HS) and headspace-solid phase microextraction (HS-SPME) for the determination of fuel volatile compounds in soil. Retos y oportunidades en la ciencia del suelo (ISBN: 978-84-8408-769-4), pp. 129-132.

INTRODUCTION

Applying an appropriate and effective analytical method for the determination of fuel volatile organic compounds (VOC), (fuel oxygenates -FO- and BTEX) in environmental samples, is the basis for carrying out solid sorption, monitorization and/or remediation studies.

The most commonly used technique to analyze volatile compounds in soils is equilibrium headspace analysis (HS) coupled to gas chromatography/mass spectrometry (GC/MS) (Esteve-Turrillas *et al.*, 2007; García Pinto *et al.*, 2011; Pavón *et al.*, 2009). The HS procedure has the advantage that very little sample manipulation is required, which minimizes the loss of contaminant. Furthermore, this method saves an enormous amount of time, and does not use organic solvents, as other extraction techniques for organic contaminants. On the other hand, head space-solid phase microextraction (HS-SPME) has been also used for VOC analysis in diverse environmental matrices (Arambarri *et al.*, 2004; Ezquerro *et al.*, 2004; Llompart *et al.*, 1999). This technique was developed in the 90s by Prof. Pawliszyn research group (Arthur and Pawliszyn, 1990; Louch *et al.*, 1992; Zhang and Pawliszyn, 1993). This technique uses selective fibers, consisting of a fused silica rod covered with a polymeric coating. HS-SPME combines the advantages of HS extraction and the concentration in a single step (Zhang and Pawliszyn, 1993).

The principal limitation of HS and HS-SPME analysis is the matrix effect in solid samples; i.e. samples with different properties would exert dissimilar degrees of sorption, modifying the analytical recovery. This matrix effect can be minimized by using surrogates, compounds with similar properties to the analytes but rarely found in environmental samples. They should be spiked to the samples and standards in a constant concentration and stabilized for a proper

amount of time to be sorbed by the sample in a similar extent than analytes, so that this matrix effect can be corrected (Hiatt, 2010; Rosell *et al.*, 2006).

The aim of the present chapter was to optimize the extraction and analysis of fuel VOC (FO and BTEX) in water and soil samples, using HS and HS-SPME with GC/MS quantification.

MATERIALS AND METHODS

Reagents and standards

The following reagents were used: benzene (purity, 99.8 %; grade, PAI-ACS (UV-IR-94 HPLC-GPC)), toluene (purity, 99.8 %; grade, PAI-ACS (UV-IR-HPLC-GPC)), ethylbenzene (purity, 99 %; grade, PS), *o*-xylene (purity, 99 %; grade, PA (Reag.USP. Ph. Eur)), *m*-xylene (purity, 99 %; grade, PA (Reag. Ph. Eur)), *p*-xylene (purity, 99 %; grade, PA (Reag. USP)), MTBE (purity, 99,7 %; grade, PAI (PAR)) and ETBE (purity, 99 %; grade, PA (Reag. USP)). Fluorobenzene (purity, 99%) was used as surrogate. All reagents were purchased from Panreac Química, S.L.U., except fluorobenzene, purchased from Sigma-Aldrich Co, LLC. Standard solutions, one of FO and BTEX and another of fluorobenzene, were prepared in methanol (purity, 99.9%; grade, PAI (PAR)), with each of the reagents at a concentration of 100 mg L^{-1}. These solutions were used for the preparation of standards and for soil and water spiking.

Preparation of water and soil samples

Spiked distilled water standards of 500 µg L^{-1} of individual FO (MTBE and ETBE) and BTEX (benzene, toluene, ethylbenzene and xylene) were used for HS and HS-SPME optimization. 2 mL of distilled water and 10 µL of standard

solution were added in 22-mL volatile organic analysis (VOA) vials and hermetically closed and homogenised before analyzing.

Samples of the A and B horizon (A_{Camb} and B_{Camb}) from an alumi-umbric Cambisol profile collected in the surroundings of Santiago de Compostela (Galicia, NW Spain) were used. According to USEPA Method 5021A (volatile organic compounds in soils and other solid matrices using equilibrium headspace analysis) (USEPA, 2003), the soil was mixed with organic free distilled water to create a slurry. One gram of sample was mixed with 2 mL of distilled water, and the slurry was spiked with the standard solution until 1000 μg Kg^{-1} of individual FO and BTEX. The slurry was stabilized in hermetically closed VOA vials at 4 °C for 7 days before analyzing.

Calibration standards were prepared with the 100 mg L^{-1} standard in VOA vials with 2 mL of distilled water. For HS, standards of 50 to 15000 μg L^{-1}, and for HS-SPME, of 0.5 to 2500 μg L^{-1} were prepared. Fluorobenzene was added to water standards at constant concentration (2500 μg L^{-1}) to be used as internal standard for calibration. In the case of soil samples, fluorobenzene was added also as surrogate or matrix effect corrector, during the spiking process and stabilized with the rest of the analytes at 4 °C for at least 7 days. Fluorobenzene concentration was also maintained constant at 5000 μg Kg^{-1}.

Instrumentation and analytical methods

The analysis instrumentation consists of an autosampler (Combi PAL, Agilent Technologies), with liquid, HS and SPME injection and an oven for heating and agitating VOA sample vials, a gas chromatograph (Model 450 GC, Agilent Technologies) and an ion trap mass spectrometer (Model 220 MS, Agilent Technologies). Cycle Composer software (Version 1.5.4; CTC Analytics AG) was used to control the Combi PAL autosampler and MS Workstation software

(Version 6.9.3; Varian, Inc.) was used to control de GC-MS system and to process the data.

In HS and HS-SPME, VOA vials containing the samples were heated in the HS oven, with constant agitation and for a suitable period of time to achieve an acceptable equilibrium between the HS and the sample. As presented in figure 3.1a, when the VOA vial contains an aqueous sample, the equilibrium takes place between the liquid and the headspace of the vial. When there is a soil/water slurry (Figure 3.1b), the equilibrium takes place among three phases (soil, water and headspace) and the interaction of soil with the analytes or sorption, will provoke a lower displacement towards the headspace, compared to water standards, where there are no sorption processes. This is known as matrix effect and should be corrected, as already said, with the addition of a standard surrogate. In HS analysis an aliquot of the HS gas is directly injected in the chromatograph. In HS-SPME, a fiber is introduced in the vial during oven equilibration, to absorb the analytes in the HS. The amount of analytes absorbed, is proportional to the concentration in the HS, and therefore, on the water or soil sample (also with matrix effect correction).

Therefore, after the equilibration time, in direct HS sampling, 1 mL of HS gas was directly injected in the chromatograph for analysis. The injector was operated at 250 °C and in split 1/10 mode. In HS-SPME method, a 75 µm Carboxen-PDMS fiber (Supelco) was exposed to the headspace during equilibration and then thermally desorbed for 5 min at 300 °C (temperature defined by the manufacturer) in the injector, that also operated with a 1/10 split ratio. Furthermore, before introducing the fiber in the vial, the sample has to stabilize in the HS oven at the incubation temperature for 5 min. After desorption, SPME fibers are recommended to suffer a bakeout process under N_2 current to clean the traces of contaminants that could remain. Usually, the

bakeout temperature is fixed 20 °C under the desorption temperature, in this case 280 °C.

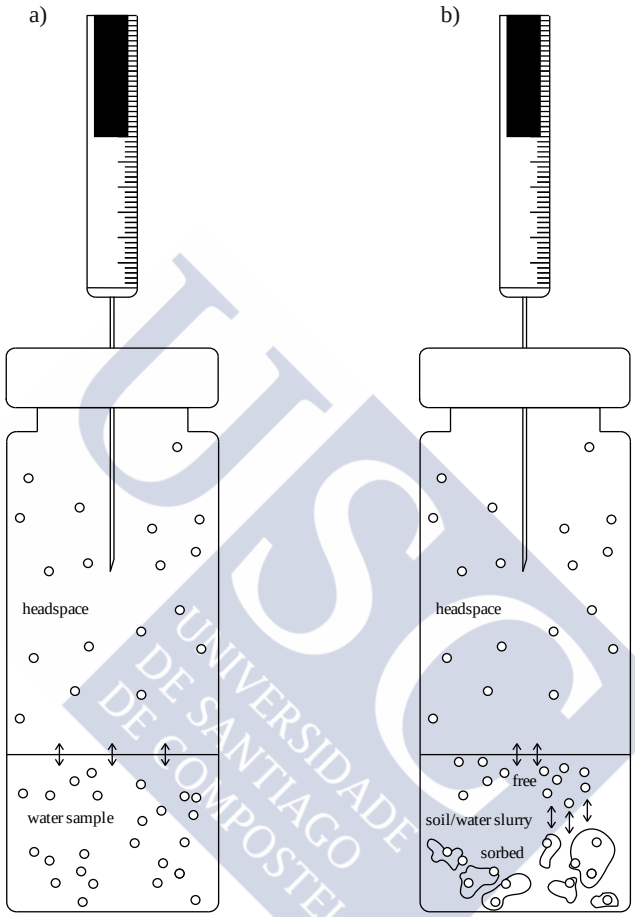

Figure 3.1. Simplification of equilibrium processes occurring in VOA vials with water (a) and soil (b) samples during HS analysis.

The chromatographic column used was a FactorFour VF-5ms EZ-Guard (supplied by Agilent Technologies) of 30m x 0.25 mm x 0.25 µm. The column oven temperature was varied as follows: 35 °C (held for 5 min), 10 °C min^{-1} up to 80 °C and 25 °C min^{-1} up to 200 °C (held for 0.7 min). The carrier gas was helium with a constant flow of 1 mL min^{-1}. The mass spectrometer operated in full scan mode. *m*- and *p*- xylene were quantified as a single peak.

The analytical performance characteristics were established for HS and HS-SPME-GC-MS methods using water spiked standards and uncontaminated blanks. Limits of detection (LOD) were calculated as 3.3 times the standard deviation of the blank (*n=10*) divided by the slope of the calibration curve. Limits of quantification (LOQ) were calculated as ten times the standard deviation of the blank (*n=10*) divided by the slope of the calibration curve (García Pinto *et al.*, 2011). The linear range goes from the LOQ to the highest standard until which the calibration curves were linear, with significant R^2 coefficients.

Optimization of VOC extraction and analysis

For VOC (FO and BTEX) analysis in water and soil samples, HS and HS-SPME conditions were optimized. The most important parameters to optimize in a HS process are the extraction temperature and the extraction time, apart from others like the sample size or the agitation speed. HS conditions were varied, in the range commonly found in the literature maintaining constant the rest of parameters. The extraction temperatures tested were 60, 80 and 90 °C, for 15 min of extraction time and 500 rpm of agitation speed. Extraction time of 10, 15 and 20 min, were used, at 80 °C and 500 rpm. The sample size and slurry ratio (1 g:2 mL and 1 g:5 mL) and agitation speed (500 and 700 rpm) were optimized at 80 °C and 15 min. The optimum values were selected in order to obtain the highest analytical response of the contaminants. HS-SPME optimum conditions were established based on HS results, and different incubation times were tested (15, 20 and 30 min). HS and HS-SPME-GC-MS methods were optimized with spiked distilled water and then validated for soil analysis with spiked soils with matrix effect correction.

RESULTS AND DISCUSSION

FO and BTEX HS-GC-MS analysis optimization

i. Optimization of HS parameters

Several parameters that highly influence the analytical sensitivity of HS analysis were optimized: extraction temperature, extraction time, sample size and agitation speed.

The peak sizes of the individual FO and BTEX obtained for each temperature and extraction time tested are presented in figure 3.2. The highest peak size was reached at 80 °C. At 60 °C, the equilibrium concentration was lower probably to the lower volatilization of the analytes towards the HS. At 90 °C, the higher vial temperature provoked a pressure increase. This could also increase the temperature of vaporization of the analytes, what could explain the lower volatilization towards the HS (Figure 3.2a). The extraction time with the highest peak size was 15 min, although only MTBE, ETBE and benzene, showed higher significant differences between 15 min and/or 10 and 20 min (Figure 3.2b). As a result, 80 °C and 15 min were used as optimum.

According to EPA method 5021A (USEPA, 2003), 10 mL of aqueous samples or 2 g of soil samples (or less in case of high concentration) + 10 mL of organic free distilled water, should be added to 22-mL VOA vials for HS analysis. By direct observation, the total column of 10 mL was very difficult to homogeneously agitate during HS incubation. Different liquid volumes from 1 to 10 mL were tested to select the volume which better agitation had. The best agitation was obtained for 2 mL. In the case of soil, lowering the slurry proportion soil/water to 1 g:2 mL also produced a more homogeneous slurry and easier to agitate than the recommended by EPA Method 5021 (2 g:10 mL or 1 g:5 mL).

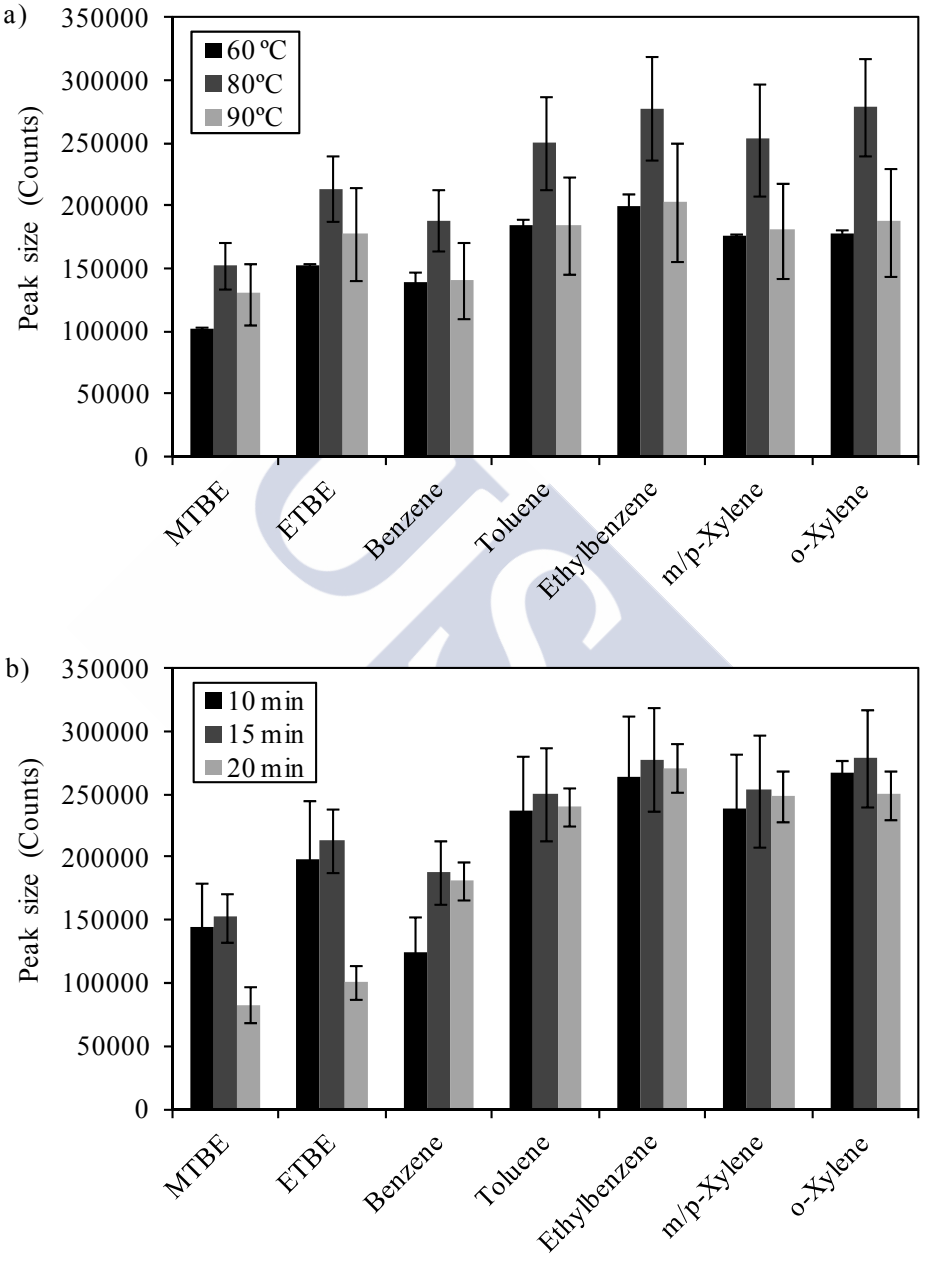

Figure 3.2. Peak sizes of individual FO and BTEX in 500 µg L^{-1} water standards analyzed by HS-GC-MS, at different incubation temperatures (a) and times (b).

To support those visual conclusions, water standards of 100, 500, 1000, 5000 and 10000 ng in 2 mL or 10 mL of distilled water were compared for peak

size resolution. An example of the results obtained for ETBE and ethylbenzene are shown in figure 3.3. The results indicated that the peak size of FO was higher in 2 mL standards, but that of BTEX was higher in 10 mL standards (6-24% higher). However, this last difference was only significant for toluene, ethylbenzene and *m*/*p*-xylene. According to the analytical results, the increase in the analytical signal was not as significant as to omit the visual conclusions of a better agitation with 2 mL. Therefore, a water volume of 2 mL for aqueous samples and soil slurries was used for HS analysis.

Agitation of the sample during HS analysis is very important since it reduces the time required to reach equilibrium by enhancing the diffusion of analytes towards the headspace (Flórez Menéndez *et al.*, 2000). By direct observation, with a speed lower than 500 rpm, water samples, and especially, soil slurries did not agitate properly. At more than 700 rpm, the sample was over-agitated and released drops on the VOA vial, over the liquid or slurry surface. The peak sizes of individual FO and BTEX were slightly higher with 700 rpm than with 500 rpm, but the difference between those agitation speeds was not significant (8-14% difference) (data not shown). Therefore, the agitation speed was fixed at 500 rpm, in order to assure the proper and homogeneous agitation of the water and soil samples.

Thus, the final parameters used for HS extraction FO and BTEX from water and soil samples are summarized in Table 3.1.

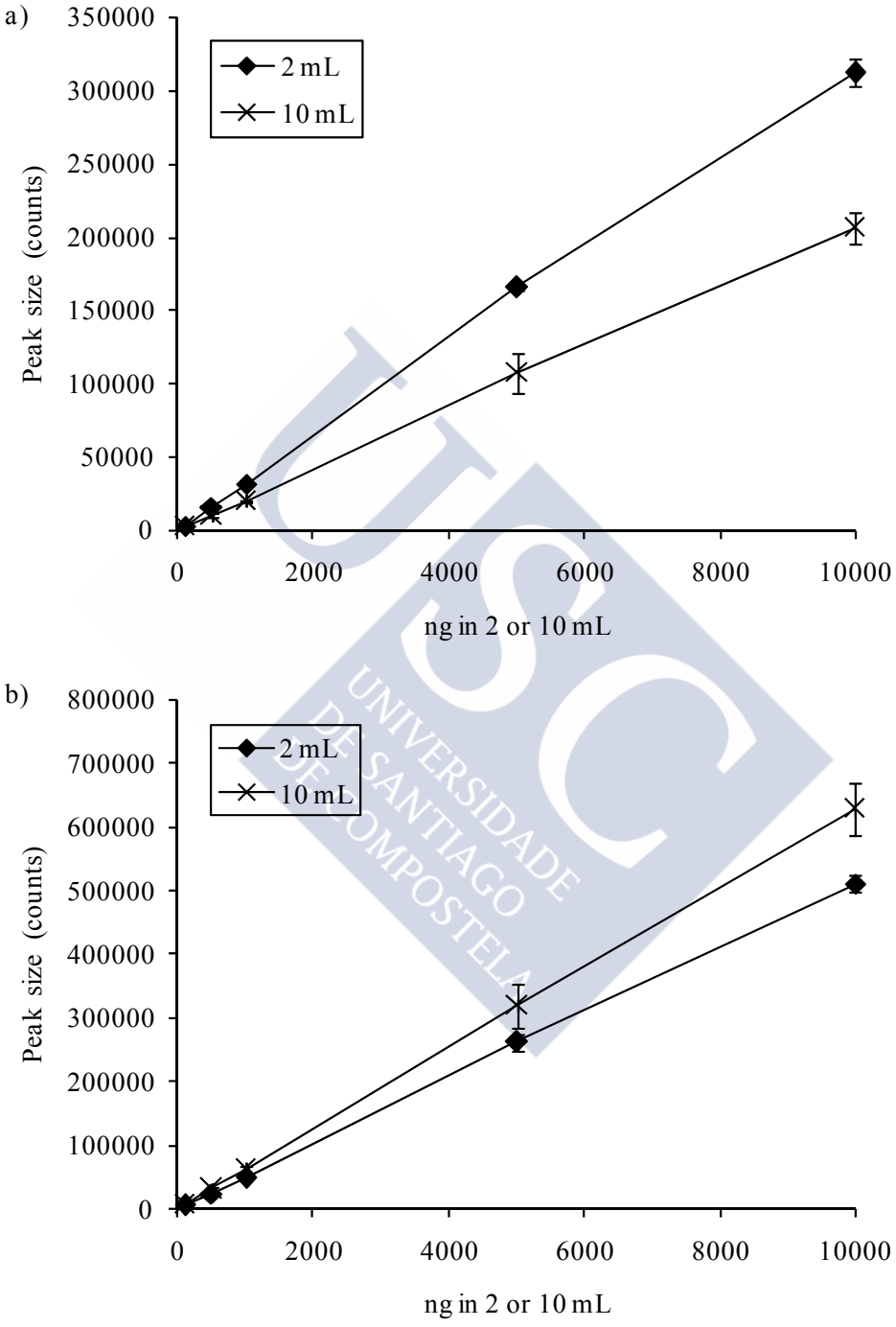

Figure 3.3. Examples of peak sizes of ETBE (a) and ethylbenzene (b) resulting from HS-GC-MS analysis of 2 mL and 10 mL standards.

Table 3.1. Optimized values of the most important parameters in HS extraction of FO and BTEX.

Extraction parameter	Optimized value
Extraction temperature	80 °C
Extraction time	15 min
Sample size of aqueous samples	2 mL
Sample size of soil samples	Slurry of 1g of soil : 2mL of water
Agitation speed	500 rpm

ii. HS analysis validation for soil samples

The principal limitation of HS analysis is the matrix effect, which could be corrected by using surrogate standards (fluorobenzene, in this case). Figure 3.4 represents the recovery of individual FO and BTEX from A_{Camb} (Figure 3.4a) and B_{Camb} (Figure 3.4b) spiked with 1000 g Kg^{-1}, without and with the surrogate correction.

The use of surrogate significantly increased the FO and BTEX recovery, especially in A_{Camb}: in A_{Camb} the recovery increased from 20-40% without surrogate, to 80-100% with the addition of surrogate; in B_{Camb}, it increased from 70-90% to 80-100%. The principal difference between the soil samples is the organic carbon content (42.6 and 3.3 g Kg^{-1} for A_{Camb} and B_{Camb}, respectively). The presence of organic matter in A_{Camb}, provoked a stronger sorption on FO and BTEX, than inorganic soil components (clays, oxides and oxihydroxides of iron and aluminium, etc.) in B_{Camb} (Balseiro-Romero and Monterroso, 2013). Therefore, surrogates should be used while HS-GC-MS analyzing solid samples, especially if they are expected to exert a strong sorption on analytes.

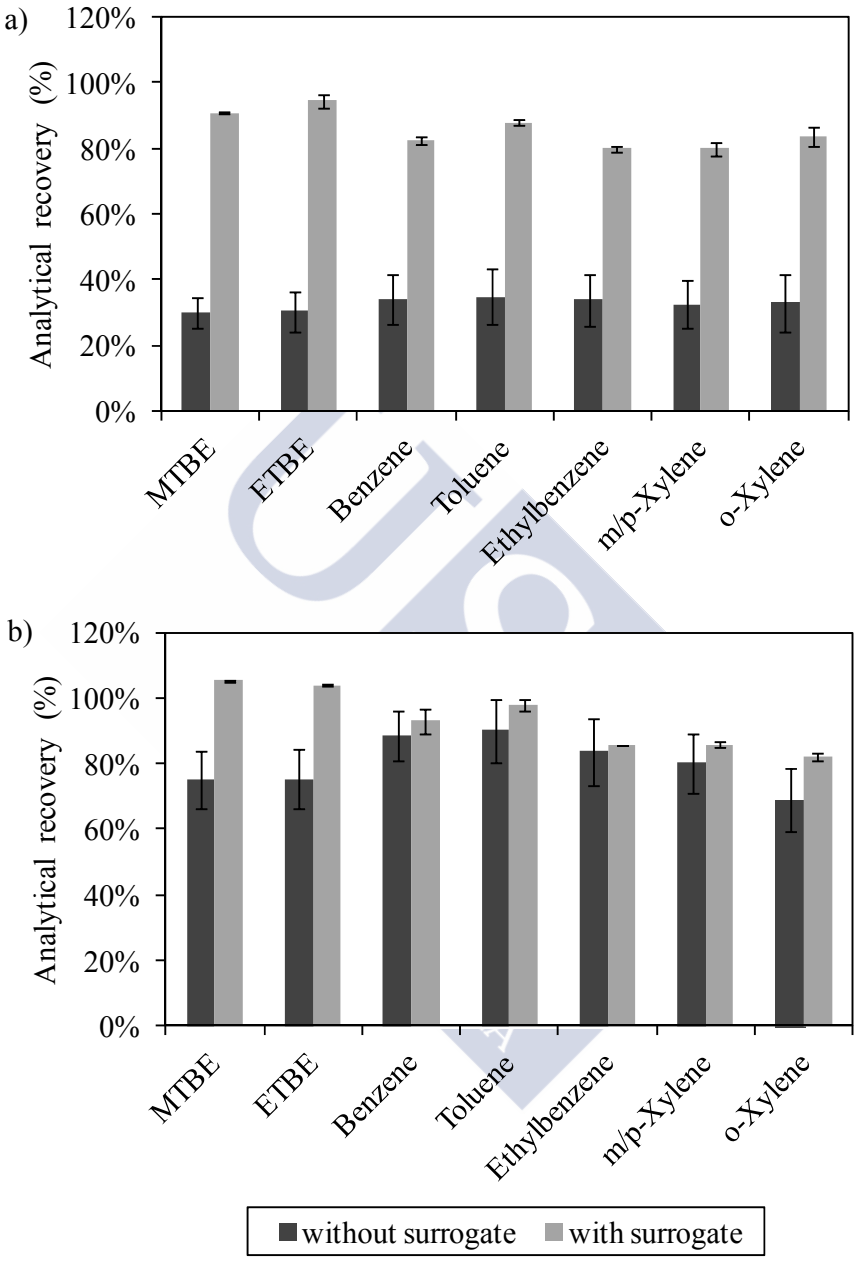

Figure 3.4. Analytical recoveries of individual FO and BTEX from A_{Camb} (a) and B_{Camb} (b) spiked with 1000 µg Kg^{-1} and analyzed by HS-GC-MS without and with the addition of surrogate (fluorobenzene, 5000 µg Kg^{-1}).

iii. Analytical performance characteristics of HS-GC-MS

The chromatographic separation of FO and BTEX was simple, considering the small amount of compounds to analyze, their relative similar properties (volatility, chemical structure) and the injection mode: the HS gas injection or fiber injection generates less peak interferences, and therefore, higher peak resolution, than liquid injection with solvents. Furthermore, based on that high resolution, the mass spectrometer (MS) operated in full scan mode, what also simplifies the GC-MS method.

When the previous extraction step is HS, following the manufacturer´s indications, the GC-MS conditions are those summarized in table 3.2. An example of a resulting chromatogram is represented in figure 3.5.

Table 3.2. Optimized GC-MS conditions for FO and BTEX analysis after HS extraction.

GS-MS condition	Optimum value
HS volume injected	1 mL
Injector temperature	250 °C
Injection mode	1/10 split
Column oven temperature pattern	35 °C (held for 5 min), 10 °C min^{-1} up to 80 °C and 25 °C min^{-1} up to 200 °C (held for 0.7 min)
Carrier gas flow	Helium at 1 mL min^{-1}
MS ionization mode	Electron impact
MS ion trap temperature	220 °C

This method (Table 3.2) could be operated in splitless mode, if more analytical signal was needed. With these conditions and the properties of the column, *m*- and *p*- xylene were hardly separated (they are isomers, and have very similar properties). Therefore, they were quantified as a single peak.

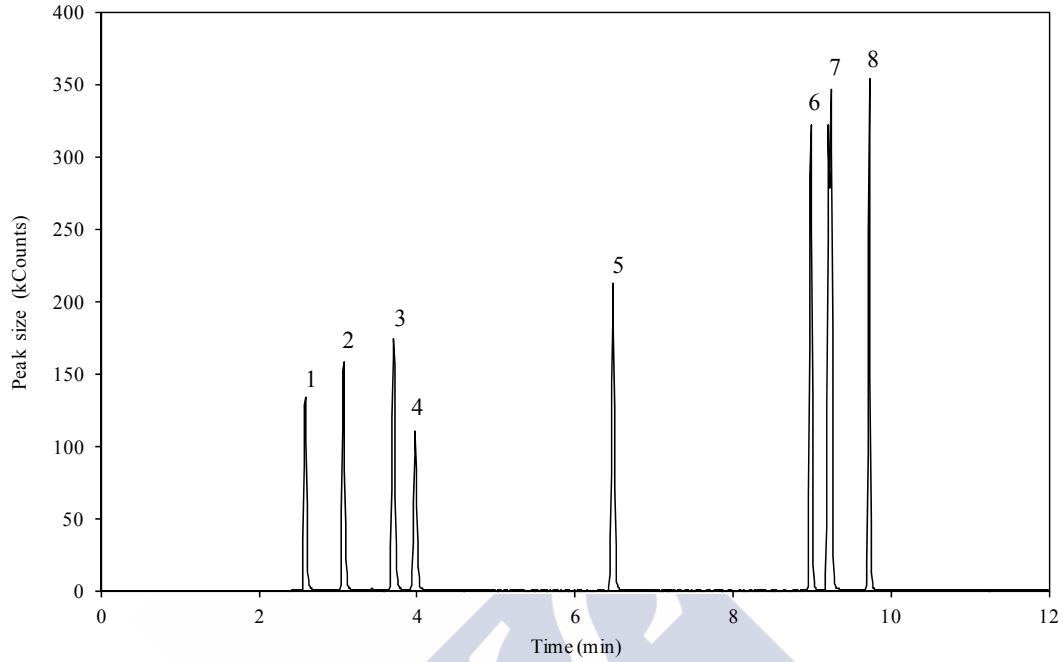

Figure 3.5. Example of a HS-GC-MS chromatogram of a 5000 µg L^{-1} water standard. The peaks correspond to MTBE (1), ETBE (2), benzene (3), fluorobenzene (4), toluene (5), ethylbenzene (6), *m*/*p*-xylene (7) and *o*-xylene (8).

The analytical performance characteristics of HS-GC-MS method for VOC analysis are summarized in table 3.3.

Table 3.3. Analytical performance characteristics of HS-GC-MS analysis of FO and BTEX.

Contaminant	LOD (µg L^{-1})	LOQ (µg L^{-1})	Linear range (µg L^{-1})	R^2
MTBE	4.6	6.7	15000	0.994
ETBE	1.9	3.4	15000	0.997
Benzene	3.1	7.0	15000	0.994
Toluene	9.8	20.9	15000	0.993
Ethylbenzene	3.7	10.8	15000	0.996
***m*/*p*-Xylene**	12.7	29.7	15000	0.996
***o*-Xylene**	11.3	26.2	15000	0.996

FO and BTEX HS-SPME-GC-MS analysis optimization

i. Optimization of HS-SPME parameters

The optimized parameters used in HS analysis can be used in HS-SPME. The main difference is the incubation time. In this case, the equilibrium takes place between the sample and HS, and then, between the HS and the fiber, and higher incubation times should be used.

Indeed, several incubation times were tested (15, 20 and 30 min) (Figure 3.6). Comparable analytical signals were obtained for MTBE and ETBE at all incubation times. However, 30 min of incubation appeared necessary to reach a higher peak size of BTEX compounds.

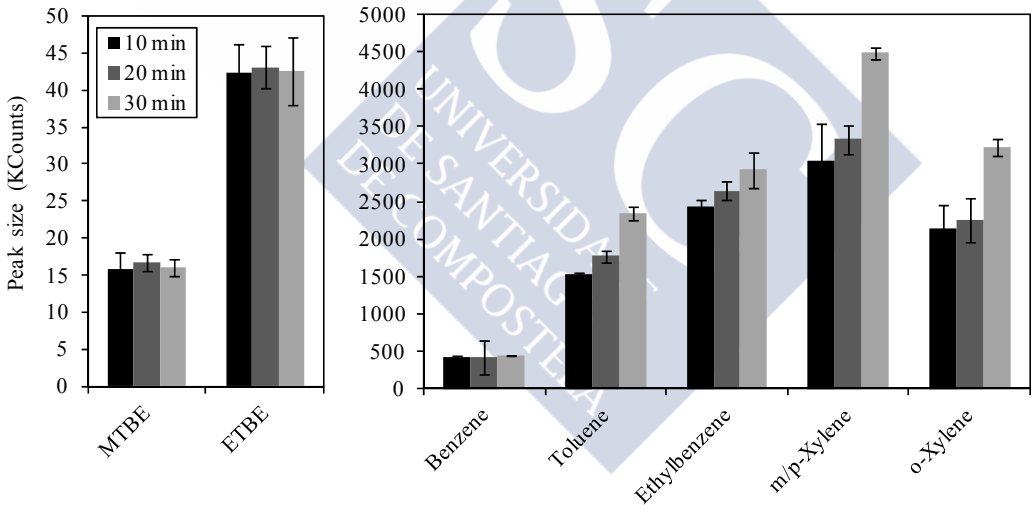

Figure 3.6. Peak sizes of individual FO and BTEX in 500 µg L-1 water standards analyzed by HS-SPME-GC-MS, at different incubation times.

Therefore, the final parameters used for HS-SPME analysis of water and/or soil samples are summarized in table 3.4.

Table 3.4. Optimized values of the most important parameters in HS-SPME extraction of FO and BTEX.

Extraction parameter	Optimized value
Extraction temperature	80 °C
Pre-heating time	5 min
Extraction time	30 min
Desorption temperature	300 °C
Desorption time	5 min
Bakeout temperature	280 °C
Bakeout time	10 min
Sample size of aqueous samples	2 mL
Sample size of soil samples	Slurry of 1g of soil : 2mL of water
Agitation speed	500 rpm

ii. HS-SPME analysis validation for soil samples

As in HS-SPME analysis, as occurred for HS analysis, matrix effect should be corrected with surrogate standards in order to accurately quantify the soil concentration. Figure 3.7 represents the recovery of individual FO and BTEX from A_{Camb} (Figure 3.7a) and B_{Camb} (Figure 3.7b) spiked with 1000 μg Kg^{-1}, without and with the surrogate correction.

The use of surrogate was necessary to reach analytical recoveries of up to 100% in both soil samples, and correct the matrix effect.

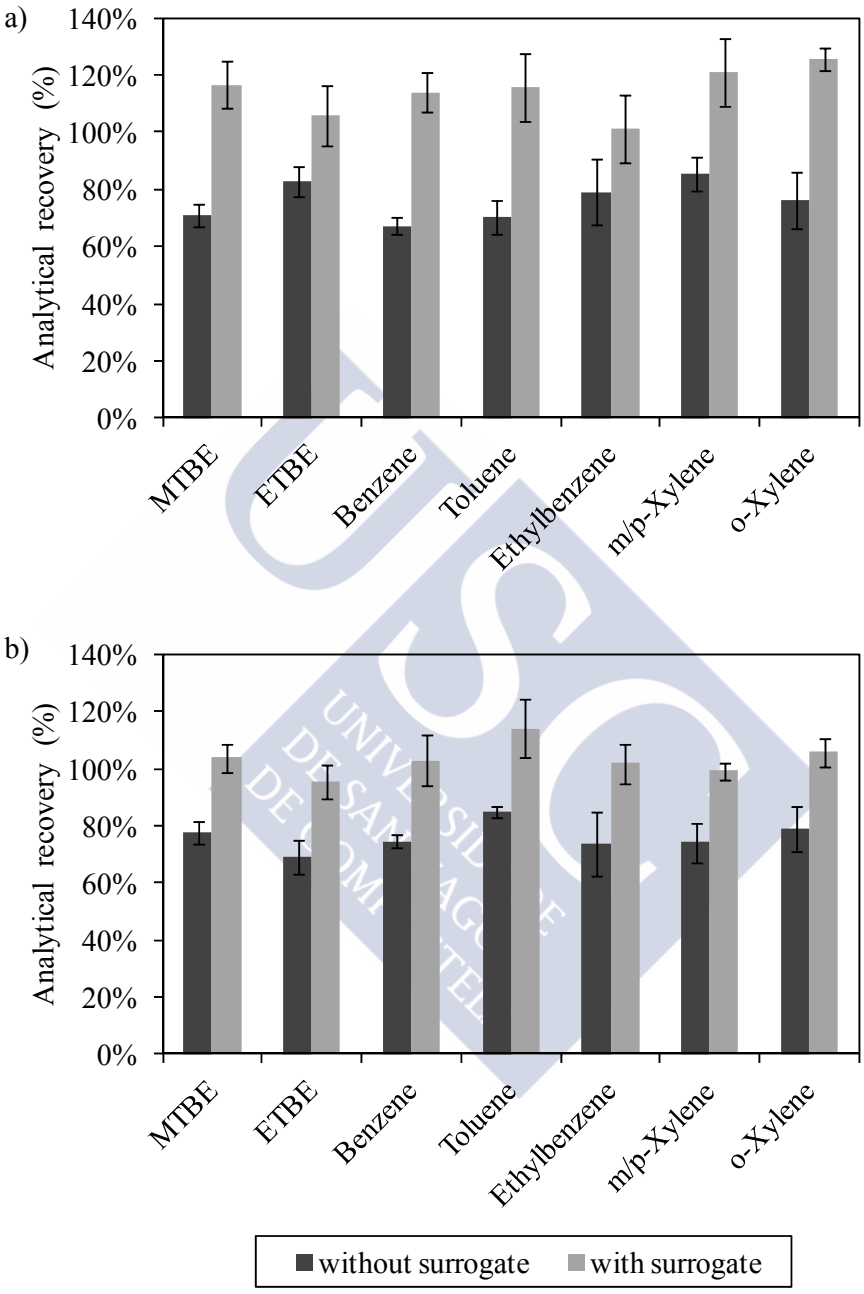

Figure 3.7. Analytical recoveries of individual FO and BTEX from A_{Camb} (a) and B_{Camb} (b) spiked with 1000 μg Kg^{-1} and analyzed by HS-SPME-GC-MS without and with the addition of surrogate (fluorobenzene, 5000 μg Kg^{-1}).

ii. Analytical performance characteristics of HS-SPME-GC-MS

When the previous extraction step is HS-SPME, the GC-MS conditions are practically the same as for HS, but the main difference is the injector temperature (Table 3.5). Since the fiber desorption takes place in the injector, the desorption temperature is that defined by the manufacturer, in this case 300 °C. An example of chromatogram is represented in figure 3.8.

Table 3.5. Optimized GC-MS conditions for FO and BTEX analysis after HS-SPME extraction.

GS-MS condition	Optimum value
Injector (desorption) temperature	300 °C
Injection mode	1/10 split
Column oven temperature pattern	35 °C (held for 5 min), 10 °C min^{-1} up to 80 °C and 25 °C min^{-1} up to 200 °C (held for 0.7 min)
Carrier gas flow	Helium at 1 mL min^{-1}
MS ionization mode	Electron impact
MS ion trap temperature	220 °C

According to figure 3.8, the sensitivity of the HS-SPME method is very different for the individual contaminants, contrasting with that of the HS method (Figure 3.5), probably due to the different affinity of the contaminants for the SPME fiber. In addition, the peaks appeared with a tail, probably due to a slow desorption from the fiber. Therefore, quantification was carried out with the peak height instead of with the peak area, as in HS-GC-MS.

The analytical performance characteristics of HS-SPME-GC-MS method are summarized in table 3.6. Detection and quantification limits, and linearity were calculated as for HS-GC-MS method.

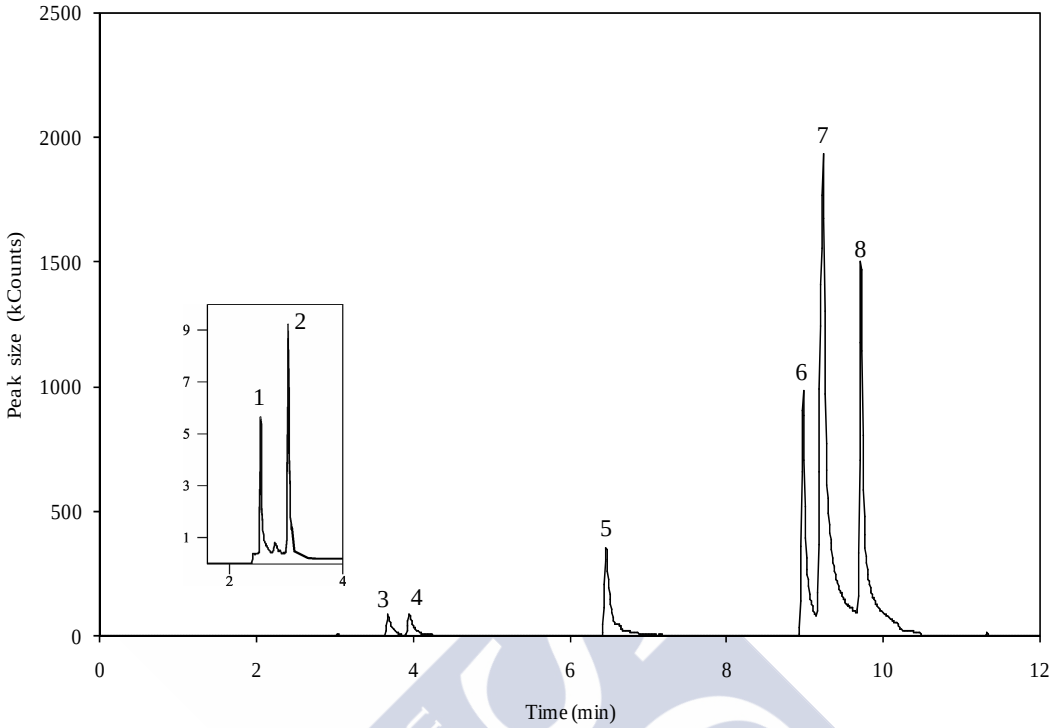

Figure 3.8. Example of a HS-SPME-GC-MS chromatogram of a 2500 μg L^{-1} water standard. The peaks correspond to MTBE (1), ETBE (2), benzene (3), fluorobenzene (4), toluene (5), ethylbenzene (6), *m*/*p*-xylene (7) and *o*-xylene (8).

Table 3.6. Analytical performance characteristics of HS-SPME-GC-MS analysis of FO and BTEX.

Contaminant	LOD (μg L^{-1})	LOQ (μg L^{-1})	Linear range (μg L^{-1})	R^2
MTBE	1.9	3.3	2500	0.990
ETBE	0.5	0.9	2500	0.981
Benzene	0.5	1.0	2500	0.996
Toluene	0.8	1.9	2500	0.991
Ethylbenzene	1.1	3.3	2500	0.991
***m*/*p*-Xylene**	0.9	2.6	2500	0.993
***o*-Xylene**	2.6	7.3	2500	0.994

CONCLUSIONS

The use of HS or HS-SPME in FO and BTEX GC/MS analysis will highly depend on the concentration of the samples. When this concentration is unknown, HS should be used as screening method, since it has a longer linear range (until 30 mg Kg^{-1} or 15 mg L^{-1}). If the analytical response of the contaminants was under or near the HS quantification limit, HS-SPME should be used. This last method amplified the analytical response of HS in more than 20 times, and its detection and quantification limits were about an order of magnitude under HS values.

The use of surrogate standards in soil analysis was essential to correct the matrix effect and to properly quantify soil concentration.

The developed HS and HS-SPME analysis methods, resulted in sensitive and accurate procedures to identify and quantify volatile organics (VOC), MTBE, ETBE and BTEX, in environmental samples. Therefore, they can be used for the characterization of the contamination in a real fuel spill episode, in a wide range of contaminant concentrations and for water and soil samples with different organic matter content.

REFERENCES

Arambarri I, Lasa M, Garcia R, Millán E. 2004. Determination of fuel dialkyl ethers and BTEX in water using headspace solid-phase microextraction and gas chromatography–flame ionization detection. J Chromatogr A 1033:193-203.

Arthur CL, Pawliszyn J. 1990. Solid phase microextraction with thermal desorption using fused silica optical fibers. Anal Chem 62:2145-2148.

Balseiro-Romero M, Monterroso C. 2013. A headspace-analysis approach to assess the sorption of fuel volatile compounds by soils. Soil Sci Soc Am J 77: 800-808.

Esteve-Turrillas FA, Armenta S, Garrigues S, Pastor A, de la Guardia M. 2007. Headspace–mass spectrometry determination of benzene, toluene and the

mixture of ethylbenzene and xylene isomers in soil samples using chemometrics. Anal Chim Acta 587:89-96.

Ezquerro Ó, Ortiz G, Pons B, Tena MT. 2004. Determination of benzene, toluene, ethylbenzene and xylenes in soils by multiple headspace solid-phase microextraction. J Chromatogr A 1035:17-22.

Flórez Menéndez JC, Fernández Sánchez ML, Sánchez Uría JE, Fernández Martínez E, Sanz-Medel A. 2000. Static headspace, solid-phase microextraction and headspace solid-phase microextraction for BTEX determination in aqueous samples by gas chromatography. Anal Chim Acta 415:9-20.

García Pinto C, Herrero Martín S, Pérez Pavón JL, Moreno Cordero B. 2011. A simplified Quick, Easy, Cheap, Effective, Rugged and Safe approach for the determination of trihalomethanes and benzene, toluene, ethylbenzene and xylenes in soil matrices by fast gas chromatography with mass spectrometry detection. Anal Chim Acta 689:129-136.

Hiatt MH. 2010. The role of internal standards and their interaction with soils impact accuracy of volatile organics determinations. Int J Environ Anal Chem 90:591-604.

Llompart M, Li K, Fingas M. 1999. Headspace solid phase microextraction (HSSPME) for the determination of volatile and semivolatile pollutants in soils. Talanta 48:451-459.

Louch D, Motlagh S, Pawliszyn J. 1992. Dynamics of organic compound extraction from water using liquid-coated fused silica fibers. Anal Chem 64:1187-1199.

Pavón JLP, Martín SH, Pinto CG, Cordero BM. 2009. Programmed temperature vaporizer based method for the sensitive determination of trihalomethanes and benzene, toluene, ethylbenzene and xylenes in soils. J Chromatogr A 1216:6063-6070.

Rosell M, Lacorte S, Barceló D. 2006. Simultaneous determination of methyl *tert*-butyl ether, its degradation products and other gasoline additives in soil samples by closed-system purge-and-trap gas chromatography-mass spectrometry. J Chromatogr A 1132:28-38.

United States Environmental Protection Agency (USEPA). 2003. Method 5021A: Volatile organic compounds in various sample matrices using equilibrium headspace analysis. Revision 1. US Environmental Protection Agency, Washington.

Zhang Z, Pawliszyn J. 1993. Analysis of organic compounds in environmental samples by headspace solid phase microextraction. J High Res Chromatogr 16:689-692.

USC
UNIVERSIDADE
DE SANTIAGO
DE COMPOSTELA

4

Development and optimization of DRO analysis in environmental samples

An accurate and sensible analytical method for the analysis of diesel range organics (DRO) is indispensable for the characterization and identification of fuel spills. In the present work, we optimized the analysis of diesel range organics (DRO) in soil and water samples. Solvent extraction procedures such as ultrasonic extraction (for water samples), accelerated solvent extraction (for soil samples) were optimized in order to achieve the highest recoveries of all DRO. In addition, a solvent-free extraction procedure, headspace-solid phase microextraction (HS-SPME), was also optimized for both soil and water samples. The use of SPME fibers has a concentration effect, so this technique is more sensible and therefore appropriate for lower DRO concentrations. Gas chromatography-mass spectrometry (GC/MS) methods were also developed to get the optimal analytical performance.

This work was included in the communication:

Balseiro-Romero M, Monterroso C. 2014. Development and optimization of diesel range organics extraction and analysis in environmental samples. 7th IECB Young Scientist Symposium, Bordeaux, France. Poster communication.

INTRODUCTION

The development of accurate and reliable analytical methods for the determination of fuel hydrocarbons in environmental samples is extremely important for assessing oil spills and their associated risks. Generally speaking, the typical methodologies for analyzing petroleum products are non-specific methods to determine total petroleum hydrocarbons (TPH) using gravimetric and infrared methods, and chromatographic methods to determine the concentration of individual components and/or a specific set of petroleum hydrocarbons (Wang and Fingas, 1997).

Diesel is one of the most common car fuels and it is a complex mixture of hydrocarbons, essentially, alkanes (mainly, C_{10}-C_{25}), cycloalkanes and polyaromates (Trapp *et al.*, 2001). Diesel range organics (DRO) is a widely spread term to refer to the range of saturated *n*-alkanes present in diesel. This is the major fraction and the most commonly analyzed, since they can be used for many purposes: as a marker for the presence of a spilled oil, for the identification of the product type, for monitoring chemical composition changes due to weathering and/or biodegradation, etc. (Wang and Fingas, 1997).

Identification and analysis of DRO from environmental samples is commonly performed by gas chromatography coupled to mass spectrometry (GC-MS) or flame ionization detection (GC-FID) (Wang *et al.*, 2002). However the most crucial step in DRO determination is the extraction procedure. Several extraction techniques were used for the extraction of semivolatile compounds from solid matrices: solid-liquid extractions, using organic solvents, such as Soxhlet extraction, accelerated solvent extraction (ASE) (also known as pressurized fluid extraction -PFE-), supercritical fluid extraction (SFE), ultrasound (US) or microwave assisted extraction (MAE); and organic solvent-free techniques, such as solid phase microextraction (SPME), or subcritical water

extraction (Cam and Gagni, 2001; Chesler *et al.*, 1997; Eriksson *et al.*, 1998; Richter *et al.*, 2006; Schantz, 2006). The extraction of organics from water samples was usually done by liquid-liquid extraction with an organic solvent, by means of a extraction separatory funnel, ultrasonic assisted extraction (US) or automated liquid-liquid extraction, and with SPME as a free-solvent technique (Eriksson *et al.*, 1998; Wang *et al.*, 2002).

The aim of the present chapter was to optimize US extraction and HS-SPME of DRO from water samples and ASE and HS-SPME from soil samples. Furthermore, GC-MS methods were developed in order to get the highest analytical resolution for an accurate identification and quantification of DRO concentration.

MATERIALS AND METHODS

Reagents, standards and reference materials

Diesel purchased from a local distribution station was used for distilled water and soil samples spiking. A 1000 mg L^{-1} standard containing a mixture of *n*-alkanes in the carbon range of C_{10}-C_{25} (DRO Mixture 1, Dr. Ehrenstorfer) was used for the preparation of calibration standards, and also for GC-MS methods optimization.

According to USEPA Method 8015C (USEPA, 2007c) regarding non-halogenated organics by gas chromatography, and USEPA Method 8270D (USEPA, 2007d) regarding the analysis of semivolatile organic compounds by gas chromatography/mass spectrometry, *p*-terphenyl-d_{14} (2000 mg L^{-1} standard solution, purchased from AccuStandard, Inc.) was used as surrogate in soil samples to correct the matrix effect during ASE and HS-SPME, and in water samples to correct the losses during US extraction.

Internal standard (IS) calibration was performed with a mix of deuterated IS, containing 1,4-dichlorobenzene-d_4, acenaphthene-d_{10}, chrysene-d_{12}, naphthalene-d_8, perylene-d_{12} and phenanthrene-d_{10} (Internal Standards Mix 33, Dr. Ehrenstorfer).

Preparation of water and soil samples

Ultrasonic extraction (US) of DRO was optimized for contaminated water, using distilled water spiked with diesel at 1 g L^{-1}. Two or five mL of distilled water were spiked with 2.5 or 6.25 µL of diesel, respectively, and added to threaded 20 or 50 mL glass tubes (depending on the amount of sample and extraction solvent). For HS-SPME optimization in DRO water samples contaminated with 25 µg L^{-1} diesel were used. The 22 mL-VOA (volatile organic analysis) vials were hermetically closed and homogenised before analysis.

Samples of the A and B horizon (A_{Camb} and B_{Camb}) from an alumi-umbric Cambisol profile collected in the surroundings of Santiago de Compostela (Galicia, NW Spain) were used for accelerated solvent extraction (ASE) and HS-SPME optimization. For ASE optimization, soil samples were spiked with diesel at 1 mg Kg^{-1} and 1000 mg Kg^{-1}, vigorously homogenised, and stabilized in glass recipients hermetically closed at 4 °C for 7 days. For HS-SPME, according to USEPA method 5021A (USEPA, 2003), the soil was mixed with organic free distilled water to create a slurry. One gram of sample was mixed with 2 mL of distilled water, and the slurry was spiked with diesel at 5 mg Kg^{-1}. The slurry was stabilized in hermetically closed 22 mL-VOA vials at 4 °C for 7 days.

Calibration standards were prepared with the 1000 mg L^{-1} DRO standard (Dr. Ehrenstorfer). In the case of liquid injection (after ASE or US extraction), hexane standards of 100 to 15000 µg L^{-1} were prepared. In the case of HS-SPME, 2 mL water standards of 0.5 to 50 µg L^{-1} were prepared in VOA vials. Internal standard calibration was carried out by adding a IS mix (Dr. Ehrenstorfer) at

constant concentration of 200 μg L^{-1} in standards and liquid extracts and of 50 μg L^{-1} in VOA vials, before analysis.

Surrogate standard, *p*-terphenyl-d_{14}, was also added to hexane standards and to water samples before US extraction and to spiked soils before the 7 days-stabilization and ASE extraction, in order to obtain, theoretically, a final concentration of 200 μg L^{-1} in the liquid extract. In HS-SPME samples, *p*-terphenyl-d_{14} was only added to soil samples before stabilization, in order to correct the matrix effect, at a constant concentration of 50 μg L^{-1}.

Instrumentation for extraction and analysis of DRO

For DRO extraction of diesel-contaminated water, an ultrasonic water bath (Ultrasons, J. P. Selecta, S. A.) extractor was used. Closed tubes containing the sample and the extraction solvent, were completely immersed in the water of the US extractor, and extracted for a suitable amount of time. Then, an aliquot of the organic phase was pipetted and dried with anhydrous Na_2SO_4, before GC-MS analyzing.

For DRO extraction of diesel-contaminated soil samples, an accelerated solvent extractor, ASE® 200 (Dionex), was used. According to USEPA method 3545 (USEPA, 2007a), 11 mL-stainless steel cells were filled with 5 g of diesel spiked soil, mixed with 1.25 g of diatomaceous earth (used as drying agent) and sand (3-4 g). During extraction, the cells are filled with the extraction solvent and statically kept with the solvent at high pressure and temperature, in order to extract the maximum amount of analytes present in the samples. After the static cycle/s, the solvent is purged with a N_2 flow and collected in vials. Figure 4.1 represents the ASE process schematically. The extract is adjusted to a fixed volume and an aliquot is analyzed by GC-MS. Extracts could be evaporated in an N_2 evaporator with water bath (TurboVap®LV, Caliper Lifesciences Inc.) until a very low volume. This is usually used when the concentration of the sample is

supposed to be very low and the extract should be preconcentrated; or when the extraction solvent cannot be injected in the GC column and should be changed to another solvent. For the chromatographic column installed, hexane is the most suitable solvent.

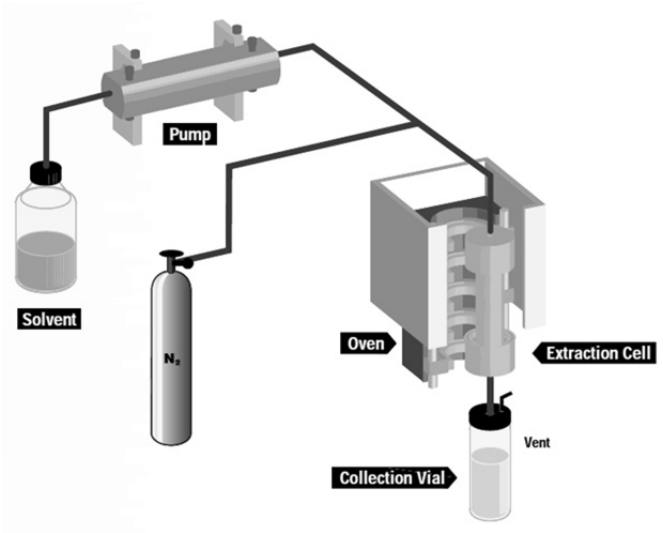

Figure 4.1. Schematic ASE process (ASE® 200 Brochure, Dionex).

In HS-SPME of DRO from contaminated water and soil samples, the VOA vials containing the samples were heated in the HS oven of the Combi PAL autosampler (Agilent Technologies), with constant agitation and for a suitable period of time to achieve an acceptable equilibrium among the SPME fiber, the HS and the sample. A 65 µm PDMS/DVB fiber (Supelco) is introduced in the vial during oven equilibration, to absorb the analytes in the HS. The amount of analytes absorbed, is proportional to the concentration in the HS, and therefore, on the water or soil sample (with matrix effect correction with surrogate). The fiber is then thermally desorbed for 5 min at 270 °C (temperature defined by the manufacturer) in the injector that operated in splitless mode. Furthermore, before introducing the fiber in the vial, the sample has to stabilize in the HS oven

at the incubation temperature for 5 minutes. After desorption, the fiber suffers a bakeout process at 250 °C under N_2 flow.

The analysis instrumentation was the same used in Chapter 3. The injection conditions and the column oven temperature were optimized for DRO analysis. Helium was used as carrier gas at constant flow of 1 mL min^{-1} and the mass spectrometer operated in full scan mode.

Optimization of DRO extraction and analysis

Ultrasonic extraction (US) was optimized for DRO analysis of diesel-contaminated water, following USEPA Method 3550C (USEPA, 2007b), adapted for water samples. The most important parameters to optimize in US extraction are the extraction solvent, the sample/solvent ratio, the sample size and the extraction time. Hexane, dichloromethane and acetone:hexane (1:1, *v*/*v*) were added in 1:20 ratio to samples of diesel-contaminated distilled water (1 g L^{-1}), and extracted for 30 min. Dichloromethane and acetone:hexane extracts were evaporated to a low volume and redissolved in hexane, since polar solvents may damage the chromatographic column. For the optimization of sample size (1 and 5 mL), sample/solvent ratio (1:2, 1:4 and 1:20) and the extraction time (30 min and 1 h), serial extractions were carried out by varying only one parameter at a time: 1 mL/1:2/30 min; 1 mL/1:2/1 h; 1 mL/1:4/30 min; 1 mL/1:4/1 h; 1 mL/1:20/30 min; 1 mL/1:20/1 h; and the same series for 5 mL of sample (except 1:20 ratio, that was only tested for 1 mL samples). The analytical recoveries were calculated from a theoretical extract prepared in the correspondent solvent with the 100% of diesel present in water samples.

For the optimization of ASE of DRO from diesel-contaminated soils, 1 mg Kg^{-1} spiked A_{Camb} and B_{Camb} were used. Based on based on USEPA Method 3545A (USEPA, 2007a), and Dionex Application Note 324 (Richter, 2012), the following extraction conditions were selected and optimized in order to efficiently extract

DRO: sample size, extraction solvent, extraction temperature and static cycles. Three extraction temperatures were tested: 5 g of sample were extracted at 100, 150 and 175 °C with hexane and 2 static cycles. Other extraction parameters, as pressure, preheating time, static time, flush volume and N_2 purge time, were established based on USEPA (2007a), and Richter (2012). The analytical recoveries were calculated from a theoretical extract prepared in hexane with the 100% of diesel present in soil samples. The ASE method was validated using 1000 mg Kg^{-1} diesel-spiked A_{Camb} and B_{Camb}.

HS-SPME optimum conditions for DRO extraction in water and soil samples were established based on FO and BTEX optimization results (Chapter 3), using 25 µg L^{-1} water standards. The method was validated for soils using 5 mg Kg^{-1} diesel-spiked A_{Camb} and B_{Camb}.

GC-MS methods for DRO analysis were developed for liquid injection (after US and ASE) using 1 mg L^{-1} hexane standards of DRO, and adapted for HS-SPME using 2 mL water standards of 50 µg L^{-1}. The injector temperature in liquid extract injection was optimized by using constant temperature (300 °C) or a ramp (from 60 °C to 300 °C, at 200 °C min^{-1}). The injector split was varied in split (1/20), splitless, and split/splitless mode. When the SPME fiber was used, the injector operated at 270 °C in splitless mode. The column oven temperature was optimized by testing different initial temperatures (40, 60 and 100 °C), final temperatures (250, 270 and 300 °C), and temperature ramps (50, 20 and 10 °C min^{-1}). The analytical performance characteristics were established for liquid injection and HS-SPME-GC-MS methods using hexane and water standards, and hexane and water blanks, respectively. Limits of detection (LOD) and limits of quantification (LOQ) were calculated following García Pinto *et al.* (2011).

RESULTS AND DISCUSSION

Optimization of ultrasonic (US) assisted extraction of DRO from aqueous samples

The parameters with more influence on US extraction of DRO from aqueous samples were optimized: extraction solvent, water sample size, sample/solvent ratio and extraction time.

The extraction solvents tested were hexane, dichloromethane and acetone:hexane (1:1, *v/v*), following USEPA recommendations for semivolatile organics (USEPA, 2007b). Recoveries of individual DRO analyzed in US extracts of diesel-spiked water (1 g L^{-1}) are presented in table 4.1.

Table 4.1. Analytical recoveries of individual DRO extracted with US extraction from 1 g L^{-1} diesel-contaminated water samples. Samples were extracted with hexane, dichloromethane and acetone:hexane (1:1), with a sample/solvent ratio of 1:20, for 30 min.

Contaminant	Hexane	Dichloromethane	Acetone:Hexane (1:1)
Decane (C_{10})	42%	30%	34%
Undecane (C_{11})	58%	46%	49%
Dodecane (C_{12})	74%	59%	61%
Tridecane (C_{13})	74%	62%	65%
Tetradecane (C_{14})	74%	66%	69%
Pentadecane (C_{15})	79%	66%	76%
Hexadecane (C_{16})	80%	67%	75%
Heptadecane (C_{17})	89%	73%	78%
Octadecane (C_{18})	86%	71%	79%
Nonadecane (C_{19})	83%	78%	81%
Eicosane (C_{20})	85%	74%	81%
Heneicosane (C_{21})	84%	77%	77%
Docosane (C_{22})	77%	74%	81%
Tricosane (C_{23})	79%	95%	95%
Tetracosane (C_{24})	64%	79%	86%
Pentacosane (C_{25})	>100%	>100%	>100%

The recoveries of individual DRO were generally higher with hexane, although the differences between the three solvents were not highly significant. The selected solvent was hexane, especially for avoiding the evaporation step that implied the use of dichloromethane and acetone:hexane. The recovery of the surrogate (*p*-terphenyl-*d14*) in dichloromethane and acetone:hexane evaporated extracts varied around 90-100% (data not shown) indicating that there were no losses during the evaporation step. However, due to the high volatility range of DRO, some of them could be partially evaporated during this step.

The analytical recoveries of DRO from the serial extractions carried out for the optimization of the sample size (1 and 5 mL), sample/solvent ratio (1:2, 1:4 and 1:20), and extraction time (30 min and 1 h) are summarized in table 4.2.

Table 4.2. Analytical recoveries of individual DRO extracted with hexane by US extraction from 1g L^{-1} diesel-contaminated water samples. Serial extractions were carried out varying only one parameter at a time: sample size (1 and 5 mL), sample/solvent ratio (1:2, 1:4 and 1:20) and extraction time (30 min and 1 h).

	1mL						5mL			
	1:2		1:4		1:20		1:2		1:4	
Contaminant	**30 min**	**1 h**	**30 min**	**1 h**	**30 min**	**1 h**	**30 min**	**1 h**	**30 min**	**1 h**
Decane (C_{10})	77%	91%	88%	83%	116%	75%	73%	83%	121%	128%
Undecane (C_{11})	92%	97%	96%	87%	126%	86%	79%	80%	128%	124%
Dodecane (C_{12})	89%	104%	91%	93%	127%	87%	78%	86%	118%	128%
Tridecane (C_{13})	103%	110%	99%	98%	128%	91%	83%	83%	124%	136%
Tetradecane (C_{14})	97%	106%	101%	95%	129%	95%	82%	82%	121%	127%
Pentadecane (C_{15})	99%	111%	101%	92%	123%	94%	83%	84%	119%	124%
Hexadecane (C_{16})	99%	109%	103%	98%	118%	93%	82%	83%	121%	129%
Heptadecane (C_{17})	98%	114%	102%	101%	124%	93%	81%	85%	120%	38%
Octadecane (C_{18})	98%	110%	99%	99%	120%	95%	84%	85%	120%	127%
Nonadecane (C_{19})	88%	115%	93%	107%	121%	94%	83%	85%	113%	125%
Eicosane (C_{20})	100%	107%	102%	97%	121%	94%	87%	81%	124%	123%
Heneicosane (C_{21})	95%	122%	95%	89%	110%	95%	87%	91%	113%	122%
Docosane (C_{22})	102%	111%	98%	105%	124%	103%	85%	85%	116%	130%
Tricosane (C_{23})	102%	121%	106%	105%	133%	81%	91%	88%	120%	137%
Tetracosane (C_{24})	103%	136%	114%	102%	159%	109%	86%	109%	119%	130%
Pentacosane (C_{25})	107%	103%	110%	113%	145%	151%	90%	75%	121%	148%

In general, the recoveries of individual DRO were very high (higher than 70% and near 100% in most cases). The data for the different sample sizes tested were very similar for each extraction conditions, reflecting that the amount of sample used will not influence the extraction efficiency. Therefore, the amount of sample should be optimized for each contamination episode, considering the expected concentration of the samples, and the LOQ and linear limits of the analytical method. A sample/solvent ratio of 1:2 was selected, in order to reduce the amount of solvent used, and therefore, of solvent residues. In some cases, the recovery was better with the other ratios, but the differences were lower than 10%. The extraction time of 1 h was selected, in order to assure the complete extraction of the analytes.

Therefore, for US extraction of DRO from diesel-contaminated water samples, hexane should be used as extraction solvent at 1:2 sample/solvent ratio for 1 h of extraction time. The sample size should be defined according to the sample concentration.

Optimization of accelerated solvent extraction (ASE) of DRO from soil samples

ASE parameters with the most influence on DRO extraction from diesel-spiked soils were optimized: sample size, extraction solvent, extraction temperature and extraction static cycles.

The sample size should be optimized according to the concentration, to ensure a proper analytical signal and sensitivity. The weight of a specific sample that a extraction cell will contain depends on the bulk density of the sample, the cell size and the amount of drying agent and/or sand that must be added (USEPA, 2007a). Generally, a 11-mL ASE cell will holds about 10 g of material (including drying agent and sand, if needed), and the lowest amount of soil that can be extracted without losing sensitivity is 1 g.

According to USEPA Method 3545A (USEPA, 2007a) DRO may be extracted with acetone:methylene chloride (1:1, *v/v*), acetone:hexane (1:1, *v/v*), or acetone:heptane (1:1 *v/v*). However, in Dionex Application Note 324 (Richter, 2012), for GC determination, hexane or pentane are the suitable solvents for dry samples extraction, while acetone:hexane (1:1, *v/v*), should be used to extract wet samples (greater than 40% water). According to this and to the GC column specifications (only apolar solvents can be injected), hexane was selected as extraction solvent. In case of wet samples, acetone/hexane (1:1, *v/v*) can be used, but the extract should be evaporated to a very small volume and redissolved in hexane.

Three extraction temperatures were tested: the recommended by Dionex Application Note 324 (Richter, 2012), 100 °C, the recommended by USEPA Method 3545A (USEPA, 2007a), 175 °C, and an intermediate temperature, 150 °C. The rest of extraction parameters were held constant. The peak sizes of the individual DRO obtained for each temperature are presented in figure 4.2.

In general, peak sizes of DRO in A_{Camb} extracts (Figure 4.2a) at 100 and 150 °C are very similar, and the sizes significantly increased at 175°C. In B_{Camb} (Figure 4.2b), at 100 °C higher amounts of DRO was extracted than at 150°C. The extraction temperature of 175°C was not considered, in spite of having, in general, the best extraction results, since it provoked an over pressure on the equipment and some collecting vials were broken during N_2 purge. Then, 100 °C was selected as extraction temperature, following the manufacturer recommendations (Richter, 2012).

Both Dionex Application Note 324 (Richter, 2012), and USEPA Method 3545A (USEPA, 2007a), recommend 1 extraction cycle. However, one cycle could not be enough while extracting DRO from weathered soils. Due to the wide carbon range of the DRO analyzed (C_{10} to C_{25}), they could be sorbed by

soils with very different sorption strengths. Then, 2 extraction cycles were used for DRO ASE extraction.

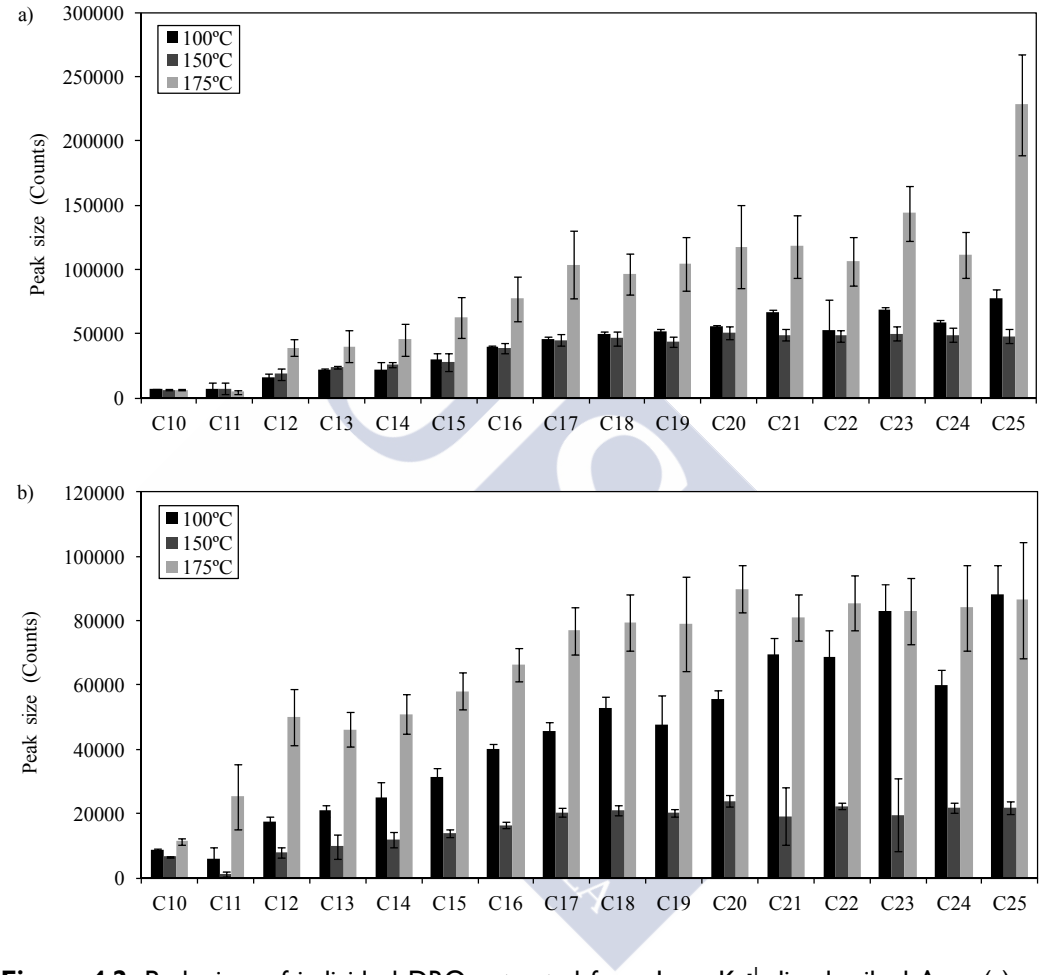

Figure 4.2. Peak sizes of individual DRO extracted from 1 mg Kg^{-1} diesel-spiked A_{Camb} (a) and B_{Camb} (b) by ASE at different temperatures (100, 150 and 175 °C).

Other extraction parameters, such as pressure, preheating time, static time, flush volume and N_2 purge time, were established based on USEPA (2007a), and Richter (2012). Table 4.3 summarizes the optimized conditions for ASE extraction of DRO from diesel-contaminated soil.

Table 4.3. Optimized values of the most important parameters in ASE of DRO from soil samples.

ASE condition	Optimum value
Sample size in 11-mL cells	1-10 g (depending on concentration)
Extraction solvent	Hexane for dry samples; acetone/hexane (1:1) for wet samples
Extraction temperature	100 °C
Number of extraction cycles	2
Pressure	1500 psi
Preheating time	8 min
Static time	5 min
Flush volume	60% of cell volume
N_2 purge time	60 s

Analytical recoveries of individual DRO extracted with ASE optimized method from 1000 mg Kg^{-1} diesel-spiked A_{Camb} and B_{Camb}, are presented in table 4.4. Matrix effect correction was carried out with the standard surrogate. Analytical recoveries of all DRO resulted between 70 and 100 %, except for decane, what validated the ASE extraction method for the majority of DRO in soils with different properties.

Table 4.4. Analytical recoveries of individual DRO extracted from 1000 mg Kg^{-1} diesel-spiked A_{Camb} and B_{Camb} by optimized ASE method.

Contaminant	A_{Camb}	B_{Camb}
Decane (C_{10})	43%	46%
Undecane (C_{11})	73%	72%
Dodecane (C_{12})	83%	80%
Tridecane (C_{13})	92%	85%
Tetradecane (C_{14})	88%	85%
Pentadecane (C_{15})	89%	85%
Hexadecane (C_{16})	91%	86%
Heptadecane (C_{17})	89%	86%
Octadecane (C_{18})	89%	85%
Nonadecane (C_{19})	88%	86%
Eicosane (C_{20})	88%	87%
Heneicosane (C_{21})	90%	88%
Docosane (C_{22})	>100%	>100%
Tricosane (C_{23})	>100%	>100%
Tetracosane (C_{24})	>100%	>100%
Pentacosane (C_{25})	>100%	>100%

HS-SPME extraction of DRO from aqueous and soil samples

The HS-SPME process and the optimized parameters for DRO extraction are very similar to that used for FO and BTEX in Chapter 3. The main difference is the extraction temperature. Due to the lower volatility of DRO comparing to FO and BTEX, different extraction temperatures were tested, 70, 80 and 90°C (with 30 min of incubation time). Figure 4.3 shows the peak sizes of individual DRO of a 25 μg L^{-1} water standard at the different extraction temperatures.

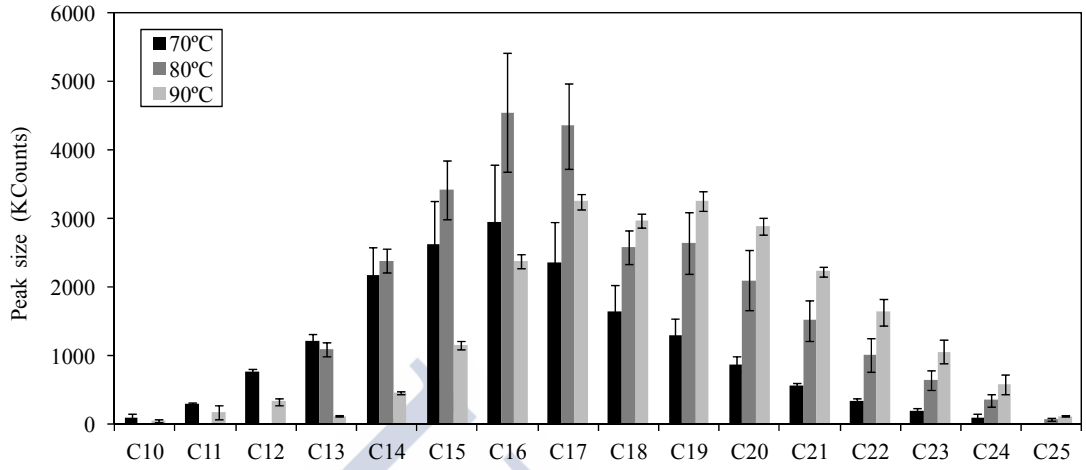

Figure 4.3. Peak sizes of individual DRO in 25 µg L^{-1} water standard analyzed by HS-SPME-GC-MS, at different incubation temperatures, and 30 min of incubation time.

The peak size of the individual DRO obtained at the extraction temperatures tested was very different: the analytical signal of C_{10}-C_{14} was higher at 70 °C, that of C_{15}-C_{17}, at 80 °C, and that of C_{18}-C_{25}, at 90 °C (Figure 4.3). Since performing 3 extractions at different temperatures would be sample and time-consuming, the extraction temperature of 90 °C was selected. This temperature offers the better signal for the highest-molecular weight DRO, which are those that would be more strongly sorbed in diesel weathered soils. Furthermore, for the rest of compounds, the analytical signal was perfectly quantifiable in the calibration range used.

The fiber desorption temperature is that recommended for a PDMS/DVB fiber, 270 °C (Supelco); and the bakeout temperature was fixed 20 °C under the desorption temperature, 250 °C. Consequently, the final parameters used for HS-SPME analysis of water and/or soil samples are summarized in table 4.5.

Table 4.5. Optimized values of the most important parameters in HS-SPME extraction of DRO from aqueous and soil samples.

Extraction parameter	Optimized value
Extraction temperature	90 °C
Pre-heating time	5 min
Extraction time	30 min
Desorption temperature	270 °C
Desorption time	5 min
Bakeout temperature	250 °C
Bakeout time	10 min
Sample size of aqueous samples	2 mL
Sample size of soil samples	Slurry of 1g of soil : 2mL of water
Agitation speed	500 rpm

As in chapter 3, this method was optimized for soil analysis, with 5 mg Kg^{-1} diesel-spiked soils, A_{Camb} and B_{Camb}. Matrix effect correction was necessary to get an accurate recovery of DRO (90-100 %) (data not shown).

GC-MS method optimization for analyzing DRO in liquid extracts and fiber injection

GC-MS methods for DRO analysis were optimized for liquid injection (after US and ASE) and then adapted for HS-SPME fiber injection. The injection conditions and the column oven temperature were optimized.

The injector temperatures tested were a constant temperature of 300 °C and a temperature ramp from 60 °C to 300 °C, at 200 °C min^{-1}. The analytical signal was 3-5 times higher when the ramp was programmed. The initial temperature is slightly lower than the vaporization temperature of hexane (69 °C), what favours a concentration effect of the analytes in the injector.

The principal problem of liquid injection is minimizing the solvent interferences and separating them from the peak analytes. The injection mode can highly influence on solvent interferences. In splitless mode, the solvent front

interferes with the analyte peaks, and in split mode (1/20), the analytical signal of the analytes decreases. The best solution was using a split/splitless mode. In this mode, the split was opened at 1/20 only a tenth of second to eliminate the solvent (if it was opened for a longer time, the signal of the first DRO decreased). Then the split was closed for 10 minutes to let the analytes enter the column and opened at 1/100 to eliminate any trace of solvent or analyte.

The DRO analyzed (C_{10}-C_{25}) have similar chemical properties as being chain alkanes. The main difference between one DRO and the previous and following compound, is a CH_2- group, whose molecular weight is always 14 g mol^{-1}. Therefore, achieving a suitable chromatographic separation of DRO was relatively simple. The main aspects when optimizing the GC-MS method was improving the analytical response of the compounds. The column oven temperature was optimized by testing different initial temperatures (40, 60 and 100 °C), final temperatures (250, 270 and 300 °C), and temperature ramps (50, 20 and 10 °C min^{-1}). The optimized the GC-MS conditions with liquid injection are those summarized in table 4.6.

Table 4.6. Optimized liquid injection-GC-MS conditions for DRO analysis after ASE or US extraction.

GS-MS condition	Optimum value
Extract volume injected	1-2.5 µL (depending on concentration)
Injector temperature	60 °C to 300 °C (held for 35 min), at 200 °C min^{-1}
Injection mode	split/splitless
Column oven temperature pattern	40 °C (held for 10 min) to 300 °C, at 10 °C min^{-1}
Carrier gas flow	Helium at 1 mL min^{-1}
MS ionization mode	Electron impact
MS ion trap temperature	220 °C

An example of chromatogram of a 1000 µg L^{-1} DRO standard is represented in figure 4.4.

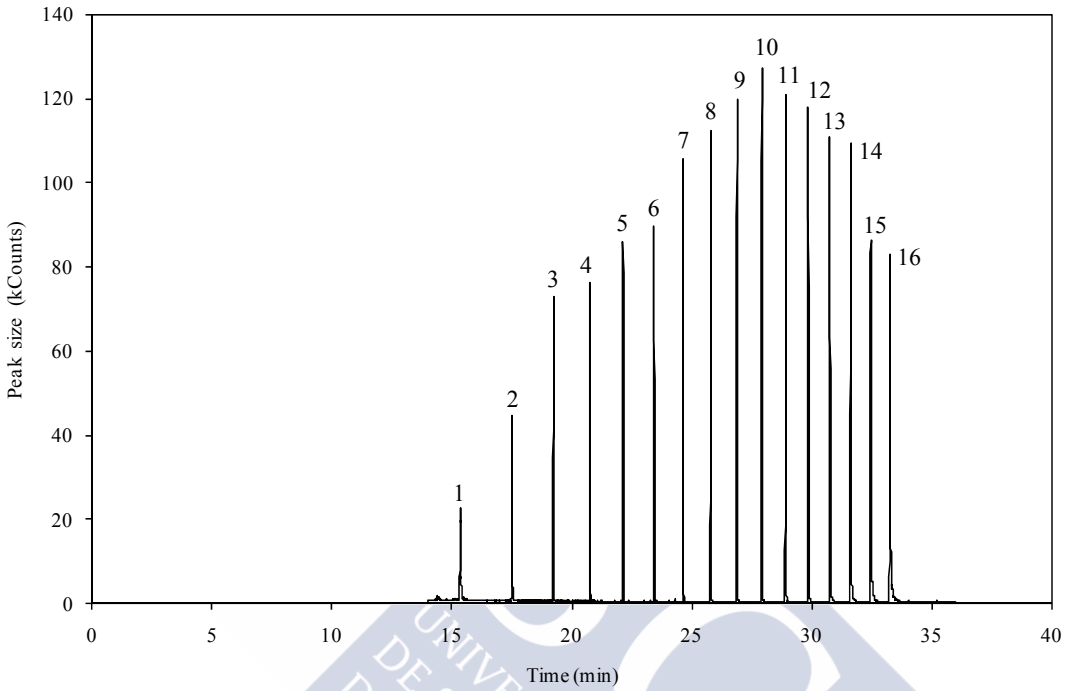

Figure 4.4. Example of liquid injection-GC-MS chromatogram of a 1000 µg L^{-1} DRO standard. The peaks correspond from decane (C_{10}) to pentacosane (C_{25}) (1 to 16).

The analytical performance characteristics of GC-MS method with liquid injection are summarized in table 4.7. Detection and quantification limits, and linearity were calculated following García Pinto *et al.* (2011).

When the previous extraction step is HS-SPME, the GC-MS conditions are those summarized in table 4.8. The main difference in the GC/MS method is the injector temperature, fixed for fiber desorption in 270 °C, in splitless mode.

Table 4.7. Analytical performance characteristics of liquid injection-GC-MS analysis of DRO.

Contaminant	LOD ($\mu g\ L^{-1}$)	LOQ ($\mu g\ L^{-1}$)	Linear range ($\mu g\ L^{-1}$)	R^2
Decane (C_{10})	4.7	10.9	15000	0.992
Undecane (C_{11})	6.2	11.6	15000	0.995
Dodecane (C_{12})	4.9	11.6	15000	0.997
Tridecane (C_{13})	1.6	3.6	15000	0.998
Tetradecane (C_{14})	6.1	12.3	15000	0.999
Pentadecane (C_{15})	5.3	8.9	15000	0.997
Hexadecane (C_{16})	5.5	10.1	15000	0.998
Heptadecane (C_{17})	5.7	10.8	15000	0.999
Octadecane (C_{18})	4.9	9.6	15000	0.999
Nonadecane (C_{19})	4.2	10.3	15000	0.999
Eicosane (C_{20})	2.9	7.0	15000	0.999
Heneicosane (C_{21})	3.0	7.2	15000	0.999
Docosane (C_{22})	2.8	6.6	15000	0.998
Tricosane (C_{23})	6.7	17.0	15000	0.999
Tetracosane (C_{24})	3.5	9.2	15000	0.999
Pentacosane (C_{25})	5.0	13.5	15000	0.999

Table 4.8. Optimized GC-MS conditions for DRO analysis after HS-SPME extraction.

GS-MS condition	Optimum value
Injector (desorption) temperature	270 °C
Injection mode	splitless
Column oven temperature pattern	40 °C (held for 10 min), 10 °C min^{-1} up to 300 °C (held for 5 min)
Carrier gas flow	Helium at 1 mL min^{-1}
MS ionization mode	Electron impact
MS ion trap temperature	220 °C

An example of chromatogram of a 50 $\mu g\ L^{-1}$ standard is represented in figure 4.5.

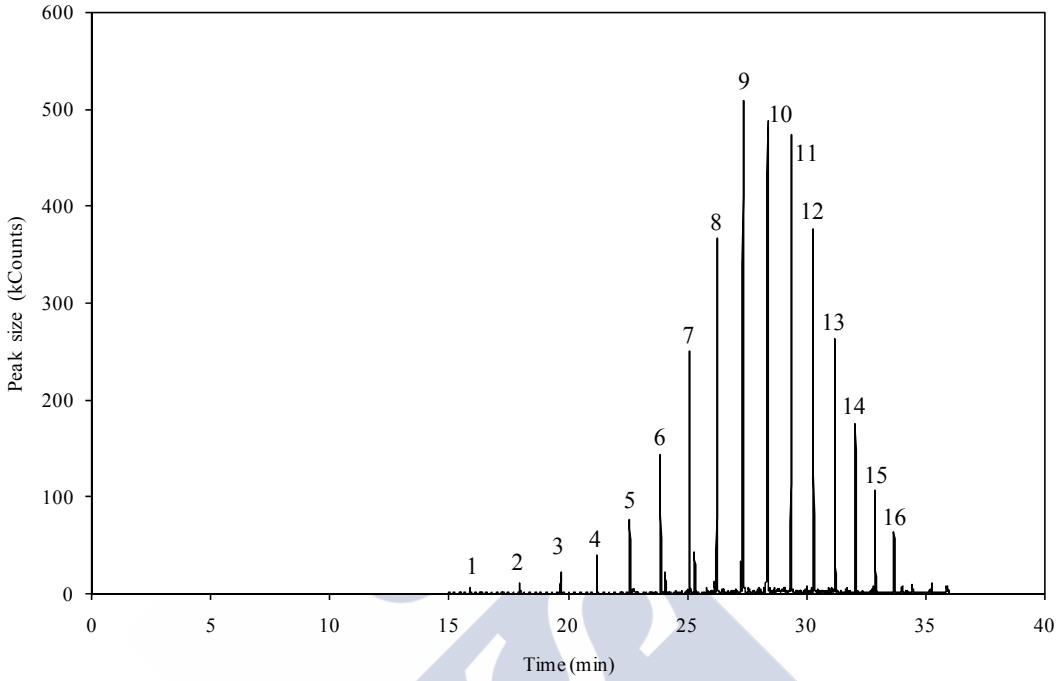

Figure 4.5. Example of HS-SPME-GC-MS chromatogram of a 50 µg L^{-1} DRO water standard. The peaks correspond from decane (C_{10}) to pentacosane (C_{25}) (1 to 16).

The analytical performance characteristics of HS-SPME-GC-MS method are summarized in table 4.9.

Table 4.9. Analytical performance characteristics of HS-SPME-GC-MS analysis of DRO.

Contaminant	LOD ($\mu g\ L^{-1}$)	LOQ ($\mu g\ L^{-1}$)	Linear range ($\mu g\ L^{-1}$)	R^2
Decane (C_{10})	2.8	5.7	50.0	0.978
Undecane (C_{11})	1.7	4.1	50.0	0.941
Dodecane (C_{12})	2.0	4.8	50.0	0.951
Tridecane (C_{13})	1.8	3.8	50.0	0.996
Tetradecane (C_{14})	0.9	2.2	50.0	0.966
Pentadecane (C_{15})	1.2	3.2	50.0	0.986
Hexadecane (C_{16})	0.9	2.5	50.0	0.987
Heptadecane (C_{17})	0.5	1.3	50.0	0.994
Octadecane (C_{18})	0.3	0.9	50.0	0.988
Nonadecane (C_{19})	0.4	1.0	50.0	0.985
Eicosane (C_{20})	0.5	1.0	50.0	0.987
Heneicosane (C_{21})	0.8	2.0	50.0	0.992
Docosane (C_{22})	1.0	2.1	50.0	0.993
Tricosane (C_{23})	1.9	4.3	12.5	0.996
Tetracosane (C_{24})	2.6	5.5	12.5	0.996
Pentacosane (C_{25})	4.2	8.0	12.5	0.988

CONCLUSIONS

The use of organic solvent extractions (US or ASE) or SPME, will depend on the concentration of the samples. SPME resulted in a more sensitive method since the quantification limits were about an order or magnitude lower than liquid extractions. Therefore SPME should be used for detect trace concentrations in environmental samples, while US extraction or ASE, are more appropriate for highly contaminated samples.

The extraction methods optimized for water and soil samples (US, ASE and SPME), efficiently extracted diesel range organics, and are therefore adequate to be used in a real contamination episode for its risk evaluation, monitorization or to make decisions about the appropriate protection of the contaminated site.

REFERENCES

Cam D, Gagni S. 2001. Determination of petroleum hydrocarbons in contaminated soils using solid-phase microextraction with gas chromatography-mass spectrometry. J Chomatogr Sci 39:481-486.

Chesler SN, Emery AP, Duewer DL. 1997. Recovery of diesel fuel from soil by supercritical fluid extraction–gas chromatography. J Chromatogr A 790:125-130.

Eriksson M, Swartling A, Dalhammar G. 1998. Biological degradation of diesel fuel in water and soil monitored with solid-phase micro-extraction and GC-MS. Appl Microbiol Biotechnol 50:129-134.

García Pinto C, Herrero Martín S, Pérez Pavón JL, Moreno Cordero B. 2011. A simplified Quick, Easy, Cheap, Effective, Rugged and Safe approach for the determination of trihalomethanes and benzene, toluene, ethylbenzene and xylenes in soil matrices by fast gas chromatography with mass spectrometry detection. Anal Chim Acta 689:129-136.

Richter P, Jiménez M, Salazar R, Maricán A. 2006. Ultrasound-assisted pressurized solvent extraction for aliphatic and polycyclic aromatic hydrocarbons from soils. J Chromatogr A 1132:15-20.

Richter B. 2012. Dionex Application Note 324. Accelerated solvent extraction of hydrocarbon contaminants (BTEX, diesel and TPH) in soils.

Schantz M. 2006. Pressurized liquid extraction in environmental analysis. Anal Bioanal Chem 386:1043-1047.

Serrano A, Gallego M. 2006. Sorption study of 25 volatile organic compounds in several Mediterranean soils using headspace–gas chromatography–mass spectrometry. J Chromatogr A 1118: 261-270.

Trapp S, Köhler A, Larsen L, Zambrano K, Karlson U. 2001. Phytotoxicity of fresh and weathered diesel and gasoline to willow and poplar trees. J Soils Sediments 1:71-76.

United States Environmental Protection Agency (USEPA). 2003. Method 5021A: Volatile organic compounds in various sample matrices using equilibrium headspace analysis. Revision 1. US Environmental Protection Agency, Washington.

United States Environmental Protection Agency (USEPA). 2007a. Method 3545A: Pressurized fluid extraction (PFE). Revision 1. US Environmental Protection Agency, Washington.

United States Environmental Protection Agency (USEPA). 2007b. Method 3550C: Ultrasonic Extraction. Revision 3. US Environmental Protection Agency, Washington.

United States Environmental Protection Agency (USEPA). 2007c. Method 8015C: Nonhalogenated organics by gas chromatography. Revision 3. US Environmental Protection Agency, Washington.

United States Environmental Protection Agency (USEPA). 2007d. Method 8270D: Semivolatile organic compounds by gas chromatography/mass spectrometry (GC/MS). Revision 4. US Environmental Protection Agency, Washington.

Wang Z, Fingas M. 1997. Developments in the analysis of petroleum hydrocarbons in oils, petroleum products and oil-spill-related environmental samples by gas chromatography. J Chromatogr A 774:51-78.

Wang Z, Li K, Fingas M, Sigouin L, Ménard L. 2002. Characterization and source identification of hydrocarbons in water samples using multiple analytical techniques. J Chromatogr A 971:173-184.

USC
UNIVERSIDADE
DE SANTIAGO
DE COMPOSTELA

5

Characterization and fingerprinting of soil and water contamination sources around a fuel distribution station in Galicia (NW Spain)

Soil and groundwater contamination around a fuel distribution station in Tomiño (Spain) was evaluated. For this purpose, several samples of superficial and subsuperficial soils and groundwater were sampled in piezometers, in addition to private well water samples. Samples were analyzed by HS-SPME-GC-MS to identify and quantify volatile organic compounds (MTBE, ETBE and BTEX) and diesel range organics (DRO). Analysis and fingerprinting data suggested that the contamination of soil and groundwater was provoked by continuous leaking of underground storage tanks. From tank nearby soils, contaminants probably migrated to surrounding soils and leached to groundwater, following a SW direction. Fingerprinting also revealed the continuity of the leak, reflected by the presence of volatiles in some samples, which only appeared in fresh leaks. MTBE was detected in very high concentration in groundwater samples, but not in fresh fuels, indicating also an old source of contamination, probably starting in the late 90s or early 2000s.

USC
UNIVERSIDADE
DE SANTIAGO
DE COMPOSTELA

INTRODUCTION

Transportation and consumption of petroleum products around the world has created the potential for oil spills into the environment. Most spills take place on marine environment, by tanker spills, and on land, including oils spills from pipelines, underground storage tanks, and aboveground storage containers (Wang *et al.*, 2006). Statistics from CONCAWE (Conservation of Clean Air and Water in Europe), reported 457 spills occurred in European pipelines from 1971 to 2012, spilling more than 80,000 m^3 of oil, and contaminating more than 100,000 m^2 of land per year, most of which was used for agricultural or industrial activities.

The fate and behaviour of spilled oils once in the soil environment, depends on a wide variety of natural processes known as weathering, including volatilization, biodegradation, photodecomposition, chemical oxidation, bioaccumulation, dispersion, diffusion, binding to soil and leaching to groundwater (Asquith *et al.*, 2012). These processes can modify the composition of the spilled oil, altering its toxicity, and also provoke the contamination of other environmental compartments. Thus, soil contamination with petroleum products involve important environmental and health risks, and therefore, it is very important to characterize, indentify, categorize, and quantify hydrocarbon sources, in order to assess those risks and applying effective clean-up procedures (Wang *et al.*, 2006).

Environmental forensics and fingerprinting are methodologies that have been developed as tools in the environmental assessment of fuel contaminants, whose main objectives are: to characterize the type of fuel causing the contamination, to quantify the concentration of potentially environmentally hazardous compounds, to investigate the degree of chemical and biological degradation of contaminants, and to determine their source, fate and transport in the environment, using the

compositional patterns of the fuel contaminants (Alimi *et al.*, 2003). In order to carry out these fingerprinting procedures, several instrumental techniques are used, including gas chromatography (GC), gas chromatography-mass spectrometry (GC/MS), high-performance liquid chromatography (HPLC), infrared spectroscopy (IR), and isotope ratio mass spectrometry (IRMS). A wide variety of target analytes can be determined by those techniques in order to characterize the contamination episode and identify the sources: a) aliphatic hydrocarbons, including *n*-alkanes, and isoprenoids as pristane and phytane; b) single-ring volatile aromatic hydrocarbons (so-called BTEX compounds) and other volatiles (fuel oxygenates as MTBE, ETBE or TAME); c) polycyclic aromatic hydrocarbons (PAH); d) biomarkers, including terpanes and steranes; and e) total petroleum hydrocarbons (TPH) and unresolved complex mixtures (UCM), in some cases (Wang *et al.*, 1999).

In this context, the aim of the present work was to evaluate soil and groundwater contamination levels of volatile organic compounds (VOC) including MTBE, ETBE and BTEX, and diesel range organics (DRO), including *n*-alkanes from C_{10} to C_{25}, derived from a spill caused by an fuel distribution station in Tomiño (Galicia, NW Spain). With these data, we fingerprinted the direction of the spill plume, estimated its age and discriminated direct from indirect contamination sources.

MATERIALS AND METHODS

Description of the study area

The study area is located in Tomiño, a small town from the south of Galicia (NW Spain) (Figure 5.1). The climate is humid oceanic, with arid trend during the summer period. Annual average temperatures ranged from 8 to 17 °C and annual rainfall was 1895 mm (2013 data).

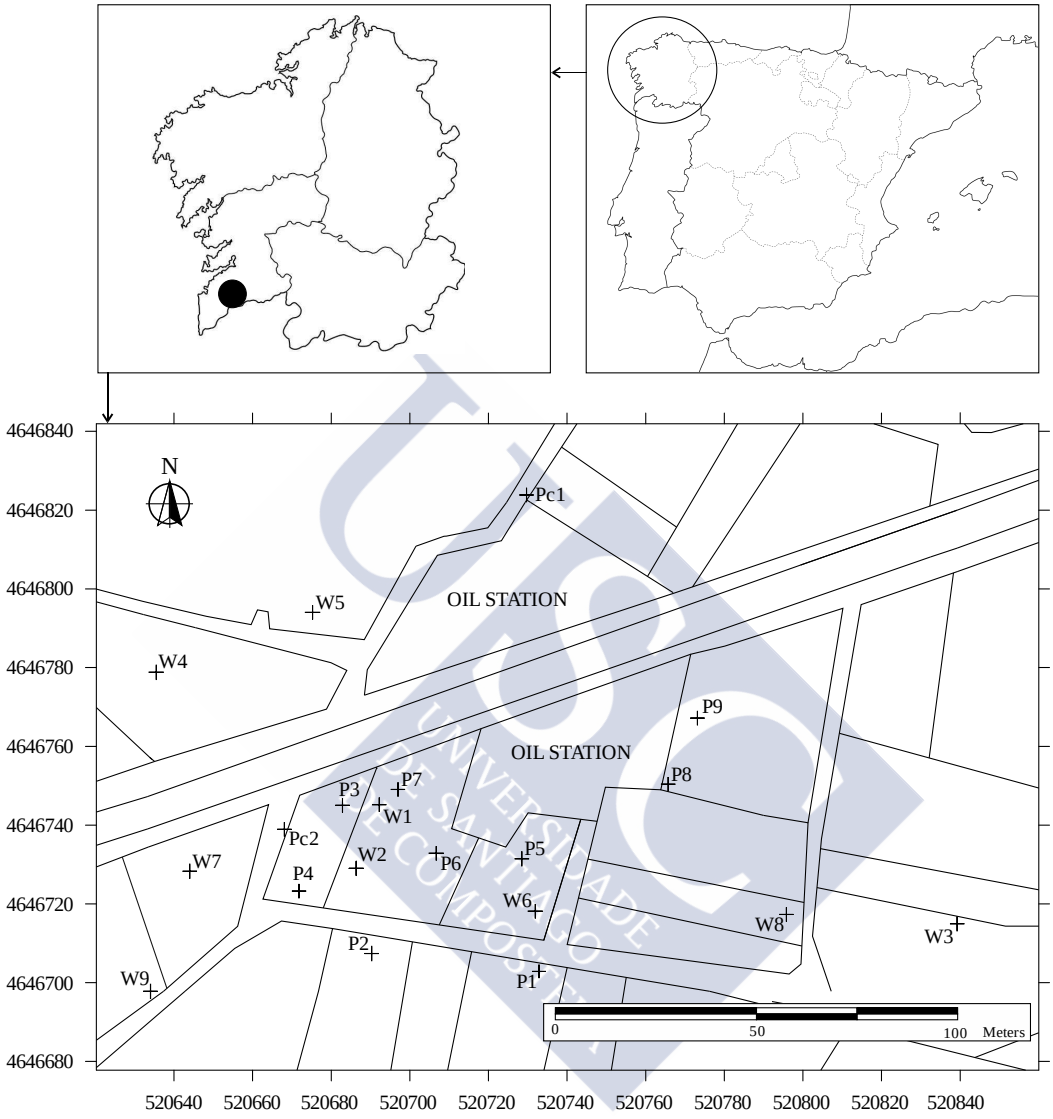

Figure 5.1. Location of the study area in Tomiño (NW Spain) and the sampling points.

The area is surrounded by mountains and valleys around the Miño river, the most important river of Galicia, and a natural frontier between Spain and North Portugal. Geologically, Tomiño is included in a metasedimentary precambric formation, with granitic, pegmatitic and quartztic intrusions. Near Miño river basin, there are quaternary alluvial deposits, principally formed by sand and

gravels, over the metasedimentary materials. Soils developed over these materials, are derived from granite and granodiorite alteration, with a sandy loam texture and ochre colours. The predominant vegetation are brushwood, and oak, alder, bay laurel or birch forest, alternating with important extensions dedicated to agriculture and residential areas.

The contamination episode was provoked by two oil distribution stations built in 1984 and located at both sides of a high-traffic road. They are immediately surrounded by parcels with private houses, gardens and agricultural fields (Figure 5.1). Furthermore, the area is crossed by many small rivers that flow with a north-southwest direction into Miño river, located at only 700 m from the oil stations.

Sampling procedures

i. Groundwater sampling

In August and October of 2012, groundwater samples were collected from nine private wells (W1-W9) and from eleven piezometers (P1-P9 and two control piezometers previously placed by the government, Pc1 and Pc2) situated in the vicinity of the oil stations. Brown jars were used to collect the samples, and they were completely filled, leaving no headspace. The samples were sealed, labelled and stored at 4 °C until analysis.

Groundwater samples collected in wells an piezometers tended to acidity or neutrality (pH=6.41±0.67 in piezometers and 5.17±0.35, in wells) and presented low ionic concentrations (conductivity=301.44±104.38 μS cm^{-1} in piezometers and 183.67±30.73 μS cm^{-1} in wells) (Table 5.1). Relatively high nitrate concentrations were found, especially, in well samples (NO_3^-=20.44±14.81 mg L^{-1} in piezometers and 35.18±13.52 mg L^{-1} in wells), reflecting the agricultural activity developed in the site.

Table 5.1. Chemical composition of water samples collected in the vicinity of the oil stations in August (2012). Mean values (± standard deviation, SD), and minimum (min) and maximum values (max), of piezometer and well samples are presented.

	Piezometers			Wells		
	mean ± SD	min	max	mean ± SD	min	max
pH	6.41 ± 0.67	5.26	7.48	5.17 ± 0.35	4.78	5.72
Conductivity ($\mu S\ cm^{-1}$)	301.44 ± 104.38	185.00	464.00	183.67 ± 30.73	151.00	243.00
Cl^- ($mg\ L^{-1}$)	20.42 ± 3.20	16.09	24.22	18.90 ± 3.00	14.59	22.94
NO_3^- ($mg\ L^{-1}$)	20.44 ± 14.81	1.02	40.60	35.18 ± 13.52	17.30	53.06
SO_4^{-2} ($mg\ L^{-1}$)	25.39 ± 16.33	10.25	63.19	19.08 ± 4.37	13.65	27.54
Ca ($mg\ L^{-1}$)	45.51 ± 31.61	13.00	100.60	10.65 ± 2.20	7.81	15.20
Mg ($mg\ L^{-1}$)	5.27 ± 2.24	3.20	10.00	3.29 ± 0.64	2.40	4.60
Na ($mg\ L^{-1}$)	20.49 ± 6.95	10.15	34.96	17.60 ± 2.59	13.67	20.38
K ($mg\ L^{-1}$)	7.25 ± 3.36	1.66	12.11	7.33 ± 2.37	2.82	10.21

ii. Soil sampling

Two samples of two different depths (between 0.4 and 6.4 m) were collected from the purge of the piezometers P1-P9 (18 samples). The sample depths were chosen based on organoleptic observation, such as smell, changes in colour, etc (Table 5.2). Samples showed a humidity of 5-24% (*w/w*), tended to acidity pHs (pH=5.7±0.6) and had a low carbon concentration (3.1±1.4 g Kg^{-1}). Furthermore, 4 superficial samples were collected in October (2012) in the nearness of selected piezometers (P3, P4, P6 and P7).

Soil samples were stored in brown jars completely filled, without headspace. Then, they were sealed, labelled and stored at 4 °C until analysis.

Table 5.2. Depths of each soil sampling point (piezometers sampled in August, 2012), chosen for analysis.

	P1	P2	P3	P4	P5	P6	P7	P8	P9
Chosen sample depths (m)	0.4	0.9	3.8	1.5	1.7	4.1	1.8	2.8	1.9
	1.5	3.0	5.0	3.2	3.6	6.4	3.5	4.8	4.6

Extraction and analysis of VOC and DRO

Volatile organic compounds (VOC), including fuel oxygenates (FO), i.e. MTBE and ETBE, and BTEX (benzene, toluene, ethylbenzene and xylene) and diesel range organics (DRO) were analyzed by head space-solid phase microextraction (HS-SPME) in both soil and groundwater samples (Chapters 3 and 4).

In HS-SPME analysis of contaminated water and soil samples, VOA (volatile organic analysis) vials containing the samples (2 mL in case of water or a slurry in case of soil samples, 1 g of sample:2mL of distilled water) were heated in the HS oven of the Combi PAL autosampler (Agilent Technologies), at 80°C for VOC and 90°C for DRO, with constant agitation, for 30 min. A 75 µm Carboxen-PDMS fiber, in case of VOC, and a 65 µm PDMS/DVB fiber (Supelco) in case of DRO analysis, was introduced in the vial during oven equilibration, to absorb the analytes in the HS. The fiber was then thermally desorbed in the injector for 5 min at 300 °C in 1/10 split, or at 270 °C in splitless mode, respectively. VOC and DRO water and soil concentrations were determined by gas chromatography (Model 450 GC, Agilent Technologies) coupled to mass spectrometry (Model 220 MS, Agilent Technologies) (GC/MS). Fluorobenzene (Sigma Aldrich Co, LLC) was added to VOC soil vials at 2500 µg L^{-1}, and *p*-terphenyl-d_{14} (AccuStandard, Inc.) was added to DRO soil vials at 50 µg L^{-1}, and stabilized for 7 days before analysis, in order to correct the soil matrix effect.

VOC calibration standards were prepared in VOA vials with 2 mL of distilled water containing 0.5 to 2500 µg L^{-1} of individual MTBE, ETBE and BTEX (Panreac Química, S.L.U.). DRO calibration standards, were prepared with a mixture of C_{10}-C_{25} *n*-alkanes (DRO mix, Dr. Ehrenstorfer) in the range of 0.5 to 50 µg L^{-1}.

Chromatographic separations were performed by a FactorFour VF-5ms EZ-Guard capillary column (30 m x 0.25 mm x 0.25 µm, Agilent Technologies) that

operated with the following oven temperature programs: for BTEX, 35 °C (held for 5 min), 10 °C min^{-1} up to 80 °C and 25 °C min^{-1} up to 200 °C (held for 0.7 min); and for DRO, 40 °C (held for 10 min) to 300 °C, at 10 °C min^{-1} (held for 5 min). Helium was used as carrier gas, at constant flow 1 mL min^{-1}. The mass spectrometer operated in full scan mode. Ionization of the molecules was carried out by electron impact (EI) and the ion trap temperature was fixed at 220 °C.

Gasoline and diesel purchased in the north distribution station were also analysed (in water dilution) by HS-SPME-GC-MS to characterize the VOC and DRO profile (this last only for diesel).

Calculation of hydrocarbon indices with DRO analysis data

The analysis data of the 16 individual *n*-alkane, or diesel range organics (DRO), from C_{10} (decane) to C_{25} (pentacosane), in soil and groundwater samples was used to calculate the concentration of the sum of DRO (∑DRO) and other hydrocarbon indices: carbon preference index (CPI) (odd to even *n*-alkane concentration ratio), low ($\leq C_{20}$) to high molecular weight ($\geq C_{21}$) alkanes concentration ratio (L/HMW), concentration ratio of ∑DRO to hexadecane (C_{16}) (C_{16} ratio) and the carbon number with the maximum concentration (C_{max}).

Statistical analysis

PASW Statistics software (Version 20.0.0; IBM SPSS Statistics, Inc.) was used to analyze the data.

Pearson correlations were carried out between individual VOC and DRO concentrations in all soil or water samples.

Principal component analysis with VOC or DRO concentrations was used to simplify the analysis data by decreasing the dimension, to explain hydrocarbon composition of soil and water samples, and to discriminate pollution sources

(Faure *et al.*, 2007; Zhang *et al.*, 2012). Individual VOC or DRO concentrations in soil and groundwater were chosen as variables, and the sampling points as cases. In addition, for DRO, carbon preference index (CPI) was included as a variable in order to help in discriminating direct or indirect sources.

RESULTS

Concentration of volatile organic compounds (VOC) in soil and groundwater samples

Soil VOC concentration varied from values under the limits of detection (LOD) to very high values. High concentrations of BTEX compounds were found, especially, in P3, P4, P5, P6, P7, P8 and P9 (between 219 and 3837 μg ∑BTEX Kg^{-1} in P9 (1.9 m) and P4 (0.0 m), respectively) (Table 5.3). Only very high concentrations of MTBE and ETBE were found in superficial soils: up to 3589 μg MTBE Kg^{-1} and 1419 μg ETBE Kg^{-1} were analyzed in P3 (0.0 m) (Table 5.4).

Spanish law on contaminated soils (Real Decreto 9/2005) establishes contamination limits of 0.1, 3.0, 2.0 and 35.0 mg Kg^{-1} of benzene, toluene, ethylbenzene and xylene, respectively, for the protection of ecosystems. Following those limits, samples soils would not involve any risk, except superficial samples (0.0 m) of P3, P4, P6 and P7, which doubled in some cases, the limit concentration of benzene.

Table 5.3. Concentration of individual VOC (μg Kg^{-1}) in soil samples collected in August (2012) from piezometer material at selected depths. Samples of superficial soils (0.0 m depth) collected in October (2012) are also included.

Sample	MTBE	ETBE	Benzene	Toluene	Ethylbenzene	*m/p*-Xylene	*o*-Xylene
P1 (0.4 m)	<LOD	<LOD	<LOD	<LOD	<LOD	<LOD	<LOD
P1 (1.5 m)	<LOD	<LOD	<LOD	<LOD	<LOD	<LOD	<LOD
P2 (0.9 m)	<LOD	<LOD	<LOD	<LOD	<LOD	75.51	<LOD
P2 (3.0 m)	<LOD	<LOD	<LOD	<LOD	<LOD	<LOD	<LOD
P3 (0.0 m)	3588.82	1419.05	187.96	646.22	884.55	667.12	931.64
P3 (3.8 m)	<LOD	<LOD	<LOD	129.46	88.38	70.92	<LOD
P3 (5.0 m)	<LOD	34.54	<LOD	116.42	79.05	63.54	<LOD
P4 (0.0 m)	2878.65	1326.88	235.35	823.64	1018.51	746.09	1013.40
P4 (1.5 m)	108.81	53.16	<LOD	126.83	89.87	74.18	88.20
P4 (3.2 m)	<LOD	54.46	<LOD	122.75	86.61	66.31	<LOD
P5 (1.7 m)	<LOD	<LOD	<LOD	<LOD	<LOD	<LOD	<LOD
P5 (3.6 m)	103.33	51.68	<LOD	134.17	96.07	79.02	88.20
P6 (0.0 m)	2671.95	1261.87	133.48	599.73	884.21	720.55	1053.12
P6 (4.1 m)	185.27	202.06	<LOD	154.69	124.15	93.64	137.30
P6 (6.4 m)	100.90	43.38	<LOD	120.05	82.67	67.36	81.90
P7 (0.0 m)	2623.70	1192.12	170.54	555.24	733.29	546.17	804.01
P7 (1.8 m)	<LOD	<LOD	<LOD	<LOD	<LOD	65.09	<LOD
P7 (3.5 m)	<LOD	<LOD	<LOD	<LOD	<LOD	<LOD	<LOD
P8 (2.8 m)	<LOD	<LOD	<LOD	<LOD	<LOD	<LOD	<LOD
P8 (4.8 m)	<LOD	40.49	<LOD	122.41	86.74	66.78	87.66
P9 (1.9 m)	<LOD	<LOD	<LOD	140.64	<LOD	75.61	<LOD
P9 (4.6 m)	<LOD	36.27	<LOD	127.87	87.22	69.50	86.20

<LOD: under limit of detection, i.e. 1.9, 0.5, 0.5, 0.8, 1.1, 0.9, and 2.6 μg L^{-1} for MTBE, ETBE, benzene, toluene, ethylbenzene, m/p-xylene and o-xylene, respectively.

Water samples with high VOC contamination (Table 5.4), were taken in sampling points in the southwest of the site: P3, P7, Pc2, W1 and W7. They mainly contain fuel oxygenates (MTBE and ETBE): MTBE concentrations varied from 25 to 692 μg L^{-1}; and ETBE concentrations, varied from 17 to 689 μg L^{-1}. Low concentrations of BTEX were found in groundwater samples (under 7 μg Kg^{-1}, except for benzene in P3-O and P7-O).

Table 5.4. Concentration of individual VOC (μg L^{-1}) in water samples collected in August (2012) (sample code-A) and October (2012) (sample code-O) from piezometers and wells.

Sample	MTBE	ETBE	Benzene	Toluene	Ethylbenzene	*m/p*-Xylene	*o*-Xylene
P1-A	<LOD	7.11	<LOD	<LOD	<LOD	<LOD	<LOD
P1-O	<LOD	24.46	<LOD	<LOD	<LOD	4.58	<LOD
P2-A	<LOD	<LOD	<LOD	<LOD	<LOD	5.53	<LOD
P2-O	<LOD	<LOD	<LOD	<LOD	<LOD	<LOD	<LOD
P3-A	600.58	689.08	<LOD	<LOD	<LOD	<LOD	<LOD
P3-O	256.29	207.55	34.24	<LOD	<LOD	<LOD	<LOD
P4-A	<LOD	<LOD	<LOD	<LOD	<LOD	4.97	<LOD
P4-O	<LOD	<LOD	<LOD	<LOD	<LOD	<LOD	<LOD
P5-A	<LOD	42.92	<LOD	<LOD	<LOD	4.88	<LOD
P5-O	<LOD	42.82	<LOD	<LOD	<LOD	<LOD	<LOD
P6-A	<LOD	<LOD	<LOD	<LOD	<LOD	4.89	<LOD
P6-O	<LOD	<LOD	<LOD	3.86	5.99	6.75	4.65
P7-A	691.49	399.23	<LOD	<LOD	<LOD	<LOD	<LOD
P7-O	165.90	154.16	394.84	4.20	<LOD	15.11	11.65
P8-A	<LOD	<LOD	<LOD	<LOD	<LOD	5.47	<LOD
P9-A	<LOD	<LOD	<LOD	<LOD	<LOD	4.84	<LOD
Pc1-A	<LOD	<LOD	<LOD	<LOD	<LOD	4.86	<LOD
Pc2-A	25.25	16.68	<LOD	<LOD	<LOD	<LOD	<LOD
Pc2-O	58.41	39.96	<LOD	<LOD	<LOD	<LOD	<LOD
W1-A	503.04	278.64	<LOD	<LOD	<LOD	4.85	<LOD
W1-O	90.62	82.76	<LOD	<LOD	<LOD	3.95	<LOD
W2-A	<LOD	<LOD	<LOD	<LOD	<LOD	5.15	<LOD
W2-O	42.12	15.80	<LOD	<LOD	<LOD	<LOD	<LOD
W3-A	<LOD	<LOD	<LOD	<LOD	<LOD	<LOD	<LOD
W4-A	<LOD	<LOD	<LOD	<LOD	<LOD	5.25	<LOD
W5-A	9.12	<LOD	<LOD	<LOD	6.66	2.45	6.52
W6-A	<LOD	<LOD	<LOD	<LOD	<LOD	<LOD	<LOD
W6-O	<LOD	<LOD	<LOD	<LOD	<LOD	<LOD	<LOD
W7-A	94.92	67.11	<LOD	<LOD	<LOD	5.03	<LOD
W7-O	148.37	82.14	<LOD	<LOD	<LOD	4.33	<LOD
W8-A	<LOD	<LOD	<LOD	<LOD	<LOD	5.21	<LOD
W9-A	9.40	<LOD	<LOD	<LOD	<LOD	4.89	<LOD

<LOD: under limit of detection, i.e. 1.9, 0.5, 0.5, 0.8, 1.1, 0.9, and 2.6 μg L^{-1} for MTBE, ETBE, benzene, toluene, ethylbenzene, m/p-xylene and o-xylene, respectively.

VOC concentrations in October were higher than in August, in P1, P6, Pc2, W2 and W7, and were lower in P2, P3, P4, P5, P7 and W1.

Spanish law on the quality of water for human consumption (Real Decreto 140/2003), establishes a limit of 1 μg L^{-1} for benzene, exceeded in October in P3 and P7 samples. USEPA (1997) establishes the odour and taste threshold of MTBE in 20 and 40 μg L^{-1}, respectively, and these values can be used as the limit for human consumption. Spanish regulation on groundwater quality (Real Decreto 1514/2009) does not establish limits for organic contaminants. Thus, Dutch reference quality values for groundwater are often used: 0.2, 4, 7 and 0.2 μg L^{-1} of benzene, toluene, ethylbenzene and xylene, respectively. In general, within those values, VOC contaminated groundwater samples exceeded the quality limits required.

Concentration of diesel range organics (DRO) in soil and groundwater samples and hydrocarbon indices

The sum of 16 *n*-alkanes analyzed in soil samples, C_{10}-C_{25} (∑DRO), varied from 39 to 951 μg Kg^{-1} (in P6 (6.4 m) and P6 (0.0 m), respectively), being always significantly higher in less deep soils (Table 5.5). In groundwater samples (Table 5.6), ∑DRO concentration did not varied in such a wide range as soil samples (6-109 μg L^{-1}). Groundwater ∑DRO concentrations in a same sampling point were in general comparable or higher in August than in October, except in P2 and P7.

Carbon preference index (CPI) can help to determine the origin of the hydrocarbon contamination. Values around 1, indicate the presence of petroleum derived *n*-alkanes (Harji *et al.*, 2008). Generally, CPI of superficial soils (0.0 m) and P1 (0.4 m), P1 (1.5 m) or P4 (1.5 m) were lower or higher than unity (Table 5.5), indicting another type of source. Deeper soil samples had CPI values around 0.8-1.0 (Table 5.5), except P7, indicating a petrogenic origin of the contamination.

CPI values of groundwater samples (Table 5.6) were generally lower than unity, indicating than the contamination was not directly spilt into groundwater.

Low to high molecular weight *n*-alkane concentration ratio (L/HMW) of petroleum sources is close to unity, whereas it is higher in plankton and algae, and lower in higher plants (Zhang *et al.*, 2012). This ratio is normally calculated with *n*-alkanes up to C_{35} or C_{40}, whereas in these soil samples (Table 5.5) only alkanes in the diesel range (up to C_{25}) were quantified. Therefore, those indexes were higher than unity in most cases. Despite the calculation, L/HMW index can be used to assess the distribution of DRO in soil depth profile. In general, L/HMW decreased with the increasing depth, except P7, indicating and enrichment of superficial layers with light DRO. Groundwater samples (Table 5.6) showed very high L/HMW ratios, indicating a higher concentration of light alkanes (also the least hydrophobic).

∑DRO to hexadecane concentration ratio (C_{16} ratio) is usually higher for biogenic hydrocarbons (i.e. 50) and low (i.e. 15) for petroleum-contaminated samples. Hexadecane was suggested to be characteristic of petrogenic hydrocarbons and it is rarely found in biolipids (Zhang *et al.*, 2012). C_{16} ratio values of soil samples (Table 5.5) were generally near 30, indicating a probable petrogenic input except for the superficial soils (0.0 m) and not very deep soils (<2 m). C_{16} ratio values of groundwater samples (Table 5.6) varied from 7.95 to 118.07. This high variation probably reflected a non-direct spill in groundwater.

C_{max} gave an idea of the alkanes with the highest concentration in samples. In soil (Table 5.5), except superficial soils, HMW alkanes were those with the highest concentration. In groundwater samples (Table 5.6), the C_{max} was completely the opposite, and LMW DRO were those appearing in higher proportion.

Table 5.5. Concentration of the sum of DRO and hydrocarbon indices of soil samples collected in August (2012) from piezometer material at selected depths. Samples of superficial soils (0.0 m depth) collected in October(2012) are also included.

Sample	∑DRO (μg Kg^{-1})	CPI [a]	L/HMW [b]	C_{max} [c]	C_{16} ratio [d]
P1 (0.4 m)	286.50	0.45	2.31	C_{10}	68.80
P1 (1.5 m)	143.38	1.24	1.13	C_{25}	47.27
P2 (0.9 m)	61.30	0.95	1.23	C_{24}	31.12
P2 (3.0 m)	49.74	0.92	1.01	C_{24}	32.97
P3 (0.0 m)	330.26	0.77	1.83	C_{12}	26.10
P3 (3.8 m)	133.04	0.88	1.59	C_{25}	25.95
P3 (5.0 m)	67.10	0.80	1.67	C_{10}	37.12
P4 (0.0 m)	786.44	0.98	1.48	C_{10}	50.81
P4 (1.5 m)	254.89	0.78	1.52	C_{10}	64.79
P4 (3.2 m)	88.80	1.01	0.72	C_{25}	33.96
P5 (1.7 m)	44.00	1.00	0.74	C_{24}	31.69
P5 (3.6 m)	60.46	0.79	0.72	C_{25}	29.39
P6 (0.0 m)	951.14	1.28	2.19	C_{10}	49.02
P6 (4.1 m)	55.59	0.97	0.99	C_{24}	34.26
P6 (6.4 m)	39.22	0.85	1.03	C_{24}	29.13
P7 (0.0 m)	256.44	1.41	0.62	C_{25}	46.72
P7 (1.8 m)	56.01	0.74	1.64	C_{10}	26.96
P7 (3.5 m)	50.88	0.73	1.64	C_{10}	34.50
P8 (2.8 m)	51.84	0.76	1.42	C_{24}	27.81
P8 (4.8 m)	47.83	0.84	1.21	C_{24}	27.61
P9 (1.9 m)	47.56	0.93	1.12	C_{24}	34.12
P9 (4.6 m)	49.15	0.96	0.97	C_{24}	29.59

[a] *CPI: Carbon preference index: odd to even n-alkane concentration ratio.*
[b] *L/HMW: low (≤C_{20}) to high molecular weight (≥C_{21}) n-alkane concentration ratio.*
[c] *C_{max}: carbon number of maximum concentration in decreasing order.*
[d] *C_{16} ratio: ratio of ∑DRO to hexadecane concentration.*

Neither Spanish regulation on contaminated soils (Real Decreto 9/2005) nor Dutch regulation, establish limits for chain hydrocarbons. On the other hand, Dutch objective quality values of groundwater determine the limit concentration of mineral oil (alkanes from C_{10} to C_{40}) in 50 μg L^{-1}. Despite only alkanes to C_{25} were analysed, the majority of water samples had ∑DRO values that exceeded the quality value (Table 5.6).

Table 5.6. Concentration of the sum of DRO and hydrocarbon indices of groundwater samples collected in August (2012) (sample code-A) and October (2012) (sample code-O) from piezometers and wells.

Sample	∑DRO (μg L^{-1})	CPI [a]	L/HMW [b]	C_{max} [c]	C_{16} ratio [d]
P1-A	55.35	0.27	19.05	C_{10}	49.56
P1-O	6.24	0.86	8.13	C_{14}	7.95
P2-A	27.66	0.56	18.17	C_{10}	14.77
P2-O	49.06	0.50	3.79	C_{10}	46.45
P3-A	45.99	0.49	65.05	C_{10}	28.32
P3-O	43.67	0.72	74.68	C_{10}	54.75
P4 -A	101.36	0.65	18.45	C_{10}	118.07
P4-O	19.61	2.54	12.65	C_{11}	20.42
P5-A	90.06	0.27	80.80	C_{10}	81.17
P5-O	57.16	0.32	72.28	C_{10}	63.39
P6-A	89.81	0.30	24.89	C_{10}	56.22
P6-O	53.71	0.39	30.10	C_{10}	52.27
P7-A	35.74	0.28	37.91	C_{10}	39.35
P7-O	79.32	0.31	28.37	C_{10}	52.11
P8-A	60.30	0.20	63.28	C_{10}	83.70
P9 -A	75.35	0.48	98.10	C_{10}	70.27
Pc1-A	109.37	0.63	7.50	C_{10}	10.93
Pc2-A	103.72	0.31	19.71	C_{10}	109.96
Pc2-O	33.10	2.61	4.30	C_{11}	27.06
W1-A	61.77	0.84	8.63	C_{10}	50.16
W1-O	65.40	0.51	19.46	C_{10}	47.19
W2-A	22.83	0.28	16.71	C_{10}	14.61
W2-O	12.67	0.58	11.57	C_{12}	8.56
W3-A	83.46	0.34	103.30	C_{10}	57.01
W4-A	23.64	0.99	3.43	C_{11}	22.91
W5-A	35.00	0.65	6.86	C_{10}	32.50
W6-A	64.39	0.94	5.36	C_{11}	15.17
W6-O	54.88	0.58	10.27	C_{10}	67.01
W7-A	48.05	0.62	10.78	C_{10}	45.84
W7-O	31.01	0.79	15.96	C_{10}	29.87
W8-A	94.55	0.43	26.89	C_{10}	72.61
W9-A	38.99	0.34	23.05	C_{10}	36.43

[a] *CPI: Carbon preference index: odd to even n-alkane concentration ratio.*
[b] *L/HMW: low (≤C_{20}) to high molecular weight (≥C_{21}) n-alkane concentration ratio.*
[c] *C_{max}: carbon number of maximum concentration in decreasing order.*
[d] *C_{16} ratio: ratio of ∑DRO to hexadecane concentration.*

Correlation between VOC and DRO concentrations in soil and groundwater samples

Correlations between individual VOC and DRO concentrations in all soil or water samples were carried out, in order to investigate if the source of all contaminants was consistent (Tables 5.7 and 5.8). Significant correlations were found in soil samples between all contaminants analyzed (Table 5.7); whereas, only significant correlations were found among BTEX or DRO in groundwater samples (Table 5.8).

DISCUSSION

Source identification and fingerprinting of DRO and VOC in the fuel spill

Soil samples taken near the oil stations were analysed for MTBE, ETBE, BTEX and *n*-alkanes in the diesel range (DRO) (C_{10}-C_{25}). In general, high concentrations of those contaminants were found in sampling points around the south oil distribution station (P3, P4, P5, P6, P7, P8 and P9). Volatile organics concentrations were higher in superficial samples (Table 5.3), especially of MTBE and ETBE, what can be probably related to the watering of those soils (placed in private gardens and agricultural fields) with contaminated well water enriched in MTBE and ETBE (Table 5.4). Carbon preference indices (CPI) of deep soil samples (Table 5.5) were, in general, near unity, and C_{16} ratios were high, indicating a petrogenic origin, and that the leak was taking place in subsuperficial soil layers. CPI values of superficial soils were far from unity (Table 5.5), reflecting a non-direct contamination source, what would agree with the contribution by irrigation with contaminated water.

Table 5.7. Coefficients of Pearson correlations performed between the concentration of individual VOC and DRO in all soil samples (Significant correlation: *p<0.05; **p<0.01).

	MTBE	ETBE	Benzene	Toluene	Ethylbenzene	*m*/*p*-Xylene	*o*-Xylene	C_{10}	C_{11}	C_{12}	C_{13}	C_{14}	C_{15}	C_{16}	C_{17}	C_{18}	C_{19}	C_{20}	C_{21}	C_{22}	C_{23}	C_{24}	C_{25}
MTBE	1	0.99**	0.97**	0.95**	0.98**	0.98**	0.98**	0.78**	0.74**	0.54**	0.86**	0.85**	0.84**	0.87**	0.82**	0.79**	0.77**	0.79**	0.87**	0.79**	0.83**	0.70**	0.77**
ETBE		1	0.97**	0.96**	0.99**	0.99**	0.99**	0.74**	0.74**	0.55**	0.87**	0.84**	0.87**	0.88**	0.90**	0.82**	0.80**	0.83**	0.90**	0.82**	0.86**	0.71**	0.79**
Benzene			1	0.96**	0.97**	0.96**	0.96**	0.68**	0.63**	0.54**	0.86**	0.83**	0.82**	0.86**	0.90**	0.77**	0.74**	0.79**	0.87**	0.80**	0.85**	0.74**	0.81**
Toluene				1	0.98**	0.98**	0.97**	0.68**	0.68**	0.48*	0.84**	0.81**	0.84**	0.86**	0.90**	0.77**	0.75**	0.80**	0.88**	0.80**	0.84**	0.71**	0.79**
Ethylbenzene					1	0.99**	0.99**	0.72**	0.74**	0.48*	0.87**	0.84**	0.89**	0.89**	0.91**	0.82**	0.80**	0.84**	0.91**	0.84**	0.88**	0.73**	0.81**
***m*/*p*-Xylene**						1	0.99**	0.72**	0.76**	0.47*	0.87**	0.83**	0.90**	0.88**	0.91**	0.83**	0.82**	0.84**	0.92**	0.86**	0.89**	0.72**	0.80**
***o*-Xylene**							1	0.71**	0.76**	0.48*	0.89**	0.82**	0.91**	0.89**	0.92**	0.85**	0.84**	0.87**	0.93**	0.86**	0.89**	0.73**	0.81**
C_{10}								1	0.81**	0.13	0.44*	0.68**	0.51*	0.69**	0.49*	0.48*	0.42*	0.47*	0.52*	0.52*	0.53**	0.47*	0.54**
C_{11}									1	0.03	0.60**	0.66**	0.80**	0.79**	0.67**	0.76**	0.73**	0.76**	0.75**	0.78**	0.77**	0.62**	0.69**
C_{12}										1	0.66**	0.63**	0.38	0.50*	0.59**	0.50*	0.46*	0.41*	0.47*	0.36	0.41	0.39	0.36
C_{13}											1	0.85**	0.91**	0.84**	0.95**	0.93**	0.94**	0.92**	0.94**	0.87**	0.89**	0.75**	0.78**
C_{14}												1	0.75**	0.90**	0.85**	0.82**	0.74**	0.77**	0.80**	0.76**	0.77**	0.72**	0.74**
C_{15}													1	0.85**	0.95**	0.95**	0.96**	0.98**	0.98**	0.94**	0.96**	0.77**	0.86**

Table 5.7. (Continuation).

	C_{16}	C_{17}	C_{18}	C_{19}	C_{20}	C_{21}	C_{22}	C_{23}	C_{24}	C_{25}
C_{16}	1	0.93**	0.91**	0.84**	0.90**	0.89**	0.92**	0.92**	0.88**	0.91**
C_{17}		1	0.95**	0.92**	0.96**	0.96**	0.94**	0.96**	0.85**	0.89**
C_{18}			1	0.98**	0.99**	0.94**	0.96**	0.95**	0.84**	0.86**
C_{19}				1	0.97**	0.95**	0.92**	0.92**	0.75**	0.78**
C_{20}					1	0.96**	0.98**	0.98**	0.86**	0.89**
C_{21}						1	0.92**	0.95**	0.76**	0.82**
C_{22}							1	0.99**	0.93**	0.95**
C_{23}								1	0.91**	0.95**
C_{24}									1	0.99**
C_{25}										1

Table 5.8. Coefficients of Pearson correlations performed between the concentration of individual VOC and DRO in all groundwater samples (Significant correlation: *p<0.05; **p<0.01).

	MTBE	ETBE	Benzene	Toluene	Ethylbenzene	*m/p*-Xylene	*o*-Xylene	C_{10}	C_{11}	C_{12}	C_{13}	C_{14}	C_{15}	C_{16}	C_{17}	C_{18}	C_{19}	C_{20}	C_{21}	C_{22}	C_{23}	C_{24}	C_{25}
MTBE	1	0.93**	0.08	-0.01	-0.12	-0.19	-0.01	-0.04	0.16	-0.24	-0.18	0.10	-0.04	0.07	-0.01	-0.05	-0.16	-0.13	-0.19	-0.20	-0.19	-0.14	-0.23
ETBE		1	0.10	0.01	-0.13	-0.20	0.01	0.02	0.24	-0.22	-0.20	0.23	0.07	0.18	0.07	0.01	-0.12	-0.09	-0.17	-0.20	-0.21	-0.17	-0.24
Benzene			1	0.72**	-0.04	0.62**	0.81**	0.21	0.10	0.21	-0.07	0.07	-0.10	-0.04	-0.08	-0.06	-0.11	-0.05	-0.03	-0.06	-0.02	-0.08	-0.12
Toluene				1	0.42*	0.61**	0.82**	0.19	0.06	0.15	-0.11	0.03	-0.12	-0.08	-0.12	-0.11	-0.15	-0.10	-0.07	-0.09	-0.05	-0.12	-0.16
Ethylbenzene					1	0.11	0.53**	-0.03	-0.08	0.06	-0.12	-0.06	-0.11	-0.11	-0.13	-0.11	-0.09	-0.05	-0.01	-0.06	0.02	-0.05	-0.16
***m/p*-Xylene**						1	0.59**	0.17	-0.09	0.27	0.08	0.06	-0.05	-0.04	-0.06	-0.03	0.01	-0.06	-0.04	-0.08	0.04	0.02	-0.02
***o*-Xylene**							1	0.16	0.03	0.23	-0.12	0.03	-0.14	-0.09	-0.11	-0.10	-0.13	-0.06	-0.02	-0.07	0.01	-0.08	-0.18
C_{10}								1	0.51**	0.15	-0.18	0.24	-0.01	0.21	0.13	0.14	0.01	-0.01	-0.03	-0.09	-0.13	-0.15	-0.11
C_{11}									1	0.16	-0.04	0.48**	0.35*	0.51**	0.42*	0.42*	0.24	0.32	0.23	0.10	0.21	0.22	0.19
C_{12}										1	0.75**	0.38*	0.33*	0.10	0.20	0.32	0.53**	0.61**	0.65**	0.39*	0.54**	0.56**	0.49**
C_{13}											1	0.37*	0.49**	0.13	0.18	0.26	0.60**	0.62**	0.70**	0.46**	0.58**	0.57**	0.50**
C_{14}												1	0.83**	0.84**	0.72**	0.71**	0.73**	0.73**	0.62**	0.33*	0.40*	0.36*	0.26
C_{15}													1	0.79**	0.76**	0.73**	0.79**	0.84**	0.71**	0.50**	0.58**	0.53**	0.37*

Table 5.8. (Continuation).

	C_{16}	C_{17}	C_{18}	C_{19}	C_{20}	C_{21}	C_{22}	C_{23}	C_{24}	C_{25}
C_{16}	1	0.96**	0.93**	0.74**	0.73**	0.55**	0.39*	0.46**	0.50**	0.41*
C_{17}		1	0.96**	0.75**	0.74**	0.55**	0.47**	0.56**	0.62**	0.52**
C_{18}			1	0.86**	0.84**	0.68**	0.55**	0.58**	0.65**	0.56**
C_{19}				1	0.96**	0.90**	0.67**	0.63**	0.65**	0.54**
C_{20}					1.	0.94**	0.72**	0.74**	0.74**	0.62**
C_{21}						1	0.77**	0.73**	0.67**	0.58**
C_{22}							1	0.93**	0.87**	0.77**
C_{23}								1	0.93**	0.82**
C_{24}									1	0.91**
C_{25}										1

On the other hand, the ratio of low to high molecular weight alkanes (L/HMW), decreased with depth in all soils, except P7, also reflected by C_{max}. This indicated that deep soil horizons, where the contamination probably took place, were enriched of HMW alkanes. These contaminants are the least water-soluble and most hydrophobic, and tended to adsorb on soil particles. These interactions slowed down the leaching of heavy DRO towards groundwater. Alimi *et al.* (2003) also reported that the residual concentrations of *n*-alkanes in soil increased with the carbon number.

Only the most water-soluble components of fuel (VOC, especially fuel oxygenates, and LMW alkanes, C_{10} to C_{14}) were detected in piezometer and well samples (Tables 5.4 and 5.6). Indeed, L/HMW ratios were significantly higher in water samples (Table 5.6) than in soil samples (Table 5.5). Low molecular weight DRO have higher water solubilities (Appendix B) and therefore, are more probably found in groundwater, transported with leachates. Furthermore, water samples CPI indices were far from unity (Table 5.6), indicating that the contamination of water was not directly from fuel leak, but indirectly transported from contaminated soils.

Significant correlations (p<0.05) were found between individual VOC and DRO in all soil samples analyzed, but only among VOC or DRO in groundwater samples (Tables 5.7 and 5.8). This indicated again the direct petrogenic input of contamination occurring in soil, and the indirect contamination of groundwater by rainfall and irrigation water leaching through fuel contaminated soils.

Figure 5.2 shows examples of three chromatograms (fresh diesel, P3 groundwater sampled in October (2012) and P3 soil at 5.0 m depth) and the respective concentration profile of each individual *n*-alkane from the total ΣDRO. In fresh diesel, LMW alkanes (C_{10} to C_{14}) represent more than 50% of total DRO analyzed. P3 water sample is enriched of LMW alkanes (more than 80% of total DRO) and P3 (5.0 m) soil is enriched of HMW alkanes (more than 60%).

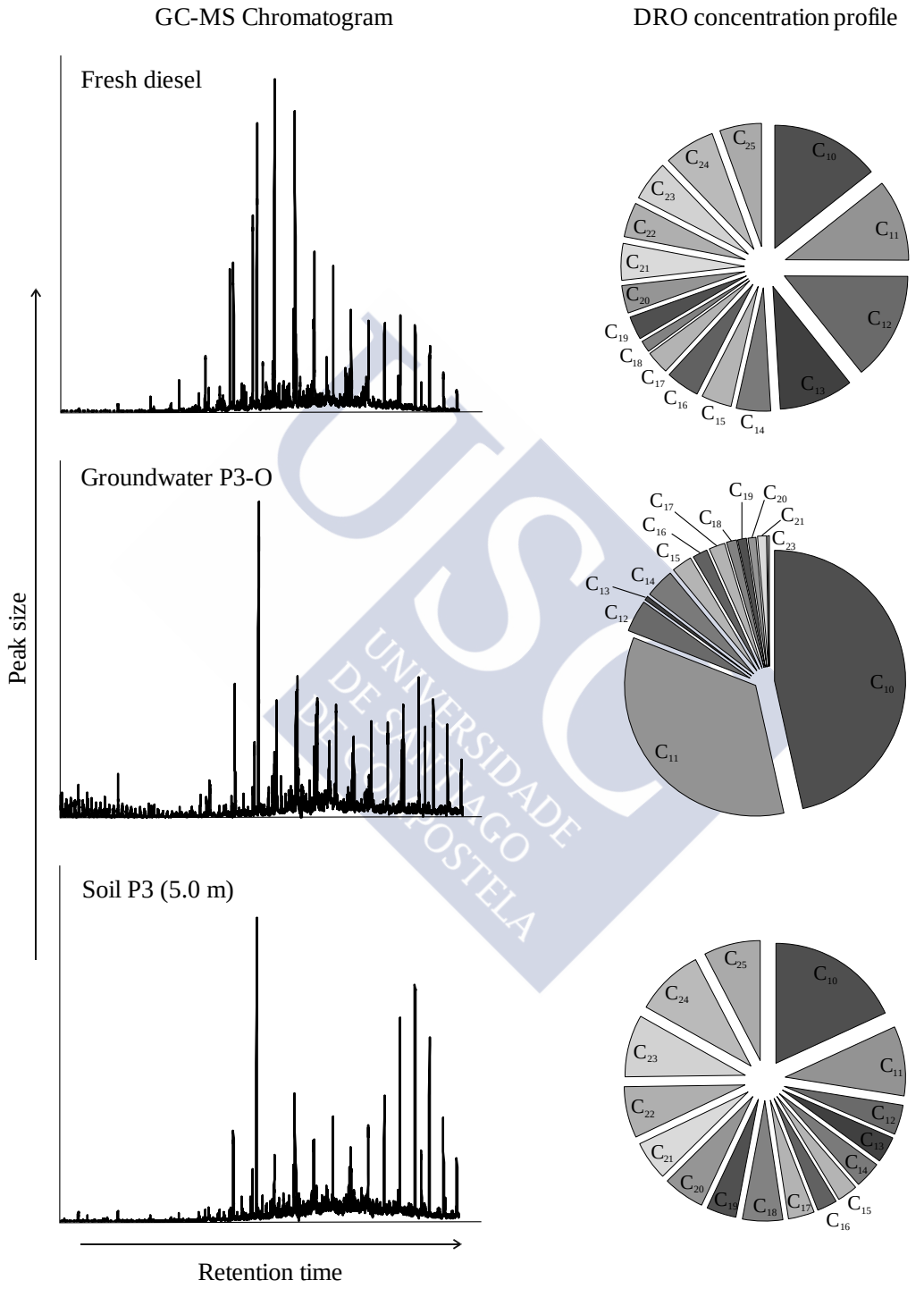

Figure 5.2. GC-MS chromatograms and individual DRO profiles of fresh diesel, P3-O groundwater and P3 soil at 5.0 m depth.

Furthermore, in the P3 soil sample chromatogram, more undefined peaks appear than in fresh diesel or water sample chromatograms. This is known as undefined complex mixture (UCM) and its proportion increases with the weathering of fuel in contaminated soils (Wang and Fingas, 1997).

The presence of MTBE in very high concentration in some groundwater samples helped to fingerprint the age of the spill. Although MTBE was not detected in gasoline and diesel purchased from the oil station (data not shown), high concentrations of this oxygenate were detected in piezometers and wells (P3, P7, W1 and W7) (Table 5.4). Indeed, while sampling, a very strong hydrocarbon odour was detected, indicating that the concentration of groundwater contaminated samples was over the odour threshold (20 µg MTBE L^{-1}) (USEPA, 1997). The presence of MTBE reflects that the spill have been leaking from years ago, probably, when MTBE started to be used as octane enhancer. This occurred in the 2000s, when the Fuel Quality Directive 98/70/EC required all EU countries to use completely lead free gasoline. The station was established in 1984, and the first odour and flavour detection in well water by neighbours was reported in 1994 (personal communication).

The use of MTBE started to be regulated in 2009 by European Renewable Energy Directive (2009/28/EC) and Fuel Quality Directive (2009/30/EC). These directives encourage the use of bio-components such as ETBE and ethanol in gasoline, and limit the use of MTBE as fuel oxygenate, due to its potential for groundwater contamination and carcinogenicity. In spite of being yet regulated, MTBE was detected in groundwater samples taken in 2012. MTBE has a very high water solubility and volatility (Appendix A). Therefore, in an oil spill, it will easily migrate to water and air compartments (Arey and Gschwend, 2005). When released in the atmosphere, MTBE is rapidly photodegraded, but in groundwater this contaminant is very slowly biodegraded and therefore the persistency of MTBE in groundwater is very high (Atienza *et al.*, 2005). Some other authors

reported the presence of very high concentrations of MTBE in aquifers and wells (Atienza *et al.*, 2005; Arey and Gschwend, 2005; Iturbe *et al.*, 2005)

Car fuels distributed in the store, diesel and gasoline, have different compositions. Gasoline is mainly composed of alkanes (up to C_{10}), cycloalkanes and monoaromates (BTEX); and diesel, of alkanes (mainly, C_{10}-C_{25}), cycloalkanes and polyaromates (Trapp *et al.*, 2001). The coexistence of aromatics, MTBE, ETBE (typically added in gasoline) and alkanes in diesel range, in the groundwater and soil samples indicated that the spill was probably composed of both gasoline and diesel. Therefore, underground tanks of both fuels could be spilling in the surrounding soils.

Some facts also reflected the continuity of the spill over time. On the one hand, the presence of volatiles (BTEX) in some soil samples (Table 5.3). VOC are the first fuel components lost while weathering, and, therefore, only appeared in fresh leaks (Wang *et al.*, 1999). On the other hand, some groundwater samples were taken in August and October of 2012 from the same sampling points near the station to screen a possible variation in contaminant concentrations. The presence of higher concentrations of VOC in October samples of some sampling points near the distribution station (P1, P6, Pc2, W2 and W7) also reflected the continuous leaking (Table 5.4).

Migration of contaminant plume

Contaminants leaked from underground tanks contaminated the station nearby soils. Results suggested than contaminants migrated from those directly-contaminated soils to groundwater (by leaching) and to further soils following the south-west direction in the sampling site (Figure 5.3). This is reflected by high VOC and DRO concentrations in sampling points surrounding the station and in that direction line.

The direction of the plume coincides with the direction where Miño river basin is located, which was probably acting as the receptor of superficial and subsuperficial flows of the study site.

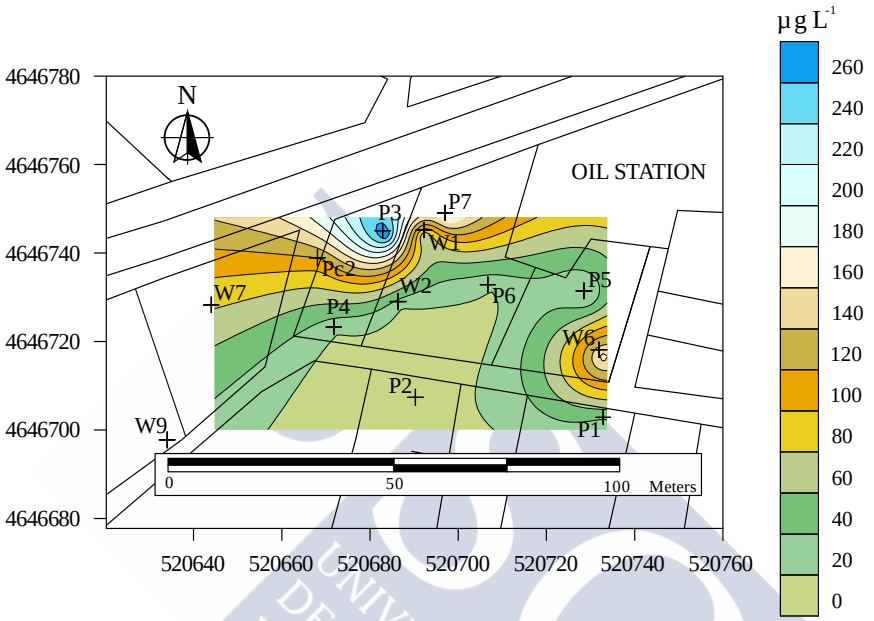

Figure 5.3. Example of spatial distribution of MTBE in groundwater samples collected in October (2012). The map shows the isoconcentration curves estimated by Surfer® Golden software (Version 12.0).

Multivariate statistical analysis: PCA

Principal component analysis (PCA) was performed for VOC (Figure 5.4) and DRO (Figure 5.5), in both soil and groundwater samples.

The variance in PCA of VOC (Figure 5.4) explained by component 1 was 46.7%, and that explained by second component was 28.7%. The concentrations of each individual VOC were used as factors for PCA. The scores of each factor in the component rotated matrix were represented in the component axis. MTBE and ETBE principally scored in component 2, and BTEX, in component 1, being the highest score for toluene, ethylbenzene and *o*-xylene. Benzene score in both axes was very low since it was not found in many samples.

Water samples are grouped on the left of the first axis, practically at a constant value of component 1, indicating a principal and variable composition of MTBE and ETBE (Figure 5.4). Those with the highest and positive scores in second axis, were those with the highest MTBE and ETBE concentrations (P3, P7 and W1, in both sampling months). These sampling points were located in SW direction, which was probably the direction of the contamination plume (Figure 5.3). P7-O, P6-O and W5-A were located far from the other water samples, at positive values of component 1 axis, due to the presence of toluene, ethylbenzene and xylene isomers.

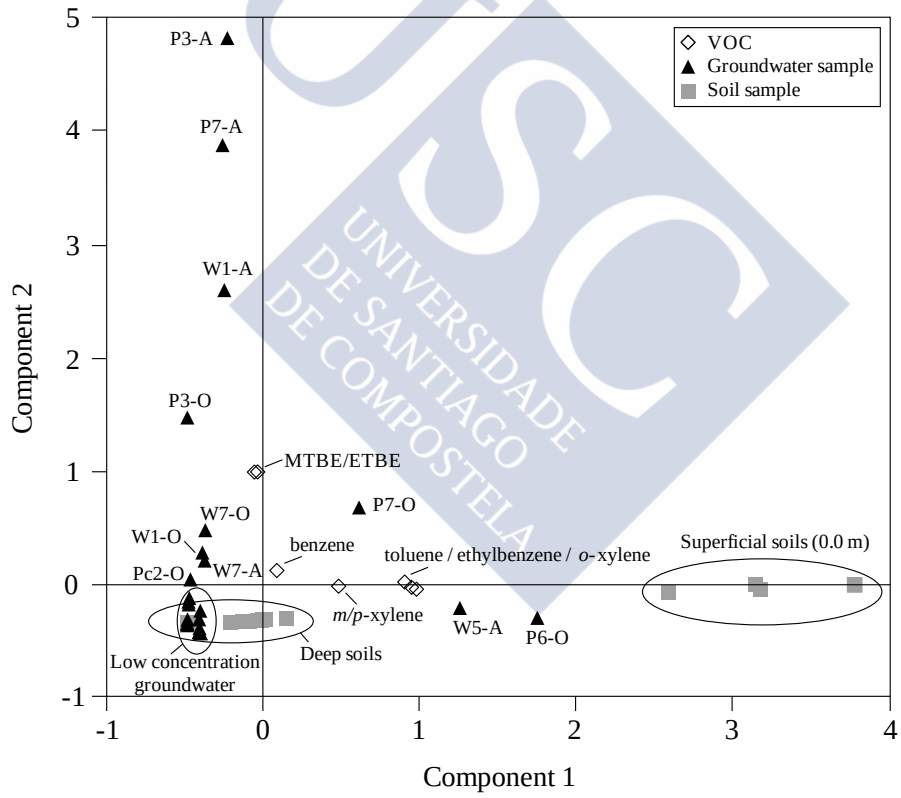

Figure 5.4. Principal component analysis (PCA) plot of scores obtained for individual VOC concentrations (factors). The component variables generated by PCA were also represented for each case (groundwater or soil samples).

Soil samples were located below the second axis, with lower scores of component 2, reflecting a lower presence of MTBE and ETBE than water samples (Figure 5.4). Superficial soils (0.0 m) had the highest scores in both components, indicating the highest concentration of both MTBE/ETBE and BTEX of all soil samples. Deep soil samples with the highest BTEX concentrations obtained positive values in component 1: P3 (3.8 m), P4 (1.5 m), P5 (3.6 m), P6 (4.1 and 6.4 m), P8 (4.8 m) and P9 (4.8 m). Therefore, deep soil surrounding the station, in which the spill took place, and surrounding soils in SW direction, towards which the spill plume was moving, were obtaining higher scores in component 1. On the other hand, superficial soil, whose contamination was due to irrigation with contaminated water, obtained the highest values in component 1 and were located on 0 value of component 2.

The variance in PCA of DRO (Figure 5.5) explained by component 1 was 76.8%, and that explained by second component was 7.9%. The concentration of each individual DRO and CPI were used as factors for PCA. DRO from C_{13} to C_{25} principally scored in component 1, while CPI and LMW *n*-alkanes from C_{10} to C_{12} had higher scores in component 2 than the other factors.

Water samples, as happened for VOC, were placed vertically at constant values of component 1. This indicates that LMW alkanes are the most abundant components of those samples. The exception to this tendency were samples Pc1-A and W6-A, which were placed at higher values of component 1, indicating the presence of higher concentrations of high molecular weight DRO with regard to the other water samples.

In Figure 5.5, superficial (0.0 m) and subsuperficial soils samples above 2 m (P1 0.4 m, P1 1.5 m, P4 1.5 m), had high punctuations in both components, indicating a higher concentrations of DRO, but especially of LMW alkanes. Deeper soils with CPI values around 1 formed a cloud at negative values of component 1 axis. Some soils with also CPI around 1 were out of this cloud, but

in the same horizontal line as the cloud (e.g. P4 3.2 m). Therefore, soils with higher punctuations on component 2 (either positive or negative), were those in which contamination was principally due to an input of contaminated water; and the majority of deep soils, with petrogenic inputs (CPI around unity), were place at negative values of component 1, and in component 2 values around 0-0.5.

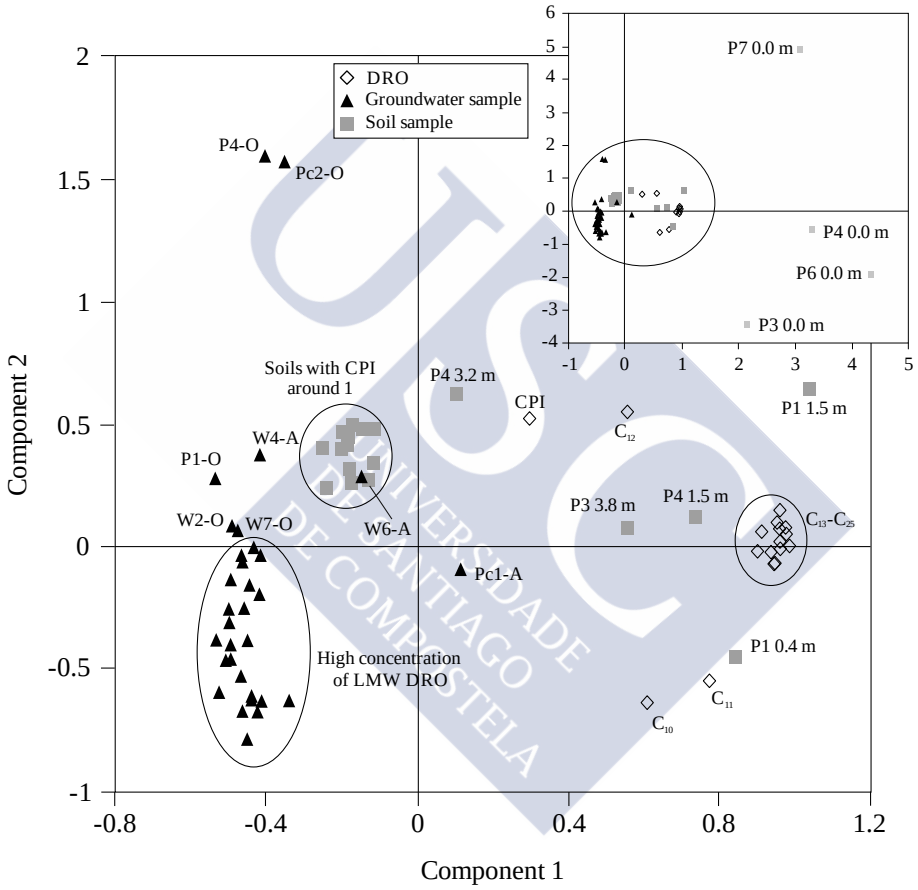

Figure 5.5. Principal component analysis (PCA) plot of scores obtained for individual DRO concentrations and CPI (factors). The component variables generated by PCA were also represented for each case (groundwater or soil samples).

CONCLUSIONS

GC-MS analysis and fingerprinting data suggested that the contamination of soil and groundwater in the surroundings of the fuel distribution station in

Tomiño was provoked by continuous leaking of underground storage tanks. This provoked the contamination of tank nearby soils, from which contaminants migrated to surrounding soils and groundwater, depending on their physicochemical characteristics and those of soils, groundwater and the site orography. Also superficial soils presented a high VOC and DRO contamination, but probably due to the irrigation with contaminated well water.

Fingerprinting also revealed the continuity of the leak, reflected by two facts: a) the presence of volatiles in some soil samples, which only appeared in fresh leaks; and b) the presence of MTBE, not detected in fuels, indicated also an old source of contamination, probably starting in the late 90s or early 2000s.

Multivariate analysis, contaminant distribution and hydrocarbon indices, helped to discriminate the contamination sources in soil and groundwater samples around the oil station.

REFERENCES

Alimi H, Ertel T, Schug B. 2003. Fingerprinting of hydrocarbon fuel contaminants: Literature review. Environ Forensics 4:25-38.

Arey JS, Gschwend PM. 2005. A physical–chemical screening model for anticipating widespread contamination of community water supply wells by gasoline constituents. J Contam Hydrol 76:109-138.

Asquith EA, Geary PM, Nolan AL, Evans CA. 2012. Comparative bioremediation of petroleum hydrocarbon-contaminated soil by biostimulation, bioaugmentation and surfactant addition. J Environ Sci Eng A 1:637-650

Atienza J, Aragón P, Herrero MA, Puchades R, Maquieira Á. 2005. State of the art in the determination of MTBE in natural waters and soils. Crit Rev Anal Chem 35:317-337.

Faure P, Mansuy-Huault L, Su X. 2007. Alkanes and hopanes for pollution source apportionment in coking plant soils. Environ Chem Lett 5:41-46.

Harji RR, Yvenat A, Bhosle NB. 2008. Sources of hydrocarbons in sediments of the Mandovi estuary and the Marmugoa harbour, west coast of India. Environ Int 34:959-965.

Iturbe R, Flores C, Flores RM, Torres LG. 2005. Subsoil TPH and other petroleum fractions-contamination levels in an oil storage and distribution station in north-central Mexico. Chemosphere 61:1618-1631.

Trapp S, Köhler A, Larsen L, Zambrano K, Karlson U. 2001. Phytotoxicity of fresh and weathered diesel and gasoline to willow and poplar trees. J Soils Sediments 1:71-76.

United States Environmental Protection Agency (USEPA). 1997. Drinking water advisory: Consumer acceptability advice and health effects analysis on methyl tertiary-butyl ether (MTBE). US Environmental Protection Agency, Washington.

Wang Z, Fingas M. 1997. Developments in the analysis of petroleum hydrocarbons in oils, petroleum products and oil-spill-related environmental samples by gas chromatography. J Chromatogr A 774:51-78.

Wang Z, Fingas M, Page DS. 1999. Oil spill identification. J Chromatogr A 843:369-411.

Wang Z, Stout SA, Fingas M. 2006. Forensic fingerprinting of biomarkers for oil spill characterization and source identification. Environ Forensics 7:105-146.

Zhang J, Dai J, Chen H, Du X, Wang W, Wang R. 2012. Petroleum contamination in groundwater/air and its effects on farmland soil in the outskirt of an industrial city in China. J Geochem Explor 118:19-29.

USC
UNIVERSIDADE
DE SANTIAGO
DE COMPOSTELA

6

A headspace-analysis approach to assess the sorption of fuel volatile compounds by soils

Sorption of fuel volatile compounds by soils affects the final environmental fate of these contaminants and strongly determines the efficiency of decontamination techniques. The headspace-analysis approach here suggested indirectly relates the sorption exerted by soils with the contaminant analytical recovery, which will be different according to the matrix effect of each particular sample. The aim of the present work was to assess the sorption of BTEX and fuel oxygenates by a wide selection of soil components and soil samples and to determine the influence of the physicochemical properties of the sample and the contaminant, the contaminant concentration, the incubation time, and the temperature on sorption. For this purpose, the samples were spiked with BTEX and fuel oxygenates in hermetically sealed vials and later analyzed by headspace-gas chromatography-mass spectrometry under several conditions (contaminant concentration, incubation time and temperature). The results were then compared to assess the sorption exerted by each sample under each scenario. Significant differences were found between the recovery of BTEX and fuel oxygenates, mainly due to the different mobility, polarity and sorption mechanisms involved while interacting with soil surface charges. Furthermore, these interactions determined the kinetic and strength of sorption, and had a strong influence on the recovery of BTEX and fuel oxygenates at different temperatures. The HS analysis approach resulted in a quick, easy, simple, automatable and environmentally friendly technique to obtain important information for understanding the behaviour of fuel volatile compounds in soil under very different scenarios. In addition, it establishes a good starting point for developing more sophisticated adsorption and soil remediation studies.

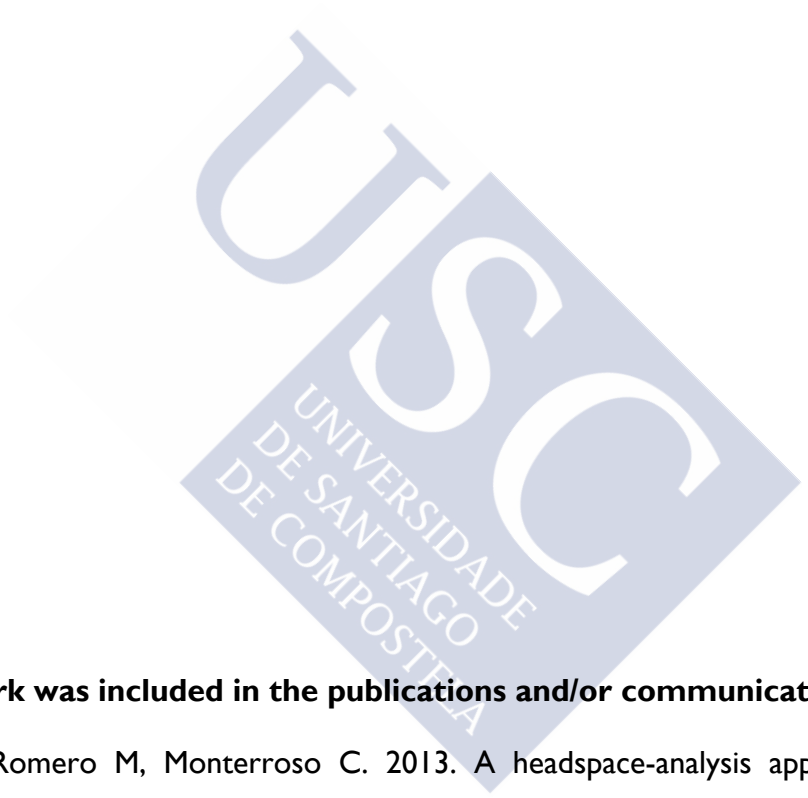

This work was included in the publications and/or communications:

Balseiro-Romero M, Monterroso C. 2013. A headspace-analysis approach to assess the sorption of fuel volatile compounds by soils. Soil Sci Soc Am J 77:800-808.

Balseiro-Romero M, Monterroso C. 2013. Sorption of xylene isomers by selected soils and soil colloids. SETAC Europe 23rd Annual Meeting, Glasgow, UK. Poster communication.

INTRODUCTION

Contamination of soil with fuel compounds is a serious and frequent problem, resulting from the poor management of wastes and emissions of petrochemical industry, accidental spills, or leakage from underground storage tanks (Kim *et al.*, 2008).

Among fuel hydrocarbons, benzene, toluene, ethylbenzene and xylene (BTEX) are of particular concern because of their high toxicity and carcinogenicity. They occur naturally in crude oil and are therefore found in fuel derived products (UK Environment Agency, 2003). Present gasoline formulations are supplemented by oxygenates as octane enhancers and ethers, particularly, methyl *tert*-butyl ether (MTBE) and ethyl *tert*-butyl ether (ETBE) are the most commonly used (EFOA Website, http://www.efoa.eu). Both BTEX and fuel oxygenates (FO) are the most volatile and water-soluble components of fuel. Therefore, contamination of soil with these compounds must not be ignored, since they can easily migrate to air and groundwater (Pavón *et al.*, 2009), causing important contamination problems in those environmental compartments. Soil sorption prevents or slows down both the biodegradation and the mobility of the contaminants, becoming a key process in determining the final fate of the contaminants in the environment (Serrano and Gallego, 2006). Soil sorption is affected by the soil components and physical and chemical properties (Margesin *et al.*, 2003), in addition to the soil water content (Albergaria *et al.*, 2010; Du *et al.*, 2011), pH (Chang Chien *et al.*, 2010) and temperature (Poppendieck *et al.*, 1999).

The Spanish law on contaminated soils (Real Decreto 9/2005) establishes levels of contamination above which soil remediation is required. Soil remediation can involve: a) "stabilization", where the physical and chemical form

of the contaminant is converted into a more inert condition (Suthersan, 1997), b) "containment", where the mobility of the contaminant is significantly reduced by means of physical barriers (Cunningham *et al.*, 1997) or c) "decontamination", where either the entire contaminated matrix is removed from the site (*ex situ*) or the contaminant is removed from the matrix (*in situ*), either by means of physicochemical processes (air sparging, soil vapour extraction, thermal desorption) or biological processes (phytoremediation, bioremediation, landfarming, composting) (Ortiz *et al.*, 2007). In particular, soil vapour extraction (SVE) and bioremediation are two of the most widespread remediation techniques for soils contaminated with volatile organic compounds (VOC) (Genovese *et al.*, 2008; Poppendieck *et al.*, 1999; Prenafeta-Boldú *et al.*, 2004; Soares *et al.*, 2010). The sorption of contaminants by soil will greatly affect the efficiency of decontamination methods (Ruiz *et al.*, 1998), as the higher the degree of sorption, the more difficult it is to decontaminate the soil and more complex decontamination methods will be required. In this sense, prior to remediation, it is essential to determine the properties of the contaminants and the soil, in order to anticipate the behaviour of the contaminants and characterize the sorption occurring in the particular soil.

Applying an appropriate and effective analytical method for the determination of BTEX and FO is the basis for carrying out solid sorption and remediation studies. The most commonly used technique to analyze volatile compounds in soils is by equilibrium headspace analysis (HS) coupled to gas chromatography/mass spectrometry (GC/MS) (Esteve-Turrillas *et al.*, 2007; García Pinto *et al.*, 2011; Pavón *et al.*, 2009). The HS procedure has the advantage that very little sample manipulation is required, which minimizes loss of the contaminant. Furthermore, this method saves an enormous amount of time. The limitation of HS quantification is the matrix effect, i.e. samples with different

properties would exert dissimilar degrees of sorption. Therefore, under equal analytical conditions, the contaminant would not be extracted in the same proportion from very dissimilar samples and the analytical results cannot always be comparable. This matrix effect is usually minimized with different calibration protocols (use of internal standards, or standard addition protocol), in order to achieve a proper quantification (Rosell *et al.*, 2006).

Here we propose the use of the HS-GC-MS analysis protocol without any matrix effect correction to assess the sorption of BTEX and FO by dissimilar soils and soil components. Traditionally, sorption studies of contaminants by soils are carried out through batch (Chang Chien *et al.*, 2010) or column (Bronner and Goss, 2011) experiments and the construction of sorption isotherms. These methods are difficult, time-consuming and usually involve great contaminant losses. The proposed HS analysis approach is a quick, easy, simple, automatable and environmentally friendly alternative with a minimum sample handling. It can lead to comparable results to more complicated techniques, since the analytical response is sensitive to soil characteristics and can be related to sorption processes. In addition, this approach could be used as an assessment, decision and diagnostic tool for remediation of contaminated soils.

Within this context, several experiments with spiked samples of different soils and soil components were designed to evaluate the influence of the sample properties and of external conditions (concentration of the contaminant and incubation time) in BTEX and FO analytical recovery and, therefore, in sorption. Furthermore, the effect of temperature on BTEX and FO analytical recovery was studied in order to establish an approach to deciding the adequacy of soil remediation by means of processes based on soil vapour extraction and thermal desorption.

MATERIALS AND METHODS

Reagents

The following reagents were used: benzene (purity, 99.8%; grade, PAI-ACS (UV-IR-94 HPLC-GPC)), toluene (purity, 99.8%; grade, PAI-ACS (UV-IR-HPLC-GPC)), ethylbenzene (purity, 99%; grade, PS), *o*-xylene (purity, 99%; grade, PA (Reag.USP. Ph. Eur)), *m*-xylene (purity, 99%; grade, PA (Reag. Ph. Eur)), *p*-xylene (purity, 99%; grade, PA (Reag.USP)), MTBE (purity, 99.7%; grade, PAI (PAR)) and ETBE (purity, 99%; grade, PA (Reag.USP)). All reagents were purchased from Panreac Química, S.L.U. (Barcelona, Spain). The spiking solution was prepared in methanol (purity, 99.9%; grade, PAI (PAR)) with each of the reagents at a concentration of 100 mg L^{-1}.

Soils and soil components samples

Four samples of natural soils with markedly different colloidal components and physicochemical properties and four samples of common soil components were selected for study (Table 6.1).

Soil samples were collected from four selected soil profiles in the surroundings of Santiago de Compostela (Galicia, NW Spain). This region has an average annual temperature of 13 °C and an average annual precipitation of 1290 mm. In general terms, the soils showed typical characteristics of Galician soils: i.e. variable charge, low pH and low cation exchange capacity dominated by aluminium (Macías and Calvo, 1992). Samples of A horizons were collected from an umbric alu-andic Andosol (A_{And}) and a haplic Podzol (A_{Pod}). The A_{And} was very dark because of the high content of organic matter, which was highly humified and stabilized by organo-aluminic complexes. The A_{Pod} was characterized by strong acidity and high content of poorly humified organic matter with high

mobility. B horizon samples were obtained from a Bws horizon of a humic Ferralsol (B_{Ferr}) and an alumi-umbric Cambisol (B_{Camb}). The B_{Ferr} had a high content of clay, mainly kaolinite, and crystalline iron oxihydroxides. The B_{Camb} had a sandy texture with low clay content. The soil samples were sieved through a 2 mm mesh and conserved in plastic containers at room temperature until use.

Table 6.1. Main properties of the samples used in the experiments.

Sample	pH [a]	$C_{Organic}$ [b] (g Kg^{-1})	C:N	ECEC [c] (cmol(+) Kg^{-1})	Surface area [d] (m^2 g^{-1})
Humic acid	1.7	490.1	-	159.3	1.1
Montmorillonite	3.3	-	-	68.8	254.9
Kaolinite	3.8	-	-	38.1	17.8
Goethite	7.0	-	-	0.5	14.2
A_{Pod}	4.0	133.8	21.2	3.4	0.5
A_{And}	4.6	91.6	13.7	1.5	17.7
B_{Ferr}	5.2	3.9	10.8	3.2	55.4
B_{Camb}	5.1	3.3	2.9	1.2	10.1

[a] Measured on an aqueous soil suspension of 1g:2.5 mL soil:water ratio.
[b] $C_{Organic}$: Organic carbon. Determined by combustion and IR detection.
[c] ECEC: Effective Cation Exchange Capacity. Determined by displacement with NH_4Cl 1M (unbuffered).
[d] Determined by BET method.

Kaolinite, montmorillonite, goethite and humic acid purchased from Sigma-Aldrich Química, S.A. (Madrid. Spain), were used as soil components samples. Montmorillonite is a 2:1 clay mineral of the smectite group with high permanent charge and a shrinking/swelling capacity on drying or wetting (Bohn *et al.*, 2001). Kaolinite is a 1:1 aluminium silicate with very low charge and cation exchange capacity (Besoain, 1985). Goethite is an iron oxihydroxide (α-FeOOH) with variable charge, formation of which is favoured at low temperatures and high soil moisture (Sumner, 2000). Humic acid is the main fraction of soil organic matter and consists of complex aromatic macromolecules joined to amino acids,

peptides, amino sugars, aliphatic acids and other organic constituents (Sumner, 2000).

Description of the experiments

As stated, the matrix effect hinders the active participation of the contaminants in the equilibrium during HS analysis, leading to different recoveries of the compound according to the properties of the sample and the external conditions. Therefore, several experiments were designed to evaluate how the recovery (i.e. sorption) of BTEX (benzene, toluene, ethylbenzene and *m*-, *p*- and *o*-xylene) and FO (MTBE and ETBE) during HS analysis of different soils and soil components is influenced by a) the concentration of the contaminant and the incubation (experiment 1), and b) the temperature (experiment 2).

In experiment 1, the four soil components and the four soils described above (Table 6.1) were used to test the influence of three spiking concentrations and of the incubation process on the recovery of BTEX and FO. According to the manufacturer's recommendations and to Method 5021A from United States Environmental Protection Agency (USEPA, 2003), the spiking procedure was carried out in the HS analytical vials containing a slurry resulting from mixing 1 g of solid sample and 2 mL of distilled water. The slurry decreases the losses due to evaporation (Serrano and Gallego, 2006) and favours the distribution of the contaminant over the soil. The appropriate volume of the spiking solution was added to the slurry to achieve three levels of contamination: 6, 30 and 60 μg g^{-1} of sample, for the sum of the six BTEX compounds (ΣBTEX) and 2, 10 and 20 μg g^{-1} of sample, for the sum of the two FO (ΣFO). These concentrations meant 1, 5 and 10 μg g^{-1} for each individual contaminant. Once the samples were spiked, the vials were quickly sealed to minimize losses by evaporation. Two parallel experiments were carried out to test the effect of an incubation process: one

experiment in which the samples were analyzed immediately after spiking (t=0 experiment) and another experiment in which the contaminated samples were incubated at 4 °C for one week (t=7 days experiment).

For experiment 2, the following soil components and soils samples were used: humic acid, montmorillonite, kaolinite, goethite, A_{And} and B_{Camb}. The experiment was carried out with spiking concentrations of 6, 30 and 60 μg ΣBTEX g^{-1} and 2, 10 and 20 μg ΣFO g^{-1}. After 7 days of incubation, the vials were subjected to a wide range of temperatures (room temperature-RT-, 40, 60, 80 and 90 °C) to study the influence of the temperature on the recovery of BTEX and FO during HS analysis.

In both experiments, the samples were contaminated in triplicate and analyzed by HS-GC-MS.

Instrumentation and analytical procedure: HS-GC-MS

The analytical system consists of an autosampler (Combi PAL, Agilent Technologies), an oven for heating the samples until headspace equilibrium, a gas chromatograph (Model 450 GC, Agilent Technologies) and an ion trap mass spectrometer (Model 220 MS, Agilent Technologies).

The headspace (HS) operating conditions were established according to the manufacturer's application notes and to the results of some preliminary experiments carried out in the laboratory. During the HS process, the sample vials from experiment 1 were heated at 80 °C in the HS oven, while in experiment 2 this temperature was varied as previously stated (RT, 40, 60, 80 and 90 °C). Each sample was maintained in the oven with constant agitation (500 rpm) for 15 minutes to achieve an acceptable equilibrium between the slurry and the HS. Then, 1 mL of gas from the HS of the vials was aspirated with a 2.5 mL-syringe (supplied by CTC Analytics AG) and was injected directly in the

chromatograph for analysis. The injector was operated at 250 °C and in split/splitless mode, with a 1/10 split ratio (Chapter 3).

The chromatographic column was a FactorFour VF-5ms EZ-Guard (supplied by Agilent Technologies) of 30 m x 0.25 mm x 0.25 µm. The column oven temperature was varied as follows: 35 °C held for 5 minutes, followed by an increase of 10 °C min^{-1} up to 80 °C and an increase of 25 °C min^{-1} up to 200 °C, which was held for 0.7 minutes. The carrier gas was helium with a constant flow of 1 mL min^{-1}.

The mass spectrometer operated in full scan mode. Ionization of the molecules was carried out by electron impact (EI) and the ion trap temperature was fixed at 220 °C. In the chromatograms obtained, *m*- and *p*-xylene appeared as a single peak and were therefore analyzed jointly.

Cycle Composer software (Version 1.5.4; CTC Analytics AG) was used to control the Combi PAL autosampler and MS Workstation software (Version 6.9.3; Varian, Inc.) was used to control de GC-MS system and to process the data.

Calibration was carried out with standards of 2 mL of water (the same volume added to the slurry of samples) containing 0.1, 0.5, 1, 5 and 10 µg of each individual contaminant; i.e. 0.6, 3, 6, 30 and 60 µg ΣBTEX and 0.2, 1, 2, 10 and 20 µg ΣFO. Through this type of calibration without matrix, the results from HS-GC-MS analysis of the samples corresponded to the quantity of contaminant recovered, which is free of sorption and actively participates in the slurry-HS equilibrium. This allowed to more easily characterizing the matrix effect and, therefore, the sorption exerted by soil components and soil samples. The standards were analyzed in triplicate by HS-GC-MS under the same analytical conditions as the samples. The calibration curves fitted well to a linear pattern (R^2>0.997).

Statistical analysis

PASW Statistics software (Version 18.0.0; IBM SPSS Statistics, Inc.) was used to analyze the data. The data of experiment 1 were analyzed by a Student's t-test for independent samples, and those of experiment 2, were analyzed by a repeated measures ANOVA. A significance level of p=0.05 was considered for all statistical analyses.

RESULTS AND DISCUSSION

Influence of contamination level and incubation on BTEX and FO recovery from soil components and soils

Figure 6.1 and 6.2 represent the results of HS-GC-MS analysis from experiment 1, which are expressed as the amount of ΣBTEX and ΣFO (µg of ΣBTEX or ΣFO g^{-1} of sample) recovered from soil components (Figure 6.1) and soils (Figure 6.2), for the different spiking concentrations and incubation times. These results varied according to the contaminant, the type of matrix, the spiking concentration and the incubation time. This reflects the participation of different sorption mechanisms influenced by the properties of the sample and the compound. At first glance, MTBE and ETBE (FO) were recovered in higher proportion than BTEX from the majority of the samples, especially after 7 days of incubation. This could be explained easily because FO are more soluble and volatile, and therefore, more mobile, than the BTEX compounds: the water solubility of FO varied from 26.0 to 51.6 g L^{-1} (EFOA Website http: www.efoa.eu) and that of BTEX varied from 0.1 to 1.8 g L^{-1} (Mackay *et al.*, 2006); and the vapour pressure (at 20-25 °C) of FO varied from 28 to 31 KPa (EFOA Website http: www.efoa.eu) and that of BTEX varied from 0.8 to 13 KPa (Mackay *et al.*, 2006) (Appendix A).

Humic acid displayed the highest sorption capacity of all soil components, since all contaminants showed the lowest recovery (Figure 6.1). In addition, the sorption kinetic of humic acid seemed to be very rapid, since the amount of BTEX and FO recovered from the total spiked was scarcely modified after incubation. The relative recovery of BTEX from humic acid (Figure 6.1a) was significant lower than that of FO (p<0.05) (Figure 6.1b). For example, at the highest spiking concentration (60 μg g^{-1} for ΣBTEX and 20 μg g^{-1} for ΣFO), about 18% of the BTEX spiked (11 μg g^{-1}) and 45% of the FO spiked (9 μg g^{-1}) was recovered. This reflects the higher affinity of BTEX for organic matter, due to the lower polarity of BTEX, with regard to FO: non-polar molecules prefer non-polar phases ("like dissolves like") (Goss and Schwarzenbach, 2003).

For inorganic soil components (montmorillonite, kaolinite and goethite), the amount of BTEX recovered was significant higher than that from humic acid (p<0.05) (Figure 6.1a). The highest amount of BTEX recovered was from goethite, at t=0 days, for the highest spiking concentration (60 μg g^{-1}) (about 95% of the BTEX spiked was recovered).

Furthermore, the sorption of BTEX by inorganic soil components was not as rapid as for the humic acid, making incubation a key factor in the sorption of BTEX by those components. However, for the FO (Figure 6.1b) the incubation time did not have such an important effect as for BTEX, and the analytical recovery was only slightly modified. Inorganic soil components (clays, oxides and hydroxides of iron and aluminium) have either negative or positive surface charges which can attract and hold either positive or negative species (Brady and Weil, 2008). While interacting with the superficial charges of soil components, MTBE and ETBE act as dipoles, since they are polar molecules due to the non-bonding electrons on the oxygen.

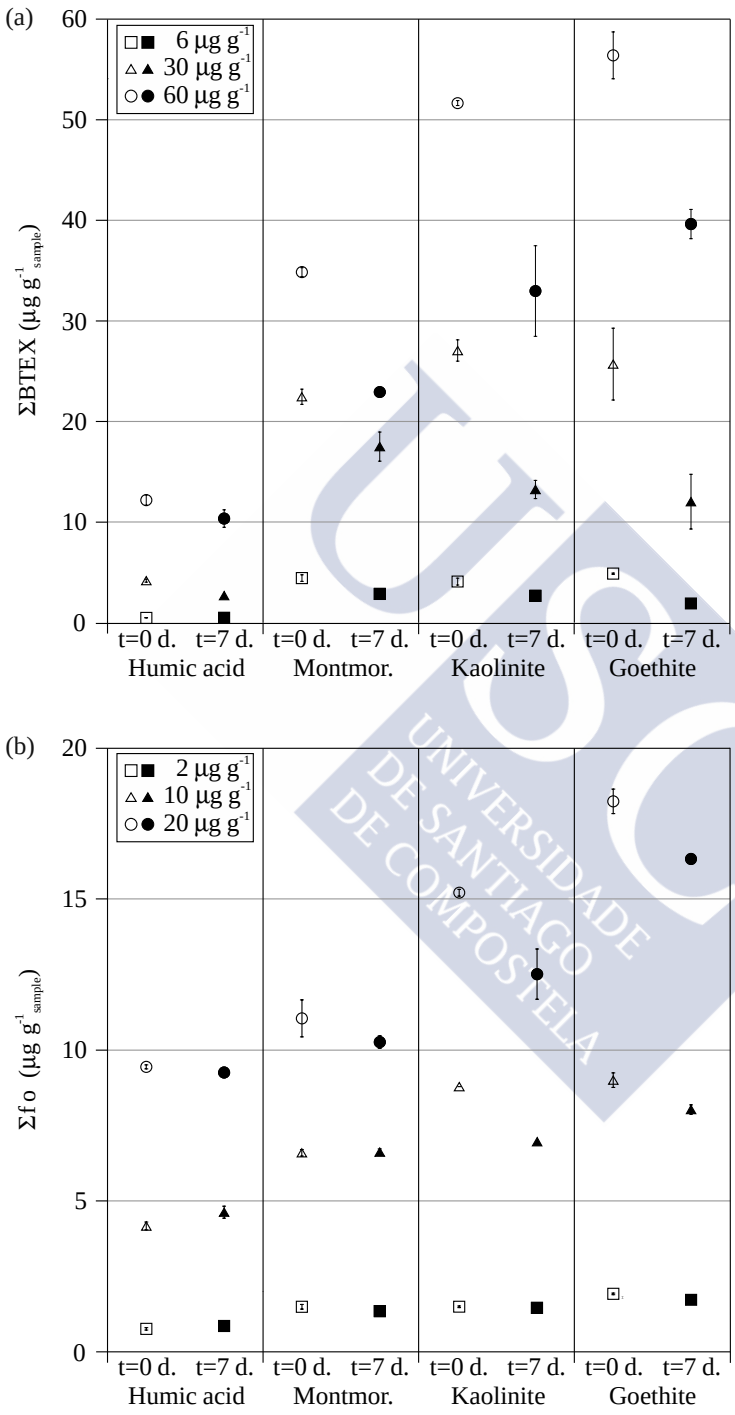

Figure 6.1. Amount of BTEX (a) and FO (b) recovered from soil components after HS-GC-MS analysis, for the different spiking concentrations (6, 30 and 60 µg ΣBTEX g^{-1} of sample and 2, 10 and 20 µg ΣFO g^{-1} of sample) and incubation times (0 and 7 days). The results are expressed in µg ΣBTEX or ΣFO g^{-1} of sample, as the mean ± the standard deviation (*n*=3). The term Montmor. corresponds to montmorillonite.

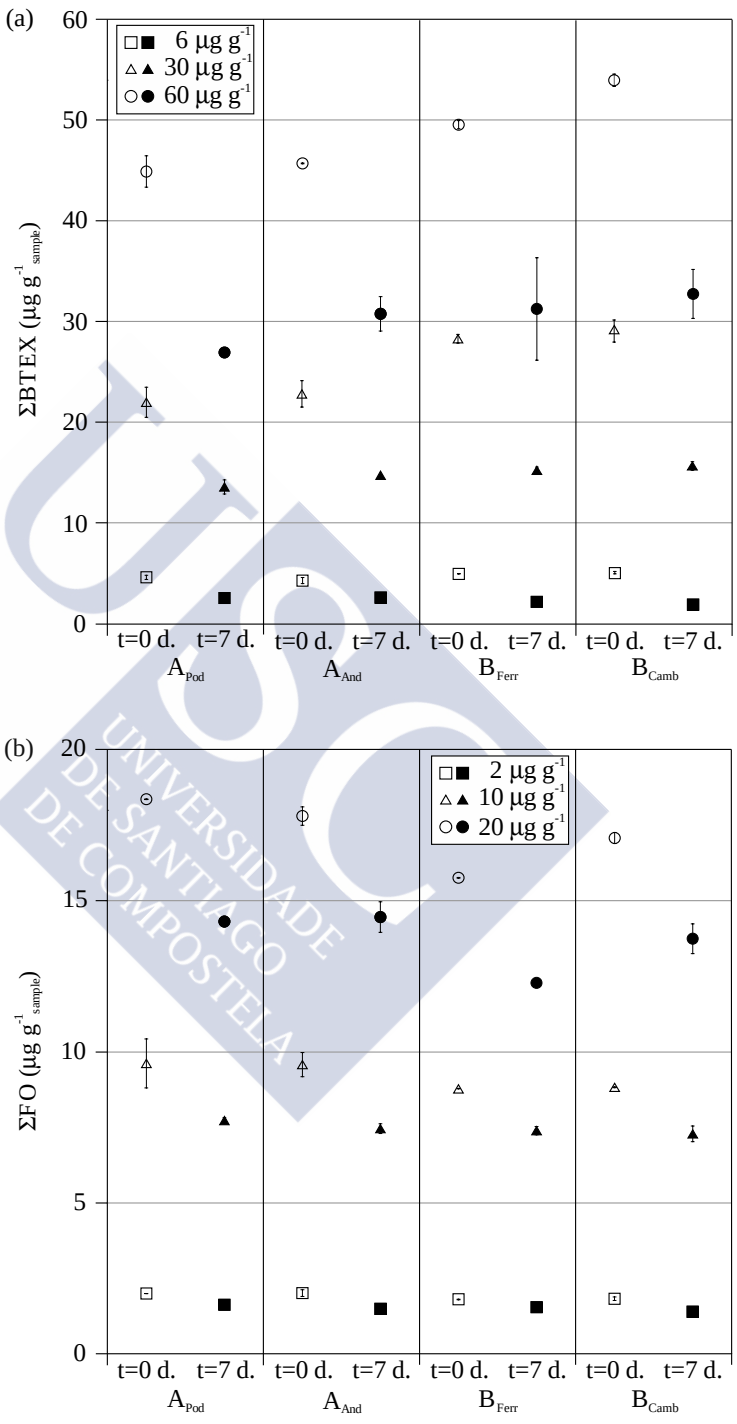

Figure 6.2. Amount of BTEX (a) and FO (b) recovered from soils after HS-GC-MS analysis, for the different spiking concentrations (6, 30 and 60 µg ΣBTEX g^{-1} of sample and 2, 10 and 20 µg ΣFO g^{-1} of sample) and incubation times (0 and 7 days). The results are expressed in µg ΣBTEX or ΣFO g^{-1} of sample, as the mean ± the standard deviation (*n=3*).

However, the BTEX compounds which are relatively non-polar, act as induced dipoles due to the presence of a π electron cloud around the aromatic ring (Sharmasarkar *et al.*, 2000). The first type of interaction (soil charges-dipole or FO) is more rapid, almost instantaneous, whereas the second (soil charges-induced dipole or BTEX) is weaker and needs the incubation time to manifest completely. Montmorillonite, kaolinite and goethite showed different behaviours in the sorption of both groups of contaminants (Figure 6.1). The amount of BTEX and FO recovered from montmorillonite with respect to the theoretically spiked was lower than the expected with a linear trend, which is the most observed trend in the samples used (the recovery or the sorption capacity is proportional to the spiking concentration). This particular behaviour of montmorillonite was more pronounced after incubation. For example, the percentage of BTEX recovered from the total spiked at t=7 days was approximately 66% for the spiking concentration of 30 μg g^{-1}, but it was only 38% for the spiking concentration of 60 μg g^{-1}. This indicated that the sorption capacity of montmorillonite increased with the increasing spiking concentration. This particular behaviour may be due to the capacity of montmorillonite to expand and produce a larger surface area: expansion of the interlayer generates a total surface area of 600 to 800 m^2 g^{-1}, with as much as 80% of the total due to internal surfaces (Bohn *et al.*, 2001). The molecular radius of the BTEX group varies between 0.40 and 0.44 nm (Morsali *et al.*, 2010), and that of FO is around 0.31 nm (Larsen *et al.*, 1995). Since the interlayer spacing of montmorillonite varies from 0.95 nm to a distance of up to tens of nanometres in full hydration (Bohn *et al.*, 2001), the entry of BTEX or FO in the interlayer is perfectly feasible in terms of size. Although it is unlikely that organic compounds will enter the interlayer and displace exchangeable cations, the present results indicate that such entry was forced at high concentrations of the contaminant. The recovery of both BTEX and FO from kaolinite and goethite, was practically proportional

to the spiking concentration, except for BTEX after 7 days of incubation. In this case, the amount of BTEX recovered from goethite at the highest spiking concentration was higher than the expected for a linear trend: the percentage of BTEX recovered from the total spiked was approximately 41% and 66%, for the spiking concentrations of 30 and 60 $\mu g\ g^{-1}$, respectively. This probably reflected the saturation of the sample, which could be due to the low surface area of this soil component (Table 6.1).

The recovery of both BTEX and FO from soil samples (Figure 6.2) showed less differences than the observed between organic and inorganic soil components. For BTEX compounds, the recovery from A horizons was slightly lower than in the B horizons, due to the affinity and consequent sorption by organic matter. On the contrary, for FO the recovery was lower from the B horizons. This could be caused by the higher polarity of MTBE and ETBE, and therefore the lower affinity for organic matter.

Comparison of the recovery of the individual compounds in experiment 1

As explained above, the differences between the two groups of contaminants as a whole were due to the dissimilar mobility and charge interaction with the samples. Within each group, several differences were also found when comparing the analytical recovery of the individual contaminants. Figure 6.3 shows the percentage of contaminant recovered with respect to the total spiked. The data used were the obtained from experiment 1 for an incubation period of t=7 days, which resulted in the highest degree of sorption, and for a spiking concentration of 1 $\mu g\ g^{-1}$ for each individual compound. This concentration allowed working with samples under non-saturation conditions. As previously stated, *m*- and *p*-xylene isomers were analyzed jointly. The recovery of

the FO varied approximately from 35 to 90% and that of BTEX varied from 0 to 50%.

At first glance, the recovery of the BTEX compounds seemed to be governed by the physical properties of the compounds, especially those that influence on their mobility, since the recovery decreased with the diminution of volatility: the volatility order of BTEX is benzene>toluene>ethylbenzene>*m*/*p*-xylene>*o*-xylene (Mackay *et al.*, 2006). In the majority of samples, benzene, toluene, ethylbenzene and *m*/*p*-xylene, were recovered in the same or lower proportion than the precedent compound in the volatility list. The exception of this tendency is the *o*-xylene, It was recovered in higher proportion than *m*/*p*-xylene and ethylbenzene, or even than benzene in some cases, except in the presence of organic matter (humic acid, and A horizons), when the sorption was comparable to the other xylene isomers. These results indicate that, apart from mobility, the differences in the chemical structure of the compounds and samples are also taking part in sorption. As already mentioned, the sorption of BTEX was partially governed by the interaction between the surface charge of soils and soil components and the charge induced in the compound (induced dipole) due to the presence of a π electron cloud around the aromatic ring. The presence of an alkyl group (methyl group in toluene and xylenes, and ethyl group in ethylbenzene) influences the dipole strength: the combination of positive inductive and resonant effects caused by σ electrons of the alkyl groups results in a greater negative charge density in the aromatic ring as regard to the absence of functional groups, as in benzene (Sharmasarkar *et al.*, 2000). According to March (1992), the dipole or nucleophilic strength, and therefore the sorption strength, depends on the type and position of the alkyl groups. The presence of a methyl group at the *m*- or *p*- positions of the ring would impart a greater sorptive affinity than a methyl group at *o*- position or an ethyl group in the ring. A possible steric

repulsion between the two adjacent methyl groups in *o*-xylene could lower its sorption strength compared to ethylbenzene and *m*- and *p*-xylene. Within this theoretical base, the results were clearly consistent for samples without organic matter (montmorillonite, kaolinite, goethite and B horizons). In humic acid and A horizons, it seemed that the nucleophilic differences between the substituted aromatic molecules did not have much influence in sorption as for inorganic samples. This could be because in the presence of organic matter, the sorption took place differently, mainly by means of dispersion interactions (Chang, 2010). This type of interaction, is probably determined only by the global sorption capacity of the sample (i.e. number of available sorption sites) rather than by differences in intermolecular interactions between the sorbate and the sorbent (Niederer *et al.*, 2007).

For the group of FO, the recovery of MTBE and ETBE from samples without organic matter (montmorillonite, kaolinite, goethite and B horizons) did not vary significantly ($p<0.05$). However, ETBE was recovered in less proportion than MTBE, i.e. ETBE was sorbed in higher proportion than MTBE. This differs from the results obtained for BTEX, for which the greatest differences between compounds of similar chemical characteristics (for example, xylene isomers) were found in inorganic soil components. As already cited, FO are very polar, and act as real dipoles due to the non-bonding electrons on the oxygen (Wade, 2003). The results indicate that while interacting with inorganic soil components, both compounds offered similar sorption strengths, probably because the charge distribution was not as dissimilar as for BTEX compounds. In the presence of organic matter (humic acid and A horizons), the high polarity hindered the sorption of FO that was clearly lower than that of BTEX.

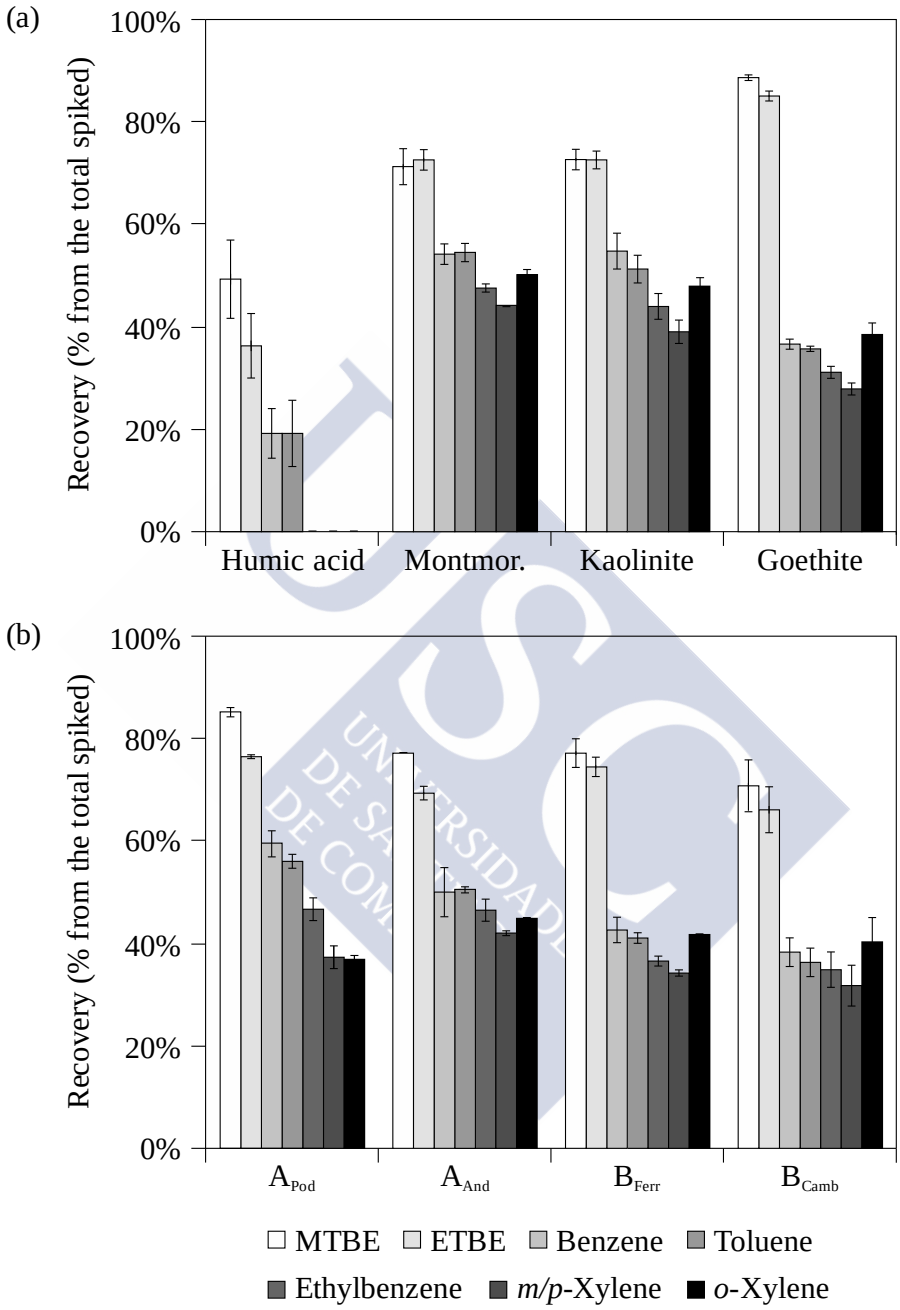

Figure 6.3. Recovery of the individual BTEX compounds and FO by soil components (a) and soils (b) for a spiking concentration of 1 μg g^{-1} of sample, for each individual compound, and an incubation time of 7 days. The results are expressed as the mean of the percentage of ΣBTEX or ΣFO recovered from the total theoretically spiked ± the standard deviation (*n=3*). The term Montmor. corresponds to montmorillonite.

This sorption was more hindered for MTBE since it has higher polarity than ETBE, making dispersion interactions with organic matter more difficult: MTBE is much more soluble (51.6 g L^{-1}) than ETBE (26 g L^{-1}) (EFOA Website, http://www.efoa.eu). This did not occur for BTEX, because the high lipophilicity softened the differences.

Influence of temperature on BTEX and FO recovery from soil components and soils

In experiment 2, the influence of temperature on the recovery of FO (MTBE and ETBE) and BTEX compounds from selected soil components and soils was tested at several temperatures: room temperature (RT) (approximately 20 °C), 40, 60, 80 and 90 °C. As expected, higher temperature led to greater volatilization of the contaminants towards the headspace (HS), as already concluded by other authors (He *et al.*, 2009; Poppendieck *et al.*, 1999). However, the amount of contaminant recovered from the samples at each temperature interval varied greatly according to the sample characteristics and to the compound itself (Figure 6.4). The results obtained in this experiment could be a good approach to study the efficiency of soil remediation methods based on soil vapour extraction (SVE) and thermal desorption.

For the BTEX compounds (Figure 6.4a), simple observation of the results revealed two groups of samples differentiated by the absence or presence of organic matter. At RT, between 40 and 60% of the spiked BTEX was recovered from inorganic soil components (montmorillonite, kaolinite and goethite) and the B_{Camb}, and between 60 and 80%, was recovered at 40 °C. Therefore, almost without any source of external heat, at environmental temperatures (up to 40 °C may be applicable to soils in very warm climates), more than 60% of BTEX present in soil could be eliminated. In the case of high contamination, the temperature could be increased. Higher temperatures would obviously require

higher inputs of energy and would alter many important soil properties, without supposing an important increase of the BTEX recovery with regard to 40 °C (up to 90%). On the other hand, at RT, the humic acid appeared to adsorb all the BTEX spiked (Figure 6.4a), and even at higher temperatures (90 °C), the recovery of the contaminants was about 20% of the quantity spiked. In the A_{And}, the presence of organic matter decreased the BTEX recovery to below that from inorganic soil components and B_{Camb}. At RT, the recovery of BTEX was around 10%, and at 40 °C, it did not reach 30%. The presence of organic matter appeared essential for the permanence of BTEX, making soil remediation by means of methods like SVE, more difficult, being more appropriate the application of alternative treatments (for example, bioremediation). In case of using SVE, the application of very high temperatures through an external source of heat appears essential.

For the FO (MTBE and ETBE) (Figure 6.4b), the results are very similar for all samples tested, except for the humic acid. At RT, the recovery of FO from inorganic soil components and the two soils was around 30%. The recovery doubled at 40 °C (around 60%), and at 60 °C reached between 80-90%. At the highest temperature (90 °C), the whole amount of FO added was recovered. For the humic acid, the recovery of FO was around 20% at RT. The increase of temperature supposed a recovery of only up to 40% of the amount of FO spiked. These results indicate that SVE could be efficiently used even unassisted with external heating for remediating soil contaminated with FO, both with and without organic matter.

In case of a fuel contamination episode, the joint remediation of BTEX and FO could be needed. The results indicate that the application of conventional vapour extraction at low temperatures (up to 40 °C) could be carried out in absence or very low presence of organic matter with very good and similar results for the two groups of contaminants. The remediation of soils with high

presence of organic matter could be more difficult since the recovery of the two groups of contaminants was very different. Since the application of two independent remediation methods for each group of contaminants is expensive and time consuming, in case of organic matter presence, combined remediation methods could be used. A good example is SVE combined with bioremediation. This technique is appropriate for this case, since it combines the effectiveness of SVE for the elimination of volatile compounds and the bioremediation to complete the decontamination process of organic compounds for which SVE is hindered (Soares *et al.*, 2010).

Some differences were appreciated when comparing the recovery of both groups of compounds (Figure 6.4). As already discussed in experiment 1, the differences between recoveries of BTEX and FO, were especially due to the dissimilar mechanisms of sorption. In samples without organic matter, at RT, the sorption of FO was stronger than the sorption of BTEX, due to the different energy of the intermolecular forces while interacting with the superficial charges of soil components: the interaction between the soil charges and a dipole of a high-polar molecule (MTBE or ETBE) is stronger than the interaction between the soil charges and an induced dipole of a low-polar molecule (BTEX) (Chang, 2010). The increase of temperature forced the release of both groups of contaminants, revealing that the mobility or volatility increase prevailed over the sorption strength. On the other hand, in samples with organic matter, the recovery of MTBE and ETBE from A_{And} is very similar to that from samples without organic matter: they were sorbed preferably by the inorganic fraction of soil due to the high polarity, and that the participation of organic matter in sorption was negligible unless organic matter was present in important proportion (humic acid). Instead, for BTEX compounds, the participation of soil organic matter in sorption is very important, even at low proportion (A_{And}). This can be due to the higher organophilicity of BTEX in comparison to FO.

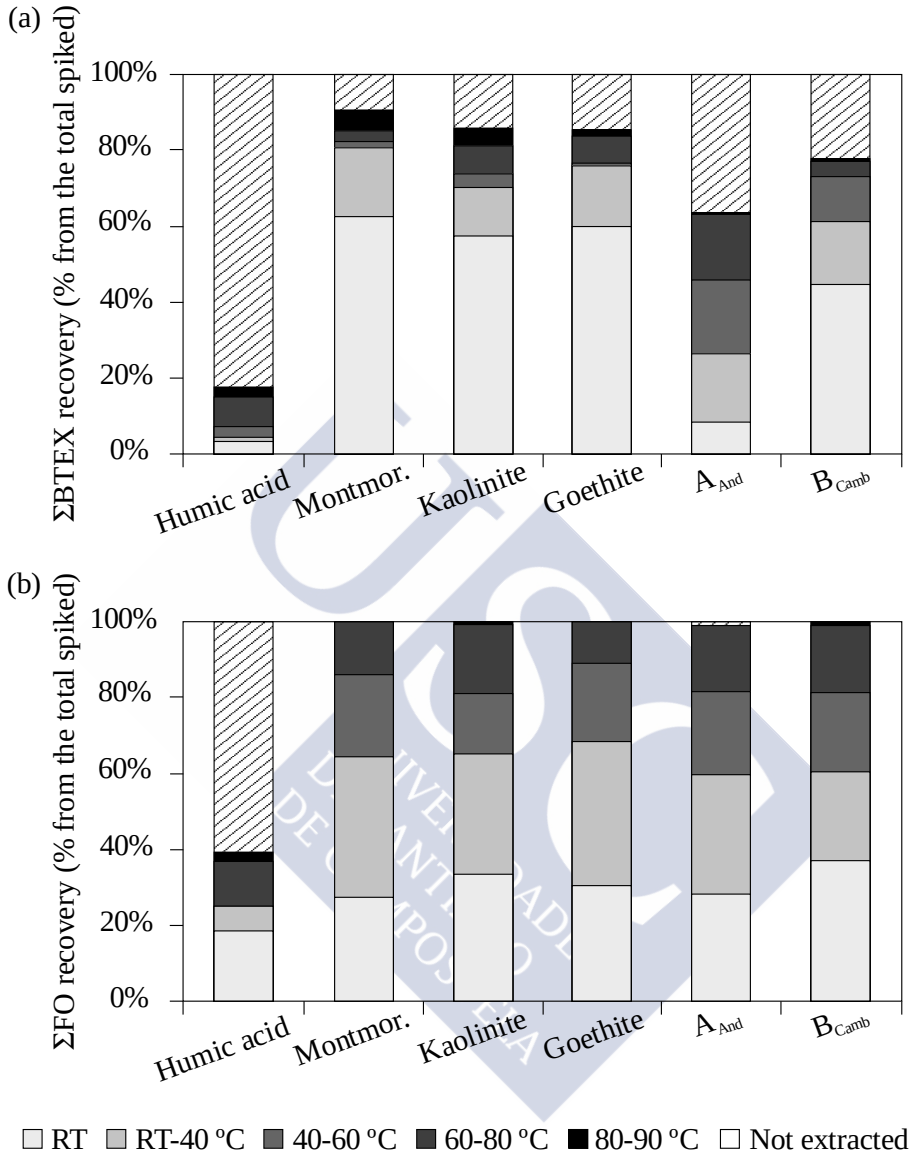

Figure 6.4. Recovery of BTEX (a) and FO (b) from selected soil components and soils at different temperatures for a spiking concentration of 6 μg ΣBTEX g^{-1} of sample or 2 μg ΣFO g^{-1} of sample and an incubation time of 7 days. The results are expressed as the mean of the percentage of ΣBTEX or ΣFO recovered from the total theoretically spiked ± the standard deviation (*n=3*). The term Montmor. corresponds to montmorillonite.

This experiment is obviously a very simple approximation to soil remediation, since in a real SVE system, the elimination of BTEX and FO would

be additionally favoured by the extraction of the soil vapour phase. In this sense, the temperatures required for a real contamination episode would be probably lower than the expected in this laboratory scale experiment. Therefore, additional experiments should be made to achieve a complete optimization of the remediation process.

CONCLUSIONS

Sorption of BTEX (benzene, toluene, ethylbenzene and *m*-, *p*- and *o*-xylene) and fuel oxygenates (FO) (MTBE and ETBE) by soils and soil components was mainly influenced by the mechanism involved in the interaction between the soil surface charges and the molecules.

The presence of organic matter had a significant effect on the sorption of BTEX, which was even perceptible at the moment of contamination. Sorption was so strong that very high temperatures were required to obtain significant recoveries of BTEX from soil. On the contrary, the kinetic sorption of BTEX by inorganic soils and soil components was slower and sorption strength was much weaker, since considerable recoveries were reached, even at room temperature. On the other hand, MTBE and ETBE are more polar than BTEX, and the sorption by organic matter was not so notable. In case of samples without organic matter, the sorption kinetic was faster and the sorption strength stronger than for BTEX and high temperatures were needed to obtain similar recoveries to that for BTEX at room temperature.

The sorption of the individual BTEX compounds decreased with the volatility increase, except for the three individual xylene isomers, for which significant differences were found in inorganic soil components and soils without organic matter, affected by the different charge distribution of the three isomers. The sorption of both FO was very similar, except in the presence of organic

matter, when sorption was comparatively hindered for the least polar oxygenate (ETBE).

The results indicate that remediation of soils contaminated with the studied fuel volatile compounds through methods based on soil vapour extraction at low temperature, could be successful in absence or very low presence of organic matter. The remediation of high carbon content soils would be more difficult, since BTEX are strongly sorbed, and very high temperatures would be necessary to achieve an adequate elimination. Soil vapour extraction combined with bioremediation could be a good and effective alternative for this type of soils.

The HS analysis approach purposed resulted in a simple and rapid method for obtaining very useful data that contribute to understand the behaviour of fuel volatile compounds in a great variety of scenarios and to establish the bases for optimizing soil remediation techniques.

REFERENCES

Albergaria JT, Alvim-Ferraz M, Delerue-Matos M. 2010. Estimation of pollutant partition in sandy soils with different water contents. Environ Monit Assess 171:171-180.

Besoain E. 1985. Mineralogía de arcillas de suelos. Instituto Interamericano de Cooperación para la Agricultura, San José.

Bohn HL, McNeal BL, O'Connor GA. 2001. Soil Chemistry. John Wiley and Sons Inc., New York.

Brady NC, Weil RR. 2008. The nature and properties of soils. Pearson Prentice Hall, Upper Sandle River.

Bronner G, Goss KU. 2011. Sorption of organic chemicals to soil organic matter: Influence of soil variability and pH dependence. Environ Sci Technol 45:1307-1312.

Chang Chien SW, Chen CY, Chang JH, Chen SH, Wang MC, Mannepalli MR. 2010. Sorption of toluene by humic acids derived from lake sediment and mountain soil at different pH. J Hazard Mater 177:1068-1076.

Chang R, 2010. Chemistry. McGraw-Hill, Boston.

Cunningham SD, Shann JR, Crowley DE, Anderson TA. 1997. Phytoremediation of contaminated water and soil. In: Krueger E *et al.* (eds.) Phytoremediation

of soil and water contaminants. ACS Symposium Series. American Chemical Society, Washington DC.

Du P, Sagehashi M, Terada A, Zhou S, Li F, Hosomi M. 2011. Adequacy of a simple diffusion model to predict benzene behavior in soil. Soil Sci Soc Am J 75: 2147-2157.

Esteve-Turrillas FA, Armenta S, Garrigues S, Pastor A, de la Guardia M. 2007. Headspace–mass spectrometry determination of benzene, toluene and the mixture of ethylbenzene and xylene isomers in soil samples using chemometrics. Anal Chim Acta 587:89-96.

European Fuel Oxygenates Association (EFOA). http://www.efoa.eu.

García Pinto C, Herrero Martín S, Pérez Pavón JL, Moreno Cordero B. 2011. A simplified Quick, Easy, Cheap, Effective, Rugged and Safe approach for the determination of trihalomethanes and benzene, toluene, ethylbenzene and xylenes in soil matrices by fast gas chromatography with mass spectrometry detection. Anal Chim Acta 689:129-136.

Genovese M, Denaro R, Cappello S, Di Marco G, La Spada G, Giuliano L, Genovese L, Yakimov MM. 2008. Bioremediation of benzene, toluene, ethylbenzene, xylenes-contaminated soil: a biopile pilot experiment. J Appl Microbiol 105:1694-1702.

Goss KU, Schwarzenbach RP. 2003. Rules of thumb for assessing equilibrium partitioning of organic compounds: success and pitfalls. J Chem Educ 80:450-455.

He X, Chen S, Quan X, Zhao Y, Zhao H. 2009. Temperature-dependence of soil/air partition coefficients for selected polycyclic aromatic hydrocarbons and organochlorine pesticides over a temperature range of −30 to +30 °C. Chemosphere 76:465-471.

Kim JM, Le NT, Chung BS, Park JH, Bae JW, Madsen EL, Jeon CO. 2008. Influence of soil components on the biodegradation of benzene, toluene, ethylbenzene, and *o*-, *m*-, and *p*-xylenes by the newly isolated bacterium *Pseudoxanthomonas spadix* BD-a59. App Environ Microbiol 74:7313-7320.

Larsen G, Lotero E, Márquez M, Silva H. 1995. Ethyl *tert*-butyl ether (ETBE) synthesis on H-Mordenite: gas-phase kinetics and DRIFTS studies. J Catal 157:645-655.

Macías F, Calvo de Anta R. 1992. Pedogeochemical characterisation of the soils of Galicia (NW Spain) with respect to lithological variations. Evidence of a transitional environment between temperate and subtropical humid domains. C.R. Acad Sci Paris Ser II 315:1803–1810.

Mackay D, Shiu WY, Ma KC, Lee SC. 2006. Handbook of physical-chemical properties and environmental fate for organic chemicals. CRC Press, Boca Raton.

March J. 1992. Advanced organic chemistry: Reactions, mechanisms and structure. John Wiley & Sons, New York.

Margesin R, Walder G, Schinner F. 2003. Bioremediation assessment of a BTEX-contaminated soil. Acta Biotechnol 23:29-36.

Morsali A, Beyramabadi SA, Bozorgmehr MR, Raanaee M, Keyvani B, Jafari GR. 2010. Prediction of gas chromatography retention of BTEX and other substituted benzenes based on quantum chemical parameters. Sci Res Essays 5:349-351.

Niederer C, Schwarzenbach RP, Goss KU. 2007. Elucidating differences in the sorption properties of 10 humic and fulvic acids for polar and non-polar organic chemicals. Environ Sci Technol 41:6711-6717.

Ortiz I, Sanz J, Dorado M, Villar S. 2007. Técnicas de recuperación de suelos contaminados. Círculo de Innovación en Tecnologías Medioambientales y Energía (CITME), University of Alcalá.

Pavón JLP, Martín SH, Pinto CG, Cordero BM. 2009. Programmed temperature vaporizer based method for the sensitive determination of trihalomethanes and benzene, toluene, ethylbenzene and xylenes in soils. J Chromatogr A 1216:6063-6070.

Poppendieck DG, Loehr RC, Webster MT. 1999. Predicting hydrocarbon removal from thermally enhanced soil vapor extraction systems: 1. Laboratory studies. J Hazard Mater 69:81-93.

Prenafeta-Boldú FX, Ballerstedt H, Gerritse J, Grotenhuis JTC. 2004. Bioremediation of BTEX hydrocarbons: Effect of soil inoculation with the toluene-growing fungus *Cladophialophora* sp. strain T1. Biodegradation 15:59-65.

Rosell M, Lacorte S, Barceló D. 2006. Simultaneous determination of methyl *tert*-butyl ether, its degradation products and other gasoline additives in soil samples by closed-system-purge-and-trap gas chromatography-mass spectrometry. J Chromatogr A 1132:28-38.

Ruiz J, Bilbao R, Murillo MB. 1998. Adsorption of different VOC onto soil minerals from gas phase: Influence of mineral, type of VOC, and air humidity. Environ Sci Technol 32:1079-1084.

Serrano A, Gallego M. 2006. Sorption study of 25 volatile organic compounds in several Mediterranean soils using headspace–gas chromatography–mass spectrometry. J Chromatogr A 1118:261-270.

Sharmasarkar S, Jaynes WF, Vance GF. 2000. BTEX sorption by montmorillonite organo-clays: TMPA, ADAM, HDTMA. Water Air Soil Pollut 119:257-273.

Soares AA, Albergaria JT, Domingues VF, Alvim-Ferraz MdCM, Delerue-Matos C. 2010. Remediation of soils combining soil vapor extraction and bioremediation: Benzene. Chemosphere 80:823-828.

Sumner ME. 2000. Handbook of soil science. CRC Press, Boca Raton.

Suthersan SS. 1997. Remediation engineering: Design concepts. Lewis Publishers, Boca Raton.

United Kingdom Environment Agency. 2003. Review of the fate and transport of selected contaminants in the soil environment. Environment Agency, Bristol.

United States Environmental Protection Agency (USEPA). 2003. Method 5021A: Volatile organic compounds in various sample matrices using equilibrium headspace analysis. Revision 1. US Environmental Protection Agency, Washington.

Wade LG. 2012. Organic chemistry. Pearson Prentice Hall, Upper Sandle River.

7

Influence of plant root exudates on the mobility of fuel volatile compounds in contaminated soils

Vegetation and its associated microorganisms play an important role in the behaviour of soil contaminants. One of the most important elements is root exudation, since it can affect the mobility, and therefore, the bioavailability of soil contaminants. In this study, we evaluated the influence of root exudates on the mobility of fuel derived compounds in contaminated soils. Samples of humic acid, montmorillonite, and an A horizon from an alumi-umbric Cambisol were contaminated with volatile contaminants present in fuel: oxygenates (MTBE and ETBE) and monoaromatic compounds (benzene, toluene, ethylbenzene and xylene). Natural root exudates obtained from *Holcus lanatus* and *Cytisus striatus* and ten artificial exudates (components frequently found in natural exudates) were added to the samples, individually and as a mixture, to evaluate their effects on contaminant mobility. Fuel compounds were analyzed by headspace-gas chromatography-mass spectrometry. In general, the addition of natural and artificial exudates increased the mobility of all contaminants in humic acid. In A horizon and montmorillonite, natural or artificial exudates (as a mixture) decreased the contaminant mobility. However, artificial exudates individually had different effects: carboxylic components increased and phenolic components decreased the contaminant mobility. These results established a base for developing and improving phytoremediation processes of fuel-contaminated soils.

This work was included in the publications and/or communications:

Balseiro-Romero M, Kidd PS, Monterroso C. 2014. Influence of plant root exudates on the mobility of fuel volatile compounds in contaminated soils. Int J Phytorem 16:824-839.

Balseiro-Romero M, Kidd PS, Monterroso C. 2013. Influence of plant root exudates on the mobility of fuel volatile compounds in contaminated soils. 9th International Phytotechnology Society Conference, Hasselt, Belgium. Oral communication.

INTRODUCTION

Contamination of soil with fuel compounds is a serious and frequent problem, resulting from the poor management of wastes and emissions of the petrochemical industry, accidental spills, or leakage from underground storage tanks (Kim *et al.*, 2008).

Among fuel hydrocarbons, benzene, toluene, ethylbenzene and xylene (BTEX) are of particular concern because of their high toxicity and carcinogenicity. They occur naturally in crude oil and are therefore found in fuel derived products (UK Environment Agency, 2003). Present gasoline formulations are supplemented by oxygenates as octane enhancers and ethers, particularly, methyl *tert*-butyl ether (MTBE) and ethyl *tert*-butyl ether (ETBE) are the most commonly used (EFOA Website, http://www.efoa.eu). Both BTEX and fuel oxygenates (FO) are very volatile and water-soluble. Therefore, contamination of soil with these compounds must not be ignored, since they can easily migrate to air and groundwater (Pavón *et al.*, 2009), causing important contamination problems in those environmental compartments. In this sense, applying an appropriate and effective soil remediation technique appears essential to avoid and reduce the impact of this type of contaminants on the environment and on human health.

Traditional strategies to treat fuel contaminated soils include various physical and chemical engineering-based technologies such as thermal desorption, air sparging, soil washing, vapour extraction, solidification or stabilization (Zhang *et al.*, 2010). However, these techniques are either too expensive or have a high energy consumption, making them often financially impossible, especially when large areas or volumes of soil were contaminated. Furthermore, soil structure may be damaged, making the land unsuitable for agricultural use (Zhang *et al.*, 2010).

Phytoremediation is an alternative technology which uses plants to extract, contain, degrade, and/or immobilize soil contaminants. Due to the low cost of this technique, the *in situ* nature of the treatment, the large public acceptance, and the fact that it is easy to handle (Schwitzguébel *et al.*, 2002), phytoremediation is gaining advantage over other remediation strategies. Furthermore, it is not invasive and, in principle, delivers intact, biologically active soil (Wenzel, 2009). From an environmental standpoint, plants can be seen as a "natural, solar-powered, pump-and-treat systems" for cleaning up contaminated soils (Van Acken *et al.*, 2010).

The success of phytoremediation lies in the correct understanding of the subtle and complex interactions between contaminants, soil material, plants and the associated microorganisms (Vangronsveld *et al.*, 2009). Of particular interest in this system is root exudation. The impact of root exudates on the microbial community in the rhizosphere has been widely studied: root exudates greatly influence the abundance, diversity or activity of potential degrading microorganisms in the zone surrounding the roots (Phillips *et al.*, 2012). Furthermore, root exudates can produce significant changes in physicochemical soil properties, particularly in the rhizosphere, and can greatly influence soil sorption-desorption processes, and therefore, the mobility and bioavailability of soil contaminants (Zhu *et al.*, 2009), becoming a key player in elucidating the fate of contaminants in the environment. In a previous study (Balseiro-Romero and Monterroso, 2013), we developed a headspace (HS) analysis approach to assess the sorption of BTEX and FO by a wide variety of soils and soil components, under different conditions (contaminant concentration, incubation time, temperature). Our knowledge of these contaminant-soil interactions serves as a basis for further understanding interactions between root exudates and soil contaminants and the soil itself, which could contribute towards a better

understanding of this complex soil-plant-contaminant system and to establishing a base for optimizing phytoremediation processes.

Within this context, the aim of the present study was to evaluate the influence of root exudates on the mobility of fuel volatile compounds in contaminated soils. For this purpose, both natural root exudates and artificial exudates (components usually found in natural root exudates) were added to sterile spiked matrices in a HS vial-adapted batch system.

MATERIALS AND METHODS

Reagents

The following reagents usually found in fuel were used: benzene (purity, 99.8%; grade, PAI-ACS (UV-IR-HPLC-GPC)), toluene (purity, 99.8%; grade, PAI-ACS (UV-IR-HPLC-GPC)), ethylbenzene (purity, 99%; grade, PS), *o*-xylene (purity, 99%; grade, PA (Reag. USP. Ph. Eur)), *m*-xylene (purity, 99%; grade, PA (Reag. Ph. Eur)), *p*-xylene (purity, 99%; grade, PA (Reag. USP)), MTBE (purity, 99.7%; grade, PAI (PAR)) and ETBE (purity, 99%; grade, PA (Reag. USP)). All reagents were purchased from Panreac Química, S.L.U. (Barcelona, Spain). A stock solution with each of the reagents at a concentration of 100 mg L^{-1} was prepared in methanol (purity, 99.9%; grade, (PAR) PAI). This solution was prepared daily to avoid errors due to volatilization losses.

For the artificial exudates, the following compounds usually found in natural root exudates were used (Table 7.1): pyruvic acid (purity, 98%), malonic acid (purity, 99%), succinic acid (purity, 99%), fumaric acid (disodium salt; purity, 99.9%), citric acid (anhydrous; purity≥99.5%), salicylic acid (purity, 99%), *p*-coumaric acid (purity≥98%; grade, HPLC), ferulic acid (purity, 99%) and (±) catechin hydrate (purity, 99.2%) were purchased from Sigma-Aldrich Química,

S.A. (Madrid, Spain); and oxalic acid (purity, 97%) was purchased from Merck-España (Madrid, Spain).

Table 7.1. Main properties of the individual root exudate components (REC) used.

Name	Type	%C (*w*/*w*) [a]	log P [b]
Pyruvic acid (PA)	Monocarboxylic aliphatic acid	40.9%	-1.24
Oxalic acid (OA)	Bicarboxylic aliphatic acids	19.0%	-2.22
Malonic acid (MA)		34.6%	-0.56
Succinic acid (SuA)		40.6%	-0.59
Fumaric acid (FuA)		30.0%	-0.46
Citric acid (CiA)	Tricarboxylic aliphatic acid	37.5%	-1.72
Salicylic acid (SaA)	Phenolic compounds	60.8%	2.26
***p*-Coumaric acid (CouA)**		65.8%	1.88
Ferulic acid (FeA)		61.8%	1.64
(±) Catechin hydrate (Cat)		62.0%	0.49

[a] *%C: g of carbon per 100 g of exudate component.*
[b] ***P:** water/organic matter partition coefficient. Calculated using Advanced Chemistry Development (ACD/Labs) Software V11.02. The organic phase used was octanol.*

Collection of natural root exudates

For the collection of natural root exudates, plants were grown under sterile conditions and all manipulations were carried out in a sterile laminar-flow hood. All solutions were prepared using sterile ultra pure water (Milli-Q). Seeds of *Holcus lanatus* and *Cytisus striatus* were surface-sterilized with 2.5% NaClO (10 min) and rinsed in sterile Milli-Q water. Seeds were placed in autoclaved glass Petri dishes (6 cm tall) on sterile 1:1 vermiculite:perlite mixture moistened with sterile Milli-Q water, and kept under the following growth chamber conditions: day/night cycle of 16/8 hours and 20/15 °C, 190 mmol $\cdot m^{-2} \cdot s^{-1}$ of PPFD (photosynthetic photo flux density). After 3-4 weeks, seedlings were transferred into sterile 500-mL Erlenmeyer flasks containing continuously aerated filter-sterilized 0.5-strength Hoagland's nutrient solution. Flasks were covered in aluminium paper and nutrient solutions were changed every week. Plants were

allowed to grow for 4 weeks before root exudate sampling. Exudates were collected by transferring the plants to sterile 0.4 mM $CaCl_2$ solution. After 24 hours, the plants were removed and the exudate solutions were immediately filtered (0.2 µm), frozen and lyophilized so as to minimize microbial degradation. This protocol was repeated until the required quantity of root exudate solution was obtained. The same plants were used for distinct sampling events with a 2 day break interval between each sampling (during which time they were transferred into filter-sterilized 0.5-strength Hoagland's nutrient solution).

The lyophilized exudate solutions obtained from either *H. lanatus* or *C. striatus* were then re-dissolved in sterile Milli-Q water to obtain a dissolved organic carbon concentration (DOC) of approximately 20 mg C L^{-1} for both plant species. The DOC of the final solution was measured with an organic carbon analyser (Flowsys Model, Systea).

Soil and soil components samples

Samples of two common soil components with markedly different colloidal and physicochemical properties (humic acid and montmorillonite) and a sample of an A horizon, were selected for the study. The samples of humic acid and montmorillonite were purchased from Sigma-Aldrich Química, S.A. (Madrid. Spain). Humic acid is the main fraction of soil organic matter and consists of complex aromatic macromolecules joined to amino acids, peptides, amino sugars, aliphatic acids and other organic constituents (Sumner, 2000). The sample used had a high organic carbon concentration (490.1 g Kg^{-1}) and cation exchange capacity (159.3 cmol(+) Kg^{-1}). Montmorillonite is a 2:1 clay mineral of the smectite group with high permanent charge and a shrinking/swelling capacity on drying or wetting (Bohn *et al.*, 2001). The sample used had a high surface area (254.9 m^2 g^{-1}) and a cation exchange capacity of 68.8 cmol(+) Kg^{-1}. The A horizon was collected from an alumi-umbric Cambisol (A_{Camb}) in the surroundings of

Santiago de Compostela (Galicia, NW Spain). This region has an average annual temperature of 13 °C and an average annual precipitation of 1290 mm. The sample used showed variable charge, low pH (4.9), low cation exchange capacity (2.0 cmol(+) Kg^{-1}) dominated by aluminium, and a concentration of organic carbon of 42.6 g Kg^{-1}. This soil horizon was chosen for the study since it coincides with the area of highest root proliferation and activity. It was sieved through a 2 mm mesh and conserved in plastic containers at room temperature until use.

All matrices were previously sterilized with a 0.5 mM sodium azide solution.

Description of the experiments

The different matrices were artificially spiked with BTEX (benzene, toluene, ethylbenzene and *m*-, *p*- and *o*-xylene) and fuel oxygenates (FO, MTBE and ETBE) at a concentration of 10 µg of each individual compound per g of sample. According to the manufacturer's recommendations and to Method 5021A from United States Environmental Protection Agency (USEPA, 2003), the spiking procedure was carried out in HS analytical vials containing a slurry resulting from mixing 1 g of matrix and 2 mL of distilled water. The slurry minimises losses due to evaporation (Serrano and Gallego, 2006) and favours the equal distribution of the contaminant over the soil. Once the matrices were spiked, the vials were quickly sealed with magnetic caps with silicone-PTFE septa, and stabilized for 7 days at low temperature. This HS vial-adapted batch system is hermetically closed during all the experimental steps (spiking, stabilization, addition of exudates and analysis), minimizing the contaminant losses due to evaporation in conventional batch systems.

Different parallel experiments with the addition of root exudates were carried out. On the one hand, natural root exudates (collected from *H. lanatus*

or *C. striatus*) were added to the spiked and stabilized matrices at an approximate concentration of 20 mg C L^{-1}. On the other hand, ten root exudate components (REC) usually found in natural root exudates (mono-, bi- and tricarboxylic acids and phenolic compounds) (Table 7.1) were added to the spiked matrices as a mixture, simulating an artificial root exudate, and individually, at three different concentrations, 1, 10 and 25 mM, to study the effect of each REC separately. In the case of the mixture, these global concentrations corresponded to 0.1, 1 and 2.5 mM for each individual REC.

The spiked matrices without the addition (used as controls) and with the addition of root exudates (natural or artificial) were agitated in a linear laboratory shaker for approximately 12 hours before analysis, in order to enhance contact between the exudates, the matrix and the contaminants. In all experiments, the matrices were contaminated and analyzed in triplicate by headspace-gas chromatography-mass spectrometry (HS-GC-MS).

Instrumentation and analytical procedure: HS-GC-MS

The analytical system consists of an autosampler (Combi PAL, Agilent Technologies), an oven for heating the samples until headspace equilibrium, a gas chromatograph (Model 450 GC, Agilent Technologies) and a mass spectrometer with ion trap (Model 220 MS, Agilent Technologies).

The headspace (HS) operating conditions were established according to the manufacturer's application notes and to the results of some preliminary experiments carried out in the laboratory. During the HS process, the sample vials were heated at 80 °C in the HS oven, and constantly agitated (500 rpm) for 15 minutes to achieve an acceptable equilibrium between the slurry and the HS. Then, 1 mL of gas from the HS of the vials was aspirated with a 2.5 mL-syringe (supplied by CTC Analytics AG) and was directly injected in the chromatograph

for analysis. The injector worked at 250 °C and in split mode, with a 1/10 split ratio (Chapter 3).

The chromatographic column was a Factor Four VF-5ms EZ-Guard (supplied by Agilent Technologies) of 30 m x 0.25 mm x 0.25 µm. The column oven temperature was varied as follows: 35 °C held for 5 minutes, followed by an increase of 10 °C min^{-1} up to 80 °C and an increase of 25 °C min^{-1} up to 200 °C, which was held for 0.7 minutes. The carrier gas was helium at constant flow of 1 mL min^{-1}.

The mass spectrometer operated in full scan mode. Ionization of the molecules was carried out by electronic impact (EI). The ion trap temperature was fixed at 220 °C and the transfer line temperature, at 280 °C.

In the chromatograms obtained, *m*- and *p*-xylene appeared as a single peak and were therefore analyzed jointly.

Cycle Composer software (Version 1.5.4; CTC Analytics AG) was used to control the Combi PAL autosampler and MS Workstation software (Version 6.9.3; Varian, Inc.) was used to control de GC-MS system and to process the analytical data.

Calibration was carried out with standards of 2 mL of water (the same volume added to the slurry of samples) containing 0.1, 0.5, 1, 5 and 10 µg of each individual contaminant. The standards were analyzed in triplicate by HS-GC-MS under the same analytical conditions as the samples. The calibration curves fitted well to a linear pattern (R^2>0.997).

BTEX and FO were quantified in the slurries without any matrix effect correction, in order to assess the contaminant mobility in the different matrices: the equilibrium concentration reached during HS analysis or the analytical recovery is directly related to the amount of contaminant which is free of sorption, and therefore, to the contaminant mobility. The differences in the

analytical recovery allowed for easily characterizing the effect of root exudates on the contaminant mobility in each matrix.

Statistical analysis

PASW Statistics software (Version 18.0.0; IBM SPSS Statistics, Inc.) was used to analyze the data. The data of the controls were analyzed by a one factor ANOVA, with a Tukey *post hoc* analysis. The data from the experiment with artificial exudates were analyzed by principal component analysis (rotation was carried out by Varimax method). Furthermore, the data from the samples with the addition of individual REC was correlated with some REC properties. A significance level of p=0.05 was considered for all statistical analyses.

RESULTS

Mobility of BTEX and FO in soil components and soil in the absence of exudates

Figure 7.1 represents the recovery of each contaminant from each matrix without the addition of root exudates (controls), expressed as a percentage from the total concentration spiked (10 μg g^{-1}) of each contaminant. The final recovered percentage of the contaminants varied from 15 to 85%, indicating from very high to very low sorption capacities of the different matrices. The high variation reflects the participation of different sorption mechanisms influenced by the properties of the matrix and the contaminants.

At a first glance, FO were recovered in significantly (p<0.05) higher proportions than BTEX from all the matrices: the recovery of FO varied from 55% to 85%, and that of BTEX varied from 15% to 50%. This could be easily explained because MTBE and ETBE are more soluble and volatile, and therefore,

more mobile, than the BTEX compounds: the water solubility of FO varied from 26.0 to 51.6 g L^{-1} (EFOA Website http://www.efoa.eu) and that from BTEX varied from 0.1 to 1.8 g L^{-1} (Mackay *et al.*, 2006); and the vapour pressure (at 20-25 °C) of FO varied from 28 to 31 KPa (EFOA Website http://www.efoa.eu) and that from BTEX varied from 0.8 to 13 KPa (Mackay *et al.*, 2006) (Appendix A). Furthermore, the recovery of the BTEX compounds decreased with a diminution in volatility: the volatility order of BTEX is benzene>toluene>ethylbenzene>*m*/*p*-xylene>*o*-xylene (Mackay *et al.*, 2006). The exception to this tendency was *o*-xylene, in montmorillonite and A_{Camb}, which was recovered in a higher proportion than *m*/*p*-xylene, and even than ethylbenzene (although this difference was not statistically significant).

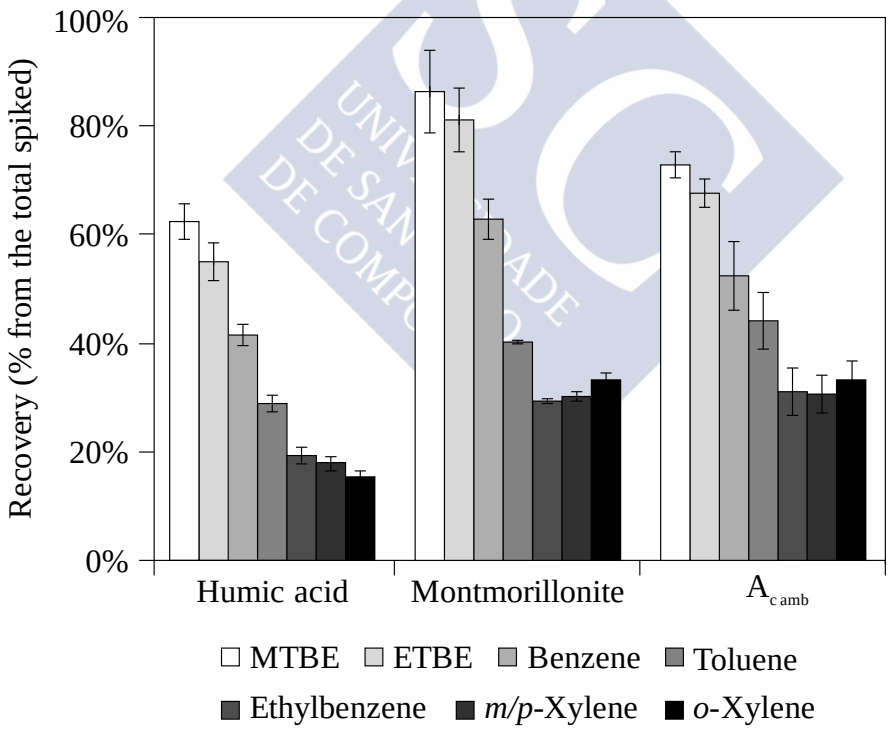

Figure 7.1. Recovery of BTEX and FO after HS-GC-MS analysis of the matrices spiked at a concentration of 10 μg g^{-1}, for each individual contaminant. The results are expressed as the mean of the percentage of each contaminant recovered from the total spiked ± the standard deviation (*n=3*).

Humic acid showed the lowest contaminant recovery of all matrices, due to its high retention capacity. The contaminant recovery varied from 15% of *o*-xylene to 60% of MTBE. Montmorillonite also showed low contaminant recovery, especially for the contaminants with the highest molecular weight, reflecting an unexpected retention capacity, in spite of the inorganic properties of this soil component: the recovery of the contaminants varied from 30% of *m*/*p*-xylene to 85% of MTBE. A_{Camb} showed contaminant recoveries which fell between those of humic acid and montmorillonite (from 30% of *m*/*p*-xylene to 70% of MTBE was recovered), since the organic and inorganic components in soil are contributing with different sorption capacities.

Influence of natural root exudates on BTEX and FO mobility

The HS-GC-MS analysis data of the matrices with the addition of natural root exudates from *H. lanatus* or *C. striatus* were normalized by dividing by the HS-GC-MS analysis results of the controls without exudate (Figure 7.2). This ratio helped to decide whether the addition of exudate increased (if the ratio is over 1) or decreased (if it is under 1) the mobility of the contaminants, previously stabilized in the spiked matrices.

In general, the addition of natural root exudates provoked a decrease in the recovery of the contaminants, and this was more pronounced in the case of exudates from *C. striatus* than those from *H. lanatus*. The addition of *C. striatus* exudates, provoked a contaminant mobility decrease of approximately 10-40% with respect to the control without exudate, and the addition of *H. lanatus* exudates. provoked a decrease of 10-20%. Only in the case of humic acid with *H. lanatus* exudates, the mobility of the contaminants increased: they provoked a mobility increase of 10-20% with respect to the controls without exudates.

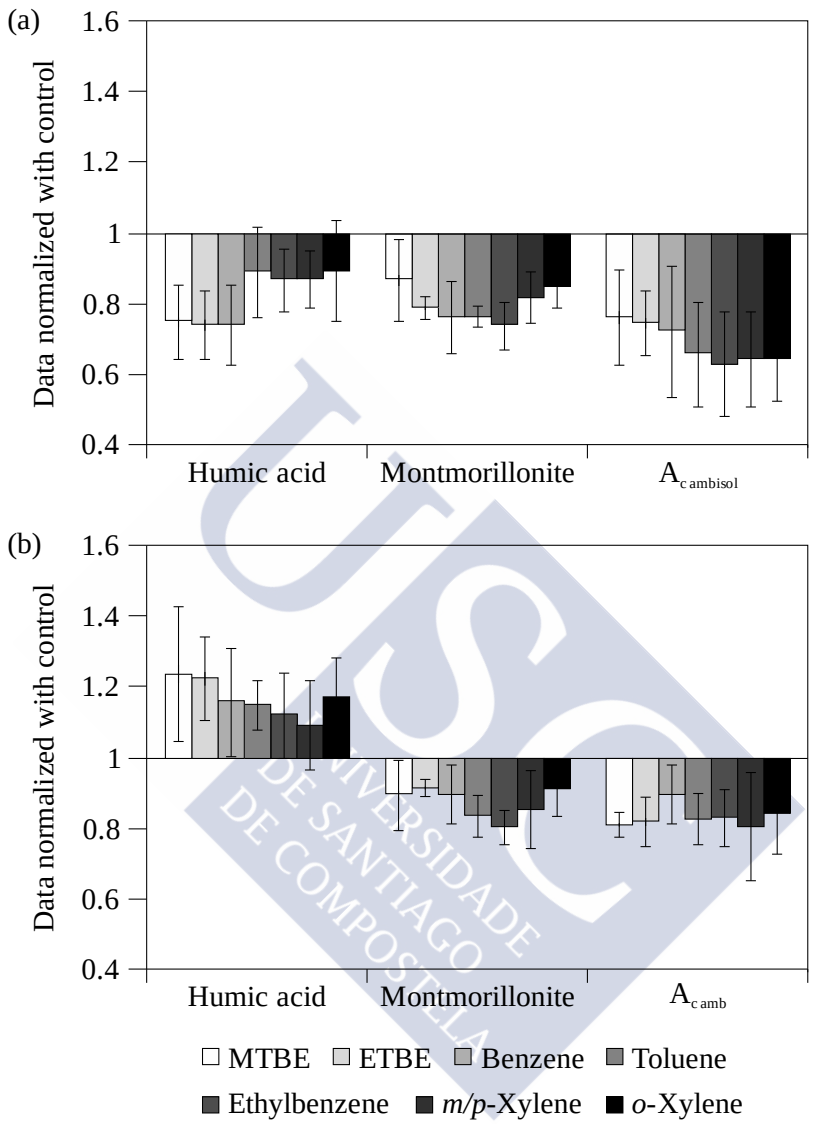

Figure 7.2. Normalized HS-GC-MS analysis data of the matrices after the addition of *Cytisus striatus* (a) and *Holcus lanatus* (b) root exudates. The normalization was carried out with the HS-GC-MS analysis data of the matrices without the addition of exudates. The results are expressed as the mean ± the standard deviation (*n=3*).

Despite the contaminants have very different mobilities (as seen for the controls), no generalized tendencies were found for the change in mobility induced by the addition of root exudates in the different matrices.

Influence of root exudate components (REC) (individually and as a mixture) on BTEX and FO mobility

The combined and individual effect of a variety of carboxylic and phenolic REC (Table 7.1) on the mobility of BTEX and FO was studied at different concentrations (1, 10 and 25 mM). Figure 7.3 represents the results of the addition of the REC mixture to the different spiked matrices, for each mixture concentration and contaminant. The addition of this artificial root exudate provoked an effect similar to that of *H. lanatus* exudates: the REC mixture increased the mobilization of the contaminants in the humic acid (between 15-80%) and increased the retention of the contaminants in the A_{Camb} and the montmorillonite (up to 80%). Furthermore, this effect grew with increasing mixture concentration, and, in most cases, very good correlations were found between the normalized HS-GC-MS analysis data and the mixture concentration (R^2=0.80–1.00).

Results showing the effect of each REC individually (at different concentrations) are detailed in Tables 7.2, 7.3 and 7.4. The effect of each REC was very different according to the type of matrix and REC. The addition of any REC to humic acid provoked an increase in the mobility of all contaminants, as occurred for *H. lanatus* exudates (the contaminant mobility increase varied from 10 to 100%, with respect to the controls without exudates) (Table 7.2). In general, carboxylic REC increased the contaminant mobility in montmorillonite and A_{Camb} (increase of up to 100%) (Tables 7.3 and 7.4), but the addition of phenolic REC to those matrices, caused a decrease in the mobilization of the contaminants, as occurred with natural root exudates (decrease of up to 80%) (Tables 7.3 and 7.4).

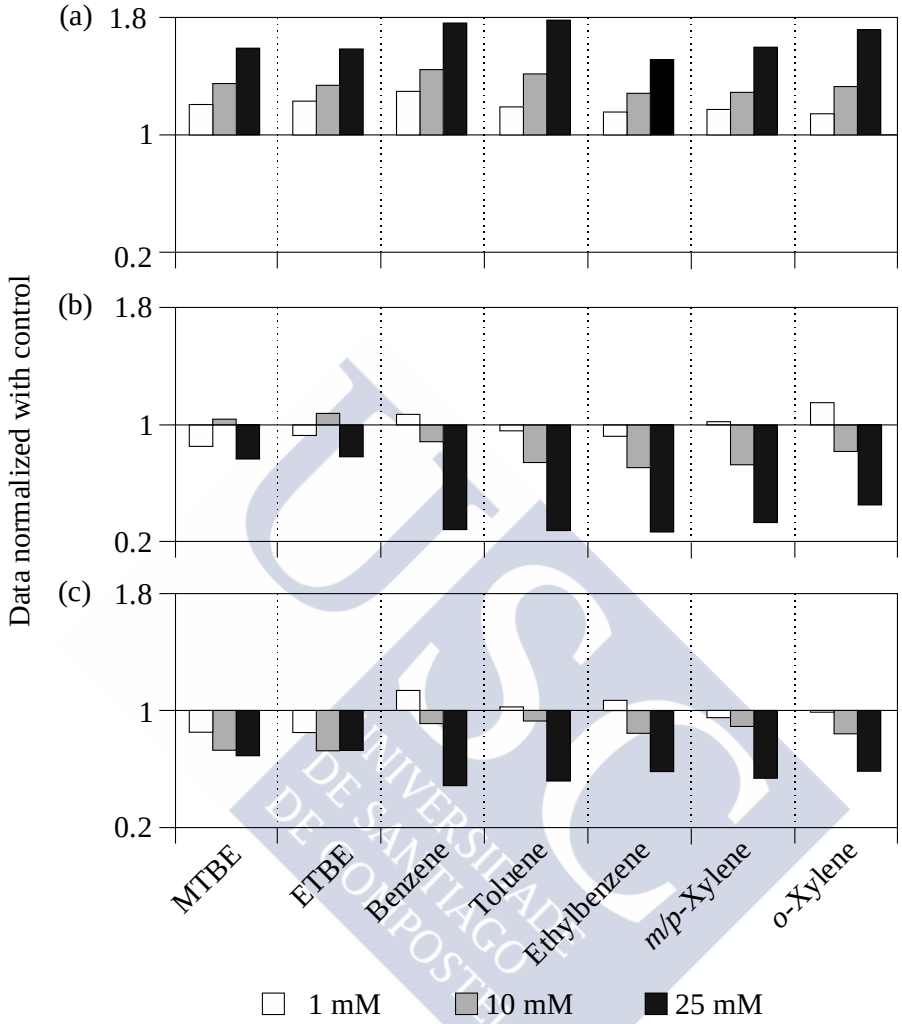

Figure 7.3. Normalized HS-GC-MS analysis data of humic acid (a), montmorillonite (b) and A_{Camb} (c) after the addition of the REC mixture at 1, 10 and 25 mM. The normalization was carried out with the HS-GC-MS analysis data of the matrices without the addition of exudates.

Table 7.2. Normalized HS-GC-MS analysis data of FO and BTEX in contaminated humic acid after the addition of individual root exudate components (REC). The results are expressed as the mean ± the standard deviation (*n=3*).

REC	Concentration (mM)	MTBE	ETBE	Benzene	Toluene	Ethylbenzene	*m/p*-Xylene	*o*-Xylene
AP	1	1.80 ± 0.18	1.33 ± 0.45	1.77 ± 0.21	1.59 ± 0.29	1.50 ± 0.36	1.55 ± 0.37	1.46 ± 0.36
	10	1.98 ± 0.30	1.33 ± 0.11	1.36 ± 0.49	1.24 ± 0.43	1.21 ± 0.41	1.40 ± 0.34	1.39 ± 0.36
	25	1.36 ± 0.47	1.39 ± 0.15	1.52 ± 0.20	1.52 ± 0.18	1.28 ± 0.17	1.41 ± 0.17	1.40 ± 0.16
AO	1	1.47 ± 0.17	1.46 ± 0.30	1.54 ± 0.22	1.53 ± 0.38	1.57 ± 0.39	1.53 ± 0.43	1.29 ± 0.23
	10	1.65 ± 0.31	1.73 ± 0.15	1.33 ± 0.25	1.38 ± 0.30	1.50 ± 0.27	1.37 ± 0.31	1.28 ± 0.22
	25	1.51 ± 0.28	1.72 ± 0.17	1.74 ± 0.42	1.80 ± 0.25	1.48 ± 0.20	1.62 ± 0.21	1.63 ± 0.23
AM	1	1.87 ± 0.13	1.69 ± 0.26	1.86 ± 0.35	2.07 ± 0.26	2.01 ± 0.32	2.15 ± 0.38	2.04 ± 0.39
	10	1.79 ± 0.24	1.13 ± 0.29	1.67 ± 0.30	1.65 ± 0.25	1.59 ± 0.23	1.59 ± 0.23	1.59 ± 0.22
	25	1.74 ± 0.21	1.23 ± 0.15	1.32 ± 0.21	1.39 ± 0.20	1.11 ± 0.17	1.21 ± 0.19	1.23 ± 0.19
ASu	1	1.38 ± 0.42	1.62 ± 0.29	1.47 ± 0.51	1.39 ± 0.41	1.17 ± 0.24	1.39 ± 0.38	1.30 ± 0.36
	10	1.40 ± 0.45	1.27 ± 0.11	1.78 ± 0.38	1.79 ± 0.28	1.57 ± 0.28	1.56 ± 0.29	1.60 ± 0.32
	25	1.65 ± 0.25	1.25 ± 0.16	1.36 ± 0.11	1.32 ± 0.11	1.08 ± 0.09	1.18 ± 0.11	1.19 ± 0.12
AFu	1	1.34 ± 0.11	1.26 ± 0.11	1.39 ± 0.20	1.31 ± 0.12	1.25 ± 0.16	1.32 ± 0.18	1.36 ± 0.32
	10	1.38 ± 0.11	1.53 ± 0.12	1.33 ± 0.15	1.29 ± 0.15	1.22 ± 0.18	1.22 ± 0.19	1.24 ± 0.21
	25	1.30 ± 0.13	1.43 ± 0.17	1.62 ± 0.25	1.64 ± 0.23	1.43 ± 0.23	1.44 ± 0.34	1.59 ± 0.28
ACi	1	1.76 ± 0.75	1.31 ± 0.14	1.78 ± 0.86	1.27 ± 0.45	1.17 ± 0.39	1.23 ± 0.39	1.18 ± 0.43
	10	1.76 ± 0.72	1.63 ± 0.14	1.38 ± 0.18	1.23 ± 0.27	1.13 ± 0.26	1.16 ± 0.26	1.19 ± 0.29
	25	1.36 ± 0.14	1.61 ± 0.15	1.75 ± 0.17	1.66 ± 0.27	1.47 ± 0.18	1.63 ± 0.20	1.56 ± 0.29
ASa	1	1.83 ± 0.11	1.20 ± 0.11	1.77 ± 0.19	1.61 ± 0.20	1.50 ± 0.18	1.55 ± 0.19	1.37 ± 0.33
	10	1.84 ± 0.13	1.66 ± 0.12	1.28 ± 0.17	1.24 ± 0.12	1.24 ± 0.30	1.17 ± 0.11	1.18 ± 0.11
	25	1.25 ± 0.12	1.70 ± 0.22	1.81 ± 0.30	1.72 ± 0.23	1.54 ± 0.27	1.77 ± 0.27	1.72 ± 0.33
ACu	1	1.30 ± 0.18	1.51 ± 0.21	1.35 ± 0.40	1.35 ± 0.42	1.30 ± 0.42	1.36 ± 0.44	1.30 ± 0.42
	10	1.29 ± 0.19	1.82 ± 0.16	1.60 ± 0.22	1.56 ± 0.23	1.41 ± 0.23	1.47 ± 0.26	1.52 ± 0.26
	25	1.57 ± 0.20	1.81 ± 0.18	1.87 ± 0.23	1.88 ± 0.21	1.60 ± 0.19	1.78 ± 0.22	1.86 ± 0.29
AFe	1	1.59 ± 0.11	1.31 ± 0.17	1.72 ± 0.14	1.60 ± 0.15	1.59 ± 0.20	1.57 ± 0.19	1.53 ± 0.21
	10	1.62 ± 0.11	1.62 ± 0.20	1.32 ± 0.12	1.22 ± 0.19	1.10 ± 0.25	1.13 ± 0.26	1.20 ± 0.23
	25	1.49 ± 0.29	1.64 ± 0.21	1.68 ± 0.28	1.60 ± 0.28	1.51 ± 0.26	1.47 ± 0.35	1.50 ± 0.35
Cat	1	1.40 ± 0.16	1.20 ± 0.13	1.75 ± 0.23	1.61 ± 0.21	1.42 ± 0.24	1.59 ± 0.26	1.47 ± 0.30
	10	1.54 ± 0.25	1.47 ± 0.14	1.24 ± 0.16	1.23 ± 0.14	1.23 ± 0.28	1.13 ± 0.15	1.17 ± 0.18
	25	1.24 ± 0.13	1.45 ± 0.12	1.58 ± 0.19	1.50 ± 0.19	1.31 ± 0.22	1.38 ± 0.22	1.40 ± 0.24

Table 7.3. Normalized HS-GC-MS analysis data of FO and BTEX in contaminated montmorillonite after the addition of individual root exudate components (REC). The results are expressed as the mean ± the standard deviation (*n=3*).

REC	Concentration (mM)	MTBE	ETBE	Benzene	Toluene	Ethylbenzene	*m/p*-Xylene	*o*-Xylene
AP	1	1.30 ± 0.13	1.47 ± 0.17	1.54 ± 47	1.35 ± 0.50	1.32 ± 0.56	1.53 ± 0.66	1.77 ± 0.41
	10	1.12 ± 0.13	1.09 ± 0.18	1.17 ± 0.35	1.20 ± 0.47	1.18 ± 0.57	1.29 ± 0.79	1.67 ± 0.53
	25	0.98 ± 0.05	1.07 ± 0.05	0.90 ± 0.32	0.80 ± 0.33	0.72 ± 0.31	0.77 ± 0.35	0.94 ± 0.21
AO	1	1.28 ± 0.16	1.44 ± 0.12	1.24 ± 0.42	1.12 ± 0.68	1.04 ± 0.75	1.28 ± 0.92	1.50 ± 0.69
	10	1.08 ± 0.09	1.03 ± 0.10	0.83 ± 0.20	0.72 ± 0.24	0.64 ± 0.28	0.85 ± 0.41	1.11 ± 0.30
	25	1.19 ± 0.05	1.27 ± 0.06	1.07 ± 0.31	1.17 ± 0.43	1.19 ± 0.57	1.22 ± 0.63	1.38 ± 0.36
AM	1	1.35 ± 0.09	1.49 ± 0.12	1.57 ± 0.65	1.44 ± 0.65	1.14 ± 0.61	1.47 ± 0.88	1.72 ± 0.60
	10	1.04 ± 0.09	1.12 ± 0.10	1.35 ± 0.39	1.18 ± 0.46	1.31 ± 0.61	1.32 ± 0.70	1.53 ± 0.39
	25	1.03 ± 0.26	1.27 ± 0.20	1.54 ± 0.82	1.51 ± 1.03	1.57 ± 1.07	1.38 ± 0.82	1.52 ± 0.57
ASu	1	1.16 ± 0.12	1.33 ± 0.13	1.60 ± 0.44	1.42 ± 0.68	1.43 ± 0.89	1.38 ± 1.10	1.84 ± 0.66
	10	0.88 ± 0.12	0.94 ± 0.10	1.02 ± 0.33	0.90 ± 0.39	0.87 ± 0.45	0.94 ± 0.52	1.06 ± 0.32
	25	1.07 ± 0.11	1.25 ± 0.19	1.20 ± 0.35	1.09 ± 0.40	1.01 ± 0.41	1.08 ± 0.50	1.39 ± 0.44
AFu	1	1.31 ± 0.10	1.40 ± 0.15	0.90 ± 0.25	0.63 ± 0.26	0.54 ± 0.30	0.88 ± 0.69	1.09 ± 0.59
	10	0.96 ± 0.08	1.03 ± 0.10	0.94 ± 0.28	0.76 ± 0.26	0.68 ± 0.32	0.78 ± 0.39	0.93 ± 0.27
	25	1.38 ± 0.08	1.54 ± 0.10	1.44 ± 0.40	1.22 ± 0.41	1.07 ± 0.45	1.15 ± 0.51	1.37 ± 0.32
ACi	1	1.23 ± 0.08	1.35 ± 0.09	1.75 ± 0.72	1.80 ± 0.95	2.09 ± 1.32	1.70 ± 1.71	2.33 ± 0.90
	10	1.26 ± 0.11	1.29 ± 0.13	1.59 ± 0.57	1.31 ± 0.83	1.31 ± 1.02	1.16 ± 0.72	1.60 ± 0.82
	25	1.26 ± 0.15	1.33 ± 0.17	1.28 ± 0.36	1.28 ± 0.50	1.23 ± 0.48	1.33 ± 0.57	1.62 ± 0.43
ASa	1	1.16 ± 0.09	1.19 ± 0.07	0.68 ± 0.24	0.46 ± 0.19	0.43 ± 0.17	0.57 ± 0.25	0.73 ± 0.17
	10	1.09 ± 0.16	1.12 ± 0.14	0.96 ± 0.36	0.61 ± 0.26	0.46 ± 0.21	0.45 ± 0.23	0.55 ± 0.15
	25	1.09 ± 0.11	1.16 ± 0.13	0.95 ± 0.29	0.71 ± 0.29	0.57 ± 0.25	0.52 ± 0.26	0.65 ± 0.19
ACu	1	0.93 ± 0.05	1.03 ± 0.07	1.11 ± 0.37	1.01 ± 0.46	0.83 ± 0.45	0.90 ± 0.49	1.05 ± 0.32
	10	0.88 ± 0.13	0.98 ± 0.19	0.96 ± 0.37	0.80 ± 0.28	0.71 ± 0.39	0.73 ± 0.43	0.85 ± 0.33
	25	0.90 ± 0.04	0.98 ± 0.07	0.51 ± 0.16	0.34 ± 0.14	0.30 ± 0.13	0.33 ± 0.15	0.39 ± 0.10
AFe	1	0.85 ± 0.06	0.93 ± 0.07	0.84 ± 0.22	0.79 ± 0.30	0.68 ± 0.34	0.77 ± 0.43	0.93 ± 0.29
	10	0.95 ± 0.04	0.90 ± 0.19	0.80 ± 0.19	0.57 ± 0.19	0.45 ± 0.18	0.48 ± 0.21	0.59 ± 0.14
	25	0.87 ± 0.07	0.88 ± 0.06	0.39 ± 0.32	0.36 ± 0.14	0.30 ± 0.13	0.34 ± 0.16	0.43 ± 0.11
Cat	1	0.83 ± 0.05	0.89 ± 0.08	0.84 ± 0.21	0.85 ± 0.41	0.73 ± 0.54	0.88 ± 0.63	0.92 ± 0.29
	10	0.97 ± 0.12	1.00 ± 0.13	0.66 ± 0.18	0.48 ± 0.19	0.41 ± 0.18	0.49 ± 0.21	0.61 ± 0.14
	25	0.84 ± 0.10	0.86 ± 0.10	0.30 ± 0.19	0.27 ± 0.14	0.22 ± 0.10	0.30 ± 0.14	0.39 ± 0.09

Table 7.4. Normalized HS-GC-MS analysis data of FO and BTEX in contaminated A_{Camb} after the addition of individual root exudate components (REC). The results are expressed as the mean ± the standard deviation (*n=3*).

REC	Concentration (mM)	MTBE	ETBE	Benzene	Toluene	Ethylbenzene	*m/p*-Xylene	o-Xylene
AP	1	0.79 ± 0.07	0.77 ± 0.06	1.22 ± 0.09	1.27 ± 0.32	1.27 ± 0.17	1.21 ± 0.12	1.14 ± 0.11
	10	1.09 ± 0.09	1.04 ± 0.05	1.70 ± 0.24	1.81 ± 0.23	1.75 ± 0.17	1.66 ± 0.09	1.54 ± 0.13
	25	0.92 ± 0.18	0.77 ± 0.10	0.81 ± 0.08	1.00 ± 0.18	1.00 ± 0.26	1.02 ± 0.24	0.96 ± 0.22
AO	1	0.76 ± 0.07	0.71 ± 0.04	0.67 ± 0.10	1.03 ± 0.26	1.09 ± 0.24	1.06 ± 0.17	1.03 ± 0.12
	10	0.89 ± 0.05	0.89 ± 0.05	1.13 ± 0.05	1.09 ± 0.13	1.00 ± 0.15	0.97 ± 0.11	1.05 ± 0.19
	25	0.89 ± 0.10	0.80 ± 0.03	1.17 ± 0.11	1.77 ± 0.47	1.95 ± 0.60	2.18 ± 0.28	1.62 ± 0.37
AM	1	0.76 ± 0.07	0.68 ± 0.08	0.67 ± 0.31	1.00 ± 0.53	0.88 ± 0.12	0.88 ± 0.05	0.88 ± 0.05
	10	0.96 ± 0.06	0.93 ± 0.05	1.60 ± 0.11	1.88 ± 0.18	1.62 ± 0.35	1.52 ± 0.23	1.49 ± 0.17
	25	0.84 ± 0.12	0.87 ± 0.16	1.10 ± 0.12	1.39 ± 0.32	1.39 ± 0.16	1.35 ± 0.09	1.23 ± 0.10
ASu	1	0.78 ± 0.06	0.71 ± 0.07	0.59 ± 0.09	0.92 ± 0.13	1.08 ± 0.10	1.03 ± 0.05	1.01 ± 0.06
	10	1.12 ± 0.07	1.11 ± 0.07	1.85 ± 0.19	2.31 ± 0.15	2.33 ± 0.15	2.34 ± 0.06	1.97 ± 0.07
	25	0.86 ± 0.08	0.79 ± 0.07	0.93 ± 0.25	1.15 ± 0.15	1.14 ± 0.10	1.12 ± 0.03	1.04 ± 0.04
AFu	1	0.69 ± 0.15	0.70 ± 0.06	0.86 ± 0.13	0.92 ± 0.06	0.98 ± 0.14	0.94 ± 0.07	0.91 ± 0.04
	10	0.79 ± 0.05	0.77 ± 0.04	1.18 ± 0.19	1.93 ± 0.46	1.95 ± 0.38	1.96 ± 0.30	1.60 ± 0.24
	25	0.99 ± 0.16	0.90 ± 0.10	0.77 ± 0.28	0.91 ± 0.28	0.92 ± 0.26	0.93 ± 0.24	0.88 ± 0.26
ACi	1	0.91 ± 0.17	0.80 ± 0.03	1.33 ± 0.34	1.90 ± 0.43	2.52 ± 0.51	2.25 ± 0.27	1.91 ± 0.10
	10	0.77 ± 0.06	0.76 ± 0.03	1.16 ± 0.11	1.29 ± 0.16	1.21 ± 0.18	1.21 ± 0.13	1.06 ± 0.10
	25	1.01 ± 0.10	0.85 ± 0.03	0.68 ± 0.23	0.95 ± 0.09	1.28 ± 0.12	1.28 ± 0.04	1.22 ± 0.08
ASa	1	0.81 ± 0.06	0.70 ± 0.10	0.38 ± 0.18	0.75 ± 0.08	0.98 ± 0.07	0.97 ± 0.06	0.98 ± 0.07
	10	0.82 ± 0.03	0.82 ± 0.07	1.01 ± 0.11	0.82 ± 0.10	0.71 ± 0.04	0.75 ± 0.02	0.73 ± 0.03
	25	0.80 ± 0.05	0.75 ± 0.05	0.92 ± 0.05	0.91 ± 0.09	0.84 ± 0.10	0.83 ± 0.06	0.79 ± 0.05
ACu	1	0.92 ± 0.10	0.85 ± 0.08	0.77 ± 0.09	0.82 ± 0.06	0.92 ± 0.07	0.88 ± 0.02	0.90 ± 0.04
	10	1.10 ± 0.08	1.06 ± 0.11	0.83 ± 0.10	0.89 ± 0.13	0.83 ± 0.15	0.88 ± 0.15	0.85 ± 0.17
	25	0.83 ± 0.04	0.75 ± 0.03	0.92 ± 0.15	0.92 ± 0.08	0.77 ± 0.19	0.69 ± 0.08	0.69 ± 0.07
AFe	1	0.71 ± 0.05	0.71 ± 0.05	1.03 ± 0.14	0.97 ± 0.22	1.16 ± 0.64	0.83 ± 0.18	0.81 ± 0.15
	10	1.15 ± 0.06	1.09 ± 0.05	1.41 ± 0.13	1.40 ± 0.11	1.23 ± 0.13	1.28 ± 0.08	1.20 ± 0.06
	25	0.53 ± 0.07	0.50 ± 0.07	0.42 ± 0.03	0.56 ± 0.10	0.54 ± 0.12	0.54 ± 0.09	0.67 ± 0.11
Cat	1	0.95 ± 0.09	0.92 ± 0.07	1.42 ± 0.07	1.40 ± 0.16	1.28 ± 0.19	1.26 ± 0.13	1.20 ± 0.11
	10	0.84 ± 0.04	0.81 ± 0.04	0.96 ± 0.21	0.88 ± 0.22	0.68 ± 0.23	0.74 ± 0.20	0.71 ± 0.17
	25	0.91 ± 0.14	0.80 ± 0.03	0.67 ± 0.22	0.60 ± 0.10	0.68 ± 0.14	0.88 ± 0.13	0.89 ± 0.07

A principal components analysis (PCA) was carried out in order to clarify the previous results. For this purpose, we chose the highest concentration of REC tested (25 mM), since the effect was more pronounced. For this statistical procedure, the cases were the different matrices (humic acid, montmorillonite and A_{Camb}), each with the addition of the ten selected REC (Table 7.1) and the mixture. The variables used were the normalized HS-GC-MS analysis data of each contaminant (MTBE, ETBE, benzene, toluene, ethylbenzene, *m*/*p*-xylene and *o*-xylene), for each case, and REC properties, particularly %C and log P (Table 7.1). The Kaisen-Meyer-Olkin value (0.815) and the significance of Barlet test of sphericity, supported the factorability of the correlations and assured the data adequacy for PCA. The PCA extracted two principal components that explained more than 85% of the total variance. The first component (65.2% of total variance) was mainly represented by the normalized analysis data of BTEX and FO, and the second component (20.5% of total variance) was related to the REC properties (%C and logP). The factor scores for each case in rotated axes are represented in figure 7.4, separately for each matrix. The control value was also included to situate the limit between contaminant mobilization increase (cases with higher punctuation than the control in the component 1 axis) or decrease (cases with lower punctuation than the control in the component 1 axis).

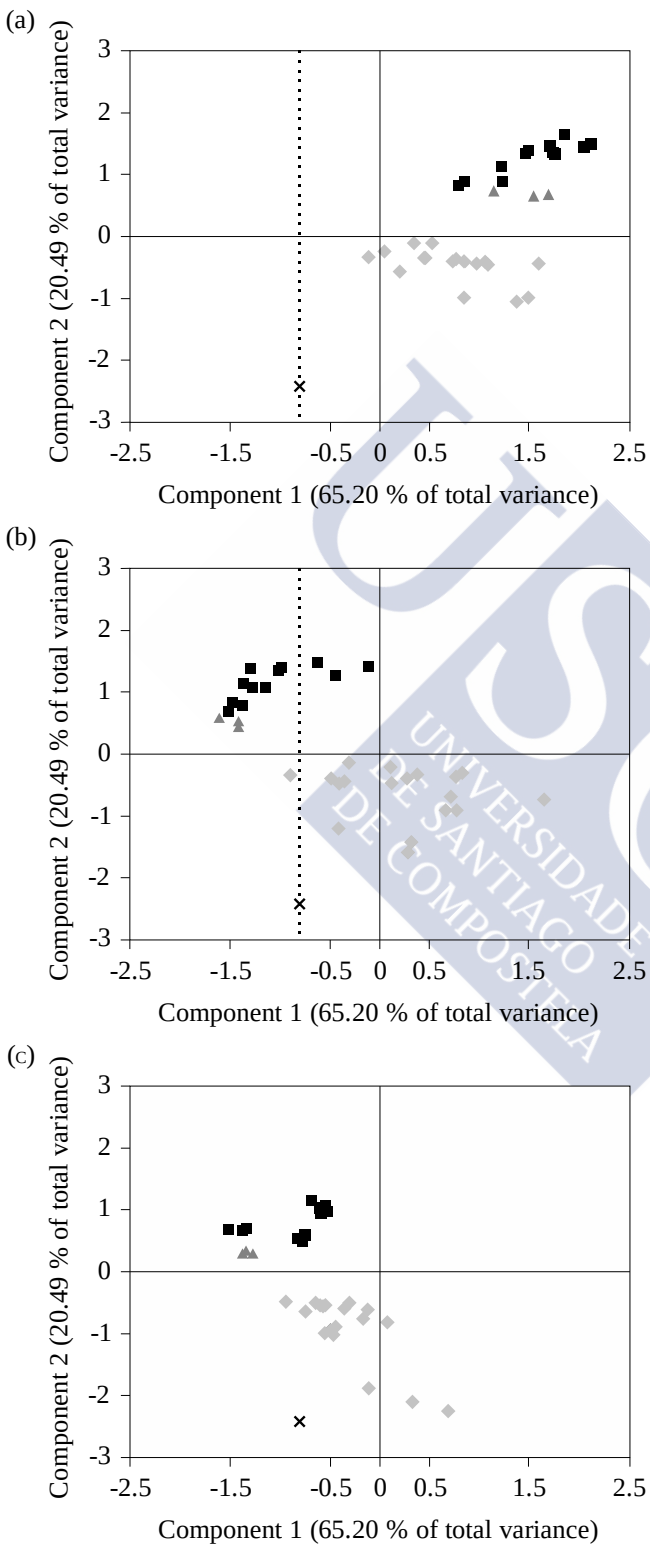

Figure 7.4. Representation of the factor scores of the cases used in PCA analysis of the individual REC experiment (at 25 mM), for humic acid (a), montmorillonite (b) and A_{Camb} (c). The cases are also differentiated according to the type of REC; i.e. carboxylic (◆) and phenolic (■). The data corresponding to the mixture of REC at 25 mM (▲) and to the control without exudate (✕) were also included.

As expected, the PCA generated two groups of cases corresponding to carboxylic and phenolic REC (Figure 7.4), and they provoked different effects on the mobility of the contaminants, particularly, in montmorillonite and A_{Camb}. The punctuation in component 1 axis of all cases of humic acid (Figure 7.4a), was higher than that of control, reflecting that the mobility of the contaminants increased regardless of the type of REC. In general, in montmorillonite (Figure 7.4b) and A_{Camb} (Figure 7.4c) the mobility of the contaminants increased in the presence of carboxylic REC (most of the cases have higher punctuation than the control in the component 1 axis) and decreased in presence of phenolic REC (most of the cases have lower punctuation than the control in the component 1 axis). The cases of the data from the REC mixture experiment were situated very near to the group of phenolic REC. Therefore, despite all REC being present in the mixture and at the same concentration, phenolic REC had a higher effect on the modification of the contaminant mobility.

To support the PCA results, regressions between the normalized analysis data of each contaminant in each matrix with the addition of the ten individual REC (Supporting Information Tables 7.2. 7.3 and 7.4) and some exudate properties (%C and log P) (Table 7.1) were calculated. The data of these regressions (R^2 and regression equations) are presented in Table 7.5. In this table, only the cases with significant coefficients were shown.

No significant coefficients were found for humic acid, which could reflect that the interaction between the contaminants and the REC is hindered because the organic matter exerted stronger sorption of the contaminants than the REC themselves. For montmorillonite, significant regression coefficients were found for all the contaminants (R^2=0.54–0.82) (Table 7.5) with the %C of REC, for the highest REC concentration studied (25 mM). This indicates that the interaction between the contaminants and the REC was easier in the absence of organic matter. Furthermore, the slope of these regressions reflected that the effect of

the REC on the mobility of FO was less important (slope=-0.80– -1.04) than on BTEX mobility (slope=-2.1– -2.76) (Table 7.5). In addition, the slopes were all negative, indicating that as the %C of the REC increased, the contaminant mobility decreased. This indicates that the exudate components with the highest %C. which are phenolic compounds, tended to interact with these contaminants, and immobilize them (the higher the %C of REC, the higher affinity for organic contaminants). This makes particular sense in the case of BTEX compounds, since they have the same chemical structure with aromatic rings, and therefore, a higher affinity for this type of REC. In the A_{Camb} the presence of organic matter hindered the interaction between the contaminant and the REC, as occurred for the humic acid, and only significant regression coefficients were found for the contaminants with the highest molecular weight (ethylbenzene and xylene isomers) at a REC concentration of 25 mM (R^2=0.60–0.72) (Table 7.5). As observed for montmorillonite, the slopes of the regressions of FO were less steep than those of BTEX.

Table 7.5. Coefficients (R^2) and equations of significant regressions found between the normalized HS-GC-MS analysis data of each contaminant in each matrix with the addition of the ten individual REC (*y*, in the equation) and the %C of those REC (*x*, in the equation) (*n*=30).

	Montmorillonite		**A_{Camb}**	
	R^2	**Regression equation**	**R^2**	**Regression equation**
MTBE	0.54*	y= -0.80x+1.42	0.27	y= -0.44x+1.06
ETBE	0.62**	y= -1.04x+1.63	0.33	y= -0.39x+0.95
Benzene	0.61**	y= -2.11x+1.92	0.26	y= -0.69x+1.15
Toluene	0.75**	y= -2.37x+1.95	0.60**	y= -1.71x+1.79
Ethylbenzene	0.75**	y= -2.47x+1.94	0.72**	y= -2.17x+2.03
***m*/*p*-Xylene**	0.82**	y= -2.45x+1.95	0.68**	y= -2.34x+2.14
***o*-Xylene**	0.79**	y= -2.76x+2.26	0.70**	y= -1.52x+1.69

* *The coefficient is significant at the 0.05 level (bilateral).*
** *The coefficient is significant at the 0.01 level (bilateral).*

DISCUSSION

In this study, the effect of root exudates (natural and artificial) on the mobility of fuel volatile compounds (BTEX and FO) was studied in several contrasting matrices (humic acid, montmorillonite and A_{Camb}).

The concentrations of artificial root exudates used (1, 10 and 25 mM) are similar to those reported by other authors in field or laboratory scale experiments. According to Vranova *et al.* (2013), the typical concentrations of organic acids in roots are approximately 10-20 mM. Mimmo *et al.* (2011), reported time averaged organic acid concentrations of 5.8-908.9 mM in percolates of microcosms planted with *Lupinus albus* L. and *Brassica napus* L. Jones (1998) summarized that organic acid concentration in the solution of soils cultivated with different plant species varied approximately from 0.8 mM (citric acid in bulk soil near *Banksia*), to 1472 mM (malonic acid in *Trifolium* rhizosphere soil). Furthermore, the organic carbon concentration of the natural root exudates used here (20 mg C L^{-1}) is within the range of the organic carbon concentration of individual REC used at the 1 mM level (17 mg C L^{-1} for oxalic acid and 180 mg C L^{-1} for catechin hydrate), and is within the same order of magnitude of REC mixture at 1 mM (80 mg C L^{-1}).

In the absence of root exudates (Figure 7.1), the mobility of BTEX and FO was highly influenced by the physical properties of the contaminants, principally, volatility and water solubility. FO were recovered in higher proportions than BTEX, and, at least in the case of the BTEX, contaminants were recovered following their volatility order (higher volatility, higher recovery), with the exception of o-xylene, in montmorillonite and A_{Camb}. As reported in Balseiro-Romero and Monterroso (2013), the differences in the chemical structure of ethylbenzene and xylene isomers influences their nucleophilic strength and sorption affinity: a possible steric repulsion between the two adjacent methyl

groups in *o*-xylene could lower its sorption strength, showing higher recovery than ethylbenzene and *m*- and *p*-xylene. For humic acid, this behaviour was not observed, probably because the interaction was determined only by the global sorption capacity of the matrix (which is very high for organic molecules due to the high concentration of organic matter). In this case, the differences in the nucleophilic strength of the contaminants were not as important as in the absence of organic matter. The mobility of all contaminants was lowest in the humic acid. Montmorillonite also showed a lower recovery than expected for some contaminants. As explained in our previous study (Balseiro-Romero and Monterroso, 2013), montmorillonite could be showing an unexpected sorption capacity due to its ability to expand the interlayer and produce a larger surface area (Bohn *et al.*, 2001).

In general, the addition of natural root exudates (Figure 7.2) provoked a decrease in the mobility of the contaminants with respect to the control. Other authors have reported similar results. Phillips *et al.* (2012) observed that root exudates had a repressive effect on the mineralization of phenanthrene, naphthalene and hexadecane compared to controls. Jones (1998) explained that due to the negative charge associated with the carboxyl groups, organic acids from root exudates can become rapidly and readily sorbed by the soil solid phase. The supply of root exudates to soil by plants can represent an important addition of organic carbon to soil (Schnoor *et al.*, 1995). As already stated, organic contaminants have a high affinity for organic phases, and therefore an increase in organic carbon concentration in humic acid and A_{Camb} or even a new contribution in montmorillonite, could easily explain the decrease in the mobility of the contaminants in the cases cited above. The mobility and bioavailability decrease, is probably the main cause of *in planta* phytoremediation and rhizodegradation failure (Wenzel, 2009). However, this situation has a positive

effect since the leaching of the contaminants and contamination of the surrounding soil and groundwater may be retarded. Increasing the bioavailability of the contaminants through the use of surfactants and other chemicals may be an alternative for improving any plant-based remediation process.

Quantities and quality of root exudation depend on plant age, health, environmental conditions, level of chemical, physical and biological stress and are known to differ between different plant species and even cultivars (Oburger *et al.*, 2013). The effect of *C. striatus* exudates was more pronounced than that of *H. lanatus* exudates (despite being added under equal organic carbon concentrations), which suggests that, in our case, *C. striatus* exuded particular compounds which magnified the retention of FO and BTEX by several matrices. The addition of *H. lanatus* exudates even caused the opposite effect, since they mobilized the contaminants bound to humic acid (Figure 7.2), in spite of the fact that this matrix showed the highest retention capacity. The most feasible explanation for this particular behaviour is that there is a specific effect of *H. lanatus* exudates by which they increase the solubility of humic acid, with the consequent liberation of the contaminants bound. Furthermore, this effect was also observed in the experiments with artificial REC (individually and as a mixture). Nardi *et al.* (1997) demonstrated that organic acids (fumaric and succinic acid) occurring in the root exudates of three maize cultivars shifted the humic matter from high to low molecular weight in size exclusion chromatograms. The organic acids enter the interior of the humic micelle-like aggregates and alter the stereochemical hydrophobic arrangement of the humic material. The developed negative charges disrupt the apparent high molecular size configuration and disperse the humic material into small-size micelles (Piccolo *et al.*, 1996). To confirm the organic matter dissolution of humic acid in the presence of root exudates of *H. lanatus*, the dissolved organic carbon (DOC) of the supernatant of humic acid vials was measured. The results showed an

increase of approximately 200% in the DOC after exudate addition (data not shown). This effect was not appreciable in A_{Camb}, in which the organic carbon concentration (42.6 g Kg^{-1}) is much lower than that of humic acid (490.1 g Kg^{-1}).

The effect of artificial root exudates as a REC mixture was clearly consistent with that of natural root exudates, and especially with those obtained from *H. lanatus*: mobilization of the contaminants increased in the humic acid and decreased in the A_{Camb} and the montmorillonite (Figure 7.3). These particular effects grew with increasing REC mixture concentration, with very good correlations in most cases. Although the composition of natural root exudates is unknown, the results of this experiment could predict that the effect of root exudates on FO and BTEX (either retention or mobilization) would be intensified with an increase in root exudation (for example, under chemical, physical or biological stress, in young specimens, etc.). The addition of individual REC to the different matrices caused different effects according to the matrix and chemical structure of the REC, as clarified in the PCA (Figure 7.4). As expected, the mobility of all contaminants increased in the humic acid. However, in the absence or a low concentration of organic matter (montmorillonite and A_{Camb}), the influence of phenolic and carboxylic REC had opposite effects: in general, carboxylic REC favoured the mobility of the contaminants, and phenolic REC, favoured the retention. Furthermore, PCA indicated that phenolic REC had a higher influence on the modification of FO and BTEX mobility, since the REC mixture data were situated in PCA axis close to phenolic REC (Figure 7.4). Therefore, when different REC are present (as in REC mixture or in natural exudates), the effect of phenolic REC will probably be more significant. This could be easily explained by the fact that the phenolic REC had a higher percentage of carbon than carboxylic REC, and therefore, higher affinity for the organic contaminants. The regressions of the data with the REC properties (Table 7.5) indicated that the modification of contaminant mobility was more

pronounced for BTEX than for FO, and that the interaction between the REC and the contaminants was easier in the absence of organic matter.

Considering these results, the role of root exudates in the soil-plant system, must not be ignored, since it could highly affect the efficiency of phytoremediation, rhizodegradation or bioremediation processes. Characterization of root exudates, and its interaction with the contaminants and the soil could be a useful step on choosing the suitable plant for each remediation process. Several authors have highlighted the role of root exudates in remediation. Toyama *et al.* (2011) discovered that the biodegradation of pyrene and benzo[*a*]pyrene in *P. australis* rhizosphere was accelerated by the *Mycobacterium*-root exudate interactions. Kim *et al.* (2010) observed that *Belamcanda chinensis* exudates behaved as natural chelating agents to enhance phytoextraction with *Echinochloa crus-galli.* Phillips *et al.* (2012) reported that *Elymus angustus* and *Medicago sativa* exudates repressed the mineralization of hexadecane, naphthalene and phenanthrene in soil microcosms.

CONCLUSIONS

The effect of root exudates on the mobility of fuel volatile contaminants (BTEX, MTBE and ETBE) highly depended on the type of matrix and on the composition of the root exudates. In general, the addition of natural root exudates of *Holcus lanatus or Cytisus striatus*, and artificial root exudates (mixture of root exudate components -REC-) provoked a decrease in the mobility of fuel volatile contaminants, except at a high concentration of humified organic matter (humic acid) which was probably due to an increase of organic matter dissolution in the presence of root exudates. However, root exudate components individually, had different effects according to their chemical properties. Again, in the presence of humified organic matter (humic acid), both carboxylic and phenolic REC increased the mobility of those contaminants, but in the absence

or low concentration of organic matter (montmorillonite and A_{Camb}) carboxylic REC increased the mobility of fuel contaminants and the phenolic REC had the opposite effect. The results reflect a higher effect phenolic REC on the modification of the contaminant mobility, easily explained by the higher percentage of carbon of phenolic REC with regard to carboxylic REC.

According to the results, before setting up an experiment, it would be necessary to characterize root exudation in each scenario, since, as concluded here, the composition of root exudates could highly influence the mobility of fuel volatile compounds in the soil-plant system, and therefore, the success of the remediation process.

The findings of this research could be useful for choosing the most appropriate phytoremediation species, according to the phytoremediation objectives (extraction, containment, immobilization or degradation). They also establish a base for developing and improving phytoremediation processes of fuel-contaminated soils.

REFERENCES

Balseiro-Romero M, Monterroso C. 2013. A headspace-analysis approach to assess the sorption of fuel volatile compounds by soils. Soil Sci Soc Am J 77:800-808.

Bohn HL, McNeal BL. O'Connor GA. 2001. Soil Chemistry. John Wiley and Sons Inc., New York.

European Fuel Oxygenates Association (EFOA). http://www.efoa.eu.

Jones D. 1998. Organic acids in the rhizosphere: a critical review. Plant Soil 205:25-44.

Kim JM, Le NT, Chung BS, Park JH, Bae JW, Madsen EL, Jeon CO. 2008. Influence of soil components on the biodegradation of benzene, toluene, ethylbenzene, and o-, m-, and p-xylenes by the newly isolated bacterium *Pseudoxanthomonas spadix* BD-a59. App Environ Microbiol 74:7313-7320.

Kim S, Lim H, Lee I. 2010. Enhanced heavy metal phytoextraction by *Echinochloa crus-galli* using root exudates. J Biosci Bioeng 109(1):47–50.

Mackay D, Shiu WY, Ma KC, Lee SC. 2006. Handbook of physical-chemical properties and environmental fate for organic chemicals. CRC Press, Boca Raton.

Mimmo T, Hann S, Jaitz L, Cesco S, Gessa CE, Puschenreiter M. 2011. Time and substrate dependent exudation of carboxylates by *Lupinus albus* L. and *Brassica napus* L. Plant Physiol Biochem 49:1272-1278.

Nardi S, Reniero F, Concheri G. 1997. Soil organic matter mobilization by root exudates of three maize hybrids. Chemosphere 35: 2237-2244.

Oburger E, Dell'mour M, Hann S, Wieshammer G, Puschenreiter M, Wenzel WW. 2013. Evaluation of a novel tool for sampling root exudates from soil-grown plants compared to conventional techniques. Environ Exper Bot 87:235-247.

Pavón JLP, Martín SH, Pinto CG, Cordero BM. 2009. Programmed temperature vaporizer based method for the sensitive determination of trihalomethanes and benzene, toluene, ethylbenzene and xylenes in soils. J Chromatogr A 1216:6063-6070.

Phillips LA, Greer CW, Farrell RE, Germida JJ. 2012. Plant root exudates impact the hydrocarbon degradation potential of a weathered-hydrocarbon contaminated soil. Appl Soil Ecol 52: 56-64.

Piccolo A, Nardi S, Concheri G. 1996. Micelle-like conformation of humic substances as revealed by size exclusion chromatography. Chemosphere 33:595-602.

Schnoor JL, Licht LA, McCutcheon SC, Wolfe NL, Carreira LH. 1995. Phytoremediation of organic and nutrient contaminants. Environ Sci Technol 29: 318A-323A.

Schwitzguébel J, van der Lelie D, Baker A, Glass D, Vangronsveld J. 2002. Phytoremediation: European and American trends successes, obstacles and needs. J Soil Sediment 2:91-99.

Serrano A, Gallego M. 2006. Sorption study of 25 volatile organic compounds in several Mediterranean soils using headspace–gas chromatography–mass spectrometry. J Chromatogr A 1118:261-270.

Sumner ME. 2000. Handbook of soil science. CRC Press, Boca Raton.

Toyama T, Furukawa T, Maeda N, Inoue D, Sei K, Mori K, Kikuchi S, Ike M. 2011. Accelerated biodegradation of pyrene and benzo [*a*]pyrene in the *Phragmite australis* rhizosphere by bacteria-root exudate interactions. Water Res 45:1629-1638.

United Kingdom Environment Agency. 2003. Review of the fate and transport of selected contaminants in the soil environment. Environment Agency, Bristol.

United States Environmental Protection Agency (USEPA). 2003. Method 5021A: Volatile organic compounds in various sample matrices using

equilibrium headspace analysis. Revision 1. US Environmental Protection Agency, Washington.

Van Aken B, Correa PA, Schnoor JL. 2010. Phytoremediation of polychlorinated biphenyls: new trends and promises. Environ Sci Technol 44:2767-2776.

Vangronsveld J, Herzig R, Weyens N, Boulet J, Adriaensen K, Ruttens A, Thewys T, Vassilev A, Meers E, Nehnevajova E, van der Lelie D, Mench M. 2009. Phytoremediation of contaminated soils and groundwater: lessons from the field. Environ Sci Pollut Res 16:765-794.

Vranova V, Rejsek K, Skene KR, Janous D, Formanek P. 2013. Methods of collection of plant root exudates in relation to plant metabolism and purpose: A review. J Plant Nutr Soil Sci 176:175-199.

Wenzel W. 2009. Rhizosphere processes and management in plant-assisted bioremediation (phytoremediation) of soils. Plant Soil 321:385-408.

Zhang Z, Zhou Q, Peng S, Cai Z. 2010. Remediation of petroleum contaminated soils by joint action of *Pharbitis nil* L. and its microbial community. Sci Total Environ 408:5600-5605.

Zhu Y, Zhang S, Huang H, Wen B. 2009. Effects of maize root exudates and organic acids on the desorption of phenanthrene from soils. J Environ Sci 21:920-926.

USC
UNIVERSIDADE
DE SANTIAGO
DE COMPOSTELA

8

Phytotoxicity of fuel to crop plants: Influence of soil properties, fuel type and plant tolerance

The aim of the present work was to characterize the effect of fuel-contaminated soils on germination, survival and early growth of six crop plants, *Brassica oleracea* L., *Trifolium repens* L., *Lactuca sativa* L., *Avena sativa* L., *Pisum sativum* L. and *Zea mays* L., grown on Cambisol A and B horizons contaminated with gasoline and diesel (0, 1.25, 2.5, 5 and 10% (*w*/*w*)). Fuel toxicity was higher in the B horizon, and diesel was more toxic than gasoline, probably due to the higher evaporation rate of this last fuel. Fuels affected germination and survival of small-seeded plants in a higher extent, reflecting the importance of the seed coat and nutrient reserves for the successful plant development on fuel-contaminated soils. In general, root growth was more affected than shoot, and plant biomass more than elongation, traduced in a lower plant branching in the presence of fuel. The findings of this study can be useful for selecting the least fuel tolerant species as soil contamination bioindicators and for determining the risks of fuel contamination. Due to the low residence time of gasoline components in soil, the phytotoxicity test resulted in a poor bioassay to assess gasoline toxicity.

This work was included in the publication:

Balseiro-Romero M, Monterroso C. Phytotoxicity of fuel to crop plants: Influence of soil properties, fuel type and plant tolerance. Toxicol Environ Chem (under review).

INTRODUCTION

Contamination of soil with petroleum products is a widespread problem, usually derived from pipeline blow-outs, disposal after drilling oil and gas wells, road accidents, leakage from underground storage tanks or uncontrolled landfill activities (Hentati *et al.*, 2013). Car fuels, such as diesel and gasoline, are complex mixtures of organic compounds and many of them are toxic and included in the list of US Environmental Protection Agency (USEPA) priority pollutants. They have different vapour pressures, water solubilities, and molecular weights (Fine *et al.*, 1997). Gasoline is mainly composed of alkanes (up to C_{10}), cycloalkanes, monoaromates, and additives (ether and alcohol oxygenates) (Xiao *et al.*, 2014), and diesel, of alkanes (mainly, C_{10}-C_{25}), isoalkanes, cycloalkanes and polyaromates (Pitz and Mueller, 2011). Because of the different physical and chemical properties of fuel components, contaminated soils have a high environmental risk, since they can contaminate other environmental compartments: the wide variety of diesel and gasoline fuel compounds can be sorbed onto soil components, released to the atmosphere or nearby surface water and/or leached to groundwater. This can lead to serious health threats and ecological stresses (Al-Mutairi *et al.*, 2008).

It is very common to assess the risk of a fuel contamination episode by analyzing the concentration of petroleum compounds (Mao *et al.*, 2009). Indeed, the Spanish law on contaminated soils (Real Decreto 9/2005) establishes levels of contamination above which soil remediation is required, regarding the risks for the human health and for ecosystems. However, chemical data alone are not sufficient to evaluate the ecological effects (Płaza *et al.*, 2005), since it is not possible to analyze all the compounds present and to measure the toxic effect caused by the interaction between them and their metabolites (Vaajasaari *et al.*, 2002). Bioassays are a good tool to assess the toxicity of this complex mixture of

contaminants. A wide variety of standardized bioassays have been developed by the Organization for Economic Cooperation and Development (OECD) on its "Guidelines for the Testing of Chemicals". Specifically, for the assessment of soil toxicity, the most spread toxicity tests include the use of earthworms (OECD Tests 207 and 222), usually observed for survival, reproduction and physical abnormalities, and/or plants, usually observed for germination, survival and early growth (OECD Test 208). Aquatic bioassays, based on enzymatic or microbial activity are commonly used to evaluate the risk of leachates from fuel-contaminated soils (Vaajasaari *et al.*, 2002).Plant toxicity bioassays can be used to evaluate the efficacy of a remediation process (Molina-Barahona *et al.*, 2005) and to screen and select the most appropriate plant for a phytoremediation process (Kirk *et al.*, 2002; Luhach and Chaudhry, 2012). Plants can be also used as bioindicators to detect soil contamination, since when growing on fuel-contaminated soils, they can suffer from observable symptoms, as the degradation of chlorophyll or the decrease in size and less production of biomass (Luhach and Chaudhry, 2012). Phytotoxicity and plant tolerance of different species to fuel-contaminated soil has previously been described by other authors. Adam and Duncan (2002) studied the effect of diesel on the germination of a wide variety of grasses, herbs, legumes and commercial crops. Tang *et al.* (2011) characterized the toxicity of the soil of an oil production plant by observing wheat, maize, cotton, corn grass and tall fescue germination and root elongation inhibition. Issoufi *et al.* (2006) evaluated germination and seedling growth of different plants growing on crude oil contaminated soil.

The present work aimed to comparatively assess and characterize the phytotoxicity of gasoline and diesel, by recording their effect on different plant growth variables (germination, survival and early root and shoot development). Unlike other previous works, we evaluated the phytotoxicity of the two most common car fuels, gasoline and diesel, concurrently, and in a wider variety of

scenarios than the commonly found in the literature: different gasoline and diesel concentrations (0, 1.25, 2.5, 5 and 10% (*w*/*w*), dissimilar contaminated soil samples (A and B horizons of a Cambisol) and a variety of test plants (*Brassica oleracea* L., *Trifolium repens* L., *Lactuca sativa* L., *Avena sativa* L., *Pisum sativum* L. and *Zea mays* L.).

MATERIALS AND METHODS

Collection and preparation of soil samples

The experiment was carried out in pots using two natural soil samples artificially spiked with gasoline and diesel. Samples of A and B horizon (A_{Camb} and B_{Camb}) from an alumi-umbric Cambisol profile were collected in the surroundings of Santiago de Compostela (Galicia, NW Spain). In general terms, they showed typical characteristics of Galician soils: i.e. variable charge, low pH (4.9 for A_{Camb} and 5.1 for B_{Camb}) and low cation exchange capacity (2.0 for A_{Camb} and 1.2 cmol(+) Kg^{-1} for B_{Camb}) dominated by aluminium (Macías and Calvo de Anta, 1992). Both samples have sandy loam texture and the principal difference between them was the organic carbon content: 42.6 and 3.3 g C Kg^{-1}, for A_{Camb} and B_{Camb}, respectively. The higher organic matter content of A_{Camb} gives it better properties for plant development, i.e. higher nutrient content, better moisture conservation, higher microbiological activity, etc. Soil samples were air dried, sieved through a 2 mm mesh and conserved in plastic containers at room temperature until use.

Prior to the spiking process, soil samples were limed with $CaCO_3$ (Panreac Química, S.L.U.), to a pH around 6, following the common dose used in the area (3-5 t ha^{-1}) and mixed with sand at a 1:5 ratio (sand/soil). These samples were spiked with gasoline and diesel purchased in a local distribution station at different concentrations: 1.25, 2.5, 5 and 10% (*w*/*w*). The suitable amount of each

fuel was added to the soil and properly mixed until reaching homogeneity. The spiked soils were stabilized in hermetically-closed recipients, with minimum headspace, for at least 2 weeks at 4°C, in order to avoid evaporation losses to the extent possible.

Plant germination and early growth

Several agricultural crop species were selected for the experiment, the final selection was made so as to represent the main crops cultivated in the area of Santiago de Compostela and also to represent species which are commonly used in plant bioassays. In the final selection two monocotyledonae were chosen (maize, *Zea mays* L. and oat, *Avena sativa* L.); two dicotyledonae which included legumes (white clover, *Trifolium repens* L. var. Grasslands Huia , and pea, *Pisum sativum* L. var. macrocarpum), a cruciferous (cabagge, *Brassica oleracea* L. convar. capitata var. alba) and a composit (lettuce, *Lactuca sativa* L. var. Trocadero Ribera). All seeds were purchased in a local agricultural supplier. *Avena sativa* L. was previously used by Calvelo Pereira *et al.* (2010) to evaluate the phytotoxicity of hexachlorocyclohexane. All test species chosen, positively followed the criteria established by OECD guidelines (OECD 208, section 11) (OECD, 2006). Seeds were surface sterilized with 2.5% NaClO (10 min agitation) and vigorously rinsed with sterile tap water to eliminate NaClO remains.

Polypropylene pots were filled in triplicate with approximately 100 g of the spiked soils. Between 4 and 8 seeds (4 for pea and maize, 5 for oat and 8 for clover, cabbage and lettuce) were placed in each pot at 1-2 cm depth. Pots with uncontaminated soils were also prepared in triplicate to be used as a control. The experiment was carried out under greenhouse conditions: temperature of 22 ± 10 °C, humidity of 70 ± 25% and a photoperiod of 16 hours of light and 8 hours of dark. The soil water content was adjusted at the start of the experiment and checked daily to maintain it approximately constant at field

capacity. The duration of the test ranged from 21 to 34 days, depending on each plant species. According to OECD guidelines (OECD, 2006), the plants were allowed to grow for about 2 weeks after 50% of the control plants have emerged.

During the test, plants were observed for emergence, and visual phytotoxicity and mortality. At the end of the test, the total of emerged seeds and surviving plants were recorded to calculate germination and survival indices (percentage from the total sowed seeds in the three replicate pots). Furthermore, plants were harvested and rinsed with tap water to eliminate adhered rhizosphere soil. Fresh shoot and root biomass (fresh weight) and elongation from surviving plants were determined immediately after harvesting. The samples were then allowed to dry at greenhouse conditions and weighted again for obtaining dry shoot and root biomass.

Other indices were calculated from the previous data. Root/shoot elongation and root/shoot biomass ratios were calculated from elongation and biomass data. Specific shoot and root length (SSL and SSR), were calculated as the shoot or root elongation (m) per unit dry shoot or root biomass (g), respectively. All ratios were calculated using the mean values. Maximal effective concentration causing a 50 % reduction of each growth variable (germination, survival and plant elongation and biomass) (EC_{50}), was also estimated for each plant species growing on either gasoline and diesel-contaminated A_{Camb} and B_{Camb}.

Statistical analysis

PASW Statistics software (Version 20.0.0; IBM SPSS Statistics, Inc.) was used to analyze the data. One factor ANOVA was used to compare the plant growth at different contamination episodes (soils and type and concentration of contaminant). Non-parametric Kruskal-Wallis test was used when the growth variables did not meet the normality test (Kolmogorov-Smirnov) and the

homogeneity of variances (Levene's). A significance level of p=0.05 was considered for all statistical analyses.

RESULTS

Plant germination and survival indices

Germination and survival indices (percentage of seeds germinated and wealthy plants at the end of the experiment from the total sowed in the three replicate pots, respectively) were calculated for each plant species in each contamination case (A_{Camb} and B_{Camb} contaminated with gasoline or diesel, and uncontaminated controls). The results are presented in Table 8.1.

In the absence of contamination, germination and survival indices were, in general, very high, but there were some differences between both soils and plant species. In A_{Camb}, all the planted seeds of pea and maize germinated and survived, while in B_{Camb}, there was a slight reduction of less than 10% in pea germination and survival, and maize survival. On the other hand, germination and survival of cabbage, clover, lettuce and oat was very high in B_{Camb} (92-100%), but lower in A_{Camb}, especially for lettuce (71% of germination and 63% of survival) and cabbage (88% of germination and 63% of survival).

The addition of diesel and gasoline to soils provoked a visible effect on germination and survival, affected by the type of contaminant (gasoline or diesel) and its interaction with both soils. The toxicity of both fuels was different in each soil, being generally higher in B_{Camb}. Diesel appeared to be the most toxic of both fuels, since germination and survival were both reduced. For example, the germination and survival was reduced in B_{Camb} more than 50% for cabbage, clover, lettuce and oat with the lowest diesel concentration used (EC_{50}<1.25%), and maize and pea reached this reduction with middle concentrations (EC_{50} of 3.5 and 5.4% for maize and pea, respectively). Gasoline was toxic at very high

concentrations in both soils (EC_{50}=5-10%), being again pea and maize the most tolerant species.

In general, most of germinated seeds, survived wealthy until the end of the experiment (wealthy plants at the end of the experiment were more than 90% of germinated seeds), except cabbage in the A_{Camb}, in all contaminant levels, included the control, and in some isolated contamination cases of the other plant species, only in contaminated soils.

Table 8.1. Germination and survival indexes of the plant species used, for the different contamination cases (soil and contaminant type and concentration). Germination indexes (first value) were calculated as the percentage of seeds germinated from the total sowed in the three replicate pots. Survival indexes (indicated in parenthesis) were calculated as the percentage of wealthy plants at the end of the experiment from the total seeds sowed in the three replicate pots.

Contaminant	Soil	Concentration (%,w/w)	Plant species					
			Cabbage	Clover	Lettuce	Oat	Pea	Maize
Gasoline	A_{Camb}	0	88 (63)	88 (88)	71 (63)	93 (93)	100 (100)	100 (100)
		1.25	96 (96)	88 (79)	71 (71)	100 (100)	100 (92)	100 (100)
		2.5	46 (25)	71 (63)	75 (75)	100 (87)	100 (92)	100 (92)
		5	17 (0)	46 (33)	50 (50)	100 (100)	100 (100)	100 (92)
		10	58 (46)	88 (63)	29 (17)	93 (93)	100 (92)	92 (83)
	B_{Camb}	0	96 (92)	100 (100)	100 (96)	100 (93)	92(92)	100 (92)
		1.25	88 (83)	100 (100)	75 (75)	93 (93)	100 (100)	92 (92)
		2.5	88 (88)	-	79 (75)	93 (93)	100 (100)	100 (92)
		5	88 (88)	42 (42)	58 (38)	87 (60)	100 (92)	50 (25)
		10	33 (29)	17 (17)	0 (0)	13 (13)	58 (33)	83 (67)
Diesel	A_{Camb}	0	88 (63)	88 (88)	71 (63)	93 (93)	100 (100)	100 (100)
		1.25	92 (71)	83 (67)	4 (4)	67 (60)	100 (92)	100 (92)
		2.5	25 (13)	17 (17)	0 (0)	93 (33)	100 (83)	100 (83)
		5	46 (25)	4 (0)	0 (0)	73 (40)	92 (83)	100 (75)
		10	0 (0)	0 (0)	0 (0)	0 (0)	92 (58)	0 (0)
	B_{Camb}	0	97 (92)	100 (100)	100 (96)	100 (93)	92 (92)	100 (92)
		1.25	38 (21)	25 (25)	0 (0)	47 (40)	100 (100)	92 (83)
		2.5	17 (8)	0 (0)	0 (0)	7 (7)	75 (58)	75 (42)
		5	25 (25)	0 (0)	0 (0)	0 (0)	33 (17)	0 (0)
		10	0 (0)	0 (0)	0 (0)	0 (0)	17 (0)	0 (0)

Plant early growth and development

Root and shoot elongation and biomass of selected plant species with the best survival indices (cabbage, oat, pea and maize) are represented in Figures 8.1 and 8.2 for every contamination case (A_{Camb} and B_{Camb} contaminated with gasoline or diesel, and uncontaminated controls). In Table 8.2, specific shoot and root length (SSL and SRL) are shown for each contamination episode and plant.

In the absence of contamination, the early growth of all plant species followed several patterns in A_{Camb} and B_{Camb} controls. In general, biomass development in A_{Camb} was similar to that in B_{Camb}, except for cabbage, for which root biomass was significantly higher in A_{Camb} ($p<0.05$). Plant elongation was also similar in both soils, except pea and maize root elongation, which was significantly higher in A_{Camb} ($p<0.05$). For all species in both soils, root was always longer than shoot (Figure 8.1); however, root biomass was lower than shoot biomass, except for maize (Figure 8.2). SSL or SRL values of A_{Camb} and B_{Camb} controls (Table 8.2) were similar, except cabbage in B_{Camb}, with higher SSL or SRL than A_{Camb}, and pea and maize, for which SRL was higher in A_{Camb}.

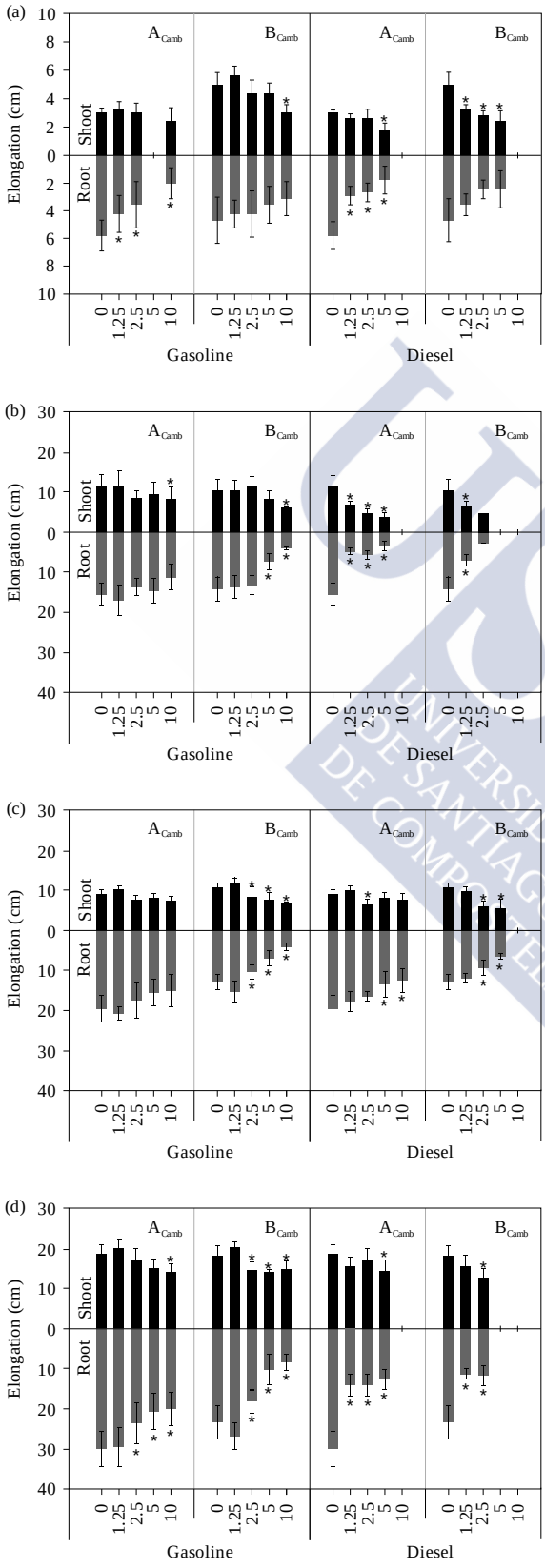

Figure 8.1. Mean elongation (cm) ± standard deviation of shoot and root of selected plant species (a-cabbage, b-oat, c-pea and d-maize) grown in A_{Camb} and B_{Camb} uncontaminated and contaminated with gasoline and diesel at different concentrations (%, *w*/*w*) (*n=24* for cabbage; *n=15* for oat; and *n=12* for pea and maize). Significant differences with the control (0% concentration) are indicated with an asterisk on top of the bar ($p<0.05$).

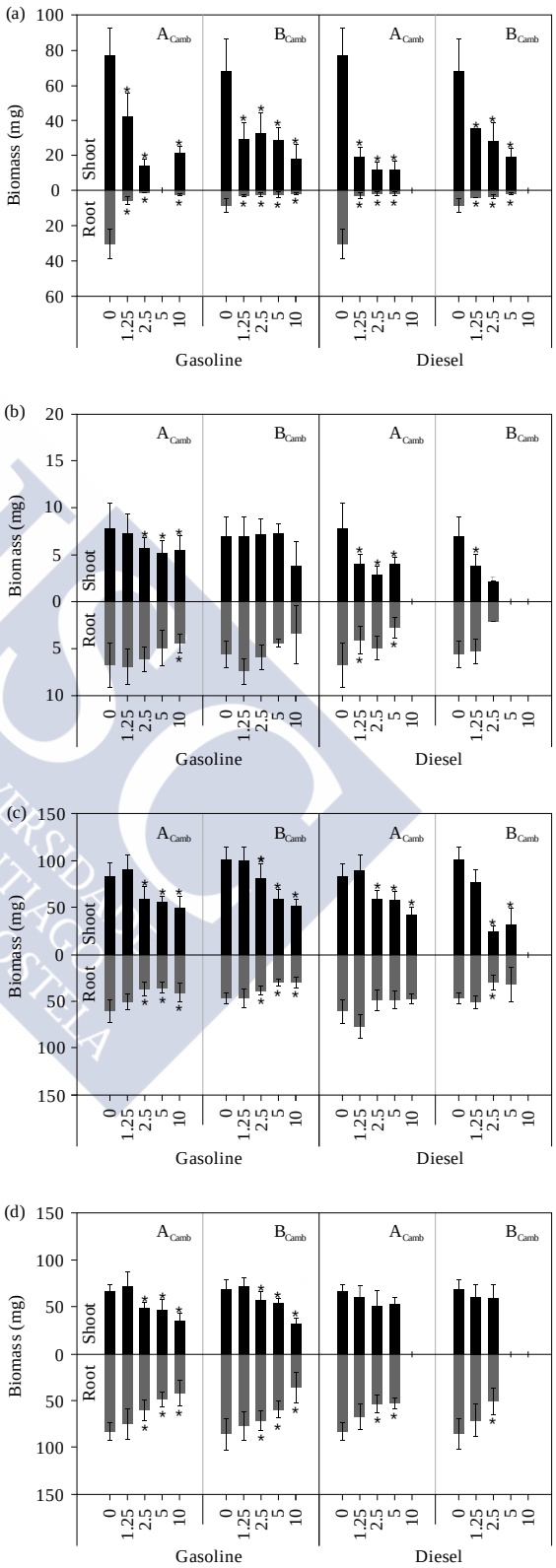

Figure 8.2. Mean dry biomass (mg) ± standard deviation of shoot and root of selected plant species (a-cabbage, b-oat, c-pea and d-maize) grown in A_{Camb} and B_{Camb} uncontaminated and contaminated with gasoline and diesel at different concentrations (%, *w/w*) (*n=24* for cabbage; *n=15* for oat; and *n=12* for pea and maize). Significant differences with the control (0% concentration) are indicated with an asterisk on top of the bar ($p<0.05$).

In contaminated soils, the growth response of the plant species used was very different in each contamination case, what complicated the establishment of any identifiable pattern. In general, elongation and biomass of root and shoot decreased with the increasing concentration of both fuels, gasoline or diesel. As occurred for germination and survival, diesel was in general more toxic for plant development, and this effect was more significant in B_{Camb} than in A_{Camb} ($p<0.05$) (for the majority of plants, there was even no seedling development at the highest diesel concentrations, 5-10%). The lowest observed effect levels (LOEL), i.e. the lowest contaminant concentration with significant effect with respect to the control ($p<0.05$) (significant differences with the control were marked with an asterisk in Figures 8.1 and 8.2), were observed to be generally lower on diesel-contaminated soils than on gasoline-contaminated soils. For example, for maize root elongation (Figure 8.1d), LOEL of gasoline in B_{Camb} was 2.5% and that of diesel, 1.25%. For oat shoot biomass (Figure 8.2b), LOEL of gasoline in A_{Camb} was 2.5% and that of diesel, 1.25%.

Root/shoot elongation and root/shoot biomass ratios for the same fuel and soil, were, in general, lower or comparable to that of the control, indicating a decrease or maintenance of root development under a fuel stress, with respect to shoot.

On the other hand, SSL and SRL of the different plant species grown on contaminated soils (Table 8.2) were in general comparable or higher than the control values: in the presence of fuel contamination, elongation of shoot and, especially, of root per unit biomass was relatively higher than in the absence of contamination, i.e. the plant was growing proportionally more in longitude than in biomass. This effect was slightly shown in some species such as pea or maize, but it was very significant for cabbage: e.g. the reduction of cabbage root biomass in gasoline-contaminated B_{Camb}, in the range of concentrations tested, was around 60-80%, leading to a significantly higher SRL than for control (Table 8.2). A

notable exception to this tendency was oat, for which the SRL decreased with the increasing concentration of gasoline in B_{Camb}, and, especially in the presence of diesel in both soils, even at the lowest concentration tested (1.25%) (Table 8.2).

Table 8.2. Specific shoot and root length (SSL and SRL, respectively) of the plant species used, for the different contamination cases (soil and contaminant type and concentration). These indexes were calculated as the mean shoot or root elongation (m) per unit mean dry shoot or root biomass (g).

Contaminant	Soil	Concentration (%, w/w)	Plant species											
			Cabbage		Clover		Lettuce		Oat		Pea		Maize	
			SSL	SRL	SSL	SRL	SSL	SRL	SSL	SRL	SSL	SRL	SSL	SRL
Gasoline	A_{Camb}	0	0.4	1.9	2.4	50.9	2.3	16.3	14.6	23.4	1.1	3.2	2.6	3.5
		1.25	0.8	7.2	5.7	61.5	1.1	9.5	15.6	24.4	1.4	3.8	2.6	3.5
		2.5	2.1	29.2	5.9	59.9	1.3	14.0	14.6	22.6	1.3	4.6	3.2	3.9
		5	-	-	8.5	51.4	1.4	9.4	17.8	29.3	1.5	4.3	3.0	4.0
		10	1.2	8.2	5.8	49.0	2.4	16.8	14.8	25.3	1.3	3.2	3.8	4.3
	B_{Camb}	0	0.7	5.4	2.1	45.9	2.3	17.6	15.2	25.4	1.1	2.6	2.5	2.5
		1.25	1.9	14.0	2.4	55.7	-	-	14.0	18.2	1.2	3.3	2.8	3.3
		2.5	1.4	17.8	-	-	2.0	23.7	15.9	21.8	1.0	2.6	2.5	2.3
		5	1.5	16.0	2.3	46.9	2.2	19.3	11.7	16.0	1.3	2.2	2.1	1.6
		10	1.7	14.9	1.2	93.8	-	-	15.8	11.2	1.3	1.4	3.6	1.5
Diesel	A_{Camb}	0	0.4	1.9	2.4	50.9	2.3	16.3	14.6	23.4	1.1	3.2	2.6	3.5
		1.25	1.3	10.1	4.1	58.6	-	-	17.5	11.1	1.2	2.2	2.3	2.0
		2.5	2.2	13.3	6.8	66.7	-	-	16.6	11.0	1.1	3.2	2.4	3.1
		5	1.5	11.0	-	-	-	-	9.6	11.7	1.3	2.7	2.3	2.3
		10	-	-	-	-	-	-	-	-	1.9	2.6	-	-
	B_{Camb}	0	0.7	5.4	2.1	45.9	2.3	17.6	15.2	25.4	1.1	2.6	2.5	2.5
		1.25	0.9	9.2	3.0	29.2	-	-	16.2	12.6	1.4	2.2	2.4	1.5
		2.5	1.0	7.8	-	-	-	-	21.7	11.9	2.0	3.1	1.8	2.2
		5	1.3	13.2	-	-	-	-	-	-	1.8	2.0	2.6	3.5
		10	-	-	-	-	-	-	-	-	-	-	2.6	3.5

DISCUSSION

The contamination of A_{Camb} and B_{Camb} soils with common car fuels, gasoline and diesel, provoked a visible toxic effect on germination, survival and plant development with regard to uncontaminated soils. This effect clearly depended

on the biological features of each plant species, but also on the type and concentration of contaminant and on the soil properties.

Hydrocarbons can affect the plants directly, by contact and interaction with the tissues, and indirectly, by disturbing the physical, chemical and microbiological soil properties. The type and concentration of contaminant and the biological features of each particular plant are usually used as baseline factors in determining phytotoxicity and plant tolerance (Sharonova and Breus, 2012). Apart from the plant and the contaminant, the soil should be also taken into account as a phytotoxicity determining factor. Soil properties including organic matter content, mineralogy, texture and moisture status, are usually ignored in phytotoxicity experiments, but they can highly impact on plant development and on the fate of fuel components (sorption, volatilization, leaching, etc.) (Fine *et al.*, 1997), and therefore, on phytotoxicity and plant tolerance to fuel. The phytotoxicity of fuel was generally higher in B_{Camb} than in A_{Camb}, in the majority of plant species. This was especially reflected by a higher decrease in germination and survival in gasoline and diesel-contaminated B_{Camb} (Table 8.1). A_{Camb} had better pedological properties for plant development, such as higher organic matter and nutrient content, better moisture conservation, etc. On the other hand, the presence of organic matter in A_{Camb} can act as a protective element (Calvelo Pereira *et al.*, 2010): hydrocarbons present in fuel were more strongly sorbed in A_{Camb} than in B_{Camb}, because of its higher organic matter content, and therefore hydrophobic contaminants were less bioavailable for plants, lowering its toxic effect. This general trend was only different for cabbage, for which gasoline toxicity was higher in A_{Camb} than in B_{Camb}, particularly, in germination and survival results (Table 8.1).

Concerning the type of contaminant, the results indicated that diesel was the most toxic fuel for the majority of plants used. Germination and survival indices and plant growth on diesel-contaminated soils was highly reduced at lower

concentrations than on gasoline-contaminated soils. Adam and Duncan (2002) also found low germination rates for white clover (18% at 14 days), in 5% diesel-contaminated soil. Tang *et al.* (2011) found an EC_{50} for maize and wheat germination inhibition of 3.04 and 2.86% of total petroleum hydrocarbons respectively. These data are concordant with the obtained in the present work for diesel-contaminated soil.

Fresh gasoline was supposed to be more toxic than diesel, as already observed by Trapp *et al.* (2001). Fuel hydrocarbon toxicity is strongly correlated with the lower boiling point fractions (Tang *et al.*, 2011), i.e. with the more volatile, soluble and lowest molecular weight components. Because of these properties, they can easily penetrate through membranes into plant cells, and also chemically react with components of plant cells disturbing vital functions (Sharonova and Breus, 2012). The lowest phytotoxicity of gasoline with regard to diesel, found in the present study, is inconsistent with literature data. This could be justified by the gasoline weathering during the 1-month assay, especially by the volatilization of light components, which are also the most toxic. For example, soil half-lives of gasoline monoaromates (BTEX) varied from 120-384 h of benzene, to 168-672 h of xylene isomers (Mackay *et al.*, 2006). Indeed, a bioluminescence bacterial test carried out in our laboratory with leachates from gasoline and diesel-contaminated soils (0.625, 1.25, 2.5, 5 and 10%, *w*/*w*), showed a higher toxicity of gasoline, principally due to its higher solubility and leachability. Luminescence inhibition reached was higher than 50% in gasoline-contaminated soils and less than 20% in diesel-contaminated soils. Furthermore, gasoline and diesel freshly contaminated water presented EC_{50} of 70 and 250 mg L^{-1}, respectively, using the same bioluminescence bacterial assay (data not published).

Diesel is a mixture of more complex and heavier components, whose half-lives in soil are significantly higher than that of gasoline components. Indeed, we

recorded a maximum diesel loss of 20-30% in 2-months greenhouse experiment carried out with the same soils planted with yellow lupine (*Lupinus luteus*) (data not published). Plants can hardly uptake complex diesel components, such as long alkanes and 2, 3 and 4 ring-PAH (Trapp and Legind, 2011). However, they may act as a physical barrier due to their high hydrophobicity or water repellent property. A diesel film around the seeds or the roots may reduce gas and water exchange and nutrient absorption; it may also enter the seeds and alter the metabolic reactions and/or kill the embryo by direct acute toxicity (Serrano *et al.*, 2009). This water repellence was especially visible while watering the pots containing soil contaminated with the highest diesel concentration used (10%): it took the water longer time to enter the soil surface and leach through the whole pot depth. Therefore, diesel toxicity appeared to be probably provoked by a very strong physical stress caused to the plant, in addition to the inherent chemical stress.

Pea, maize, and oat in less magnitude, appeared to be the most tolerant species to fuel contamination, regarding germination and survival results (Table 8.1): in general, germination and survival indices of those species were higher than 50% even at the highest fuel concentrations used (5-10%), except in B_{Camb} contaminated with diesel. Therefore, these plants can successfully germinate in fuel-contaminated soils and develop wealthy plants, even at very high concentrations. In general, the smallest plants, or plants with the smallest seeds (cabbage, lettuce, and clover), were the species whose germination and survival was more hindered with the addition of fuel (Table 8.1). Seeds have a primary line of defence preventing fuel penetration: their seed coat. The integrity and hardness of the seed coat affects the rate of fuel penetration (Adam and Duncan, 2002), and therefore the effect of fuel on the primary seed development. Large seeds such as pea, maize, or oat, have probably harder seed coats than the other small-seeded species, and more volume with more internal nutrition reserves

and stored energy, which they can use to develop the seedlings under adverse conditions (Clark *et al.*, 2004). Therefore, they could be showing higher resistance to gasoline and diesel in the early stages, presenting higher germination and survival indices for a same contamination episode (soil and fuel type). Robson *et al.* (2004) reported that plants with larger seed mass were more commonly found in hydrocarbon contaminated soils than small-seeded plant species. Furthermore, Fenner and Kitajima (1999) observed that larger-seeded plants are established in nutrient deficient soils more often than plants with small seeds, indicating that they will probably support environmental stresses, as a contamination stress, better than smaller-seeded plants.

The effect of the fuels on root and shoot development was different. For most of plant species tested, the results indicated that fuel preferably affected root development, since root elongation and/or biomass had a comparable or higher reduction than shoot, with respect to controls (Figures 8.1 and 8.2). Root was directly exposed to the contaminant in the rhizosphere, and shoot was indirectly affected by the fuel, because of the lowest root development. In some cases, this preferably effect on root was very clear, as for cabbage root elongation and biomass in A_{Camb} (Figures 8.1a and 8.2a), or maize root elongation (Figure 8.1d). In other cases, root and shoot had a relative similar development to that of the control, as occurred for oat and pea biomass on gasoline-contaminated soils (Figures 8.2b and 8.2c), indicating that root and shoot were affected by fuel contamination in a similar extent. Additionally, in contaminated soils, most of plants grew proportionally more in longitude than in biomass, traduced in less branching of shoot and root (higher SSL and SRL) than plants developed in uncontaminated controls (Table 8.2). Clark *et al.* (2004) also observed that biomass of either shoot or root appeared to be more sensitive to organic contamination than elongation.

CONCLUSIONS

Contamination of soils with common car fuels (gasoline and diesel) provoked a decrease in germination, survival and early growth of several plant species. Germination was highly hindered for plant species with small seeds (cabbage, clover and lettuce). The hardness of the seed coat and internal nutrition reserves appeared to be a key factor in germination and survival of plants growing in fuel-contaminated soils. The reduction of root or shoot biomass and elongation was not affected in a proportional way. In general, the root was more affected than the shoot, as being in direct contact with the contaminated soil. Furthermore, the reduction in biomass was relatively higher than in elongation, reflecting the negative influence of fuel contamination on plant branching. The most fuel tolerant species to fuel contamination were pea and maize. Clover and cabbage were the least tolerant species, and could be used as bioindicators to detect soil fuel contamination.

The phytotoxic effect was higher in diesel than in gasoline-contaminated soils, particularly in B_{Camb}. Diesel provoked a physical stress in plants, enhancing the inherent chemical stress, and B_{Camb} lacked the protective sorption effect of organic matter present in A_{Camb}. Gasoline showed a lower toxicity, principally due to the lower half-life of its components in soil. Taking into account gasoline characteristics and dynamics, phytotoxicity standardized bioassays should not be used to characterize fresh gasoline toxicity.

REFERENCES

Adam G, Duncan H. 2002. Influence of diesel fuel on seed germination. Environ Pollut 120:363-370.

Al-Mutairi N, Bufarsan A, Al-Rukaibi F. 2008. Ecorisk evaluation and treatability potential of soils contaminated with petroleum hydrocarbon-based fuels. Chemosphere 74:142-148.

Calvelo Pereira R, Monterroso C, Macías F. 2010. Phytotoxicity of hexachlorocyclohexane: Effect on germination and early growth of different plant species. Chemosphere 79:326-333.

Clark J, Ortego LS, Fairbrother A. 2004. Sources of variability in plant toxicity testing. Chemosphere 57:1599-1612.

Fenner M, Kitajima K. 1999. Seed and seedling ecology. In: Pugnaire FI, Valladares F (eds.). Handbook of functional plant ecology. Marcel Dekker, New York.

Fine P, Graber ER, Yaron B. 1997. Soil interactions with petroleum hydrocarbons: Abiotic processes. Soil Technol 10:133-153.

Hentati O, Lachhab R, Ayadi M, Ksibi M. 2013. Toxicity assessment for petroleum-contaminated soil using terrestrial invertebrates and plant bioassays. Environ Monit Assess 185:2989-2998.

Issoufi I, Rhykerd RL, Smiciklas KD. 2006. Seedling growth of agronomic crops in crude oil contaminated soil. J Agron Crop Sci 192:310-317.

Kirk JL, Klirnomos JN, Lee H, Trevors JT. 2002. Phytotoxicity assay to assess plant species for phytoremediation of petroleum-contaminated soil. Bioremediation J 6:57-63.

Luhach J, Chaudhry S. 2012. Effect of diesel fuel contamination on seed germination and growth of four agricultural crops. U J Environ Res Technol 2:311-317.

Macías F, Calvo de Anta R. 1992. Pedogeochemical characterisation of the soils of Galicia (NW Spain) with respect to lithological variations. Evidence of a transitional environment between temperate and subtropical humid domains. CR Acad Sci II 315:1803–1810.

Mackay D, Shiu WY, Ma KC, Lee SC. 2006. Handbook of physical-chemical properties and environmental fate for organic chemicals. CRC Press, Boca Raton.

Mao D, Lookman R, Weghe HVD, Weltens R, Vanermen G, Brucker ND, Diels L. 2009. Estimation of ecotoxicity of petroleum hydrocarbon mixtures in soil based on HPLC–GCXGC analysis. Chemosphere 77:1508-1513.

Molina-Barahona L, Vega-Loyo L, Guerrero M, Ramírez S, Romero I, Vega-Jarquín C, Albores A. 2005. Ecotoxicological evaluation of diesel-contaminated soil before and after a bioremediation process. Environ Toxicol 20:100-109.

Organization for Economic Cooperation and Development (OECD). 2006. Guidelines for the Testing of Chemicals. Test 208: Terrestrial plant test. Seedling emergence and seedling growth test.

Pitz WJ, Mueller CJ. 2011. Recent progress in the development of diesel surrogate fuels. Prog Energ Combust Sci 37:330-350.

Płaza G, Nałęcz-Jawecki G, Ulfig K, Brigmon RL. 2005. The application of bioassays as indicators of petroleum-contaminated soil remediation. Chemosphere 59:289-296.

Robson DB, Germida JJ, Farrell RE, Knight DJ. 2004. Hydrocarbon tolerance correlates with seed mass and relative growth rate. Bioremediation J 8:185-199.

Serrano A, Tejada M, Gallego M, Gonzalez JL. 2009. Evaluation of soil biological activity after a diesel fuel spill. Sci Total Environ 407:4056-4061.

Sharonova N, Breus I. 2012. Tolerance of cultivated and wild plants of different taxonomy to soil contamination by kerosene. Sci Total Environ 424:121-129.

Tang J, Wang M, Wang F, Sun Q, Zhou Q. 2011. Eco-toxicity of petroleum hydrocarbon contaminated soil. J Environ Sci 23:845-851.

Trapp S, Köhler A, Larsen L, Zambrano K, Karlson U. 2001. Phytotoxicity of fresh and weathered diesel and gasoline to willow and poplar trees. J Soils Sediments 1:71-76.

Trapp S, Legind C. 2011. Uptake of organic contaminants from soil into vegetables and fruits. In: Swartjes FA (ed.). Dealing with contaminated sites. Springer Netherlands: Dordrecht.

Vaajasaari K, Joutti A, Schultz E, Selonen S, Westerholm H. 2002. Comparisons of terrestrial and aquatic bioassays for oil-contaminated soil toxicity. J Soils Sediments 2:194-202.

Xiao J, Wu L, Wu Y, Liu B, Dai L, Li Z, Xia Q, Xi H. 2014. Effect of gasoline composition on oxidative desulfurization using a phosphotungstic acid/activated carbon catalyst with hydrogen peroxide. Appl Energy 113:78-85.

USC
UNIVERSIDADE
DE SANTIAGO
DE COMPOSTELA

9

Characterization and degrading potential of diesel-degrading bacterial strains for its application in soil remediation

Bioremediation of polluted soils is a promising technique, with very low environmental impact, which uses soil organisms (plants, bacteria and/or fungi) to degrade soil contaminants. In the present study, 10 bacterial strains isolated from a diesel-contaminated soil were screened for diesel-degrading ability, biosurfactant production, biofilm formation and tolerance to different individual hydrocarbons, desirable characteristics for the application of bacterial strains in diesel-contaminated soils. Furthermore, the diesel degradation rate was measured by *in vitro* incubation in minimal medium with diesel as solely carbon source. Strains 5, 12 and 26 presented the best results for biosurfactant, biofilm, and solvent tolerance assays. DRO degradation rates of 5 and 12 strains reached 15-25% from total DRO in 10 days of incubation, while strain 26 degradation rate reached 90%. On the basis of these results strain 26 could be a good candidate for further remediation assays with diesel-contaminated soils.

This chapter was a collaboration with the Centre for Environmental Sciences (CMK) (University of Hasselt, Belgium) and with the Instituto de Investigacións Agrobiolóxicas de Galicia (CSIC, Spain).

INTRODUCTION

Biodegradation of diesel hydrocarbons by natural populations of microorganisms allows for the conversion of those contaminants into less or nontoxic forms (Ibrahim *et al.*, 2013). Several authors have described the potential of microorganisms to degrade numerous petroleum hydrocarbons (Das and Mukherjee, 2007; von der Weid *et al.*, 2007; Zhang *et al.*, 2014).

The application of diesel degrading strains to contaminated soils for its remediation, solely (bioremediation) or in association with plants (phyto- and/or rhizoremediation) is an inexpensive and non-invasive technique that is getting importance, due to the promising results. Many laboratory protocols have been described to screen the hydrocarbon degrading potential of bacterial strains in mineral liquid media, as the DCPIP assay (Kubota *et al.*, 2008) or *in vitro* degrading protocol (Zhang *et al.*, 2010). However, when degrading strains are applied to soil for remediation, apart from having a good degrading potential, other properties are desirable for the successful development in soil and for getting acceptable degradation rates.

One of the most important properties is the production of biosurfactants. The principal limitation of bioremediation is the limited bioavailability of hydrocarbons in soil due to the low water-solubility and the interactions with the soil matrix (Szulc *et al.*, 2014). Microbial surfactants, or biosurfactants (BS), exert some influences on hydrocarbon-water interfaces, and can make them more mobile and, therefore, more available for bioremediation (Bordoloi and Konwar, 2009). On the other hand, the capacity of biofilm formation in the presence of hydrocarbons can improve the efficiency of bioremediation and rhizoremediation procedures. Biofilms are aggregates of single or multiple populations that can adhere to environmental surfaces, biotic or abiotic, through extracellular polymeric substances (Singh *et al.*, 2006). Bioremediation with

biofilm formatting bacterial strains presents a proficient and safer alternative to planktonic microorganisms since in a biofilm, cells exhibit better metabolic activity, survival rate (as they are protected within the matrix of external stresses) and rate of gene transfer (Arutchelvi *et al.*, 2011). Biofilm formatting strains are especially suitable for the remediation of recalcitrant compounds, since the ability to immobilize compounds and the high cell density accelerates the usage of xenobiotics (Singh *et al.*, 2006). In the case of rhizoremediation, the rhizosphere forms an environment that fulfils the requirements for biofilm formation, including sufficient moisture and supply of nutrients, which are provided by the plant (Rinaudi and Giordano, 2010). Microorganisms can colonize both soil particles and root tissue, and produce many benefits to plant, including control against pathogens or growth promotion. This plant-bacteria association can substantially improve the degradation of hydrocarbons in soil.

The aim of the present study was to screen a wide collection of bacterial strains isolated from a diesel-contaminated soil, for diesel-degrading ability, biosurfactant production and biofilm formation in the presence of hydrocarbons, and to evaluate their tolerance to different individual hydrocarbons. Furthermore, the diesel degradation rate was measured by *in vitro* incubation in minimal medium with diesel. The results will help to select diesel-degrading strains for application in bio and/or phytoremediation of contaminated soils.

MATERIALS AND METHODS

Screening for diesel-degrading ability of isolated bacterial strains

A wide collection of bacterial strains isolated from a diesel-contaminated site in Genk (Belgium), were provided by the Centre for Environmental Sciences (CMK) of the University of Hasselt (Belgium). The diesel-degrading ability was screened with a modified protocol from Kubota *et al.* (2008). 2,6-dichlorophenol

indophenol (DCPIP), an oxidation-reduction indicator, detects the oxidation of NADH to NAD^+, which is related to hydrocarbon degradation by bacteria. Strains were pre-cultured in 5 mL of rich 869 medium (Mergeay *et al.*, 1985) at 30 °C and 160 rpm. Cultures were centrifuged at 3000 rpm for 5 min, washed twice with $MgSO_4$ 10 mM, and cell density was adjusted to an optical density of 1, at 660 nm ($OD_{660\ nm}$). After sterilization, 750 µL of W medium (Fe-free), 50 µL of 150 µg mL^{-1} $FeCl_3 \cdot 6H_2O$ solution, 50 µL of 100 µg mL^{-1} 2,6-DCPIP solution, 80 µL of bacterial suspension and 5 µL of filter-sterilized diesel (PTFE 0.45 µm filter; Millipore) were added in 1.5 mL sterile microtubes, and cultivated at 30 °C and 120 rpm for 48 h. W medium contains (g L^{-1}): $(NH_4)_2SO_4$, 2; Na_2HPO_4, 14.320; KH_2PO_4, 5.444; NaCl, 0.5; $MgSO_4$, 0.247; $CaCl_2 \cdot 2H_2O$, 0.015; $ZnSO_4 \cdot 7H_2O$, 0.002; $(NH_4)_6Mo_7O_{24} \cdot 4H_2O$, $1.5 \cdot 10^{-4}$; $CuSO_4 \cdot 5H_2O$, $2 \cdot 10^{-4}$; $CoCl_2 \cdot 6H_2O$, $4 \cdot 10^{-4}$; $MnSO_4 \cdot 5H_2O$, 0.001; KNO_3, 0.3 (Koma *et al.*, 2003). After incubation, the colour of the tube was observed, and evaluated as positive for microbial diesel-degradation ability if colourless, and negative, if blue. When positive, the experiment was repeated with autoclaved cells, to assure that the positive result was due only to bacterial degradation.

Bacterial strains which showed positive results for diesel-degrading ability were selected for biosurfactant and biofilm production screening assays and for the evaluation of organic solvent tolerance.

Screening assays for biosurfactant production

Seed culture was prepared by growing the strains in nutrient broth (NB) medium (in g L^{-1}: D(+) glucose, 1; peptone, 15; NaCl, 6; yeast extract, 3) at 37 °C and 120 rpm for 10-12 h. After incubation, $OD_{660\ nm}$ was adjusted to 1. The culture at 3% was used to inoculate 50 mL of BS production selective medium, with diesel as the sole carbon source, in 250 mL-Erlenmeyer flasks (*n=3*). Inocula

were incubated at 37 °C and 160 rpm. BS producing selective medium contains (g L^{-1}): $(NH_4)_2SO_4$, 10; NaCl, 1.1; KCl, 1.1; $FeSO_4 \cdot 7H_2O$, $2.8 \cdot 10^{-4}$; $K_2HPO_4 \cdot 3H_2O$, 4.4; KH_2PO_4, 3.4; $MgSO_4$, 0.5; yeast extract, 0.5; trace element solution, 0.5 mL; filter-sterilized diesel (PTFE 0.45 µm filter; Millipore), 2% (*v*/*v*) (Sriram *et al.,* 2011a). The composition of the trace elements solution was (g L^{-1}): $CaCl_2$, 0.24; $ZnSO_4$, 0.29; $MnSO_4$, 0.17; $CuSO_4$, 0.25). The trace element solution was filter-sterilized (0.2 µm, Millipore), added to the production media after autoclaving, and vigorously agitated to homogenise the media.

After incubation, cultures were centrifuged at 3000 rpm for 5 min to get the supranatant (SN) and the pellets (PEL). Pellets were resuspended in the same volume of $MgSO_4$ 10 mM. Both SN and PEL were used to perform the BS screening assays: oil displacement test, drop collapsing test, emulsification assay and lipase production (Sriram *et al.*, 2011b). All tests were done in triplicate and Milli-Q sterile water was used as negative control.

i. Drop collapsing test

2-3 µL of mineral oil was added to each well of a 96-well microtitre plate and allowed to equilibrate 1 h at 37 °C. Then 5 µL of culture SN or PEL were added to the centre of the wells over the oil film. The shape of the oil drop was examined after 1 min. Flattened drops were considered positive for BS production, and intact drops were considered negative.

ii. Oil displacement test

15 µL of weathered crude oil was added to a 150 mm-diameter petri plate containing 40 mL of distilled water. 10 µL of SN and PEL were carefully added to the centre of the oil film, and after 30 s of incubation the diameter of the clear halo zone was measured.

iii. Emulsification assay

4 mL of culture SN and PEL and 4 mL of *n*-hexadecane or diesel were vortex-mixed for 5 min. The mix was left 24 h undisturbed and the height of the emulsion layer was measured. The emulsification activity was expressed as the percentage of the emulsion layer height from the total liquid height (cm).

iv. Lipase production

Agar plates were prepared according to Sriram *et al.* (2011a): 2% Tween 80, 2.5 % agar, and 0.5 % methyl red. 20 µL of culture SN and PEL were added to a cut in the plates, and incubated overnight at room temperature. Strains were positive for lipase production when a zone of clearance around the cut was observed.

Biofilm formation assay

This assay is based on the ability of bacterial strains to form biofilms on plastics, usually polystyrene (PS), polypropylene (PP) and polyvinylchloride (PVC) (O'Toole and Kolter, 1998; Shimada *et al.*, 2012; Tribelli *et al.*, 2012).

Seed culture was prepared by growing the strains in Luria-Bertani medium (LB) (in g L^{-1}: tryptone, 10; NaCl, 10; yeast extract, 5) at 30 °C and 120 rpm for 12-24 h. After incubation, $OD_{600\ nm}$ of the inocula was adjusted to 0.3 (Shimada *et al.*, 2012). PS and PP 96-well plates were prepared with a total volume of 300 µL: 3 µL of culture (100-fold dilution), 15 µL of filter-sterilized contaminant (diesel or *n*-hexadecane) (5%, *v/v*), as the sole carbon source, and 285 µL of W minimal medium (Koma *et al.*, 2003) (*n=3*). Negative controls wells were also prepared with 3 µL of LB medium incubated without inoculant. The plates were closed with parafilm and covered with aluminium foil, and were incubated at 30 °C for 7 days in static conditions (Tribelli *et al.*, 2012).

Following the method described by Tribelli *et al.* (2012), after incubation, the supranatant with planktonic cells was very gently pipetted to special UV plates to measure absorbance at 600 nm (absorbance of planktonic cells: APL). In the PS or PP plates, 100 µL of $MgSO_4$ 10 mM was added to solubilise the remaining planktonic cells. After approximately 20 min, the $MgSO_4$ was eliminated and 25 µL of 1% crystal violet solution (Sigma Aldrich Co, LLC), which will stain the biofilm-formatting cells attached to the plastic plates (O'Toole and Kolter, 1998). After 20 min incubation at room temperature, plates were washed 4 times with sterile distilled water, to free crystal violet. Attached biofilm cells were solubilised with 200 µL of ethanol 96% and incubated 20 min. Then, the liquid was transferred to specific UV-plates and absorbance at 550 nm was measured (absorbance of crystal violet: ACV).

With the two absorbance values, APL and ACV, the adherence index was calculated (Equation 9.1):

$$\text{Adherence index} = \frac{\text{ACV (Absorbance of crystal violet} - \text{Biofilm cells)}}{\text{APL (Absorbance of planctonic cells)}}$$

Equation 9.1

Organic solvent tolerance (OST)

This test can give an easy idea of the extent of growth of the strains in the presence of hydrocarbons. Following Oh *et al.* (2012), strains were grown for 12 h at 37 °C and 120 rpm on LB modified medium (LBGMg) that contains (g L^{-1}): D(+) glucose, 1; peptone, 8; NaCl, 8, yeast extract, 4; $MgSO_4 \cdot 7H_2O$, 2,465. Cultures were resuspended with the same medium to OD_{600nm}=0.5. Bacterial suspensions were diluted in ten-fold serial steps up to the 10^{-6} dilution stage. 5 µL of each dilution were spotted on LBGMg agar plates, and 4 mL of the organic solvents were gently added to the plate surface: hexane, octane, dodecane and hexane/cyclohexane (1:1). Negative control plates were also prepared with

LBGMg medium incubated without inoculant. Plates were closed with parafilm to avoid evaporation losses. After 20 h of incubation at 30 °C, plates were observed for bacterial growth at the different serial dilutions.

Measurement of diesel degradation: *in vitro* protocol

Selected strains, 5, 12 and 26, were precultivated in LB medium for 24 hours at 30°C and 150 rpm. Cultures were centrifuged at 3000 rpm for 10 min, and the pellets were washed twice and resuspended in Bushnell Haas modified mineral medium (BH2), that contains (g L^{-1}): K_2HPO_4, 1.32; KH_2PO_4, 1; NH_4Cl, 0.81; $NaNO_3$, 0.84; $FeSO_4 \cdot 7H_2O$ 0.01; $MgSO_4 \cdot 7H_2O$, 0.42 (Bushnell and Haas, 1941). $OD_{590\ nm}$ of inocula was adjusted to 1, and 0.5 mL was added to culture sterile tubes with 4.5 mL of BH2 medium and 1 g L^{-1} of filter-sterilized diesel, as the sole carbon source. The tubes were incubated at 30°C and 150 rpm. At each fixed time (0, 2, 4, 6, 8 and 10 days), six flasks were sacrificed and used for residual hydrocarbon determination and CFU counting. Abiotic controls were also set up for all times. A heat killed cells control (autoclaved inocula) was incubated for 10 days to assure that hydrocarbon losses were due to bacterial degradation.

After incubation, 100 µL of serial ten-fold dilutions of the cultures were plated in 1:10 diluted 869 agar medium. After 7 days of incubation at 28 °C, colony forming units (CFU) were counted and calculated per mL of medium.

The hydrocarbons were extracted from the culture by ultrasonic assisted extraction with hexane (1:2, sample-solvent), for 1 h (Chapter 4). Gas chromatography (Model 450 GC, Agilent Technologies) coupled to mass spectrometry (Model 220 MS, Agilent Technologies) (GC/MS) was used to analyse the diesel range organics (DRO), alkanes from C_{10} to C_{25}. Before analysis, a mix of deuterated internal standards, containing 1,4-dichlorobenzene-d_4, acenaphthene-d_{10}, chrysene-d_{12}, naphthalene-d_8, perylene-d_{12} and phenanthrene-

d_{10} (Internal Standards Mix 33, Dr. Ehrenstorfer), was added to the extracts at 0.2 mg L^{-1} as a constant concentration. Calibration of DRO was carried out with a standard containing a mixture of C_{10}-C_{25} *n*-alkanes (DRO mix, Dr. Ehrenstorfer). The calibration standards were prepared in hexane, at several concentrations: 0.1, 0.5, 1.0, 2.5, 5, 7.5 and 10.0 mg L^{-1}. Internal standards were also added to standards in the same concentration as for the samples (0.2 mg L^{-1}). Chromatographic separations were performed by a FactorFour VF-5ms EZ-Guard capillary column (30 m x 0.25 mm x 0.25 µm; Agilent Technologies) that operated with the following oven temperature program: 40 °C (held for 10 min) to 300 °C, at 10 °C min^{-1}. Helium was used as carrier gas, at constant flow 1 mL min^{-1}. The injector was operated with a temperature ramp from 60 °C to 300 °C (held for 35 min), at 200 °C min^{-1}, and samples (1 µL) were injected in split/splitless mode. The mass spectrometer operated in full scan mode. Ionization of the molecules was carried out by electron impact (EI) and the ion trap temperature was fixed at 220 °C (Chapter 4).

Statistical analysis

PASW Statistics software (Version 20.0.0; IBM SPSS Statistics, Inc.) was used to analyze the data. One factor-ANOVA was used to compare the adherence indices in biofilm formation protocol. A significance level of p=0.05 was considered for statistical analyses.

RESULTS AND DISCUSSION

Diesel-degrading ability of bacterial strains: DCPIP protocol

Strains isolated from a diesel-contaminated site were screened for diesel-degrading ability with the DCPIP protocol. Figure 9.1 shows the DCPIP test results for strain 12.

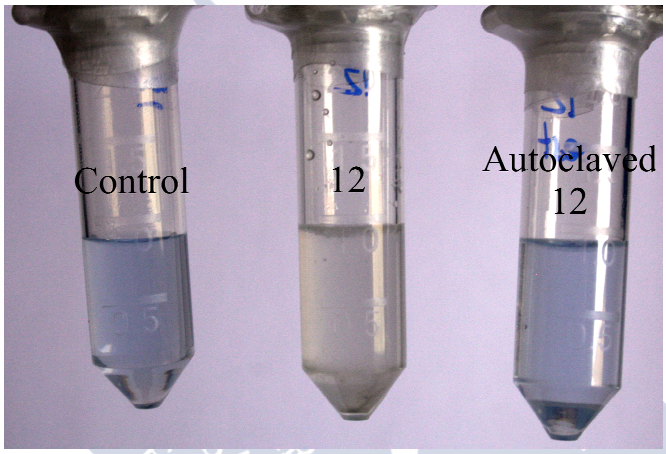

Figure 9.1. Results of the DCPIP diesel-degrading ability of strain 12. The colourless tube indicated that the test was positive, and the blue colour in autoclaved tube, indicated that the degradation was due to the bacterial strain.

Ten positive strains for diesel-degrading ability test were selected (Table 9.1) to screen for biosurfactant production, biofilm formation and organic solvent tolerance.

Table 9.1. Collection of diesel-degrading bacteria isolated from a contaminated site by CMK (Hasselt University) and selected for this study.

Strain	Species
1	*Arthrobacter* sp.
5	*Staphylococcus aereus*
11	*Pseudomonas brassicacearum*
12	*Pseudomonas putida*
14	*Pseudomonas putida*
15	*Pseudomonas fluorescens*
17	*Pseudomonas* sp.
25	*Pseudomonas brassicacearum*
26	*Staphylococcus aereus*
27	*Pseudomonas* sp.

Screening protocols for biosurfactant production

The biosurfactant production assays (Table 9.2) showed positive results for some of the strains tested. In the case of drop collapsing test, strains 5, 25, 26 and 27 culture supranatant and 11, 12 and 14 pellet suspension, showed flattened drops on mineral oil. The culture supranatant of strains 5, 11, 14, 25 and 26 produced a clear halo zone with a diameter higher than 1 cm, during oil displacement experiment performance. In general, most of strains were capable of emulsifying hydrocarbons, reflected by an evident emulsified layer. This layer was especially developed in the presence of hexadecane: emulsifications activities of strains 5, 12, 15, 17, 25, 26 and 27 supranatants were higher than 50%. Emulsification activity in the presence of diesel was significantly lower, since diesel is a heavy mix of compounds, more difficult to emulsify. Lipase production was recorded with 1, 5, 14 and 15 supranatant.

Table 9.2. Results of the biosurfactant production screening assays of the tested strains, with supranatant (SN) and pellet suspension (PEL). Negative results are indicated with "-".

Strain	Drop collapsing		Oil displacement (halo diameter, cm)		Emulsification assay (emulsification activity, %)				Lipase production	
					Hexadecane		Diesel			
	SN	PEL	SN	PEL	SN	PEL	SN	PEL	SN	PEL
1	-	-	0.5	0.5	slight layer	slight layer	30.0%	-	+	-
5	++	-	1.1	0.4	60.0%	slight layer	-	-	+	-
11	-	+	1.2	0.6	-	-	50.0%	-	-	-
12	-	+	1.2	-	60.0%	slight layer	-	14.3%	-	-
14	-	++	-	-	40.0%	slight layer	35.0%	-	+	-
15	-	-	0.8	0.3	60.0%	slight layer	55.0%	-	+	-
17	-	-	0.6	0.4	60.0%	5.0%	45.0%	-	-	-
25	++	-	1.1	0.5	65.0%	10.0%	40.0%	-	-	-
26	++	-	1.3	-	60.0%	slight layer	-	51.4%	-	-
27	+	-	0.4	0.4	60.0%	slight layer	35.0%	-	-	-

Other authors also found similar results for biosurfactant producing strains. Ibrahim *et al.* (2013) screened a wide variety of strains (*Micrococcus kristinae, Bacillus licheniformis, Bacillus firmus, Bacillus lentus, Serratia marcescens, Pseudomonas paucimobilis*). They found halos of 23 to 51 mm in the oil displacement test; positive results for the drop collapsing test; and emulsification activities of 40-90%. Sriram *et al.* (2011b) found a clear halo zone of 2.95 cm^2 in the oil displacement test and an emulsification activity with *n*-hexadecane of 62% for *Bacillus cereus* NK1 isolate.

In general, the best biosurfactant assays results were those of culture supranatant, indicating that biosurfactant production of the strains was preferably extracellularly produced.

On the basis of these results (Table 9.2), the best biosurfactant producing strains were 5, 12, 25 and 26. Figure 9.2 shows some examples of the positive results of strain 26 for different biosurfactant screening tests.

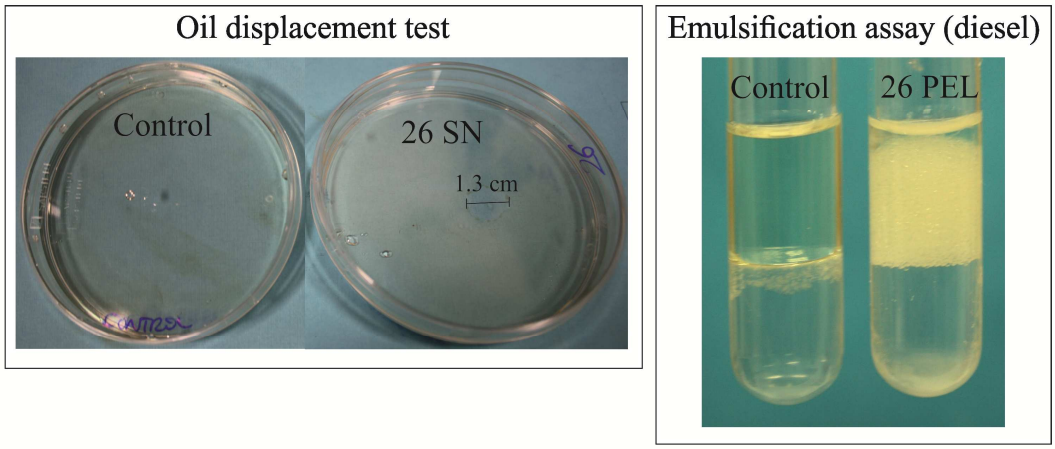

Figure 9.2. Oil displacement and emulsification assay with diesel for strain 26 SN and PEL, respectively.

Biofilm formation in the presence of hexadecane and diesel

Adherence indices (Equation 9.1) resulted from the biofilm formation (Table 9.3) in the presence of hexadecane and diesel of all strains were higher than the respective negative control, but only few strains had significant differences (p<0.05). As happened in the biosurfactant assays, biofilm results in the presence of diesel were less significant than with hexadecane. The strains with the best results in hexadecane were 5, 11, 12, 15, 17, 26 and 27, showing adherence indices between 9.1 and 128.0 in PP (3.5 for the control), and between 14.9 and 114.0 in PS (1.9 for the control). The best results in diesel were those of 5 y 26 in PP, with adherence indices of 43.1 and 46.0, respectively (2.3 for the control).

Ramey *et al.* (2004) reviewed that some species of *Pseudomonas* are known to form biofilms on biotic or abiotic surfaces. *P. putida* can respond rapidly to the

presence of root exudates in soils, converging at root colonization sites and establishing stable biofilms.

Table 9.3. Adherence indices of the bacterial strains in polypropylene (PP) and polystyrene (PS) plates in the presence of hexadecane or diesel. The results are expressed as the mean ± the standard deviation (*n=3*). Significant differences with the respective control are indicated with asterisks.

	Hexadecane		Diesel	
Strain	**PP**	**PS**	**PP**	**PS**
Control	3.5 ± 0.7	1.9 ± 1.0	1.3 ± 0.5	2.3 ± 0.4
1	10.1 ± 0.9	10.6 ± 8.2	6.0 ± 4.7	8.4 ± 2.1
5	62.6 ± 3.8**	55.5 ± 5.0**	5.8 ± 2.5	43.1 ± 3.9**
11	9.1 ± 3.0	19.4 ± 5.4**	3.2 ± 0.9	12.1 ± 7.7
12	16.7 ± 3.6*	14.9 ± 3.2*	3.0 ± 1.4	13.3 ± 4.0
14	4.2 ± 1.3	7.3 ± 0.4	4.3 ± 3.8	7.3 ± 1.4
15	20.6 ± 1.0**	16.0 ± 6.3*	6.1 ± 2.2	16. 3 ± 2.9
17	35.5 ± 9.1**	22.6 ± 3.1**	3.7 ± 0.2	19.2 ± 5.8
25	14.1 ± 4.2	10.6 ± 3.2	5.2 ± 2.7	11.8 ± 3.1
26	128.0 ± 4.5**	114.0 ± 10.3**	6.1 ± 3.5	46.0 ± 10.7**
27	23.9 ± 6.7**	14.6 ± 1.6	2.0 ± 1.4	22.2 ± 20.1

** p<0.05; ** p<0.01.*

Organic solvent tolerance (OST) spot assay

The strains tested showed very good results for OST (organic solvent tolerance) assay, since, in general, up to 10^{-3}-fold dilution grew in the presence of the organic solvents (Table 9.4), except strain 1. Therefore, any of the strains would have an acceptable growth on organic xenobiotics, and probably on diesel, what can also be predicted by the DCPIP assay positive results. Figure 9.3, shows the results of OST test of strain 5.

Sardessai and Bhosle (2012) reviewed that a large number of the reported organic solvent tolerant bacteria are *Pseudomonas* strains (most of strains in Table 9.1 are *Pseudomonas* sp.), especially *P. putida*, and that in general, Gram-negative bacteria are better candidates to cope with the solvent induced shock.

Table 9.4. Growth of bacterial strains ten-fold dilutions (10^{-1} to 10^{-6}) on LBGMg agar medium overlaid with several organic solvents. The extent of growth was visually characterized with +++, ++ and +, from high to slight growth.

Strain	Hexane	Octadecane	Dodecane	Hexane/Cyclohexane
1	10^{-1} (+)	-	10^{-4} (++), 10^{-5} (+)	-
5	10^{-4} (++)	10^{-4} (+)	10^{-4} (++)	10^{-3} (++), 10^{-4} (+)
11	10^{-3} (+++), 10^{-2} (++)	10^{-3} (++), 10^{-2} (++)	10^{-4} (+++), 10^{-5} (++), 10^{-6} (+)	10^{-3} (++), 10^{-4} (+)
12	10^{-2} (+++), 10^{-3} (+)	10^{-2} (++), 10^{-3} (+)	10^{-3} (++)	10^{-2} (+++), 10^{-3} (+)
14	10^{-5} (++), 10^{-6} (+)	10^{-4} (+++), 10^{-5} (+), 10^{-6} (+)	10^{-4} (+++), 10^{-5} (+)	10^{-5} (++), 10^{-6} (+)
15	10^{-4} (+++), 10^{-5} (+)	10^{-3} (+++), 10^{-4} (++), 10^{-5} (+)	10^{-3} (+++), 10^{-4} (++), 10^{-5} (+)	10^{-4} (+++), 10^{-5} (++)
17	10^{-5} (+++), 10^{-6} (++)	10^{-4} (++), 10^{-5} (+)	10^{-4} (+++), 10^{-5} (++), 10^{-6} (+)	10^{-4} (+++), 10^{-5} (++), 10^{-6} (+)
25	10^{-5} (+++)	10^{-5} (+++), 10^{-6} (+)	10^{-5} (++), 10^{-6} (+)	10^{-5} (++), 10^{-6} (+)
26	-	10^{-2} (++), 10^{-3} (+)	10^{-3} (+++), 10^{-4} (+)	-
27	10^{-5} (++), 10^{-6} (++)	10^{-5} (++), 10^{-6} (++)	10^{-5} (++), 10^{-6} (++)	10^{-5} (++), 10^{-6} (++)

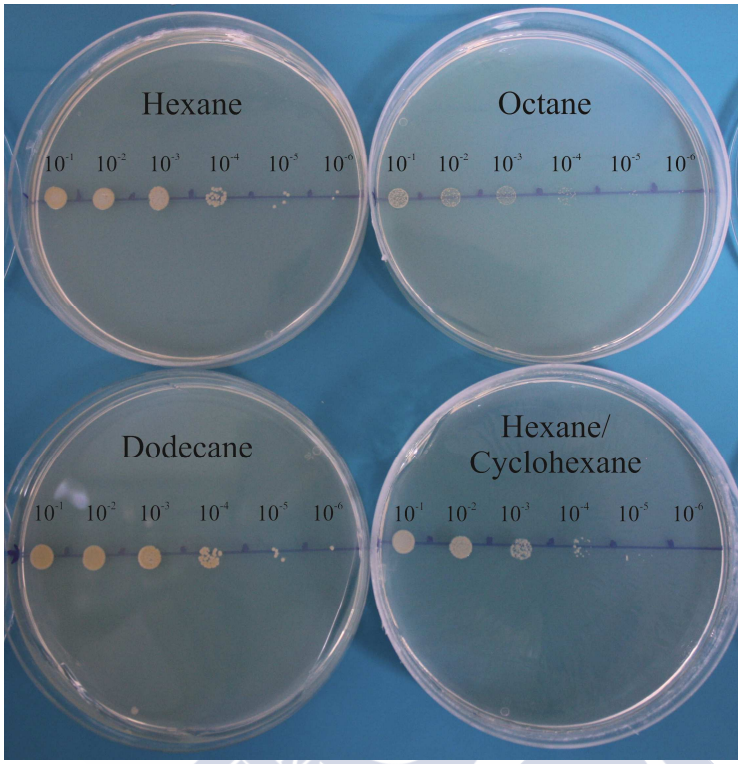

Figure 9.3. Bacterial growth of 5 µL of ten-fold dilutions of strain 5 in OST (organic solvent tolerance) test with 4 mL of hexane, octadecane, dodecane and hexane/cyclohexane (1:1, *v/v*).

Diesel range organics degradation by selected strains: *in vitro* protocol

Three strains of those with the best results in biosurfactant, biofilm and OST assays were selected for the *in vitro* diesel degradation experiment, with GC/MS determination of DRO: strains 5, 12 and 26.

The results of GC/MS analysis of DRO are represented in figures 9.4, 9.5 and 9.6. The percentage of DRO degraded at each incubation time, was calculated by the difference with the respective non-inoculated control.

The sum of the 16 alkanes analyzed (∑DRO, from C_{10} to C_{25}) was represented, in addition to two examples of individual alkanes: a low and a high-molecular weight alkane, C_{12} and C_{22}, respectively.

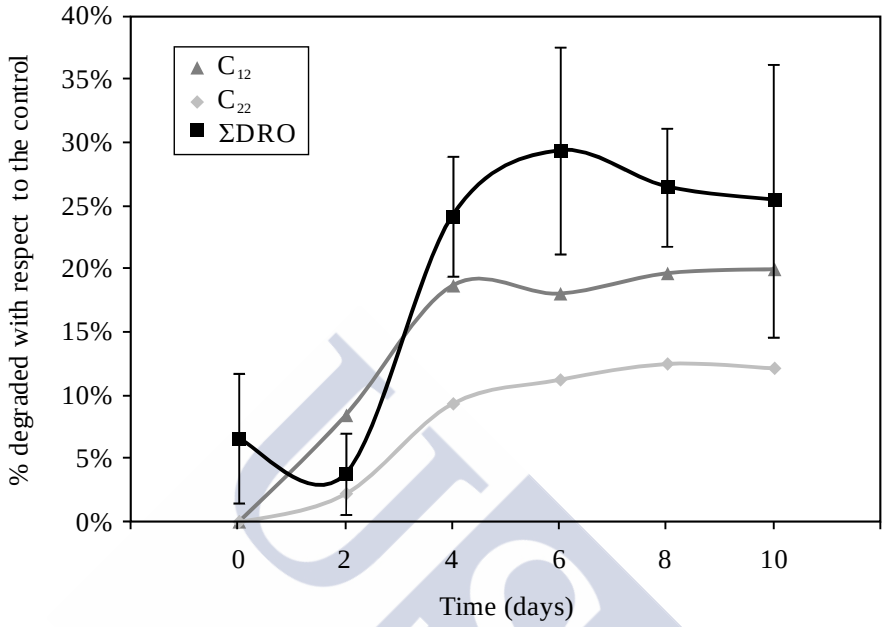

Figure 9.4. Percentage of DRO degraded by strain 5 with respect to the non-inoculated control based on GC/MS analysis, at different incubation times.

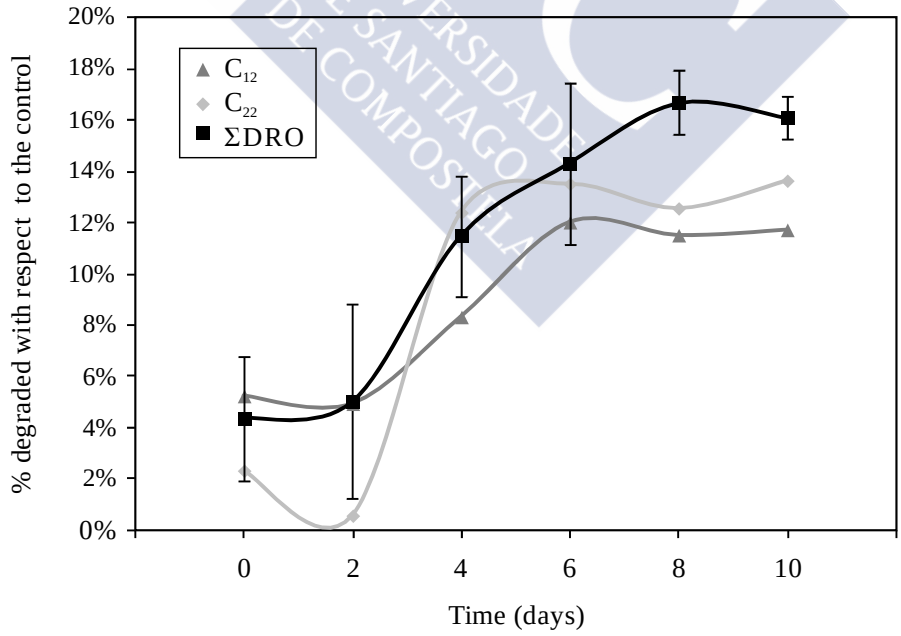

Figure 9.5. Percentage of DRO degraded by strain 12 with respect to the non-inoculated control based on GC/MS analysis, at different incubation times.

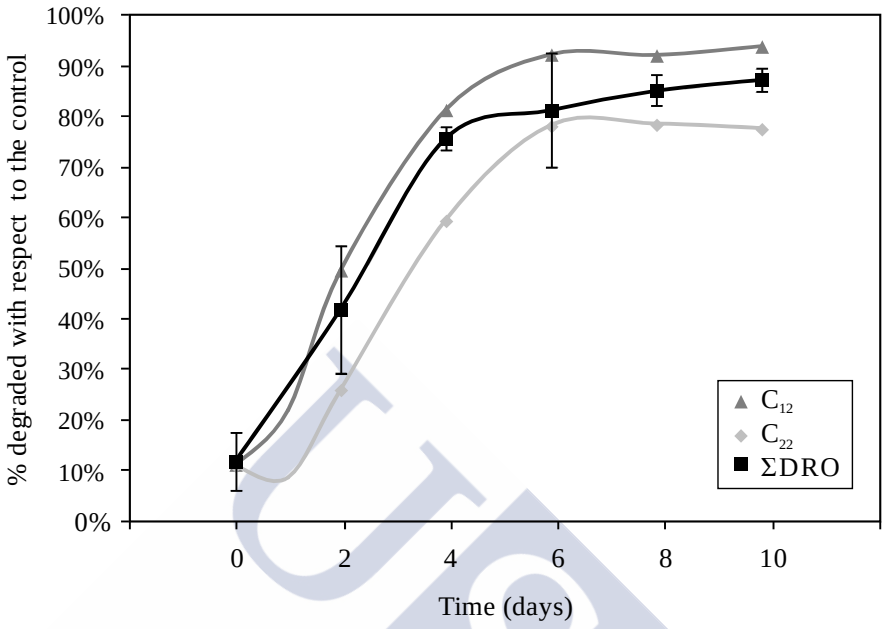

Figure 9.6. Percentage of DRO degraded by strain 26 with respect to the non-inoculated control based on GC/MS analysis, at different incubation times.

The degrading kinetics of the strains was very similar: the degradation was very fast for the first 4 days, after a variable acclimatization period, and then the degradation rate was stabilized until the end of the experiment. Strain 12, appeared to be the slowest of the degrading strains tested, with a relatively longer acclimatization period (2 days) and a low degradation rate until its stabilization at 6-7 days (Figure 9.5).

Strain 5 and 12 (Figure 9.4 and 9.5) had acceptable degradation rates, since 15-25% of the analyzed ∑DRO were degraded by the end of the experiment (10 days). On the other hand, strain 26 showed extremely promising results, with near 90% of ∑DRO degraded (Figure 9.6). Other authors have reported high diesel degradation rates by several bacterial strains. Zhang *et al.* (2014) reported diesel degradation rates of 30-60% in culture medium (mineral medium with diesel as sole carbon source) with different surfactants, using *Pseudomonas aeruginosa* endophytes isolated from *Scirpus triqueter*. Deng *et al.* (2014) isolated a

hydrocarbon-degrading strain, *Achromobacter* sp. HZ01, which degraded up to 90% diesel in 10 days of incubation in minimal salt medium (MSM) with 2% (*w*/*v*) of evaporated diesel oil.

Concerning the individual DRO, in general, the low-molecular weight alkanes (C_{10}-C_{14}) were more easily degraded than the high-molecular weight alkanes (C_{16}-C_{25}). Figures 10.4 to 10.6 show an example of each group of compounds, C_{12} and C_{22}. The lightest compounds are shorter carbon chains, and therefore, they were more easily degraded than the heaviest DRO (very long carbon chains). von der Weid *et al.* (2007), also reported higher degradation rates of the lightest alkanes with *Dietzia cinnamea*.

Taking into account the data of colony forming units (CFU) counting, CFU mL^{-1} of strains 5 and 12 were very similar at the different incubation times, and even slightly decreased with time for strain 5. However, strain 26, had a light CFU mL^{-1} increase from $1 \cdot 10^{-8}$ to $5 \cdot 10^{-8}$ at the end of the experiment (data not shown). This indicates that this strain would comfortably grow in the presence of diesel.

The *in vitro* degradation protocol offered very favourable conditions for bacterial growth: high and constant temperature, no bacterial competition for carbon source, easily available carbon and nutrients, liquid medium to grow, etc. Thus, these degradation rates would not probably be obtained in soil. Nevertheless, strain 26 showed a very good degrading capacity, and could be a good candidate for further remediation assays with diesel-contaminated soils.

CONCLUSIONS

Biosurfactant production, biofilm formation and organic solvent tolerance, are properties required for the successful application and development of diesel degrading bacterial strains to contaminated soils. The screening tests performed,

helped us to select the strains with the best properties, to carry out the *in vitro* degradation protocol.

Strains 5, 12 and 26 showed very good results in the *in vitro* degradation protocol; especially strain 26, which degraded around 90% of the DRO present. For all strains, DRO degradation reached the maximum rate in 4 or 6 days incubation.

The results of the *in vitro* degradation protocol are expected to be far from those that will be obtained in soil experiments. However, the positive results for biosurfactant production, biofilm formation, solvent tolerance, and especially, the extremely high diesel degradation rate of the *in vitro* protocol, conclude that strain 26, is a promising candidate to be used in bio- and/or phytoremediation experiments with diesel-contaminated soils.

REFERENCES

Arutchelvi J, Joseph C, Doble M. 2011. Process optimization for the production of rhamnolipid and formation of biofilm by *Pseudomonas aeruginosa* CPCL on polypropylene. Biochem Eng J 56:37-45.

Bordoloi NK, Konwar BK. 2009. Bacterial biosurfactant in enhancing solubility and metabolism of petroleum hydrocarbons. J Hazard Mater 170:495-505.

Bushnell LD, Haas HF. 1941. The utilization of certain hydrocarbons by microorganisms. J Bacteriol 41:653-673.

Das K, Mukherjee AK. 2007. Crude petroleum-oil biodegradation efficiency of *Bacillus subtilis* and *Pseudomonas aeruginosa* strains isolated from a petroleum-oil contaminated soil from North-East India. Bioresour Technol 98:1339-1345.

Deng M, Li J, Liang F, Yi M, Xu X, Yuan J, Peng J, Wu C, Wang J. 2014. Isolation and characterization of a novel hydrocarbon-degrading bacterium *Achromobacter* sp. HZ01 from the crude oil-contaminated seawater at the Daya Bay, southern China. Mar Pollut Bull 83:79-86.

Ibrahim ML, Ijah UJJ, Manga SB, Bilbis LS, Umar S. 2013. Production and partial characterization of biosurfactant produced by crude oil degrading bacteria. Int Biodeterior Biodegrad 81:28-34.

Koma D, Hasumi F, Chung S, Kubo M. 2003. Biodegradation of *n*-alkylcyclohexanes by co-oxidation via multiple pathways in *Acinetobacter* sp. ODDK71. J Biosci Bioeng 95:641-644.

Kubota K, Koma D, Matsumiya Y, Chung S, Kubo M. 2008. Phylogenetic analysis of long-chain hydrocarbon-degrading bacteria and evaluation of their hydrocarbon-degradation by the 2,6-DCPIP assay. Biodegradation 19:749-757.

Mergeay M, Nies D, Schlegel HG, Gerits J, Charles P, Van Gijsegem F. 1985. *Alcaligenes eutrophus* CH34 is a facultative chemolithotroph with plasmid-bound resistance to heavy metals. J Bacteriol 162:328-334.

Oh H, Lee J, Kim O. 2012. Increase of organic solvent tolerance of *Escherichia coli* by the deletion of two regulator genes, *fadR* and *marR*. Appl Microbiol Biotechnol 96:1619-1627.

O'Toole GA, Kolter R. 1998. Initiation of biofilm formation in *Pseudomonas fluorescens* WCS365 proceeds via multiple, convergent signalling pathways: a genetic analysis. Mol Microbiol 28:449-461.

Ramey BE, Koutsoudis M, Bodman SBv, Fuqua C. 2004. Biofilm formation in plant–microbe associations. Curr Opin Microbiol 7:602-609.

Rinaudi LV, Giordano W. 2010. An integrated view of biofilm formation in rhizobia. FEMS Microbiol Lett 304:1-11.

Sardessai Y, Bhosle S. 2002. Tolerance of bacteria to organic solvents. Res Microbiol 153:263.

Shimada K, Itoh Y, Washio K, Morikawa M. 2012. Efficacy of forming biofilms by naphthalene degrading *Pseudomonas stutzeri* T102 toward bioremediation technology and its molecular mechanisms. Chemosphere 87:226-233.

Singh R, Paul D, Jain RK. 2006. Biofilms: implications in bioremediation. Trends Microbiol 14:389-397.

Sriram MI, Gayathiri S, Gnanaselvi U, Jenifer PS, Mohan Raj S, Gurunathan S. 2011a. Novel lipopeptide biosurfactant produced by hydrocarbon degrading and heavy metal tolerant bacterium *Escherichia fergusonii* KLU01 as a potential tool for bioremediation. Bioresour Technol 102:9291-9295.

Sriram MI, Kalishwaralal K, Deepak V, Gracerosepat R, Srisakthi K, Gurunathan S. 2011b. Biofilm inhibition and antimicrobial action of lipopeptide biosurfactant produced by heavy metal tolerant strain *Bacillus cereus* NK1. Colloids Surf B 85:174-181.

Szulc A, Ambrożewicz D, Sydow M, Ławniczak Ł, Piotrowska-Cyplik A, Marecik R, Chrzanowski Ł. 2014. The influence of bioaugmentation and biosurfactant addition on bioremediation efficiency of diesel-oil contaminated soil: Feasibility during field studies. J Environ Manage 132:121-128.

Tribelli P, Di Martino C, López N, Raiger Iustman L. 2012. Biofilm lifestyle enhances diesel bioremediation and biosurfactant production in the

Antarctic polyhydroxyalkanoate producer *Pseudomonas extremaustralis*. Biodegradation 23:645-651.

von der Weid I, Marques JM, Cunha CD, Lippi RK, dos Santos SCC, Rosado AS, Lins U, Seldin L. 2007. Identification and biodegradation potential of a novel strain of *Dietzia cinnamea* isolated from a petroleum-contaminated tropical soil. Syst Appl Microbiol 30:331-339.

Zhang X, Liu X, Wang Q, Chen X, Li H, Wei J, Xu G. 2014. Diesel degradation potential of endophytic bacteria isolated from *Scirpus triqueter*. Int Biodeterior Biodegrad 87:99-105.

Zhang Z, Gai L, Hou Z, Yang C, Ma C, Wang Z, Sun B, He X, Tang H, Xu P. 2010. Characterization and biotechnological potential of petroleum-degrading bacteria isolated from oil-contaminated soils. Bioresour Technol 101:8452-8456.

USC
UNIVERSIDADE
DE SANTIAGO
DE COMPOSTELA

10

Enhanced degradation of diesel in the rhizosphere soil of *Lupinus luteus* after inoculation with diesel-degrading and PGP bacterial strains

The association of plants and rhizospheric bacteria has emerged as one of the most successful techniques to degrade petroleum contaminants. An association of *Lupinus luteus* and different bacterial inoculants was applied to the A and B horizons of a umbric Cambisol (A_{Camb} and B_{Camb}) spiked with 1.25-1.5% (*w*/*w*) of diesel. Plants were set up in contaminated and uncontaminated controls, and were either not inoculated (NI), or inoculated with a diesel-degrader (D), PGP strains (PGP), or the combination of both (D+PGP), and grown for a month. Diesel range organics (DRO) dissipation was significantly higher in inoculated than in NI pots: highest DRO losses were found in A_{Camb} D+PGP pots (close to 15% higher than NI) and in B_{Camb} D pots (close to 10% higher). Water-extractable DRO fraction was significantly higher at t=30, probably due to the effects of plant root exudates. Furthermore, biosurfactant production of the degrader strain also led to a slight increase in the soluble DRO fraction. The inoculant which led to the highest solubility increase was also that with the highest DRO dissipation.

This chapter was a collaboration with the Centre for Environmental Sciences (CMK) (University of Hasselt, Belgium) and with the Instituto de Investigacións Agrobiolóxicas de Galicia (CSIC, Spain).

INTRODUCTION

Traditional soil remediation techniques involve physical (washing, excavation) and/or chemical treatments (soil flushing) that are expensive and can be environmentally destructive (Kuiper *et al.*, 2004). Bioremediation, is the use of living organisms (plants, bacteria and/or fungi) to manage or remediate polluted soils (Wenzel, 2009). This technique can be applied *in situ* and is inexpensive, clean and causes lower impacts on the environment. In particular, rhizoremediation (phytoremediation assisted with rhizosphere microorganisms) has emerged as one of the most successful techniques to degrade petroleum contaminants (MacKinnon and Duncan, 2013). Many authors have isolated bacteria from petroleum contaminated sites with hydrocarbon-degrading potential for use in soil rhizoremediation (Das and Mukherjee, 2007; Obayori, *et al.*, 2009; Tanase *et al.*,2013).

In rhizoremediation, plant-bacteria partnerships provide benefits for both sides, which in combination can substantially improve remediation efficiency. Plants create a favourable environment for the development of bacterial communities in the rhizosphere: they provide nutrients, oxygen, favourable redox conditions and supply the bacteria with readily-available carbon sources, such as sugars or organic acids, which help them to proliferate (Wang *et al.*, 2011). Moreover, root exudates, such as flavonoids, terpenes or lignin derived compounds, often have similar chemical structures to fuel contaminants, and can stimulate the bacteria to degrade those contaminants in soil (Khan *et al.*, 2013).

Rhizospheric microbial communities can in turn benefit the host plant by improving their growth under contaminant-stress conditions. Bacterial mechanisms that enhance plant growth include the production of plant growth regulators and hormones (such as indoleacetic acid (IAA), cytokinins or other

auxins); the suppression of stress ethylene production through the synthesis of 1-aminocyclopropane-1-carboxylic acid deaminase (ACCD); or other mechanisms such as the release of essential nutrients and the induction of plant defence mechanisms (Becerra-Castro *et al.*, 2013; McGuiness and Dowling, 2009; Weyens *et al.*, 2009a; Weyens *et al.*, 2009b). On the other hand, plants get further benefits from their bacteria possessing hydrocarbon-degrading potential, since these can lead to an enhanced hydrocarbon mineralization and lower both the phytotoxicity and evapotranspiration of volatile hydrocarbons (Khan *et al.*, 2013).

In addition to bacterial inoculants, the selection of the plant is also a crucial step in rhizoremediation. Yellow lupine (*Lupinus luteus*) was selected for this study since it is a leguminous plant, with a fast growth rate and high root and shoot biomass production. These characteristics make lupine an adequate plant for this type of phytoremediation procedure (Barac *et al.*, 2004; Gutiérrez-Ginés *et al.*, 2014; Weyens *et al.*, 2010).

The overall success of the rhizoremediation process will hinge on several critical factors, such as achieving a proper development of the plant, a decrease in contaminant phytotoxicity and stress, and an increase in contaminant bioavailability (Vangronsveld *et al.*, 2009; Weyens *et al.*, 2010). In addition, dealing with specific soil properties and conditions will also be vital, since these will have a significant impact on the fate of petroleum products and on their bioavailability to the degrading microorganisms (Afzal *et al.*, 2011; Fine *et al.*, 1997).

The aim of the present work was to enhance diesel degradation in the *Lupinus luteus* rhizosphere, by means of inoculation with selected bacterial strains which showed a diesel degrading ability and plant growth promotion capacity. To do this, we performed a screening assay to select those plant-growth promoting (PGP) bacterial strains with the best positive effect on lupine root growth. The best diesel degrading strain was also selected on the basis of previous results

(Chapter 9). Finally, a pot experiment, under greenhouse conditions, was performed with *L. luteus* growing in two artificially diesel-contaminated soils (1.25-1.50%, *w*/*w*), with different organic matter contents and inoculated with the most promising bacterial strains.

MATERIALS AND METHODS

Soil samples

Samples of A and B horizon from an alumi-umbric Cambisol profile (A_{Camb} and B_{Camb}) collected in the surroundings of Santiago de Compostela (Galicia, NW Spain) were used for the pot experiment. Soils were acid (pH in H_2O, 4.9-5.1), and showed low cation exchange capacity (ECEC < 2 cmol(+) Kg^{-1}) and sandy loam texture. The main difference was their organic matter content (4.2 % in soil A_{Camb} compared to < 0.5 % in soil B_{Camb}).

Soil samples were air-dried, sieved through a 2 mm mesh and conserved in plastic containers at room temperature until use. Prior to the spiking process, soil samples were mixed with sand at a 1:1 ratio (sand/soil).

Soil samples were spiked with diesel purchased in a local gasoline station. A suitable amount of fuel was added to the soil and then it was properly mixed until reaching homogeneity. The spiked soils were kept in closed recipients and stabilized at 4°C for at least 2 weeks before setting up the pots.

Perlite pot experiment for PGP bacterial strain selection

Several strains with plant growth promoting (PGP) characteristics were used to inoculate yellow lupine grown in perlite substrate, in order to select those strain/s with the best positive effect on plant development, for later application in consortium with the diesel degrading strain.

Strains ER33, ER50 and RP92 were previously isolated from *Cytisus striatus* growing in a lindane contaminated soil (Porriño, Spain) (Becerra-Castro *et al.*, 2011). Both ER33 and ER50 are root endophytes and RP92 was isolated from the rhizoplane of this plant species (Becerra-Castro *et al.*, 2011). Strains 12, 105 and 255 were isolated from hybrid poplar (*Populus deltoides* x (*trichocarpa x deltoides*) cv. Grimminge) which were planted in a diesel-contaminated soil (Genk, Belgium). Strain 12 was isolated from the rhizosphere soil and strain 105 is a root endophyte of this species. Strain 255 is a soil bacterial strain which was isolated from the same diesel-contaminated site. These strains were provided by the Centre for Environmental Sciences (CMK) of the University of Hasselt (Belgium). Table 10.1 summarizes the most important PGP characteristics, as well as the results of the diesel tolerance test.

Table 10.1. Plant growth promoting characteristics (Becerra-Castro *et al.*, 2011; CMK University Hasselt, Belgium) and diesel tolerance of bacterial strains.

Isolate		Sd [a]	P [b]	IAA [c]	Diesel tolerance [d]
ER33	*Bradyrhizobium japonicum*	-	-	+	5%
ER50	*Rhiobium pisi*	-	+	+	10%
RP92	*Streptomyces costariarus*	+	-	+	10%
12	*Pseudomonas* sp.		+	+	5%
105	*Pantoea agglomerans*		+	+	10%
255	*Bacillus licheniformis*		+	-	10%

[a] Sd, siderophore-producer; [b] P, P-solubiliser; [c] IAA, indoleacetic acid-producer.
[d] Strains were cultivated in 5 mL of 869 medium (1:10 dilution) with 0, 1.25, 2.5, 5 and 10% (v/v) diesel, for 1-2 days, at 27 ºC, 150 rpm. Maximum concentration of diesel (%, v/v), that lead to non significant differences with the 0% control, concerning OD_{680nm} and CFU count.

Seeds of lupine were surface-sterilized with 1% NaClO + Tween 80 (10 min) and rinsed in sterile tap water. Polypropylene pots were filled in quadruplicate with perlite, and three lupine seeds were placed in the substrate, at 1 cm depth. To prepare the bacterial inoculants, fresh cultures of the strains were cultivated in 869 medium at 30 °C (Mergeay *et al.,* 1985) for 1-2 days, harvested by

centrifugation (3000 rpm, 15 min) and re-suspended in 10 mM $MgSO_4$ to an optical density of 1.0 at 660 nm (OD_{660nm}) (about 10^6 CFU per mL). In addition to the strains alone (ER33, ER50, RP92, 12, 105 and 255), consortia of 2 strains were also tested: ER33+ER50, ER33+RP92, ER33+12, ER33+105, ER33+255, ER50+RP92, ER50+12, ER50+105, ER50+255, RP92+12, RP92+105, RP92+255, 12+105, 12+255 and 105+255. Pots were inoculated with 100 mL of a 1:10 dilution of the inoculants in half-strength Hoagland nutrient solution. In the case of combinations of two PGP strains, 5 mL of each bacterial suspension were added to the nutrient solution. Non-inoculated control pots were also prepared, and watered with 10 mM $MgSO_4$ 1:10 diluted with half-strength Hoagland solution. The first inoculation was carried out when setting up the pots with the seeds, and the second inoculation was carried out after one week, when germination and early development of seedlings was observed in all pots. During the experiment, pots were watered with 100 mL of half-strength Hoagland solution. Plants were grown under greenhouse conditions for 30 days. At harvest, root and shoot fresh weight and elongation were determined. The plant material was oven-dried at 45 °C, to determine dry biomass.

Pot experiment design and inoculation of lupine plants

A_{Camb} and B_{Camb} samples were spiked with diesel, at 1.25-1.5 % (*w*/*w*). This concentration was selected according to a range-finding test (RFT) carried out with the same soils contaminated with diesel at 0.625, 1.25, 2.5, 5, 10% (*w*/*w*). (data not shown). The spiking concentration used was the lowest which induced a significant effect on plant growth with respect to uncontaminated controls (root and shoot growth were reduced by 30 and 50% compared to control plants).

Polypropylene pots were filled, with approximately 300 g of spiked or uncontaminated soil (*n=6*). One-week-old lupine seedlings were transferred to each pot, and left to stabilize for 1 week before inoculation.

Three bacterial treatments were prepared: diesel degrading strain 26 (D) (selected from Chapter 9), PGP consortium, RP92+105 (PGP), and the combination of both the degrading strain and the PGP consortium (D+PGP). The PGP consortium (RP92+105) was selected on the basis of the screening assay for its positive influence on the growth of lupine. The consortium inoculants contained equal volumes of each culture. To prepare the bacterial inoculants, fresh cultures of the strains were cultivated in 869 medium (1:5 dilution) (Mergeay *et al.*, 1985) at 30 °C and 150 rpm for 1-2 days, harvested by centrifugation (3000 rpm, 10 min) and washed twice and re-suspended in 10 mM $MgSO_4$ to an OD_{660nm}=1.0 (about 10^6 CFU per mL). Plants were inoculated with 10 mL of each inoculant (*n=6*), which was added directly to the pots around the seedlings. Non-inoculated (NI) control pots were also prepared, and watered with 10 mL of 10 mM $MgSO_4$. The first inoculation was carried out 1 week after setting up the pots with the seedlings (t=0), and the second inoculation was carried out 2 weeks after the first inoculation (t=14). At this point the inoculant was added around the base of the plant stem. Plants were grown under greenhouse conditions for 30 days after the first inoculation (t=30).

At end of the experiment roots and shoots were separated, washed in deionised water, and fresh weight and elongation were determined. The plant material was oven-dried at 45 °C, to determine dry biomass, used for discussion.

During harvest, a sample of rhizosphere soil was taken from selected pots to determine bacterial densities (*n=3*). Soil was agitated for 1 h with a 1% solution of sodium hexametaphosphate (HMP) (ratio 1:10, soil/HMP). 100 µL of serial ten-fold dilutions were plated in 1:10 diluted 869 agar medium. After 7

days of incubation at 28 °C, colony forming units (CFU) were counted and calculated per gram of dry soil.

An attempt to recover the inoculated bacterial strains was made. On the one hand, 1 g of contaminated A_{Camb} and B_{Camb}, inoculated with 26 degrader, was incubated in BH2 medium with 1 g L^{-1} of filter-sterilized diesel (*n=6*), for 7 days, at 30 °C and 150 rpm. This minimal medium, with diesel as the sole carbon source, is selective for the diesel degrading strain 26. BH2 mineral medium contains (g L^{-1}): K_2HPO_4, 1.32; KH_2PO_4, 1; NH_4Cl, 0.81; $NaNO_3$, 0.84; $FeSO_4 \cdot 7H_2O$ 0.01; $MgSO_4 \cdot 7H_2O$, 0.42 (Bushnell and Haas, 1941). One g of contaminated A_{Camb} and B_{Camb}, inoculated with PGP, was incubated with 1:10 diluted 869 medium supplemented with 2 mM Zn, for 7 days, at 30 °C and 150 rpm. This medium is selective to RP92 strain, which is Zn-tolerant (Becerra-Castro *et al.*, 2011). After incubation, serial dilutions were plated in 1:10 diluted 869 agar plates, and BOX-PCR profiling was used to confirm the identity of the strains, following the methods of Becerra-Castro *et al.* (2011).

Determination of total and water-extractable fractions of diesel in soil

A sample of approximately 3 g of rhizosphere soil was taken from NI, D, PGP and D+PGP selected pots (*n=3*) at three different times: t=0, before the first inoculation; t=14 days, before the second inoculation; and t=30 days, at harvest. Samples were stored frozen until analysis.

The extraction of diesel range organics (DRO, alkanes from C_{10} to C_{25}) from soil was performed in an accelerated solvent extractor (ASE, Dionex). NI, D, and D+PGP soil samples were selected, in order to estimate the dissipation by degradation of the 26 strain. For this, 1 g of soil was mixed with diatomaceous earth at 1:2 (diatomaceous earth/soil) and quartz sand, until completely filling 11 mL-stainless steel cells. Samples were extracted with hexane, at 100 °C, 2000 psi, for 5 min, for 2 extraction cycles (Chapter 4). The DRO easily available fraction

was estimated with a water extraction of NI, D, PGP and D+PGP soil samples, to study the effect of bacterial inoculants on water-soluble DRO fraction. For this, 1 g of soil was agitated with 5 mL of Milli-Q water for 24 h. The supranatant resulting from centrifugation at 2700 rpm for 20 min, was ultrasonically extracted with hexane (1:2, sample/hexane), for 1 h (Chapter 4). Trace water in hexane extracts was eliminated with anhydrous sodium sulphate.

The total and available soil concentration of diesel was determined by analyzing extracts by gas chromatography (Model 450 GC, Agilent Technologies) coupled to mass spectrometry (Model 220 MS, Agilent Technologies) (GC/MS). Before analysis, a mix of deuterated internal standards, containing 1,4-dichlorobenzene-d_4, acenaphthene-d_{10}, chrysene-d_{12}, naphthalene-d_8, perylene-d_{12} and phenanthrene-d_{10} (Internal Standards Mix 33, Dr. Ehrenstorfer), was added to the extracts at 0.2 mg L^{-1} as a constant concentration. Calibration of DRO was carried out with a standard containing a mixture of C_{10}-C_{25} *n*-alkanes (DRO mix, Dr. Ehrenstorfer). The calibration standards were prepared in hexane, at several concentrations: 0.1, 0.5, 1.0, 2.5, 5, 7.5 and 10.0 mg L^{-1}. Internal standards were also added in the same concentration as for the samples (0.2 mg L^{-1}). Chromatographic separations were performed by a FactorFour VF-5ms EZ-Guard capillary column (30 m x 0.25 mm x 0.25 µm; Agilent Technologies) that operated with the following oven temperature program: 40 °C (held for 10 min) to 300 °C, at 10 °C min^{-1}. Helium was used as carrier gas, at constant flow 1 mL min^{-1}. The injector was operated with a temperature ramp from 60 °C to 300 °C (held for 35 min), at 200 °C min^{-1}, and samples (1 µL for soil extracts and 2.5 µL for water extracts) were injected in split/splitless mode. The mass spectrometer operated in full scan mode. Ionization of the molecules was carried out by electron impact (EI) and the ion trap temperature was fixed at 220 °C (Chapter 4).

Statistical analysis

Univariate ANOVA was performed to assess the significant differences between inoculation treatments or contaminant concentrations, for each variable growth (shoot and root, elongation and biomass), in PGP screening experiment and in the phytoremediation pot experiment.

3-way ANOVA test was performed to determine the influence of different factors (soil, contaminant concentration and inoculum) on plant growth parameters (elongation and biomass).

RESULTS

Selection of PGP bacterial strains

Inoculation of lupine in perlite substrates with different plant growth promoting (PGP) strains (Figure 10.1), generally showed a very significant improvement in plant development, and this was especially pronounced in shoots. The increase in root biomass was only significant after inoculation with RP92+12, RP92+105 and 12+105. Shoot elongation increased by 50% compared to non-inoculated (NI) controls when inoculated with RP92+105, 12+105 and 12+255 consortia and root elongation (although not being always significant) increased by 30% compared to control when treated with the RP92+105 inoculation. Shoot biomass reached an 80% increase compared to the NI control after inoculation with RP92+105 and 12+105, and root biomass reached a 50% increase compared to NI control after inoculation with RP92+105 and 12+105.

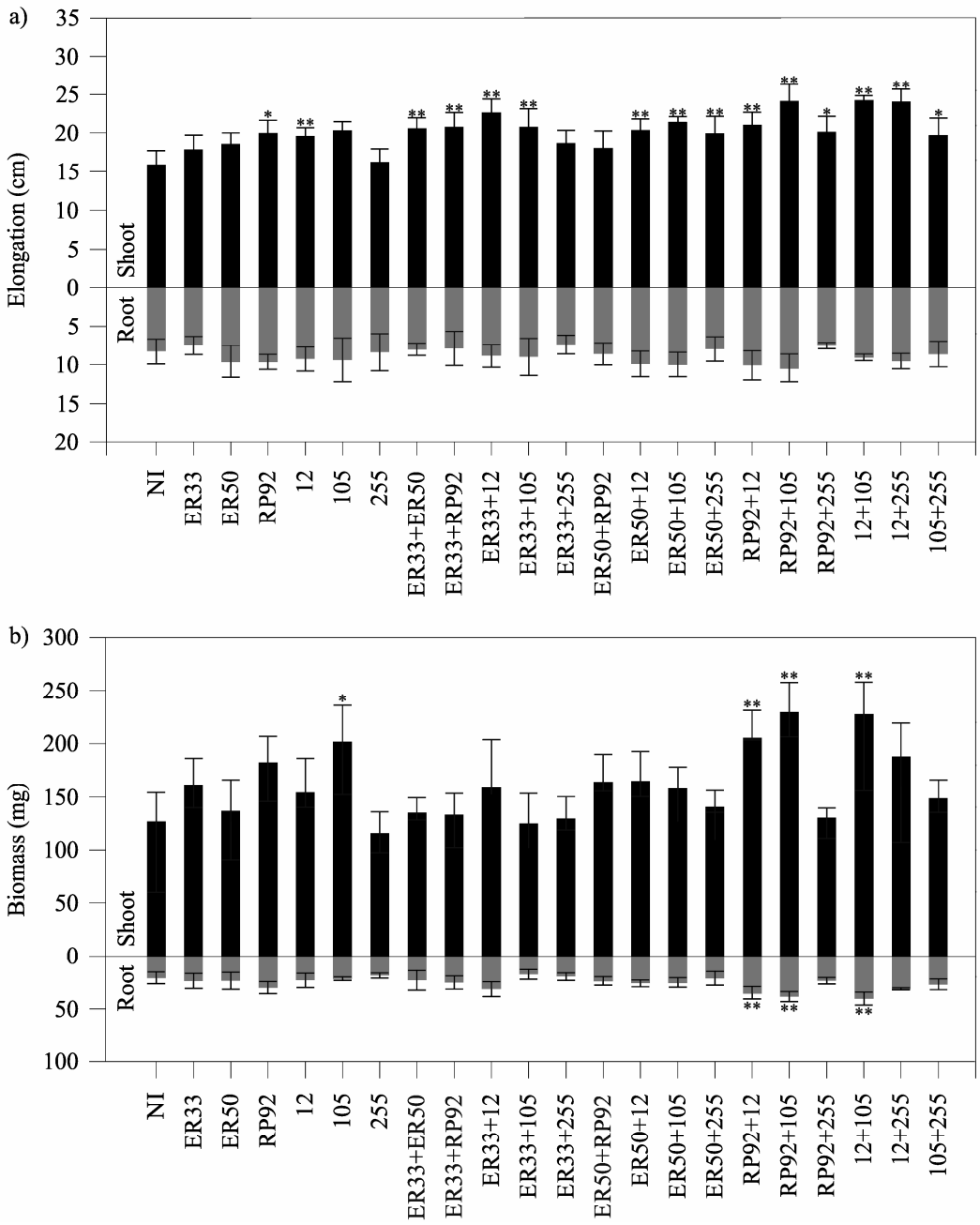

Figure 10.1. Shoot and root elongation(a) and biomass (b) of lupine growing on perlite substrate and inoculated with different PGP strains, individually or in combinations. Significant differences with the control are indicated with asterisks: * $p<0.05$ and ** $p<0.01$.

Bacterial consortia generally had more positive effect on plant growth than individual bacterial strains. For example, RP92 provoked a significant (p<0.05) increase of 25% in shoot elongation with respect to the NI control. However, when this strain was combined with strain 105, the bacterial-induced increase in shoot elongation reached 50%. Strain 105 also provoked a significant increase (p<0.05) of 60% in shoot biomass, but when in combination with strain RP92 this increase was up to 80% compared to the NI control (Figure 10.1).

Figure 10.2. Example of plants grown on non-inoculated and RP92+105 inoculated perlite.

On the basis of these results, the best combination of bacterial strains which improved all lupine growth parameters was the consortium RP92+105. Therefore, this combination was used for inoculation of the diesel-contaminated soils in the pot experiment, in order to improve lupine growth and development

under contaminant stress conditions. Figure 10.2 shows a photograph comparing the growth of plants in NI control perlite and those inoculated with RP92+105.

Plant growth in the pot greenhouse experiment

Figures 10.3 and 10.4 show the lupine growth (elongation and biomass) in contaminated and uncontaminated A_{Camb} and B_{Camb}, respectively, non-inoculated (NI) and inoculated with the degrader strain (D), plant growth promoting strains (PGP) and the combination of both (D+PGP).

After 5 weeks (1 week of stabilization + 4 weeks after inoculation), plants grown in uncontaminated and NI A_{Camb} reached a mean shoot height and root length of 24.7 and 22.1 cm, respectively, and shoot and root biomass of 330.6 and 142.8 mg, respectively (Figure 10.3). Plants grown in uncontaminated and NI B_{Camb} control reached similar values of elongation to those in A_{Camb} control (25.9 and 21.6 cm of shoot height and root length, respectively), but produced a lower biomass (234.7 and 133.2 mg shoot and root biomass, respectively), although differences between the two soils were not statistically significant (Figure 10.4).

Results of the 3-way ANOVA test (Table 10.2) indicated that shoot elongation and root biomass were significantly influenced by all three factors and their combinations: bacterial inocula (non-inoculated, D, PGP and D+PGP), soil (A_{Camb} and B_{Camb}), and contaminant concentration (contaminated or uncontaminated).

The exposure of non-inoculated (NI) plants to diesel had a significant effect ($p<0.05$) on plant growth, in both soils, and this was especially pronounced for the roots. In contaminated A_{Camb}, root biomass was reduced by 85%, with respect to uncontaminated NI soil (Figure 10.3b), and in contaminated B_{Camb}, root biomass was reduced by 73% (Figure 10.4b).

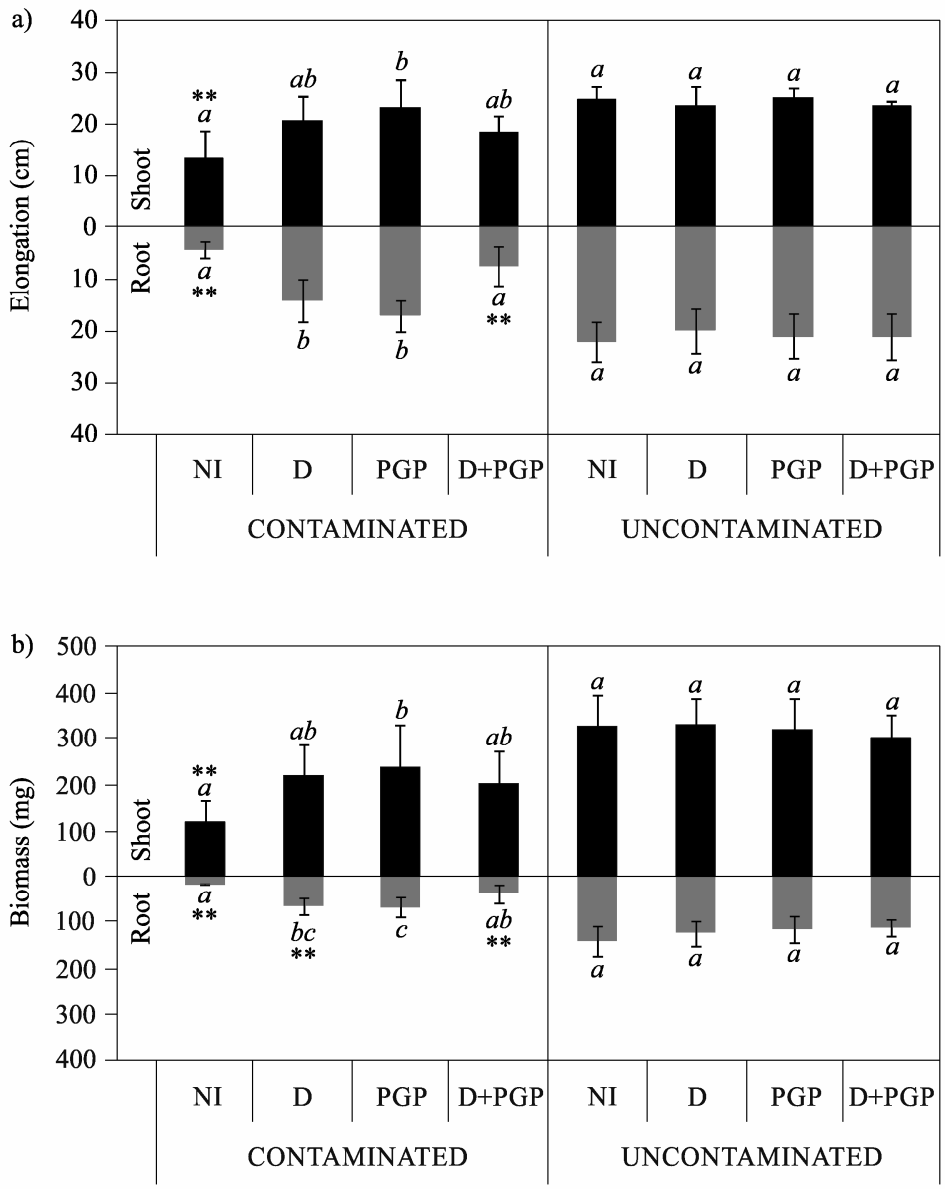

Figure 10.3. Shoot and root elongation (a) and biomass (b) of lupine grown on diesel-contaminated and uncontaminated A_{Camb}, non-inoculated and inoculated with the degrader strain (D), plant growth promoting strains (PGP) and the consortium of both (D+PGP) (n=6). Bars with different letters indicate significant differences in each plant part for contaminated or uncontaminated soil (p<0.05). Significant differences with the same inoculation treatment in uncontaminated soil are indicated with asterisks: * p<0.05 and ** p<0.01.

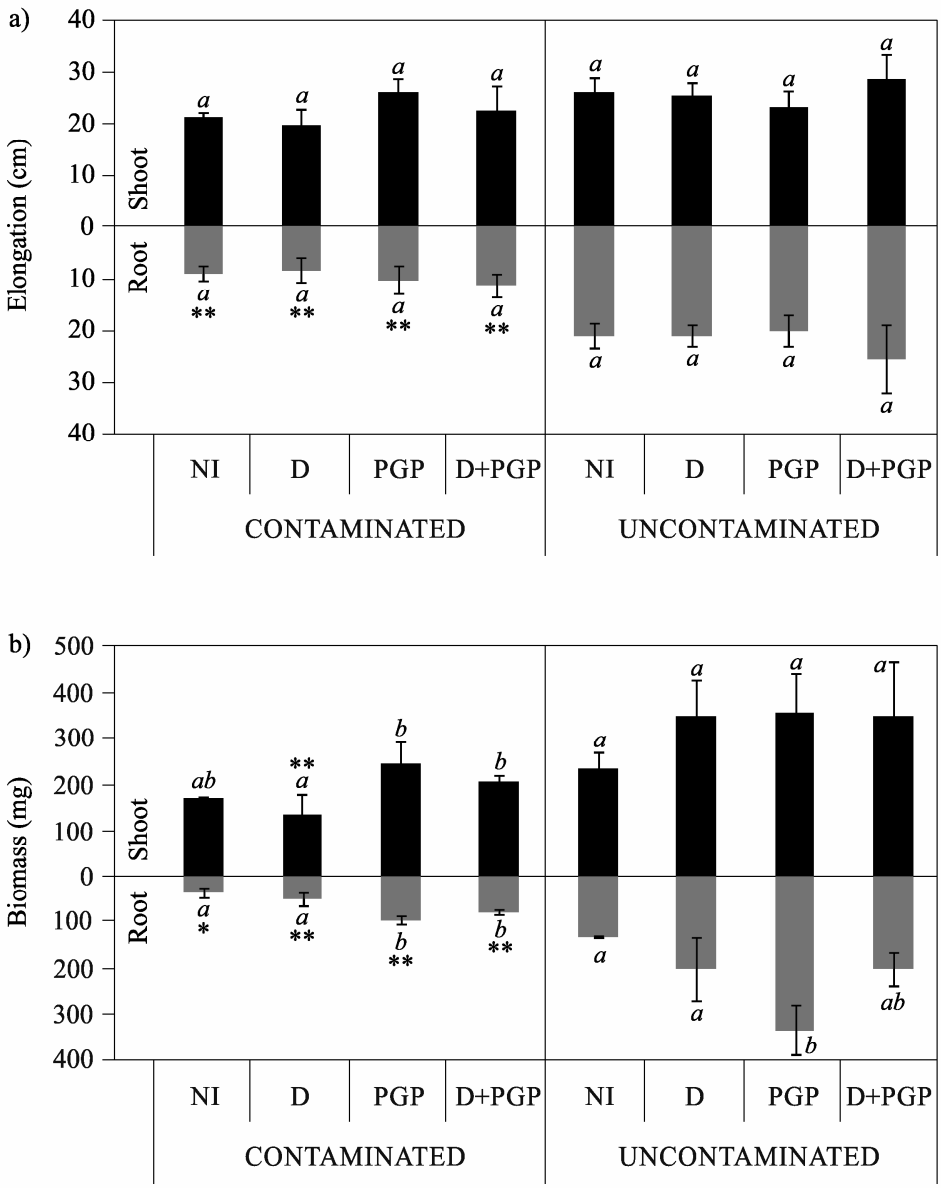

Figure 10.4. Shoot and root elongation (a) and biomass (b) of lupine grown on diesel-contaminated and uncontaminated B_{Camb}, non-inoculated (NI) and inoculated with the degrader strain (D), plant growth promoting strains (PGP) and the consortium of both (D+PGP) (*n=6*). Bars with different letters indicate significant differences in each plant part for contaminated or uncontaminated soil ($p<0.05$). Significant differences with the same inoculation treatment in uncontaminated soil respective with asterisks: * $p<0.05$ and ** $p<0.01$.

Table 10.2. Effects of soil type, bacterial inoculum and diesel concentration (contaminated or uncontaminated) on growth parameters of yellow lupine (3-way ANOVA test).

Factor	Growth feature	df	MS	F
Inoculum	**Shoot elongation**	3	58.05	6.06**
	Root elongation	3	19.39	1.56
	Shoot biomass	3	0.02	5.48**
	Root biomass	3	0.01	12.43**
Soil	**Shoot elongation**	1	72.72	7.59**
	Root elongation	1	1.23	0.10
	Shoot biomass	1	0.00	0.57
	Root biomass	1	0.04	44.30**
Concentration	**Shoot elongation**	1	167.83	17.52**
	Root elongation	1	1654.90	132.79**
	Shoot biomass	1	0.28	82.08**
	Root biomass	1	0.15	161.37**
Inoculum * Soil	**Shoot elongation**	3	34.30	3.58*
	Root elongation	3	39.87	3.20*
	Shoot biomass	3	0.01	2.58
	Root biomass	3	0.01	8.88**
Inoculum * Concentration	**Shoot elongation**	3	51.73	5.40**
	Root elongation	3	58.41	4.69**
	Shoot biomass	3	0.01	1.77
	Root biomass	3	0.00	1.42
Soil * Concentration	**Shoot elongation**	1	2.08	0.22
	Root elongation	1	21.50	1.73
	Shoot biomass	1	0.00	1.20
	Root biomass	1	0.02	26.47**
Inoculum * Soil * Concentration	**Shoot elongation**	3	28.18	2.94*
	Root elongation	3	42.48	3.41*
	Shoot biomass	3	0.01	3.65*
	Root biomass	3	0.01	7.37**

** $p<0.05$; **$p<0.01$.*

The inoculation of plants grown in A_{Camb} and B_{Camb} with the different bacterial strains/combinations (D, PGP and D+PGP), did not have a significant influence on plant development in uncontaminated soils, except the PGP inoculant which

increased the root biomass of plants grown in uncontaminated B_{Camb} (Figure 10.4b). In contrast, in contaminated soils, the different inoculation treatments had varying effects which depended on the soil.

In contaminated A_{Camb}, inoculation with D, PGP or D+PGP had a positive effect on lupine shoot growth (elongation and biomass, figures 10.3a and 10.3b, respectively). Inoculated plants presented a higher shoot height and higher biomass than in the NI contaminated control (only statistically significant in PGP treatment). This positive effect of inoculants over NI contaminated soil controls was also appreciated for root elongation and biomass, being again statistically significant in PGP treatment (Figures 10.3a and Figure 10.3b). The root of plants growing on contaminated A_{Camb} was more affected by contamination than shoot, and especially root biomass, since statistically significant differences with the respective treatments in uncontaminated A_{Camb} were found for D and D+PGP treatments.

In contaminated B_{Camb}, inoculants did not show a significant effect on shoot elongation and biomass over NI contaminated controls (Figures 10.4a and 10.4b). The consortium of the degrader and the PGP (D+PGP), and the PGP individually, provoked a significantly improvement in root biomass (Figure 10.4b), compared to the NI control or the D treatment ($p<0.05$). As in A_{Camb}, roots were highly affected by diesel contamination and significant differences with the corresponding inoculant in the uncontaminated B_{Camb} were found in all inoculation treatments, for both root elongation and biomass (Figures 10.4a and 10.4b).

Densities of culturable bacteria and recovery of inocula

Bacterial densities in contaminated A_{Camb} were an order of magnitude higher (ranging from 1.26 to 2.47 x 10^8 CFU g^{-1} of soil) than in B_{Camb} (ranging from 4.29 to 8.84 x 10^7 CFU g^{-1} of soil) (Table 10.3). Contaminated soils presented higher

bacterial densities than respective uncontaminated soils. Bacterial densities in A_{Camb} varied from 1.26 to 2.47 x 10^8 CFU g^{-1} in the contaminated soil and from 3.41 to 5.27 x 10^7 CFU g^{-1} in the uncontaminated soil (with statistically significant differences between contaminated and uncontaminated soil; $p<0.05$). In B_{Camb}, bacterial densities varied from 4.29 to 8.84 x 10^7 CFU g^{-1}, in the presence of the contaminant, and from 2.58 and 6.10 x 10^7 CFU g^{-1}, in the absence of the contaminant (with no significant differences between contaminated and uncontaminated soil; $p=0.09$).

No significant differences were found in bacterial densities between the non-inoculated and inoculation treatments for any case (soil, contaminated or uncontaminated).

Unfortunately, none of the inoculated bacterial strains were successfully re-isolated and identified by BOX-PCR profiling.

Table 10.3. Colony forming units per gram dry weight rhizosphere soil for each inoculum (*n=3*).

	Soil	Inoculum	CFU g dry $soil^{-1}$
A_{Camb}	**Contaminated**	**NI**	1.26 ± 0.59 x 10^8
		D	1.98 ± 0.52 x 10^8
		PGP	2.47 ± 0.69 x 10^8
		D+PGP	1.46 ± 0.57 x 10^8
	Uncontaminated	**NI**	4.23 ± 0.18 x 10^7
		D	3.41 ± 0.97 x 10^7
		PGP	3.66 ± 0.14 x 10^7
		D+PGP	5.27 ± 0.60 x 10^7
B_{Camb}	**Contaminated**	**NI**	4.29 ± 0.03 x 10^7
		D	4.84 ± 0.32 x 10^7
		PGP	4.30 ± 0.16 x 10^7
		D+PGP	8.84 ± 3.56 x 10^7
	Uncontaminated	**NI**	2.66 ± 0.37 x 10^7
		D	6.10 ± 1.76 x 10^7
		PGP	2.58 ± 0.21 x 10^7
		D+PGP	4.34 ± 0.56 x 10^7

Diesel range organics (DRO) concentration in soil

Concentrations of 16 individual diesel range organics (DRO, *n*-alkanes from C_{10}, decane to C_{25}, pentacosane) in rhizosphere soil were determined in selected pots of NI, D and D+PGP treatments, in contaminated A_{Camb} and B_{Camb} (*n=3*), at three different times: t=0, before first inoculation, t=14 days, before second inoculation, and t=30 days, at the end of the experiment. The analysed soil of t=0 of each pot was used as the respective initial concentrations (Table 10.4).

Table 10.4. Initial concentrations of DRO (mg Kg^{-1}) of contaminated A_{Camb} (a) and B_{Camb} (b) before first inoculation (t=0). Results are expressed as the mean of sampled soil pots ± standard deviation (*n=3*).

a)

	NI	D	D+PGP
C_{10}	11.6 ± 2.7	16.2 ± 1.5	14.5 ± 4.9
C_{11}	24.8 ± 5.4	29.6 ± 16.0	30.5 ± 8.2
C_{12}	32.5 ± 5.7	43.4 ± 11.5	39.9 ± 6.8
C_{13}	38.4 ± 4.6	54.3 ± 9.5	47.4 ± 6.7
C_{14}	43.4 ± 1.3	53.8 ± 11.7	55.9 ± 2.2
C_{15}	67.2 ± 4.5	78.3 ± 21.4	82.4 ± 5.2
C_{16}	59.3 ± 5.9	68.6 ± 21.5	72.2 ± 5.3
C_{17}	72.4 ± 6.3	81.6 ± 22.3	85.1 ± 3.7
C_{18}	58.4 ± 5.1	68.0 ± 16.0	67.9 ± 5.7
C_{19}	25.8 ± 2.5	29.5 ± 1.9	29.3 ± 3.1
C_{20}	19.8 ± 2.6	24.7 ± 0.5	25.1 ± 3.0
C_{21}	16.6 ± 2.9	20.8 ± 0.9	19.4 ± 3.1
C_{22}	12.0 ± 2.5	15.7 ± 0.4	13.9 ± 3.1
C_{23}	7.3 ± 1.7	11.5 ± 1.3	9.0 ± 3.2
C_{24}	5.1 ± 1.5	8.8 ± 0.6	6.7 ± 1.6
C_{25}	2.1 ± 0.5	4.3 ± 1.2	2.4 ± 1.4
∑DRO	496.9 ± 55.5	608.9 ± 138.2	601.7 ± 67.1

Table 10.4. (Continuation).

b)

	NI	D	D+PGP
C_{10}	28.9 ± 19.3	36.0 ± 5.3	22.4 ± 3.7
C_{11}	48.0 ± 25.7	55.6 ± 5.7	39.6 ± 4.6
C_{12}	58.5 ± 32.1	65.1 ± 4.9	49.9 ± 4.2
C_{13}	67.2 ± 40.4	73.0 ± 6.0	56.6 ± 5.3
C_{14}	76.1 ± 40.2	71.9 ± 4.0	57.9 ± 5.7
C_{15}	108.7 ± 55.0	101.4 ± 9.5	82.4 ± 9.1
C_{16}	97.0 ± 47.1	87.3 ± 5.1	73.3 ± 8.6
C_{17}	117.1 ± 52.4	102.7 ± 7.8	84.7 ± 8.2
C_{18}	88.4 ± 41.7	78.7 ± 9.5	65.9 ± 7.5
C_{19}	30.0 ± 7.6	32.2 ± 5.2	27.9 ± 3.2
C_{20}	25.4 ± 6.5	25.4 ± 3.5	22.7 ± 2.7
C_{21}	18.9 ± 6.0	20.5 ± 1.1	18.4 ± 2.4
C_{22}	12.6 ± 4.9	15.7 ± 0.8	12.7 ± 1.2
C_{23}	7.8 ± 1.1	9.8 ± 0.4	8.7 ± 1.3
C_{24}	5.7 ± 1.8	7.0 ± 0.8	6.0 ± 0.4
C_{25}	1.4 ± 0.7	2.8 ± 0.6	1.6 ± 0.8
∑DRO	791.6 ± 382.4	784.8 ± 70.2	630.8 ± 68.7

The initial concentration in A_{Camb} of the sum of 16 DRO (∑DRO) varied from 496.9 to 608.9 mg Kg^{-1} (Table 10.4a), and from 630.8 to 791.6 mg Kg^{-1} in B_{Camb} (Table 10.4b). The highest concentrations of individual DRO were found for the C_{14}-C_{18} range, and the lowest were those of the extreme DRO, C_{10} and C_{25}.

The percentage of ΣDRO dissipated and/or degraded in A_{Camb} and B_{Camb} non-inoculated (NI) and inoculated with those treatments including the degrader strain (D and D+PGP) was calculated on the basis of soil analysis data obtained at t=14 and t=30, with respect to the t=0 data (Figures 10.5 and 10.6). Furthermore, dissipation results were presented according to the DRO compounds (distinguishing C_{10} to C_{14}, C_{15} to C_{18}, and C_{19} to C_{25}). These groups were discriminated with a principal components analysis (PCA), performed with

the results of the DRO analysis and physicochemical properties of the individual alkanes (data not shown).

The percentage of DRO lost in non-inoculated (NI) soils increased with time: at t=14 DRO dissipation was less than 10%, while at t=30 dissipation reached 20-30% in both soils (Figures 10.5a and 10.6a). This dissipation can be associated with the loss of contaminants by evaporation, photodegradation, degradation by indigenous bacteria (soils were not autoclaved), and many other processes.

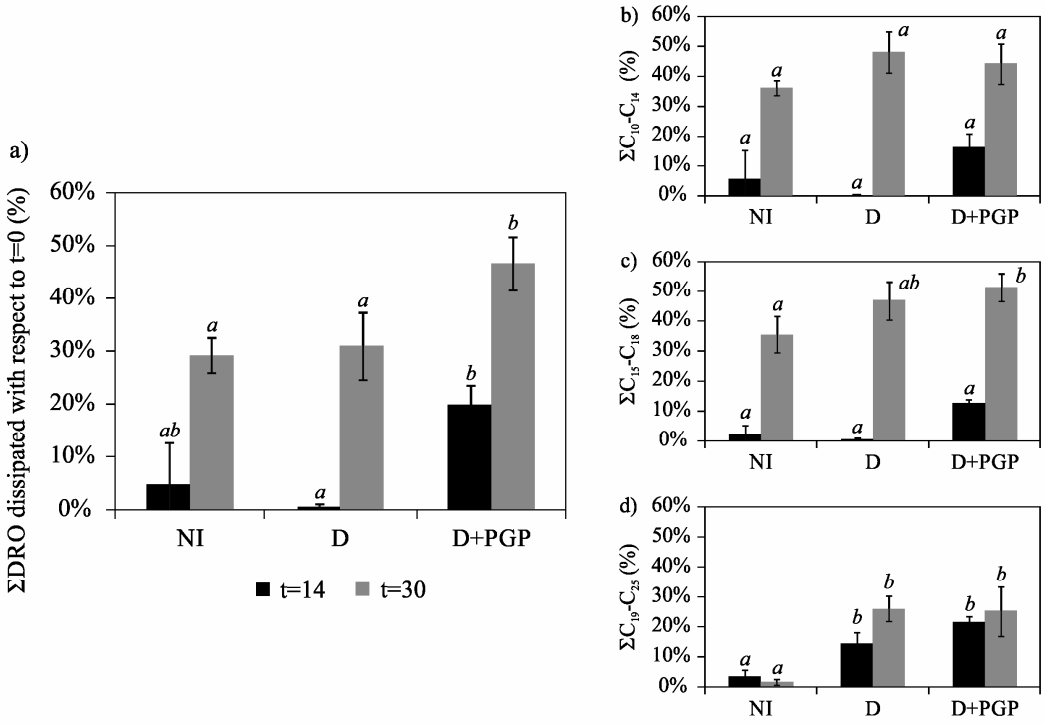

Figure 10.5. Percentage of ∑DRO (a), $\sum C_{10}$-C_{14} (b), $\sum C_{15}$-C_{18} (c) and $\sum C_{19}$-C_{25} (d) dissipated from A_{Camb} at t=14 and t=30. Percentages were calculated from the respective t=0 concentration of each DRO sum (*n=3*). Bars with different letters indicate significant differences at each time, t=14 or t=30 (p<0.05).

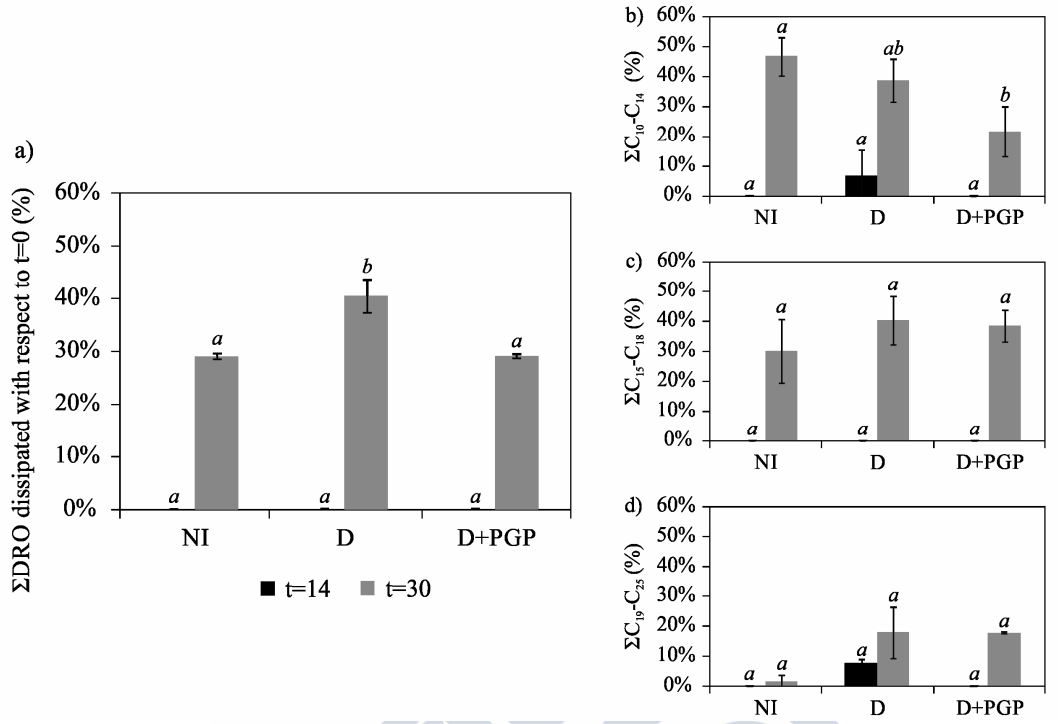

Figure 10.6. Percentage of ∑DRO (a), $\sum C_{10}$-C_{14} (b), $\sum C_{15}$-C_{18} (c) and $\sum C_{19}$-C_{25} (d) dissipated from B_{Camb} at t=14 and t=30. Percentages were calculated from the respective t=0 concentration of each DRO sum (*n=3*). Bars with different letters indicate significant differences at each time, t=14 or t=30 ($p<0.05$).

DRO dissipation in soils with the D and D+PGP inoculants could be explained by the same reasons, but in addition to these, the dissipation is likely to be related to degradation by the inoculated degrader strain, as well as the positive effect of the PGP strain on both the plant and the degrader itself. When the difference between % DRO dissipation between the NI and D, or the NI and D+PGP inoculated soils was significant ($p<0.05$), it was considered that rhizodegradation was efficiently taking place in these treatments.

In A_{Camb} (Figure 10.5a), ΣDRO dissipation in the presence of the degrader and the PGP strains (D+PGP) at t=30 was significantly higher than NI control (DRO dissipation was close to 15-20% higher in the D+PGP treatment); at t=14,

dissipation was comparable, but the difference between the D+PGP and the NI treatment was close to reaching statistical significance (p=0.059).

In B_{Camb} (Figure 10.6a), the inoculation of the PGP strain together with the degrader (D+PGP) did not have the same significant effect on DRO dissipation as was observed for A_{Camb}. In this case, the best degradation rates were obtained for the individual inoculation with the degrader (D): significant differences between ΣDRO dissipation in the D treatment and NI treatment were found (DRO dissipation was close to 10% higher in the D treatment).

In the case of the three groups of DRO (Figures 10.5 and 10.6 b, c and d, C_{10} to C_{14}, C_{15} to C_{18} and C_{19} to C_{25}, respectively), the highest losses were found for $\sum C_{10}$-C_{14} in the NI pots, and the lowest losses were found for $\sum C_{19}$-C_{25} in NI pots, in both soils. In A_{Camb}, at t=30, in addition to what was lost in NI pots a further 25% of $\sum C_{19}$-C_{25} were lost in D and D+PGP treatments, while only 15% of $\sum C_{10}$-C_{14} and $\sum C_{15}$-C_{18} was additionally lost. In B_{Camb}, at t=30, in addition to NI pots losses a further 20% of $\sum C_{19}$-C_{25} was lost in D and D+PGP treatments, while only 10% of $\sum C_{15}$-C_{18} was additionally lost.

Water extractable DRO fraction: bioavailability approach

Figure 10.7 shows the amount of ΣDRO in soil that was extracted with water. These values can give an idea of the fraction of DRO in soil which is readily available to microorganisms for degradation. In general, the water-solubilized DRO fraction was very low at t=0 and t=14 (about 20 mg Kg^{-1}), but this fraction increased at t=30 in all treatments (NI, D, PGP and D+PGP) and reached approximately 40-80 mg Kg^{-1} (generally, t=30 data were situated over 1:10 water/soil concentration ratio). This indicates that plant development and root activity influences DRO solubility, and therefore its bioavailability.

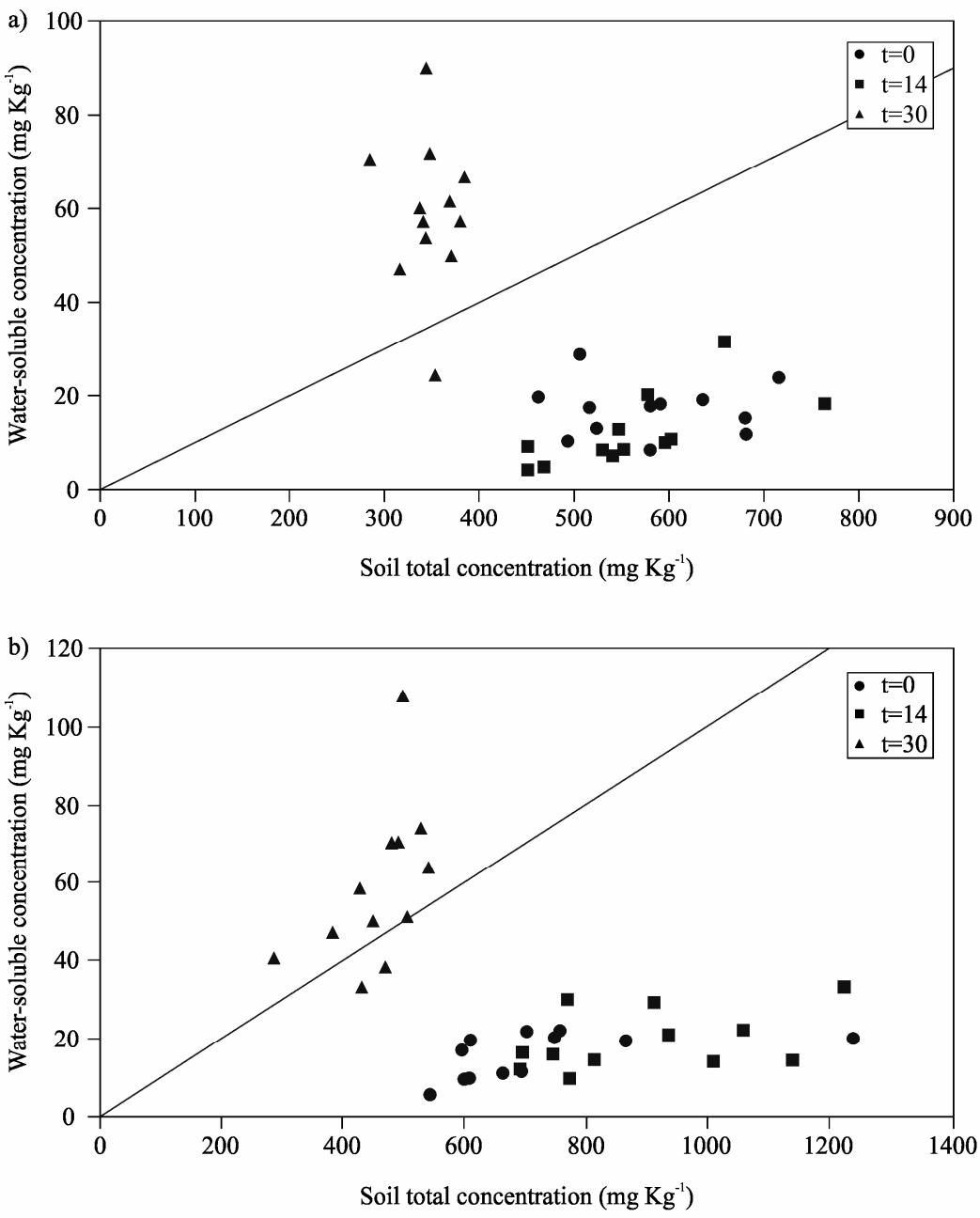

Figure 10.7. Amount of ∑DRO (C_{10}-C_{25}) solubilized in water extracts from soil with respect to the total present in the respective soil, A_{Camb} (a) and B_{Camb} (b), at t=0, t=14 and t=30 days. 1:10 water/soil concentration ratio line was represented in the figures.

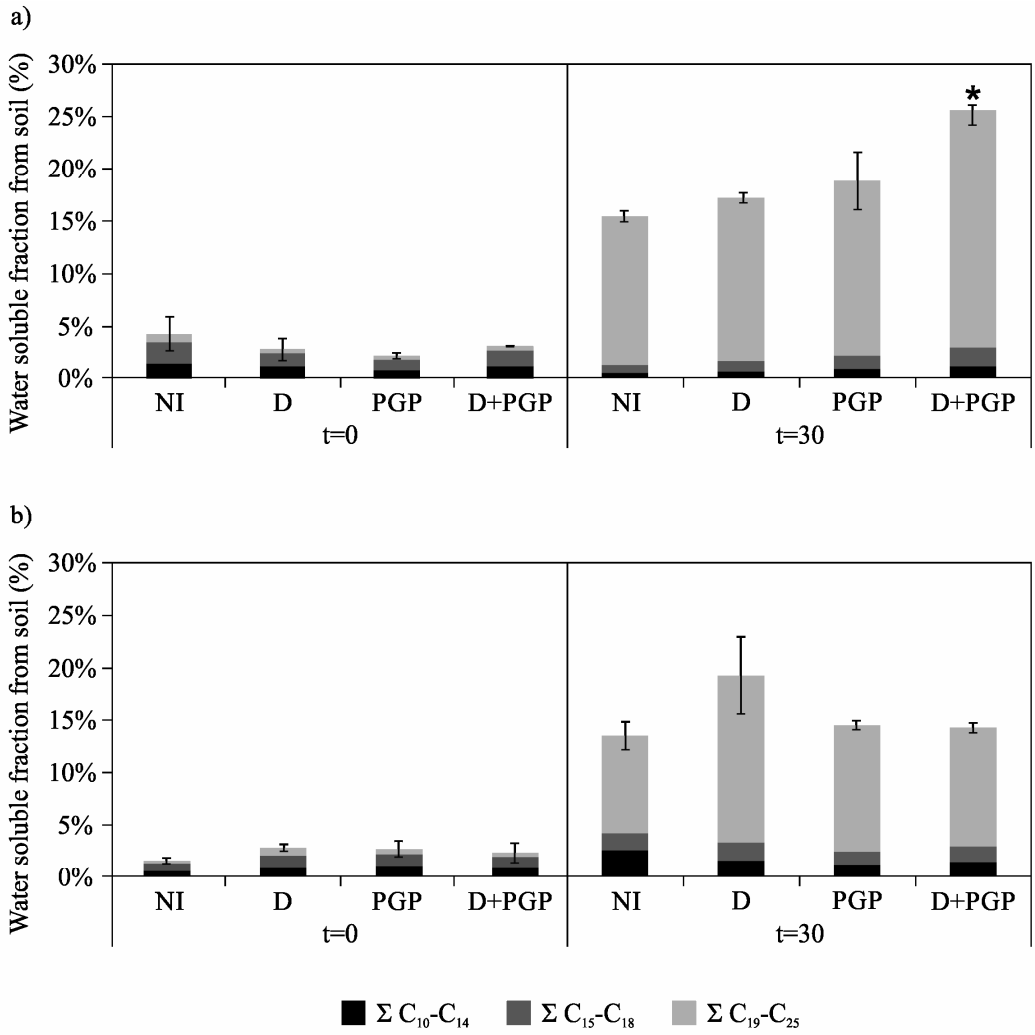

Figure 10.8. Water soluble fraction of DRO (as a percentage of the total concentration) in planted A_{Camb} (a) and B_{Camb} (b) at t=0, before any inoculation treatment, and at t=30 (*n=3*). The contributions of each group of DRO (C_{10}-C_{14}, C_{15}-C_{18}, and C_{19}-C_{25}) to ∑DRO are detailed in grey scale. Significant differences of ∑DRO (C_{10}-C_{25}) soluble fraction with the NI controls are indicated with an asterisk (p<0.05).

The inoculant treatments (D, PGP and D+PGP) provoked an increase in the water-soluble fraction, which was additional to that already observed in NI soils (Figure 10.8). In planted A_{Camb}, this increase was significant (p<0.05) with the D+PGP inoculation, showing a 10% increase in bioavailability compared to the NI soil. In planted B_{Camb}, the inoculation of the degrader (D) provoked an increase in

bioavailability of close to 5% more than that observed in the NI soil, but this was not statistically significant (p=0.170).

The group of DRO which suffered the highest increase in solubility (Figure 10.8) coincided with those which present the lowest water solubility of all the 16 alkanes analyzed, that is the group C_{19} to C_{25} (Appendix B). For the remaining DRO groups, the solubility did not suffer a significant increase with time or inoculation treatment (from t=0 to t=30).

DISCUSSION

Diesel has been shown to be phytotoxic to a wide variety of plants, as already concluded in Chapter 6 of this thesis, and reported by many authors (Adam and Duncan, 2002; Kirk *et al.*, 2002; Luhach and Chaudhry, 2012). Indeed, in this experiment lupine growth in non-inoculated (NI) contaminated A_{Camb} and B_{Camb} was significantly lower than in NI uncontaminated soils, and this was especially pronounced in root growth.

Therefore, selecting diesel-tolerant plants (Barrutia *et al.*, 2011) with an extensive root system (Khan *et al.*, 2013) is crucial for the success of the rhizoremediation process, since this will in turn influence plant performance, bacterial colonization and rhizodegradation efficiency (Afzal *et al.*, 2011; Wenzel, 2009). Yellow lupine (*Lupinus luteus*) is a leguminous plant with a deep and branched root system that has already been used in the rhizoremediation of various organic compounds (Barac *et al.*, 2004; Gutiérrez-Ginés *et al.*, 2014; Weyens *et al.*, 2010). Lupine presented a moderate diesel tolerance in the preliminary range-finding test (RFT), since the plants did not show significant symptoms of phytotoxicity, and there was no mortality until 2.5-5% (*w*/*w*) of diesel (data not shown). In Chapter 8, we also observed some diesel-tolerant plant species with potential characteristics to be used in phytoremediation: pea

and maize did not show high phytotoxicity or mortality until 5-10% (*w*/*w*) of diesel. Several authors also reported other tolerant species to be used in diesel-contaminated soils phytoremediation: poplar (*Populus* sp.), grew in 1% (*w*/*w*) diesel-contaminated soil (Tesar *et al.*, 2002); rapeseeds (*Brassica napus*), in 0.6% (*w*/*w*) (Wojtera-Kwiczor *et al.*, 2014); and bulrush (*Scirpus triqueter*), common reed (*Phragmites australis*), or "arrow head" (*Sagittaria sagittifolia*), in 2% (*w*/*w*) (Zhang *et al.*, 2013).

Although found to be diesel-tolerant, the presence of diesel in soil was still phytotoxic and provoked a poorer root development of the lupine. The phytotoxicity of contaminants is often more extreme in the root growth since the roots are in direct contact with the contaminant. For these reasons, the plants were inoculated with plant-growth promoting (PGP) rhizobacteria, which have been previously shown to decrease plant stress and improve root development under such contamination conditions (Lugtenberg and Kamilova, 2009). In this study, lupine root biomass was significantly improved with the inoculation of the PGP strain in the contaminated A_{Camb} (p<0.05), and reached a similar biomass as that recorded in the same treatment in uncontaminated soil. This improvement in root development is a vital parameter within the rhizoremediation system. On the other hand, in this soil the consortium of D+PGP did not have a significant effect with respect to NI control on root growth. However, in B_{Camb} both these inoculant treatments, PGP and D+PGP, significantly increased root length and biomass with respect to NI contaminated controls (p<0.05), although root growth did not reach a comparable root biomass as that obtained in uncontaminated soils. This indicated that in B_{Camb} the phytotoxic effect of diesel on root growth could not be fully mitigated in the presence of the PGP bacterial inoculant, as was observed in A_{Camb}.

This negative effect of diesel on plants growing in B_{Camb}, was also observed In Chapter 8. We concluded that A_{Camb} organic matter provoked a protective effect

over plants by adsorbing organic contaminants, and decreasing the phytotoxicity of diesel. A similar effect was observed in HCH-contaminated soils by Calvelo Pereira *et al.* (2010). However, this was not the case in B_{Camb} since this soil practically lacks organic matter. It is clear, that soil properties will not only affect contaminant phytotoxicity, but also plant growth and development.

Contaminated A_{Camb} and B_{Camb} showed higher bacterial densities than uncontaminated soils, regardless of the inoculant. This was especially significant in A_{Camb}, in which microbial activity increased by an order of magnitude in the presence of diesel. After a spill in soil, a new substrate becomes available to microorganisms (Siddiqui and Adams, 2002), and therefore microbial counts can substantially increase in the presence of the contaminant. On the other hand, diesel likely had a strong negative effect on soil microbial diversity and reduced the density of many protozoal, fungal and bacterial soil inhabitants. The increase in CFU detected was probably also related with the survival and proliferation of fast growing cultivable bacteria, which may have taken advantage of the abundant labile C from microbial biomass released after diesel addition. Wang and Bartha (1990) reported that bacterial population increased 100-fold in diesel-contaminated soil with lime and nutrients compared with diesel-contaminated soil with no nutrients. Therefore, the highest bacterial activity in contaminated A_{Camb} with regard to contaminated B_{Camb}, can be explained by the better conditions (nutrients, organic matter, moisture) which could have led to bacterial proliferation.

Diesel dissipation which was attributed to degradation by the degrader strain in both D and D+PGP treatments, reached around 10-20% of ΣDRO. In A_{Camb}, the highest degradation rates were obtained with the consortium D+PGP (more than 15% of diesel was degraded at t=14 and t=30), and in B_{Camb}, the degrader strain on its own (D) led to a higher loss of diesel than the combination treatment (more than 10% of diesel was degraded). Wojtera-Kwiczor *et al.*

(2014) used rapeseed and a petroleum-degrading consortium, and they removed 75-85% of diesel spiked in soil (at 6,000 mg Kg^{-1}) after eight weeks of experiment. Zhang *et al.* (2010) obtained a petroleum degradation of up to 28-67% (in soils contaminated with 10% (*w/w)* total petroleum hydrocarbons), using *Phabitis nil* and its microbial community, after 127 days of incubation. Zhang *et al.* (2013) reported an elimination of 76-80% of diesel (at 15,000 mg Kg^{-1} diesel) in estuary wetland after 60 days, in the presence of *Scirpus triqueter*, *Phragmites australis* and *Sagittaria sagittifolia* with an oil-degrading bacterium. Higher degradation rates were therefore obtained by these authors compared to the present study, but it should also be noted that those experiments were performed over a longer period of time.

The inoculation treatments in which the highest degradation rates obtained in A_{Camb} and B_{Camb} (D+PGP and D, respectively) did not correspond with the inoculants which caused the best root biomass development in A_{Camb} and B_{Camb} (D and D+PGP, respectively). However, they coincided with those treatments which induced the highest increase in water-soluble DRO concentrations at t=30. Hence, the slight differences between root growth in the different inoculation treatments did not have such a significant effect on bacterial performance as the contaminant bioavailability increase, jointly influenced by the activity of both the plant and the bacterial strains.

Although an attempt to recover the inoculated bacterial strains was made, unfortunately, none of them were successfully re-isolated. Therefore, it would be essential to work on methods for tracking the inoculants, that can help to compare the survival of the strains in different soils and treatments and to better understanding the interactions in the plant-soil-microorganism system.

Water-extractable DRO gives an estimation of the most readily-available or accessible fraction in the soil. It is generally perceived that microbes can only take up what is extractable via the aqueous phase, but they can also access other

fractions which are more strongly retained, and therefore other more exhaustive extractions processes could also be performed to predict contaminant bioavailability (Reid *et al.*, 2000).

The presence of the plant itself (at t=30) increased DRO bioavailability. It is well known that plant exudates can improve contaminant bioavailability since they can contain lipophilic substances which can increase hydrocarbon solubility, thus making them more available for microbes (Martin *et al.*, 2014). Under stress conditions, lupine excretes a high proportion of carboxylic acids in root exudates (Neumann and Römheld, 1999). In a previous study (Balseiro-Romero *et al.*, 2014), we also concluded that carboxylic acids increased the mobility of volatile hydrocarbons, regardless of the soil characteristics. This bioavailability increase was only appreciated at t=30, since the root system was more developed than at t=14, and therefore root exudation was higher. The increase in bioavailability of C_{19}-C_{25} alkanes coincided with higher degradation rates of these compounds compared to C_{10}-C_{14} and C_{15}-C_{18}, in both rhizosphere soils.

The diesel-degrading strain showed a high degrading capacity when assessed *in vitro* (Chapter 9) (80-90% of ΣDRO present in the liquid media were degraded). However, in soil, the contaminant availability is lower due to soil-contaminant interactions and a lower rate of degradation is therefore to be expected (Afzal *et al.*, 2011). The degrader strain used in this experiment was selected for its high degradation capacity, but also because it was shown to be an effective producer of biosurfactants. Biosurfactants can exert some influences on hydrocarbon-water interfaces, and can make them more mobile and, therefore, more available for bioremediation (Bordoloi and Konwar, 2009). Therefore, apart from the effect of plant root exudates on DRO bioavailability at t=30, the biosurfactants produced by the degrader strain could also be contributing to the increase in DRO bioavailability.

CONCLUSIONS

The dissipation of DRO from non-inoculated contaminated soils planted with *Lupinus luteus* reached the 30% of the initial concentration, being the lowest molecular weight hydrocarbons, those with the highest dissipation rate. The inoculation of soils with the degrader strain enhanced the DRO dissipation, and the best results showed between 45-50% of DRO lost from soil, or 15-20% in addition to NI control (obtained for A_{Camb} inoculated with D+PGP bacterial consortium). The degradation rate was especially significant for the highest molecular weight DRO, directly related to the solubility increase favoured by plant root exudation, in addition to bacterial biosurfactants excreted by the degrader strain.

The association of *Lupinus luteus* with the degrader strain and the PGP strains resulted in a good combination for application in the rhizoremediation of diesel-contaminated soils, with a moderate diesel contamination (up to 1.5%, *w*/*w*), and with an organic matter content similar to an umbric A horizon (42.6 g C Kg^{-1}). In very low concentrations of organic matter (soils type B horizon), the association lupine + degrader strain, without PGP, produced better results.

On the basis of this study, further investigations should be carried out in order to improve rhizoremediation of diesel and in general, hydrocarbon-contaminated soils: (i) evaluate the viability of the used plant-bacteria association in real contaminated soils (not spiked); (ii) identify plant species with potential use in rhizoremediation, i.e. tolerant to a wider range of diesel concentrations and with a more extensive root system; (iii) isolate new hydrocarbon-degrading and PGP strains, in order to establish other plant-bacteria associations with good results in remediation of different types of soils; and (iv) characterize the genotype of the collection of strains assayed.

REFERENCES

Adam G, Duncan H. 2002. Influence of diesel fuel on seed germination. Environ Pollut 120:363-370.

Afzal M, Yousaf S, Reichenauer TG, Kuffner M, Sessitsch A. 2011. Soil type affects plant colonization, activity and catabolic gene expression of inoculated bacterial strains during phytoremediation of diesel. J Hazard Mater 186:1568-1575.

Balseiro-Romero M, Kidd PS, Monterroso C. 2014. Influence of plant root exudates on the mobility of fuel volatile compounds in contaminated soils. Int J Phytorem 16:824-839.

Barac T, Taghavi S, Borremans B, Provoost A, Oeyen L, Colpaert JV, Vangronsveld J, van der Lelie D. 2004. Engineered endophytic bacteria improve phytoremediation of water-soluble, volatile, organic pollutants. Nat Biotech 22:583-588.

Barrutia O, Garbisu C, Epelde L, Sampedro MC, Goicolea MA, Becerril JM. 2011. Plant tolerance to diesel minimizes its impact on soil microbial characteristics during rhizoremediation of diesel-contaminated soils. Sci Total Environ 409:4087-4093.

Becerra-Castro C, Kidd P, Prieto-Fernández Á, Weyens N, Acea M, Vangronsveld J. 2011. Endophytic and rhizoplane bacteria associated with *Cytisus striatus* growing on hexachlorocyclohexane-contaminated soil: isolation and characterisation. Plant Soil 340:413-433.

Becerra-Castro C, Kidd PS, Rodríguez-Garrido B, Monterroso C, Santos-Ucha P, Prieto-Fernández Á. 2013. Phytoremediation of hexachlorocyclohexane (HCH)-contaminated soils using *Cytisus striatus* and bacterial inoculants in soils with distinct organic matter content. Environ Pollut 178:202-210.

Bordoloi NK, Konwar BK. 2009. Bacterial biosurfactant in enhancing solubility and metabolism of petroleum hydrocarbons. J Hazard Mater 170:495-505.

Bushnell LD, Haas HF. 1941. The utilization of certain hydrocarbons by microorganisms. J Bacteriol 41:653-673.

Calvelo Pereira R, Monterroso C, Macías F. 2010. Phytotoxicity of hexachlorocyclohexane: Effect on germination and early growth of different plant species. Chemosphere 79:326-333.

Calvo de Anta R, Macías F, Rivero A. 1992. Aptitud agronómica de los suelos de la provincia de La Coruña. Diputación Provincial de A Coruña, A Coruña.

Das K, Mukherjee AK. 2007. Crude petroleum-oil biodegradation efficiency of *Bacillus subtilis* and *Pseudomonas aeruginosa* strains isolated from a petroleum-oil contaminated soil from North-East India. Bioresour Technol 98:1339-1345.

Fine P, Graber ER, Yaron B. 1997. Soil interactions with petroleum hydrocarbons: Abiotic processes. Soil Technol 10:133-153.

Gutiérrez-Ginés MJ, Hernández AJ, Pérez-Leblic MI, Pastor J, Vangronsveld J. 2014. Phytoremediation of soils co-contaminated by organic compounds and heavy metals: Bioassays with *Lupinus luteus* L. and associated endophytic bacteria. J Environ Manage 143:197-207.

Johnson JF, Allan DL, Vance CP, Weiblen G. 1999. Root carbon dioxide fixation by phosphorus-deficient *Lupinus albus* (Contribution to organic acid exudation by proteoid roots). Plant Phisiol 112:19-30.

Khan S, Afzal M, Iqbal S, Khan QM. 2013. Plant–bacteria partnerships for the remediation of hydrocarbon contaminated soils. Chemosphere 90:1317-1332.

Kirk JL, Klirnomos JN, Lee H, Trevors JT. 2002. Phytotoxicity assay to assess plant species for phytoremediation of petroleum-contaminated soil. Bioremediation J 6:57-63.

Kuiper I, Lagendijk EL, Bloemberg GV, Lugtenberg BJJ. 2004. Rhizoremediation: A beneficial plant-microbe interaction. Mol Plant-Microbe Interact 17:6-15.

Lugtenberg B, Kamilova F. 2009. Plant-Growth-Promoting rhizobacteria. Annu Rev Microbiol 63:541-556.

Luhach J, Chaudhry S. 2012. Effect of diesel fuel contamination on seed germination and growth of four agricultural crops. U J Environ Res Technol 2: 311-317.

MacKinnon G, Duncan HJ. 2013. Phytotoxicity of branched cyclohexanes found in the volatile fraction of diesel fuel on germination of selected grass species. Chemosphere 90:952-957.

Martin BC, George SJ, Price CA, Ryan MH, Tibbett M. 2014. The role of root exuded low molecular weight organic anions in facilitating petroleum hydrocarbon degradation: Current knowledge and future directions. Sci Total Environ 472:642-653.

McGuinness M, Dowling D. 2009. Plant-associated bacterial degradation of toxic organic compounds in soil. Int J Environ Res Public Health 6:2226-2247.

Mergeay M, Nies D, Schlegel HG, Gerits J, Charles P, Van Gijsegem F. 1985. *Alcaligenes eutrophus* CH34 is a facultative chemolithotroph with plasmid-bound resistance to heavy metals. J Bacteriol 162:328-334.

Neumann G, Römheld V. 1999. Root excretion of carboxylic acids and protons in phosphorus-deficient plants. Plant Soil 211:121-130.

Obayori OS, Adebusoye SA, Adewale AO, Oyetibo GO, Oluyemi OO, Amokun RA, Ilori MO. 2009. Differential degradation of crude oil (Bonny Light) by four *Pseudomonas* strains. J Environ Sci 21:243-248.

Reid BJ, Jones KC, Semple KT. 2000. Bioavailability of persistent organic pollutants in soils and sediments—a perspective on mechanisms, consequences and assessment. Environ Pollut 108:103-112.

Siddiqui S, Adams WA. 2002. The fate of diesel hydrocarbons in soils and their effect on the germination of perennial ryegrass. Environ Toxicol 17:49-62.

Tanase A, Ionescu R, Chiciudean I, Vassu T, Stoica I. 2013. Characterization of hydrocarbon-degrading bacterial strains isolated from oil-polluted soil. Int Biodeterior Biodegrad 84:150-154.

Tesar M, Reichenauer TG, Sessitsch A. 2002. Bacterial rhizosphere populations of black poplar and herbal plants to be used for phytoremediation of diesel fuel. Soil Biol Biochem 34:1883-1892.

Vangronsveld J, Herzig R, Weyens N, Boulet J, Adriaensen K, Ruttens A, Thewys T, Vassilev A, Meers E, Nehnevajova E, van der Lelie D, Mench M. 2009. Phytoremediation of contaminated soils and groundwater: lessons from the field. Environ Sci Pollut Res. 16:765-794.

Wang X, Bartha R. 1990. Effects of bioremediation on residues, activity and toxicity in soil contaminated by fuel spills. Soil Biol Biochem 22:501-505.

Wang Z, Xu Y, Zhao J, Li F, Gao D, Xing B. 2011. Remediation of petroleum contaminated soils through composting and rhizosphere degradation. J Hazard Mater 190:677-685.

Wenzel W. 2009. Rhizosphere processes and management in plant-assisted bioremediation (phytoremediation) of soils. Plant Soil 321:385-408.

Weyens N, van der Lelie D, Taghavi S, Newman L, Vangronsveld J. 2009a. Exploiting plant–microbe partnerships to improve biomass production and remediation. Trends Biotechnol 27:591-598.

Weyens N, van der Lelie D, Taghavi S, Vangronsveld J. 2009b. Phytoremediation: plant–endophyte partnerships take the challenge. Curr Opin Biotechnol 20:248-254.

Weyens N, Croes S, Dupae J, Newman L, van der Lelie D, Carleer R, Vangronsveld J. 2010. Endophytic bacteria improve phytoremediation of Ni and TCE co-contamination. Environ Pollut 158:2422-2427.

Wojtera-Kwiczor J, Żukowska W, Graj W, Małecka A, Piechalak A, Ciszewska L, Chrzanowski Ł, Lisiecki P, Komorowicz I, Barałkiewicz D, Voss I, Scheibe R, Tomaszewska B. 2014. Rhizoremediation of diesel-contaminated soil with two rapeseed varieties and petroleum degraders reveals different responses of the plant defense mechanisms. Int J Phytoremediation 16:770-789.

Zhang X, Wang Z, Liu X, Hu X, Liang X, Hu Y. 2013. Degradation of diesel pollutants in Huangpu-Yangtze River estuary wetland using plant-microbe systems. Int Biodeterior Biodegrad 76:71-75.

Zhang Z, Zhou Q, Peng S, Cai Z. 2010. Remediation of petroleum contaminated soils by joint action of *Pharbitis nil* L. and its microbial community. Sci Total Environ 408:5600-5605.

11

Final synthesis and conclusions

The optimal conditions for extracting and analysing fuel derived compounds, will highly depend on the characteristics of the contaminant, its concentration and the characteristics of the samples. Effective, sensitive and precise extraction and analysis methods were developed and optimized for the analysis of fuel organic compounds, volatiles (MTBE, ETBE and BTEX), and diesel range organics (C_{10}-C_{25} *n*-alkanes) (DRO), in environmental samples (water and soil samples with different organic matter content) in wide range of concentrations. Those methods resulted adequate to be used in a real contamination episode for its risk evaluation, monitorization or to make decisions about the appropriate protection of the contaminated site. They were the base for efficiently performing the studies included in this thesis.

The characterization and fingerprinting of the hydrocarbon levels in a real contamination episode around a fuel distribution station in Tomiño (NW Spain) allowed us to identify and characterize the age of the spill (due to the detection

of MTBE in groundwater, not detected in current fuels), the continuity of the spill (due to the presence of volatiles in soil and groundwater samples) and the location of the spill (by discriminating the samples with several hydrocarbon indices and principal component analysis).

The study of sorption-desorption processes by the HS analysis-approach, in a closed *in vitro* environment, allowed to comparatively assess the sorption of fuel volatile compounds (MTBE, ETBE and BTEX) in dissimilar soils and soil components. This study reflected the importance of soil organic matter in the permanence of BTEX in soil, especially of the most apolar (ethylbenzene and/or xylene) and discriminated the sorption by soil mineral components as a slower and weaker mechanism. Sorption can also influence the evaporation of volatiles from soils, which can affect to remediation techniques such as soil vapour extraction. With the HS approach, we concluded that soils with organic matter would need higher temperatures to reach an acceptable evaporation rate, especially of BTEX, while soils without organic matter would require lower temperatures, due to the weaker sorption strength. The HS analysis approach proposed resulted in a simple and rapid method for obtaining very useful data that contribute to understanding the behaviour of fuel volatile compounds in a great variety of scenarios and to establishing the bases for optimizing soil remediation techniques.

Plant root exudates substantially modified the mobility of fuel volatile compounds in soils, widely depending on soil characteristics and on exudates composition. In general, in the absence or very low content of organic matter, root exudates reduced the mobility of MTBE, ETBE and BTEX, and in a high concentration of organic matter, they increased the mobility, due to the solubilisation of soil organic matter components. Individual root exudate components had different effects according to their chemical properties and

concentration. Therefore, the net effect of exudates would be specific in each soil-plant system and would even change throughout plant growth.

Contamination of soils with common car fuels (gasoline and diesel) provoked a decrease in germination, survival and early growth of several crop plant species. Diesel resulted more toxic than gasoline, principally due to a physical stress (water repellence) in addition to a chemical stress. Gasoline weathering (principally due to evaporation) during the experiment decreased its phytotoxicity. Fuel preferably affected the root, with regard to the shoot, and the biomass, with regard to elongation, affecting root branching. Regarding rhizoremediation, where a good root development is required, it would be essential to select fuel tolerant species, with the minimum negative effects on root, and/or to select bacterial inoculants with plant growth promotion properties.

In order to develop an efficient rhizoremediation procedure assisted with bacteria for cleaning up diesel-contaminated soils, we first selected bacterial strains with diesel-degrading or with plant growth promoting (PGP) abilities. The best strains were inoculated to *Lupinus luteus*, a leguminous plant with a rapid growth and a moderate diesel tolerance. The selected diesel-degrading strain had positive results for biosurfactant production and biofilm formation in the presence of hydrocarbons, and presented a DRO degradation rate of 90% in liquid medium (10 days-incubation). PGP strains selected from greenhouse pot experiment in perlite substrate, increased *Lupinus luteus* shoot biomass in 80% with respect to non-inoculated controls. The inoculation of *Lupinus luteus* with the bacterial consortium of the degrader and the PGP strains obtained promising results in a greenhouse pot experiment with diesel-contaminated soils with different organic matter content: after one month, close to 50% of DRO was dissipated in the presence of the degrader, corresponding to a 15-20% enhancement of DRO losses with regard to non-inoculated soils. Furthermore,

the degradation rates were directly related with an increase in DRO bioavailability, due to the effect of root exudates and bacterial biosurfactants.

In conclusion, the present thesis helped to understand the behaviour of the most mobile fractions of fuel (oxygenates and monoaromates) and thoroughly developed a procedure for the rhizoremediation of diesel (a less mobile fraction) in contaminated soils.

Appendix

Physicochemical properties of VOC and DRO

USC
UNIVERSIDADE
DE SANTIAGO
DE COMPOSTELA

A. Volatile organic compounds (VOC)

	Benzene [a]	Toluene [a]	Ethyl-benzene [a]	o-Xylene [a]	m-Xylene [a]	p-Xylene [a]	MTBE [a,b]	ETBE [b]
Formula	C_6H_6	C_7H_8	C_8H_{10}	C_8H_{10}	C_8H_{10}	C_8H_{10}	$C_5H_{12}O$	$C_6H_{14}O$
Molecular weight ($g\ mol^{-1}$)	78.11	91.14	106.17	106.17	106.17	106.17	88.15	102.18
Melting point (°C)	5.9	-95.0	-95.0	-25.2	-47.8	13.2	-108.6	-94.0
Boiling point (°C)	80.1	110.6	136.2	144.5	139.1	138.4	55.0	69.0
Density ($g\ cm^{-3}$, 20°C)	0.8765	0.8669	0.8670	0.8802	0.8842	0.8611	0.7578	0.7450
Water solubility ($g\ L^{-1}$, 25°C)	1.80	0.47	0.14	0.20	0.17	0.20	51.6	26.0
log K_{ow}	2.16	2.69	3.15	3.15	3.20	3.15	1.06	1.48
log K_{oc}	1.92	2.39	1.98	2.35	2.11	2.52	1.05	1.57
Vapour pressure (Pa, 25°C)	12654	3786	1546	767	833	787	31156	28000
Henry's law constant ($Pa\ m^3\ mol^{-1}$, 25 °C)	576	474	559	542	731	762	59	166

[a] *Mackay et al.* 2006. Handbook of physical-chemical properties and environmental fate for organic chemicals. CRC Press, Boca Raton.
[b] *EFOA Website www.efoa.eu*

B. Diesel range organics (DRO)

DRO	Formula	Molecular weight (g mol^{-1})	Melting point (°C)	Boiling point (°C)	Density (g cm^{-3})
Decane (C_{10})	$C_{10}H_{22}$	142.29	−29.7	174.1	0.7300
Undecane (C_{11})	$C_{11}H_{24}$	156.31	−25.6	195.9	0.7402
Dodecane (C_{12})	$C_{12}H_{26}$	170.34	−9.6	216.3	0.7487
Tridecane (C_{13})	$C_{13}H_{28}$	184.37	−5.4	235.4	0.7562
Tetradecane (C_{14})	$C_{14}H_{30}$	198.39	5.9	253.5	0.7627
Pentadecane (C_{15})	$C_{15}H_{32}$	212.42	9.9	270.6	0.7683
Hexadecane (C_{16})	$C_{16}H_{34}$	226.45	18.2	286.8	0.7734
Heptadecane (C_{17})	$C_{17}H_{36}$	240.47	21	302.0	0.7770
Octadecane (C_{18})	$C_{18}H_{38}$	254.50	28–30	317.0	0.7770
Nonadecane (C_{19})	$C_{19}H_{40}$	268.53	32–34	330.0	0.7860
Eicosane (C_{20})	$C_{20}H_{42}$	282.55	36.7	342.7	0.7886
Heneicosane (C_{21})	$C_{21}H_{44}$	296.58	40.5	356.5	0.7920
Docosane (C_{22})	$C_{22}H_{46}$	310.61	42	224.0	0.7780
Tricosane (C_{23})	$C_{23}H_{48}$	324.63	48–50	380.0	0.7970
Tetracosane (C_{24})	$C_{24}H_{50}$	338.66	52	391.3	0.7970
Pentacosane (C_{25})	$C_{25}H_{52}$	352.69	54	401.0	0.8010

Griesbaum et al. 2000. Hydrocarbons. In: Ullmann's Encyclopaedia of Industrial Chemistry. Wiley-VCH.

DRO range	Water solubility (mg L^{-1})	Vapour pressure (Pa)	Henry's law constant (cm^3 cm^{-3})	log K_{oc}
C_{10}-C_{12}	0.0340000	63.8	120	5.4
C_{13}-C_{16}	0.0007600	4.9	520	6.7
C_{17}-C_{21}	0.0000013	0.1	4900	8.8

GSI Chemical properties database (http://www.gsi-net.com/en/publications/gsi-chemical-database.html)

USC
UNIVERSIDADE
DE SANTIAGO
DE COMPOSTELA

USC
UNIVERSIDADE
DE SANTIAGO
DE COMPOSTELA

AGRADECIMIENTOS

En primer lugar quiero agradecer a Carmela su confianza desde el primer momento, hace ya unos cuantos años, cuando empecé el proyecto de máster. Gracias por tu amistad, apoyo y tantas horas de ayuda, y sobre todo por creer en que podía hacerlo, que siempre me dio fuerzas para luchar por ello.

Al profesor Felipe Macías, por su apoyo como coordinador del doctorado y del grupo de investigación. Gracias por confiar en las líneas de trabajo y por darnos la oportunidad de colaborar contigo.

A Petra, por darme la oportunidad de colaborar contigo y por tu ayuda en temas que se escapaban de mis conocimientos. Gracias a toda la gente del CSIC (Ángeles, Marian, Mariana, Vanessa, Bea, Cristina, María, Maribel), gracias por toda vuestra ayuda en el tema de micro, y el tiempo que perdisteis enseñándome. Pero sobre todo por hacerme sentir tan cómoda con vosotras.

I want to thank Dr. Jaco Vangronsveld, to give me the opportunity to work in his lab, and for his help and dedication. I especially want to thank Panos Gkorezis for all his help and orientation in my experiments in Hasselt, and also for your patience. To Nele Weyens, for her unconditional help in my first months at the University, and to all my lab and university colleagues, especially Arek. I really found a good friend in you.

Gracias a mis compañeros del Instituto y del departamento: Raquel, Paula, Patricia, Maca, Ramón, Darío, Ruth, Diego, Elena, Tere, Carmen, Adriana, Raiana... Por todos los buenos momentos, dentro y fuera del laboratorio. Por esto realmente echaré de menos mi etapa de tesis.

A mis amigos de Vigo y Santiago, por todos los momentos de desconexión, sobre todo en la etapa de redacción ermitaña. Y mil gracias a la gran pintora Natalia Mallo por su dibujo para la portada. A la gente de Ingeniería Química, con los que empecé en esto de la Investigación, y con quien pasé y paso muy buenos momentos.

Por supuesto quiero agradecer a mi familia. A mis padres, por las fuerzas que siempre me da que estéis orgullosos de mi, que vayáis presumiendo de hija diciendo que "es científica" y trabaja "limpando a terra contaminada". No se puede desear una familia mejor, ni más unida que la nuestra (aún estando un poco separados). Vuestro "exceso" de preocupación por mi futuro, mi bienestar, mi felicidad, estoy segura que me llevó a ser así, y a hacer todo lo que hice. Nunca dejasteis de apoyarme en todas mis decisiones, y con vosotros se me hace menos complicado pensar en la nueva etapa que se me viene ahora encima. A mi hermano. No me cansaré de decir que eres mi modelo a seguir desde que era una enana, que la persona que soy es mucho por culpa tuya o gracias a ti. Papá siempre dice que no sabe cómo le salieron dos hijos tan iguales, pero eso a mí me enorgullece y siempre me alegra saber que me parezco a mi hermano mayor, por poco que sea.

Y por último, pero no menos importante, a ti que siempre me ayudaste en los malos momentos, cuando nadie más que tú sabía que los estaba pasando. Por tu forma de hacerme reír, por tu optimismo y calma contagiosa. No podemos ser más iguales, ni tampoco más diferentes, pero eso hace que todo funcione con la precisión de un reloj suizo. Gracias por transmitirme siempre la ilusión de vivir el momento.

"Pero esa es otra historia y debe ser contada en otra ocasión"

M. Ende

Investigación financiada por:

Consellería de Innovación e Industria de la Xunta de Galicia
(INCITE08PXIB200136PR)

Ministerio de Ciencia e Innovación y FEDER
(CTM2009-14576-C02-01 y CTM2009-14576-C02-02).

Beca de **Formación de Personal Investigador** (FPI) concedida a **María Balseiro Romero** por el Ministerio de Ciencia en Innovación en 2010 hasta 2014 (Referencia: BES-2010-030923).

The contamination of soil with petroleum derived products is an environmental problem with a considerable concern, since it involves important risks for human health and for the ecosystems. Therefore, it is essential to study the behaviour and dynamics of the fuel contaminants in the soil system and to develop effective remediation procedures to protect it from degradation.

For this purpose, analytical methods were developed, and applied to the characterization of the hydrocarbon contamination around fuel distribution station. Sorption of volatile organic compounds was studied in different soils and soil components, and the effect of root exudates on their mobility was characterized. Toxicity of diesel and gasoline was evaluated with crop plants bioassays and the development of a phytoremediation procedure, assisted with diesel-degrading and plant growth promoting bacteria, was optimized in soils with different organic matter content.

USC
UNIVERSIDADE
DE SANTIAGO
DE COMPOSTELA

Programa de Doctorado
Medio Ambiente y Recursos Naturales

Portada: Dibujo original de Natalia Mallo